UNIVERSITÀ DEGLI STUDI DI MILANO

Ph.D. Programme in Food Systems

Department of Food, Environmental and Nutritional Sciences (DeFENS)
Division of Chemistry and Biochemistry

XXXIII Cycle

Synthesis, SAR and biological studies of natural and nature-inspired polyphenols

[CHIM/06]

Luce Micaela Mattio

R12014

Tutor: Prof. Sabrina Dallavalle

Ph.D. Dean: Prof. Ella Pagliarini

2019/2020

“Felix qui potuit rerum cognoscere causas…
Fortunatus et ille deos qui novit agrestis
Panaque Silvanumque senem Nymphasque sorores”

(Virgilio, Georg., II, 490; 493-94)

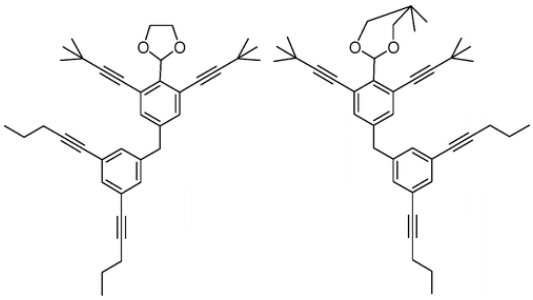

Index

ABBREVIATIONS

4CL	4-coumarate-CoA ligase
Å	Ångström
Ac_2O	acetic anhydride
ACN	acetonitrile
AIBN	2,2-azobisisobutyronitrile
BACE	beta-secretase 1
BBr_3	boron tribromide
BCl_3	boron trichloride
$Bi(OTf)_3$	bismuth(III) trifluoromethanesulfonate
BMI	body mass index
Boc	*tert*-butyloxycarbonyl
C4H	cinnamate-4-hydroxylase
CBr_4	carbon tetrabromide
CCl_4	carbon tetrachloride
CD_3OD	deuteromethanol
$CDCl_3$	deuterochloroform
CH_3I	methyl iodide
$CHCl_3$	chloroform
CHS	chalcone synthase
CHX	cyclohexane
Cs_2CO_3	caesium carbonate
$CuBr_2$	copper(II) bromide
CuI	copper Iodide
$CuSO_4 \cdot 5H_2O$	copper(II) sulfate pentahydrate
DCM	dichloromethane
DDQ	2,3-dichloro-5,6-dicyano-1,4-benzoquinone
DIPEA	*N*,*N*-diisopropylethylamine
DMA	*N*, *N'*-dimethylacetamide
DMAP	4-dimethylaminopyridine

DMF	*N*,*N*-dimethylformamide
DMP	Dess-Martin periodinane
DMSO	dimethyl sulfoxide
DPPA	diphenylphosphorylazide
dppp	1,3-Bis(diphenylphosphino)propane
DXN	*α*,*β*-dihydroxanthohumol
EDC·HCl	*N*-(3-dimethylaminopropyl)-*N*′-ethylcarbodiimide hydrochloride
eq	equivalent
Et_2O	diethylether
EtOAc	ethyl acetate
EtOH	ethanol
GABA	γ-aminobutyric acid
HDL	high-density lipoprotein
Hex	hexane
HFD	high-fat-diet
HIO_4	periodic acid
HoBt	1-hydroxybenzotriazole
HRP	horseradish peroxidase
IC_{50}	half maximal inhibitory concentration
IX	isoxanthohumol
K_2CO_3	potassium carbonate
KF	potassium fluoride
KOH	potassium hydroxide
LDA	lithium diisopropylamide
LDL	low-density lipoprotein
$LiAlH_4$	lithium aluminium hydride
$LiOH·H_2O$	lithium hydroxide monohydrate
m.p.	melting point
MBC	minimal bactericidal concentration

m-CPBA	*meta*-chloroperbenzoic acid
MeOH	methanol
MIC	minimal inhibitory concentration
min	minute
MOMCl	chloromethyl methyl ether
MW	microwave
$NaBH_4$	sodium borohydride
NaH	sodium hydride
$NaIO_4$	sodium periodate
NaN_3	sodium azide
NaOH	sodium hydroxide
NBS	*N*-bromosuccinimide
n-BuLi	butyllithium
NF-κB	nuclear factor kappa B
$NH_2NH_2{\cdot}H_2O$	hydrazine monohydrate
NIS	*N*-iodosuccinimide
$P(Cy){\cdot}HBF_4$	tricyclohexylphosphine tetrafluoroborate
$P(OEt)_3$	triethylphosphite
PAL	phenylalanine ammonia lyase
PBr_3	phosphorus tribromide
PBS	phosphate-buffered saline
$Pd(OAc)_2$	palladium acetate
$Pd(PPh_3)_4$	tetrakis(triphenylphosphine)palladium
$PdCl_2(PPh_3)_2$	bis(triphenylphosphine)palladium (II) dichloride
PPh_3	triphenylphosphine
p-TsOH	*para*-toluensulfonic acid
rt	room temperature
SIRT1	sirtuin 1
STS	stilbene synthase
TBAF	tetrabutylammonium fluoride

TBAI	tetrabutylammonium iodide
TBDMSCl	*tert*-butyl-dimethylsilyl chloride
t-BuOH	*tert*-butyl alcohol
TEA	triethylamine
TEM	transmission electron microscopy
TES	triethylsylane
TFA	trifluoroacetic acid
TG	triglycerides
THF	tetrahydrofuran
TNFα	tumour necrosis factor α
TXN	tetrahydroxanthohumol
WHO	World Health Organization
XN	xanthohumol

ABSTRACT

Polyphenols represent a wide class of diverse natural products, largely present in our diet, which have attracted the interest of several scientists in the last decades because of their beneficial effects on human health. Despite of intensive research efforts, the mechanisms of action of these compounds are still largely mysterious. This is partially due to the lack of a systematic investigation of single pure compounds with respect to several studies on complex mixtures from plant extracts. In addition, polyphenols are well known to undergo extensive hepatic and intestinal metabolism, which is of particular interest since metabolites can be responsible for both beneficial and toxic effects of dietary polyphenols.

In this scenario, the purpose of this PhD thesis was to develop synthetic strategies to obtain pure natural polyphenols and their analogues for systematic studies on their biological activity and to investigate the metabolites of this class of compounds.

The first part of this PhD thesis focused on resveratrol-derivatives, known as stilbenoids, a class of phytoalexins, produced by plants as means of defence against pathogens invasion and stress factors. In spite of the huge number of scientific reports on resveratrol, systematic studies on resveratrol-derived compounds are quite scarce. This derives from the difficulty to isolate and purify these compounds by extraction procedures from natural sources. In order to address this issue, we aimed at developing efficient and versatile biocatalytic and synthetic approaches to obtain natural-resveratrol derivatives in substantial amounts for their biological evaluation. Moreover, design and synthesis of new stilbenoid analogues were carried out for structure-activity-relationship (SAR) studies in order to identify the molecular features of the most active compounds involved in the interaction with biological targets. In addition, the synthetic strategies developed would allow to obtain new chemical entities with improved pharmacodynamic and pharmacokinetic

characteristics with respect to the natural precursors. In particular, the compounds were tested as antimicrobials and as inhibitors of α-amylase, fundamental enzyme in glucose metabolism.

The second part of this PhD thesis dealt with xanthohumol, the main prenylflavonoid found in hops and beer, endowed with several bioactivities. By LC-MS/MS, we identified and quantified xanthohumol metabolites in humans, which could be responsible for both beneficial and toxic effects of the natural precursor. The investigation of differences in xanthohumol metabolism in humans would reflect inter-individual differences in microbiota composition, and consequently in metabolic profiles. In addition, the last chapter described the development of a synthetic strategy to build a chemical probe of xanthohumol for the identification of its biological targets. In particular, efforts were made to selectively functionalize the prenyl chain of xanthohumol, without affecting the other parts of the molecule, which were supposed to be relevant to the interaction with the target.

RIASSUNTO

I polifenoli rappresentano un'ampia classe di prodotti naturali, largamente presenti nella nostra dieta. Negli ultimi anni tali molecole sono state oggetto di particolare interesse da parte della comunità scientifica per gli svariati effetti benefici sulla salute dell'uomo. Tuttavia, malgrado l'enorme ricerca scientifica, i meccanismi d'azione dei polifenoli sono ancora poco noti. Questo è in parte dovuto ai pochi studi sistematici mirati ad indagare i singoli composti, a dispetto di molti lavori incentrati sullo studio di miscele complesse di polifenoli derivanti da estratti naturali. Inoltre, questa classe di composti è nota per andare incontro a metabolismo epatico ed intestinale, punto di particolare interesse poiché proprio i metaboliti possono essere responsabili degli effetti benefici e tossici attribuiti ai loro precursori.

In tale contesto, lo scopo di questa tesi di dottorato è stato quello di sviluppare strategie sintetiche per ottenere polifenoli naturali, come singole molecole, metaboliti e analoghi sintetici per studi biologici sistematici.

In particolare, la prima parte della tesi si è incentrata sui derivati del resveratrolo, noti come stilbenoidi, una classe di fitoalessine, prodotte dalle piante come difesa da patogeni e condizioni di stress. Benché la letteratura abbondi di studi sul resveratrolo, il composto più studiato fra gli stilbenoidi, studi sistematici sui suoi derivati sono molto pochi. Ciò deriva dalla difficoltà di isolarli e purificarli da fonti naturali con procedure di estrazione classiche. Per risolvere questo problema, si sono sviluppate efficienti e versatili procedure sintetiche e biocatalitiche al fine di ottenere derivati naturali del resveratrolo in quantità sufficienti per la loro valutazione biologica. Inoltre, si sono progettati e sintetizzati nuovi analoghi stilbenici per studi di relazione struttura-attività volti ad identificare le caratteristiche molecolari indispensabili per l'interazione con il target biologico dei composti più attivi. Le strategie sintetiche sviluppate possono permettere di ottenere nuove molecole con

migliori caratteristiche farmacodinamiche e farmacocinetiche rispetto ai precursori naturali.

I composti sintetizzati sono stati testati per l'attività antimicrobica e come inibitori dell'α-amilasi, enzima fondamentale nel metabolismo del glucosio.

La seconda parte della tesi di dottorato ha riguardato lo xanthohumolo, il principale prenilflavonoide presente nel luppolo e nella birra, studiato per le sue svariate attività biologiche. Attraverso studi di cromatografia liquida-spettrometria di massa, abbiamo identificato e quantificato i metaboliti dello xanthohumolo nell'uomo. Le differenze evidenziate nel metabolismo dello xanthohumolo possono riflettere differenze inter-individuali nella composizione del microbiota, e conseguentemente nei profili metabolici.

Infine, l'ultimo capitolo descrive lo sviluppo di una strategia sintetica per costruire una sonda chimica dello xanthohumolo per l'identificazione dei suoi target biologici. In particolare, si è cercato di funzionalizzare selettivamente il prenile dello xanthohumolo, lasciando inalterate le altre parti della molecola ritenute fondamentali per l'interazione con il target.

1. INTRODUCTION

In the last century, the continuous progress in science and medicine has brought the average life expectancy at birth to double. It became evident that there were significant discrepancies in mortality and morbidity between people from different regions of the world, which have been attributed not only to genetic factors, but also to different lifestyle and environmental conditions (Kinsella 1992; Keylor et al. 2015). In this scenario, diet plays a key role as cross-cultural and epidemiological factor to stress out the differences in health life between people from different countries of the world (Ying et al. 2014)

Before the 1990s, a moderate alcohol consumption was believed to reduce the risk of coronary heart disease (CHD) (Giacosa et al. 2016). However, it was unclear if alcohol itself or particular constituents of certain alcoholic beverages were responsible for the beneficial effects observed (Rimm et al. 1996). In 1992, Siemann and Creasy (Siemann and Creasy 1992) found that resveratrol, a polyphenolic compound used as active ingredient in Japanese and Chinese folk medicines to treat disorders related to liver, skin, heart and lipid metabolism (Weiskirchen and Weiskirchen 2016), was present at high concentrations in red wine.

The discovery of the cardioprotective properties of resveratrol and its combination with other bioactive phytochemicals in wine seemed to be the key to solve the so-called “French Paradox” (Frankel et al. 1993). This expression was created by French epidemiologists to indicate that French people, well known to drink high amounts of red wine, had low incidence of CHD diseases and mortality, despite of a high fat diet and elevated smoke consumption (Richard et al. 1981). Noteworthy, a single dietary chemical constituent was suggested as responsible for health beneficial effects.

The actual role of resveratrol in the French Paradox remains contentious (Fuchs and Chambless 2007), but research interest in this simple molecule exploded as a result. Resveratrol has been reported to exert antioxidant,

antimicrobial, antifungal (Vestergaard and Ingmer 2019), anticancer (Berretta et al. 2020; Talib et al. 2020), antidiabetic (Nandurkar et al. 2020), cardioprotective (Mirabelli et al. 2020), neuroprotective (Wiciński et al. 2020a), antiaging activities (Jayaprakash et al. 2020). However, resveratrol is just one small molecule in a large and diverse class of polyphenols, natural products largely present in food and beverages we daily consume in our diet. Polyphenols have become very popular mainly because of their antioxidant properties (Wojtunik-Kulesza et al. 2020), which have been associated - by epidemiological evidence - with lower incidence of cardiovascular and neurodegenerative diseases and increased life expectancy (Valko et al. 2007). This epidemiological observation incredibly boosted the public interest in natural antioxidant supplements, which led the Global Antioxidants Market to be valued at $2,923 million in 2015 and expected to reach $4,531 million by 2022, with a CAGR (Compound Annual Growth Rate) of 6.42% in the forecast period (Eswara 2016). Despite the outstanding amount of studies on the beneficial properties of antioxidants, the results were often inconsistent with the potency and the mechanisms of action of the compound or of the class of compounds analysed in clinical trials (Tadros and Vij 2018). Indeed, besides their antioxidant activity, polyphenols have been claimed responsible for several other beneficial effects on human health, including cardioprotective, neuroprotective, chemopreventive, anti-inflammatory, immunomodulatory, antiallergic, anti-atherogenic, anti-thrombotic properties (Quideau et al. 2011; Williamson 2017; Mustafa et al. 2020). Although their antioxidant activity can contribute to all these effects, their activity in the body, which was underpinned by epidemiology, depends on both bioavailability and cellular molecular targets. Therefore, in the last decades many efforts have been made to elucidate the biochemical interactions responsible for the biological effects observed. However, the problem is not easy to solve. Polyphenols group more than 8000 different structures, and they have been often studied as mixtures of molecules from plant extracts because of the difficulty in purification procedures to obtain pure compounds in substantial

amounts for their biological evaluation. Moreover, polyphenols are well known to be low bioavailable, because they are poorly absorbed and undergo high metabolism. Indeed, only 5-10% of the total polyphenol intake is estimated to be absorbed in the small intestine, whereas 90-95% reaches the colon where the resident microbiota has been claimed by the scientific community to play a key role in the absorption and in the conversion of polyphenols into metabolites that may be more bioactive than their original precursors. Due to the inter-individual variability of the intestinal microbiota, a subsequent variability in metabolite production has also been reported, which can result in a different biological outcome due to the formation of either beneficial or toxic metabolites (Cueva et al. 2017). On their side, polyphenols are known to exert prebiotic-like effects on our intestinal microbiota, whose composition is known to affect human health (Singh et al. 2020; Wiciński et al. 2020b).

1.1 POLYPHENOLS

Nowadays, a daily intake of fruit and vegetables, drinking a cup of green tea and a glass of red wine per day, eating chocolate time to time are highly recommended to people for a healthy life. Indeed, fruits and vegetables, including tea, cocoa and grapes, contain polyphenols, a wide class of natural derivatives, which have been claimed to be responsible for several beneficial effects in humans (Quideau et al. 2011). Polyphenols include more than 8000 compounds that may be classified in several classes, depending on the chemical features or on the biosynthetic pathway. Before being named “polyphenols”, these compounds were known as “vegetable tannins” because of their presence in different plant extracts used in leather tanning. The term “tannin” derives from the French word “tan”, indicating powder of oak bark extract, used in the conversion of skin animals to leather. The word “tan” itself comes from the ancient Keltic lexical root “tann-“, meaning oak. However, today not all molecules classified as polyphenols are able to tan leather. As a matter of fact, from the second half of 20th century, these natural products

have become attractive molecules in several research fields, such as agriculture, ecology, food science, nutrition, medicine, besides their role in leather manufacture, and numerous scientist focused on their characterization and isolation (Quideau et al. 2011). In 1957, Theodore White was the first scientist to refer the term “tannins” to plant polyphenols with a molecular weight ranging from 500 to 3000 Da, and bearing enough phenol groups to form hydrogen-bond cross-linked structures with collagen molecules (White 1957). The two British phytochemists E. C. Bate-Smith and Tony Swain dedicated a great part of their research activity to plant polyphenols, which they defined as “*water-soluble phenolic compounds having molecular weights between 500 and 3000 (Da) and, besides giving the usual phenolics reactions* (tanning action)*, they have special properties such as the ability to precipitate alkaloids, gelatin and other proteins*” (Swain and Bate-Smith 1962). Later, the British physical-organic chemist Edwin Haslam, who dedicated his career to study plant polyphenols, confirmed this definition, but refined the first part, underlying that phenolics can be classified as polyphenols, if they bear 12-16 phenolic hydroxy groups on 5-7 aromatic rings per 1000 Da of relative molecular mass (Haslam and Cai 1994). From these definitions, it is important to note that the first criterion to include molecules in this class of compounds is their capacity of interaction with biomolecules (“*alkaloids, gelatin and other proteins*” from the above definition). This fundamental property of polyphenols highlights their important role as secondary metabolites in plants (i.e. chemical defence), as well as their attractive chemical-physical characteristics relevant to several applications. Eventually, Quideau *et al* defined polyphenols as “*secondary metabolites derived exclusively from the phenylpropanoid and/or the polyketide pathway, featuring more than one phenolic ring and being devoid of any nitrogen-based functional group in their most basic structural expression*” (Quideau et al. 2011). This definition allows to include in this class polyphenolic compounds lacking a tanning action, as long as they bear at least two phenol rings and share the phenylpropanoid and/or the polyketide biosynthetic pathway. Indeed, there are many natural compounds bearing

more than one phenol ring, though having different biosynthetic origins, such as some terpenoids (i.e. gossypol), or several alkaloids (i.e. norreticuline) deriving from the aminoacid tyrosine that is a primary metabolite of the phenylpropanoid pathway too (Quideau et al. 2011).

1.1.1. Biosynthesis of polyphenols

Polyphenols are secondary metabolites synthesised by plants as means of attraction of pollinators or as defence against UV radiation, microbial invasion and herbivores, like insects (Cutrim and Cortez 2018). As highlighted in the definition by Quideau *et al* (Quideau et al. 2011), polyphenols are biosynthesised through two main metabolic pathway: the phenylpropanoid and/or the polyketide metabolic pathways. The polyketide pathway involves the formation of polyketides from the binding of two-carbon units, i.e. activated acetate, and subsequent cyclization to give polyphenols (Cutrim and Cortez 2018). On the other hand, in the phenylpropanoid pathway, the aminoacid phenylalanine, deriving from the shikimate metabolic pathway, undergoes deamination by phenylalanine ammonia lyase (PAL) to give *trans*-cinnamic acid, which is converted into *p*-coumaric acid through hydroxylation of the phenyl ring by cinnamate-4-hydroxylase (C4H). *p*-Coumaric acid, through esterification of the carboxylic group and modifications on the aromatics rings, is the precursor of the subfamily of phenolic acids. On the other hand, 4-coumarate-CoA ligase (4CL) activates *p*-coumaric acid as 4-coumaroyl CoA, which undergoes the enzymatic addition of three molecules of malonyl-CoA by a type III polyketide synthase to give a linear tetraketide. The cyclization of the tetraketide intermediate, followed by the enzymatic activity of chalcone synthase (CHS) or stilbene synthase (STS), leads to the formation of chalcones, precursors of flavonoids, or stilbenoids, respectively (Chong et al. 2009; de La Rosa et al. 2010) (Figure 1.1).

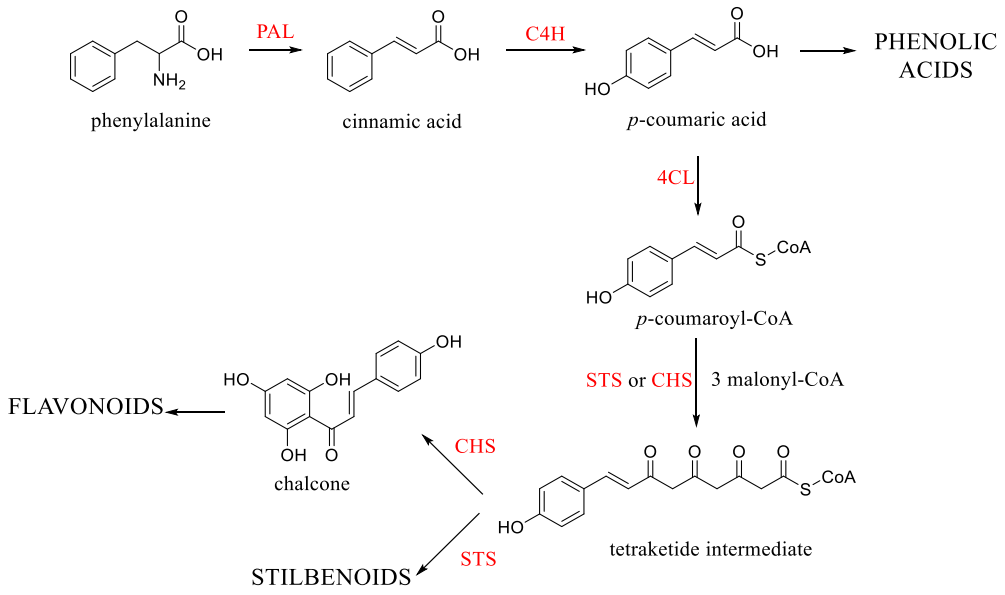

Figure 1.1. *Biosynthesis of polyphenols modified from* (Chong et al. 2009)

1.1.2. Classification of polyphenols

Polyphenols may occur in nature as aglycones or may be associated to carbohydrate moieties or organic acids. Considering the chemical features of the aglycones and the biosynthetic pathway, polyphenols may be classified into two main groups, flavonoid and non-flavonoid derivatives, differing in the number of rings and in the structural motifs that link the rings together (de La Rosa et al. 2010) (Figure 1.2).

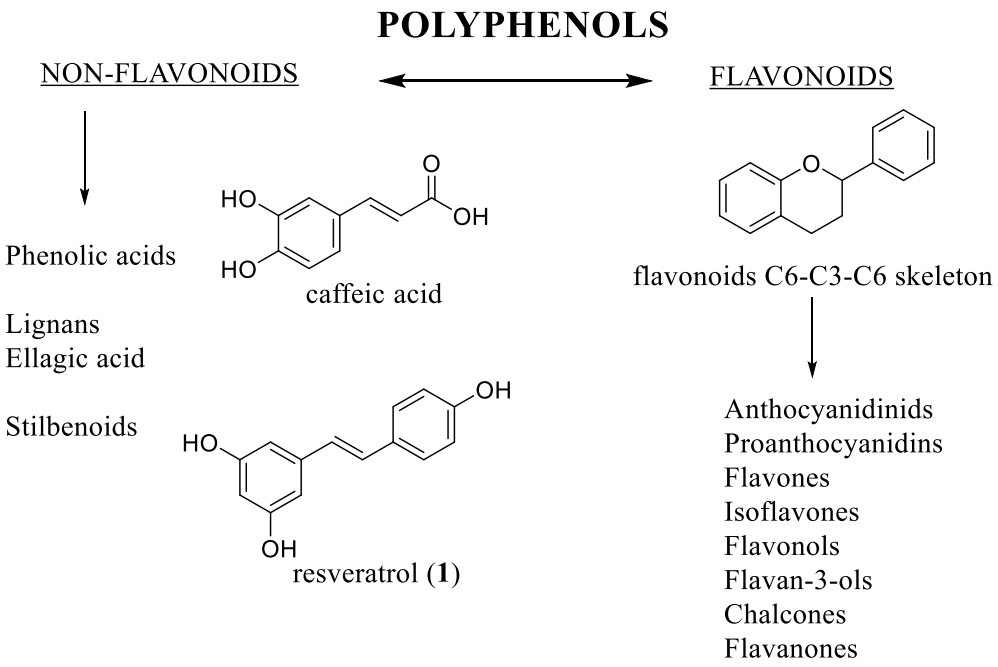

Figure 1.2. *Polyphenols classification modified from* (Han et al. 2007)

1.2. FLAVONOIDS

Flavonoids, sharing the phenylpropanoid and the polyketide biosynthetic pathways, are the most abundant class of polyphenolic compounds. Their name derives from the Latin term “flavus” meaning “yellow”, to highlight the colour of many representatives of this class. Flavonoids are involved in several physiological roles in plants, such as allelopathy, pollinator attraction, protection from UV radiation, defence against pathogens and herbivores, plant growth and development (Tauchen et al. 2020). These compounds are largely present in human diet, besides their abundance in medicinal plants and dietary supplements. Indeed, there is increasing evidence that these molecules may exert several beneficial effects on human health, such as antioxidant, anti-inflammatory, anticarcinogenic, neuroptrotective,

cardioprotective, antidiabetic, antimicrobial activities (Miranda et al. 2012). From a chemical point of view, flavonoids consist of two aromatic rings linked by a three-carbon chain that forms an oxygenated ring (diphenylpropane skeleton, C6-C3-C6 structure). Considering the hydroxylation pattern and the variations of the chromane ring (C ring), flavonoids can be further grouped into anthocyanidins, proanthocyanidins, flavones, isoflavones, flavonols, flavan-3-ols, chalcones, flavanones (Figure 1.3). Within each group, individual compounds differ in the substitution pattern of A and B rings (de La Rosa et al. 2010; Tsao 2010). Chalcones, or (*E*)-1,3-diphenylpropene-1-ones, are the precursors of all flavonoids. They consist of two aromatic rings, linked by a three carbon *α*,*β*-unsaturated carbonyl bridge (Rosa et al. 2017).

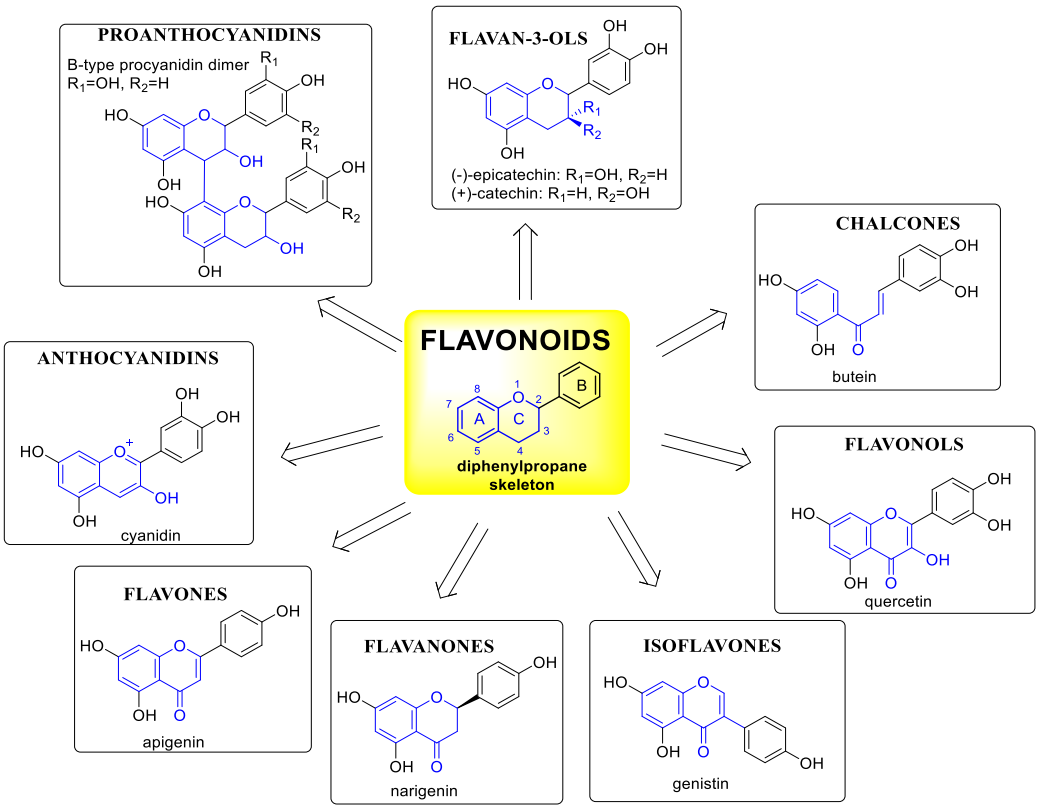

Figure 1.3. *Flavonoids classification modified from* (Tsao 2010)

Anthocyanidins, thanks to their positively charged oxonium salt structure, the flavylium cation, are water-soluble molecules constituting pigments in flower

petals and fruits, such as cranberries and grapes. Usually in nature they are glycosylated at the C3 and/or C5 positions, and in the glycosylated form, they are called *anthocyanins*. *Flavones* and *flavonols* bear a double bond between position 2 and 3, an oxygen at the C4 position, and they link the ring B at the C2 position. In addition, *flavonols* present a hydroxy function at the C3 position. *Flavanones* differ from *flavones* in the saturated bond between C2 and C3 positions, whereas *isoflavones* have the same structure as *flavones*, but bearing the ring B at the C3 position. *Flavan-3-ols* or *flavanols* bear a hydroxy group at the C3 position on a saturated three-carbon chain, which they have in common with *flavonols*. In nature, they occur as monomers or as *proanthocyanidins*, also known as condensed tannins, which are oligomers of 4-11 units of *flavanol*, such as (epi)catechin and epigallocatechin (Figure 1.3) (de La Rosa et al. 2010; Tsao 2010; Quideau et al. 2011; Panche et al. 2016)

1.2.1. Xanthohumol (XN)

In the last decade, among the flavonoid derivatives, xanthohumol (3'-[3,3-dimethylallyl]-2',4',4-trihydroxy-6'-methoxychalcone) (XN) (Figure 1.4) has attracted the interest of the functional food and pharmaceutical areas because of its multiple bioactivities (Liu et al. 2015), such as anti-obesity effects (Legette et al. 2013; Miranda et al. 2016; Paraiso et al. 2020), anticancer properties (Jiang et al. 2018), and central nervous system modulation *in vitro* and animal models (Miranda et al. 2018). XN is the main prenyflavonoid present in hops, the female inflorescences of the hop plant *Humulus lupulus* (Cannabinaceae), which is used as raw material in beer brewing to provide bitterness and flavour, in addition to its applications in traditional medicine (Zanoli and Zavatti 2008). Therefore, beer is the main dietary source of XN. The chalcone xanthohumol usually represents the 0.1-1% on dry weight of hops, and it can be detected along with other chalcones that occur at 10- o 100-fold lower concentrations. Most of the chalcones bear a hydroxy group at the 2' position, which can easily perform a Michael-addition on the *α,β*-unsaturated carbonyl bridge to give the corresponding flavanones. The

isomerization process can easily occur in the thermal beer brewing, explaining why xanthohumol is the main prenylflavonoid in hops, whereas its isomer isoxanthohumol (IX) (Figure 1.4) is the principal prenylflavonoid in beer (Stevens and Page 2004). XN was first isolated in 1913 by Power and coworkers, and it derives its name from its source (*Humulus*) and from its yellow colour (from the greek word "ξανθός" meaning "yellow", "blond") (Power et al. 1913).

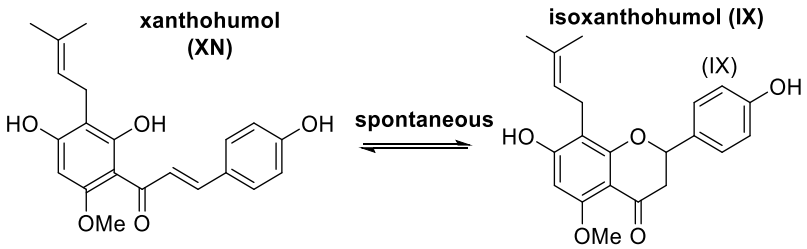

Figure 1.4. *Xanthohumol (XN) and its isomer isoxanthohumol (IX)*

1.2.1.1. Therapeutic potential of XN

1.2.1.1.1. Anticancer properties

According to WHO reports, cancer accounted for 9.6 million deaths in 2018, one-sixth of the deaths worldwide, and around one third of deaths from cancer are attributed to leading behavioural and dietary risks, including lack of physical activity, high body mass index (BMI), tobacco use, alcohol consumption and a low intake of fruit and vegetables (WHO 2018). About 30-50% of all cancer cases could be prevented, and a balanced diet with proper nutrients is an efficacious strategy in cancer prevention. In particular, a daily intake of fruit and vegetables may defend against oesophagus, colorectal, breast, endometrium, and kidney cancer. Several studies have documented the anti-carcinogenic effects of dietary polyphenols (Mustafa et al. 2020). Prevention or treatment of cancer can occur at different stages of carcinogenesis, such as initiation, promotion and progression. As anticancer agent, XN can inhibit angiogenesis, modulating Akt and NF-κB (nuclear factor

kappa B) pathways, blocking endothelial cell invasion, migration, growth, and production of angiogenic factors (Negrão et al. 2007), such as VEGF (vascular endothelial growth factor) and IL-8 (Negrão et al. 2010). Moreover, XN can inhibit proliferation and induce apoptosis in several cancer cells, by up-regulation of anti-apoptotic proteins, down regulation of pro-apoptotic proteins, and activation of procaspases (Liu et al. 2015). In addition, by upregulation of E-cadherin/catenin invasion suppressor system (Vanhoecke et al. 2005), downregulation of the metalloproteinases MMP-2 and/or MMP-9 (Young et al. 2013) and by decreasing adhesion of tumor cells to endothelial cells (Viola et al. 2013), XN can strongly inhibit cancer cell invasion (Liu et al. 2015). Noteworthy, a synergistic effect of XN with the current traditional chemotherapy and radiotherapy treatments was observed, which could allow to lower the doses of chemotherapeutic agents, like adriamycin, often responsible for severe side-effects (Jiang et al. 2018).

1.2.1.1.2. Central nervous system modulation properties

XN was found to exert different beneficial effects in the central nervous system (CNS) (Liu et al. 2015). Likely, by inhibition of inflammatory processes, apoptosis, and platelet activation, XN was showed to exert neuroprotective effects on cerebral ischemic damage in rats (Yen et al. 2012). To explain the use of hops in traditional medicine for sleeplessness and nervousnees treatment (Zanoli and Zavatti 2008), XN was investigated for sedative and anxiolytic effects. In this regard, XN was found to bind to $GABA_A$ receptors (Meissner and Häberlein 2006), but in Sprague-Dawley rat models, the anxiolytic effect was not related to $GABA_A$ receptors modulation but possibly to other neurotransmitter sites (Ceremuga et al. 2013). In mice fed a XN diet, the prenylflavonoid resulted to improve cognitive flexibility and to lower palmitate in plasma, which is associated with protein palmoitylation, resulting in poorer learning scores (Zamzow et al. 2014). Moreover, XN was found to inhibit BACE1, a potential target in Alzheimer's disease (Jung et al. 2010).

1.2.1.1.3 Effect on Metabolic syndrome (MetS)

Metabolic syndrome (MetS) indicates a complex of metabolic disorders, including hyperglycemia, hypertension, elevated triglycerides (TG) levels, low levels of high-density lipoprotein-cholesterol (HDL) in spite of elevated concentrations of low-density lipoproteins (LDL-c), and abdominal obesity. All these conditions are risk factors for type 2 diabetes (T2D) and cardiovascular diseases (Xu et al. 2019).

Different studies have demonstrated that XN can attenuate different factors of MetS. In high-fat-diet (HFD) mice, used as models for metabolic disorders, XN reduced body and liver weight gain and plasmatic TG and LDL levels, and improved dysfunctional glucose and lipid metabolism (Legette et al. 2013; Miranda et al. 2016, 2018). In a recent work (Paraiso et al. 2020), XN and its hydrogenated derivatives DXN (*α*,*β*-diihydroxanthohumol) and TXN (tetrahydroxanthohumol) (Figure 1.5) were demonstrated to modulate liver-brain axis, by decreasing the production of ceramides (a significant indicator of obesity, insulin resistance, and mitochondrial dysfunction (Torretta et al. 2019)), in both liver and hippocampus in high-fat-diet (HFD) treated mice. Moreover, XN, DXN and TXN promoted *de novo* synthesis of bile acids (BAs), which regulate FXR (farnesoid X receptor), a nuclear receptor involved in glucose, lipid and BAs homeostasis (Brandvold et al. 2019). These findings suggested that XN, DXN and TXN might be a promising approach to alleviate obesity-related metabolic impairments by modulating the bile acid-FXR-ceramide signalling axis (Paraiso et al. 2020).

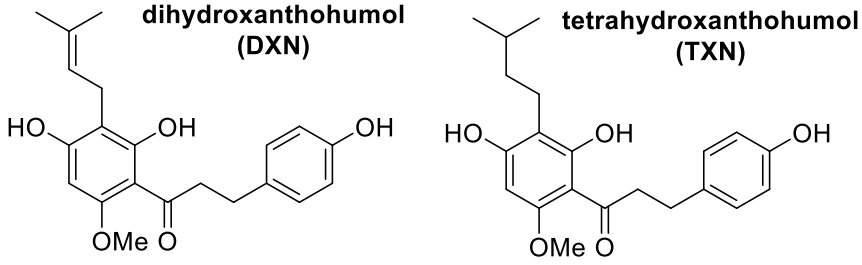

Figure 1.5. *Molecular structures of DXN and TXN, hydrogenated derivatives of XN*

1.2.1.1.4. XN metabolism

As for many polyphenols, the activity of xanthohumol seems to be highly influenced by its metabolism. Rat and human liver microsomes can convert XN into glucuronides and sulfates conjugates. *In vitro* and animal studies showed that XN is spontaneously converted into its flavanone isomer IX, which is converted into the potent phytoestrogen 8-prenylnaringenin (8-PN) by the gut microbe *E. limosum* (Possemiers et al. 2005) and by the hepatic cytochrome CYP1A2 (Guo et al. 2006). 8-PN has been demonstrated to exert estrogenic activity *in vivo*, which has raised health concerns on the use of xanthohumol in dietary supplements and medical foods (Miranda et al. 2018; Tronina et al. 2020). (Scheme 1.1)

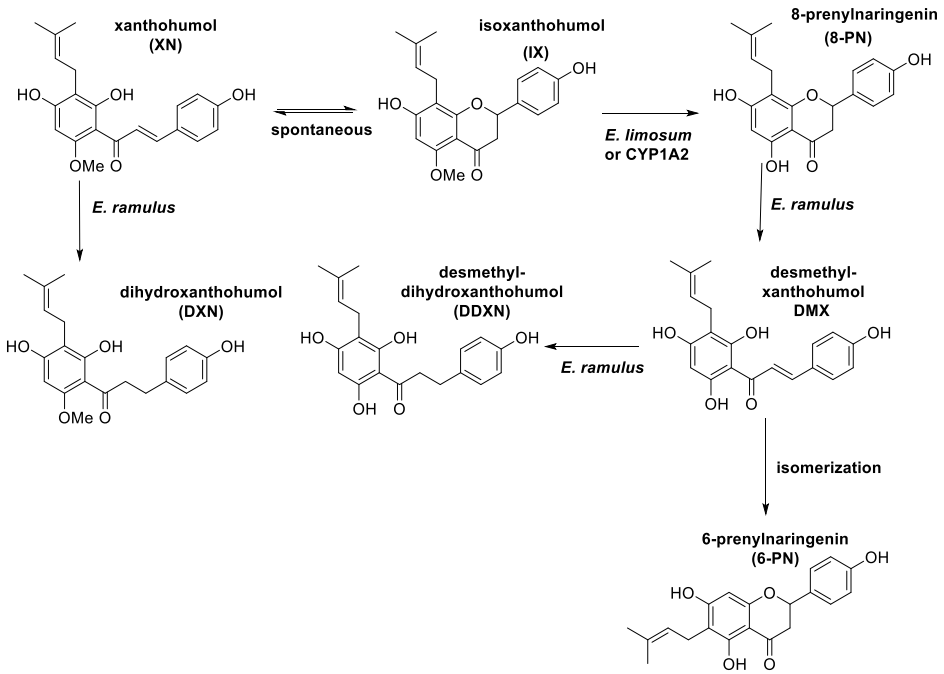

Scheme 1.1. *Metabolism of XN and its related prenylated flavonoids by gut microbiota*

In a more recent work (Paraiso et al. 2019), XN was shown in *in vitro* studies to be metabolized also by the gut microbe *E. ramulus*, belonging to the genus of *Eubacterium* (*Firmicutes* phylum). In particular, the incubation of XN with *E. ramulus* led to the formation of its hydrogenated derivative DXN, devoid of

estrogenic activity, lacking the double bond that undergoes the Michael addition in XN. Moreover, when 8-PN was incubated in presence of *E. ramulus*, desmethylxanthohumol (DMX) and desmethyldihydroxanthohumol (DDXN) (Scheme 1.1) were detected by LC-MS/MS analysis, whereas the incubation of IX with *E. ramulus* did not show any metabolic conversion. Overall, these data showed that *E. ramulus* is able to selectively hydrogenate the *α*,*β*-double bond of XN to yield DXN, and to metabolize 8-PN into DDXN. Co-culture experiments with both *E. ramulus* and *E. limosum* in presence of XN, IX, or 8-PN were also performed. XN and 8-PN showed similar results as in the monocultures involving just *E. ramulus*. IX was converted into 8-PN and DDXN, as expected. Due to the multiple biotransformation of XN, we should consider that XN metabolites, such as the extrogenic 8-PN, may contribute to the biological activity of their precursor. Therefore, considering the multiple bioactivities of XN and its safety in animal and humans (Legette et al. 2012, 2014; Liu et al. 2015), it would be important to identify and quantify XN metabolites in humans and to observe differences related to microbiota composition.

1.3. NON-FLAVONOID COMPOUNDS

1.3.1. Lignans and lignin

Para-coumaric acid is the precursor of phenolic acids that are grouped into hydroxybenzoic and hydroxycinnamic acid derivatives (Figure 1.6). The first ones include vanillic and gallic acids, less common than hydroxycinnamic acid-derived structures, such as ferulic acid, sinapic acid, *p*-coumaric acid and caffeic acid. Even if in the literature these monophenolic compounds are commonly referred to as “polyphenols”, they actually do not comply with the definition of polyphenols (Quideau et al. 2011), but they are the precursors of many non-flavonoid polyphenols.

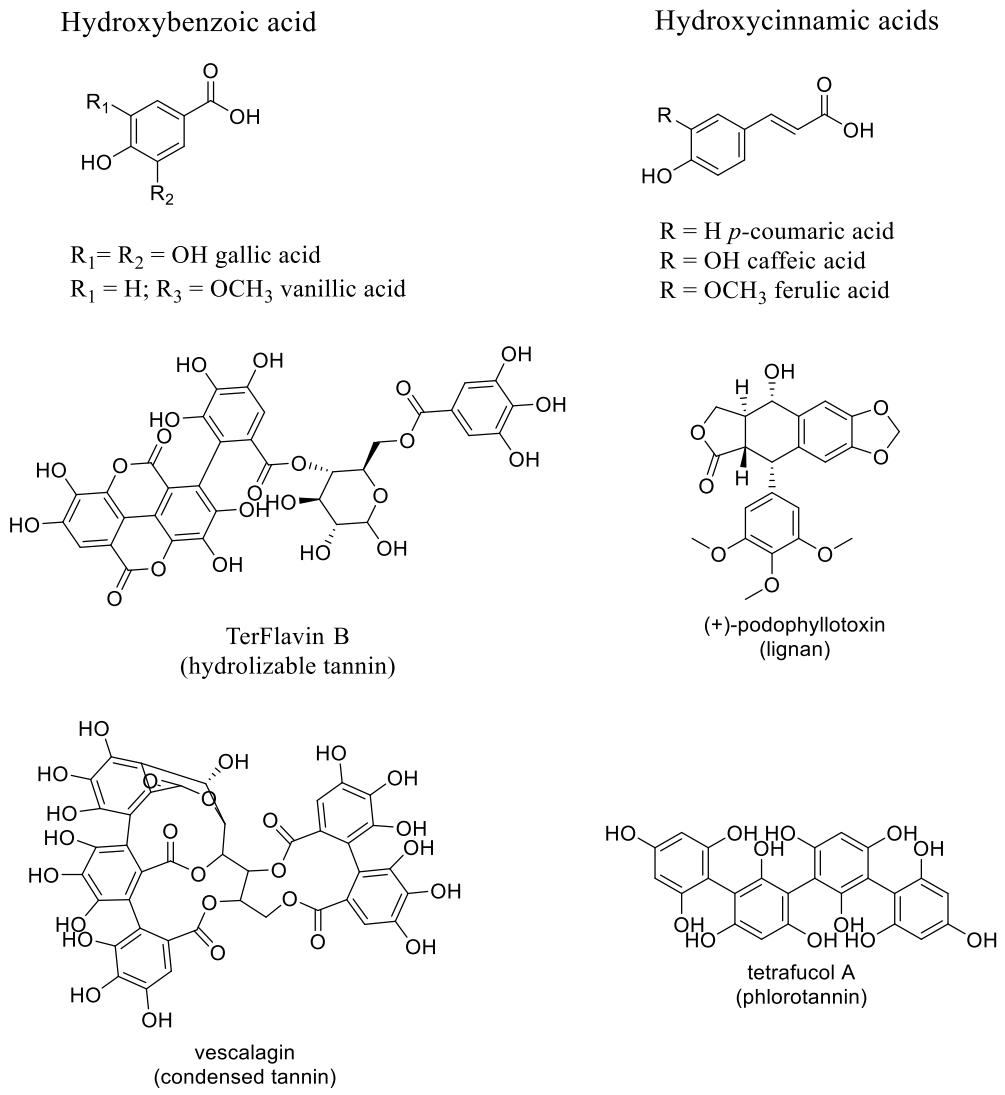

Figure 1.6. *Phenolic acids and examples of lignins and tannins*

The corresponding alcohols of ferulic acid, *p*-coumaric acid and sinapic acid constitute the so-called “monolignols” that can dimerize to give lignans, which are used by plants as defense against bacteria and fungi. Some compounds belonging to this family, like podophyllotoxin (Figure 1.6), have been used against cancer and acquired immunodeficiency syndrome (AIDS). From oxidative radical coupling of monolignols, polymerization processes take to

the formation of lignin, a strong, hydrophobic three-dimensional structure, covalently linking cellulose and proteins within the cell wall. Lignin composition varies among species: high content of coniferyl alcohol can be found in conifers, while higher amounts of coumaryl alcohol are present in cereal lignans. Lignin is a constitutive component of secondary cell walls, since it is fundamental to provide the mechanical properties that allow plants to attain height and conduct water under tension through xylem cells. On the other hand, lignin is also produced in response to infections and wounds as physical and physiological barrier (de La Rosa et al. 2010).

1.3.2. Tannins

Tannins derive from the polymerization of phenolic compounds and may be grouped in three main subclasses. Polymerization of flavan-3-ol units results in *proanthocyanidins*, also known as *condensed tannins* (i.e. vescalagin, Figure 1.6), thus belonging to flavonoid polyphenols. The *gallo*- and *ellagitannins*, known as *hydrolyzable tannins* (i.e. TerFlavin B, Figure 1.6), derive from the polymerization of other phenolics, like gallic acid (3,4,5-trihydroxybenzoic acid), and simple sugars (mainly D-glucose), through esterification and phenolic oxidative coupling reactions. Their content is especially high in the bark and galls of oaks. The third group, the *phlorotannins* (i.e. tetrafucol A, Figure 1.6), includes products of oligomerization of phloroglucinol (1,3,5-trihydroxybenzene), particularly present in red-brown algae (de La Rosa et al. 2010; Quideau et al. 2011).

1.3.3. Stilbenoids

Stilbenoids, or polyhydroxystilbenes, share the same hybrid phenylpropanoid/polyketide biosynthetic pathway with flavonoids, differing only in the last enzymatic step, which consists in the aldol-type cyclization of the tetraketide intermediate performed by stilbene synthase (STS) to give stilbenoids (Figure 1.1) (Chong et al. 2009). STS genes are transcribed in response to biotic and abiotic stress factors, such as microbes and fungi infections, UV radiations, physical trauma, highlighting the fundamental role

of these secondary metabolites in plant protection (Lu et al. 2012). Indeed, stilbenoids are both woody constitutive metabolites and phytoalexins, substances produced by plants in response to microbial infections and stress factors (Niesen et al. 2013). Notably, stilbenoids are expressed in lignified stem tissues, whereas they are completely absent in photosynthetic tissues where they have been demonstrated to be detrimental for the ion transport and associated redox processes. This observation suggests the role of resveratrol and its derivatives in interfering with cellular mechanisms, resulting in the protection of the plant against pathogens invasions (Keylor et al. 2015). Monomeric stilbenoid compounds share a common skeleton consisting of a central carbon-carbon double bond conjugated with two phenolic moieties and differing in the number and position of functional groups, such as hydroxy, methoxy, prenyl, geranyl, or farnesyl groups. The ethylene bridge can be found in the *E* or *Z* configuration, but *trans* isomers are usually the most stable and thus the most common in nature. Radical oxidative couplings of monomeric stilbenoids, commonly occurring in nature, lead to the formation of oligomeric stilbenoids (Akinwumi et al. 2018) (Figure 1.7). Therefore, this big class of polyphenols include not only mere stilbenoid structures, but also 2-arylbenzofurans, phenanthrenes, and related compounds (Rivière et al. 2012). All these compounds can be isolated in nature as aglycones or glycosides (Akinwumi et al. 2018).

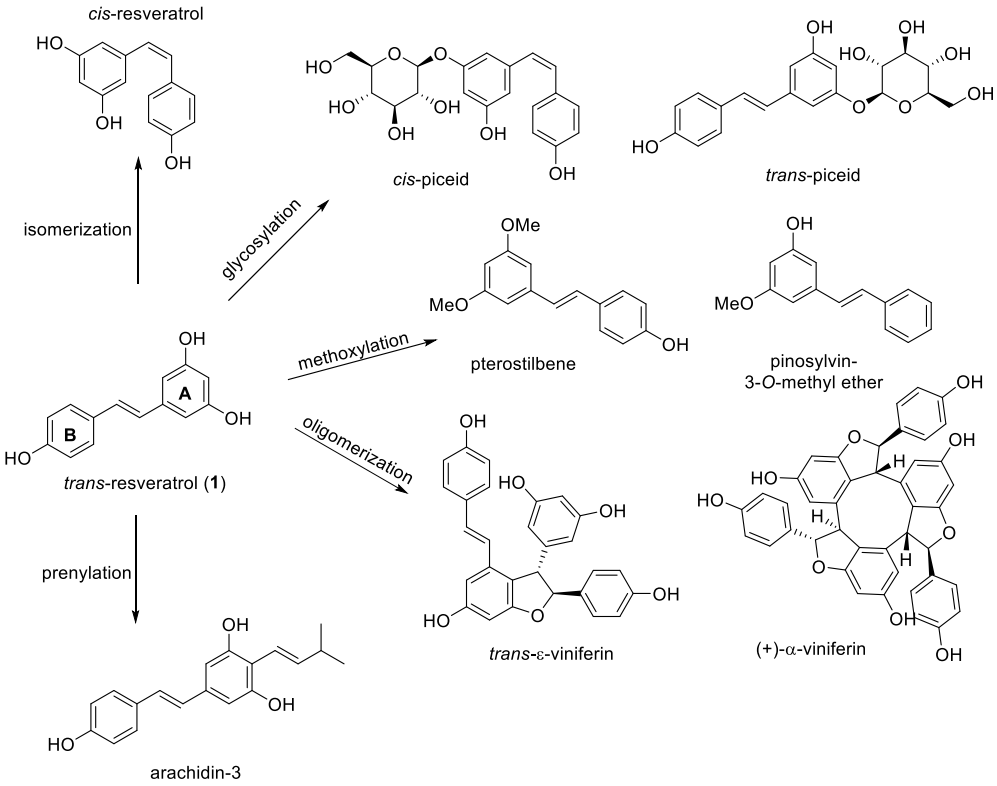

Figure 1.7. *Resveratrol post-synthetical modification modified from* (Chong et al. 2009)

1.1.3.1. Monomers

Resveratrol is the most known and studied natural phytoalexin, belonging to the large family of stilbenoids. Resveratrol was first isolated in 1939 from the roots of the white hellebore *Veratrum grandiflorum*, from which presumably derives its name, but *Polygonum cuspidatum*, a plant used in the traditional Chinese medicine, is the richest source of resveratrol (Arichi et al. 1982; Berretta et al. 2020). Later, resveratrol was found in several other plants and fruits, such as grapes, apples, raspberries, blueberries, pistachios, peanuts, and many other medicinal and edible plant species. Through several experimental and preclinical studies, resveratrol was found to exert cardioprotective, anticancer, anti-inflammatory, anti-diabetic, antimicrobial, neuro-protective properties (Weiskirchen and Weiskirchen 2016; Jayaprakash

et al. 2020). However, resveratrol is well known to be highly metabolized and poorly bioavailable, which has limited its use in humans (Pecyna et al. 2020). Resveratrol has been demonstrated to undergo different structural modifications increasing its antifungal and antioxidant properties. Piceid (Figure 1.7), its glycosylated derivative (resveratrol-3-*O*-glucoside), is believed to preserve resveratrol from oxidation while it is stored in plant cell tissues (Chong et al. 2009). Pterostilbene (*trans*-3,5-dimethoxy-4'-hydroxystilbene) (Figure 1.7) derives from the methylation of two hydroxy groups of resveratrol by *O*-methyltransferase enzymes, resulting in higher bioavailability in comparison to resveratrol. Pterostilbene was isolated in plant species such as *Pterocarpus marsupium, Vitis,* and *Vaccinium* species (blueberries), and has been studied for its antifungal, antimicrobial, anticancer, antidiabetic and neuroprotective activities (Kim et al. 2020; Lin et al. 2020). Piceatannol, (*trans*-3',4',3,5-tetrahydroxystilbene), (Figure 1.7) is commonly present in berries, grapes, passion fruit and white tea. This compound derives from the hydroxylation of resveratrol, performed by the enzyme CYP1B1 in humans (Piotrowska et al. 2012). Thanks to the presence of an additional hydroxy group at the *ortho*-position on the phenolic ring, generating a catechol, piceatannol is able to form a semiquinone radical with increased antioxidant power compared to that of resveratrol (Akinwumi et al. 2018). Noteworthy, the two adjacent hydroxy groups are able to chelate metal ions, an important function in plant pigmentation, as well as in plant cationic nutrition (i.e. Ca, Mg, Mn, Fe, Cu). Moreover, the additional hydroxy group at the *ortho* position displaces the maximum absorption from 270 nm, typical of simple phenols, to UV-B light range (280-320 nm), resulting in prevention of DNA damage against harmful solar radiation (Lattanzio et al. 2008; Quideau et al. 2011).

1.1.3.2 Oligomers

Oxidative radical couplings of resveratrol lead to the formation of three-dimensional and chiral polyphenolic compounds, consisting of 2-8 units of

resveratrol, known as “resveratrol oligomers” (Keylor et al. 2015). Their presence in plants has been correlated with their biological role in plants defence. In the 1970s, Langcake and Pryce were the first ones to describe the biological role of resveratrol and its oligomers in plants. They demonstrated the antifungal properties of resveratrol, which was found to cause fluorescent lesions on the leaves of *Vitis Vinifera* after infection with the plant pathogen *Botrytis cinerea* and *Plasmopora viticola* (Langcake and Pryce 1976). However, fungal lesions on the leaves of resistant species were shown to have relatively low amounts of resveratrol compared with the high concentrations of resveratrol oligomers, such as α-vinifein and ε-viniferin. This finding suggested that resveratrol, which is not a potent antifungal compound, could be just a precursor of the actual phytoalexins deriving from its oligomerization processes (Langcake 1981).

The resulting oligomers may be classified depending on the regioisomeric mode of their dimerization (Keylor et al. 2015). Resveratrol arenes could be indicated as A_1/A_2 for the phenol and the resorcinol rings, respectively. The dimerization process consists in the regioisomeric coupling of oxidatevely generated phenoxyl radicals: the 8-10’ coupling (i.e. ε-viniferin) (Oshima et al. 1993), the 8-8’ coupling (i.e. pallidol) (Ducrot et al. 1998; Adesanya et al. 1999) (Scheme 1.2), the 3-8’ coupling (δ-viniferin), and the less common 8-12’ (gnetin C) (Lins et al. 1982) and 12-12’ couplings (amurensin M) (Huang et al. 2001) (Scheme 1.3). Upon dimerization, highly reactive *para*-quinone methides may further undergo Friedel-Crafts reactions, tautomerization processes, or nucleophilic trappings to give the diverse and complex architectures of resveratrol oligomers (Keylor et al. 2015).

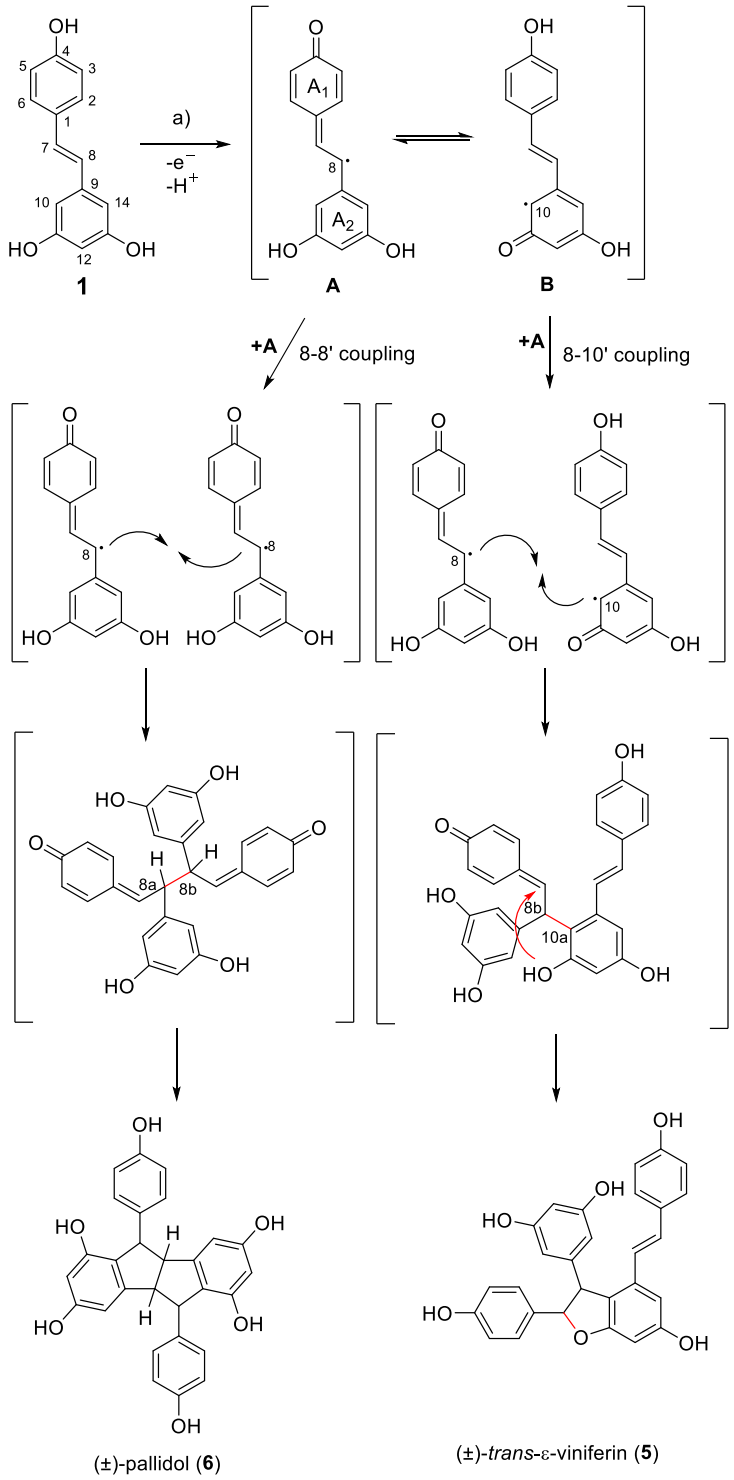

Scheme 1.2. *Proposed mechanisms of 8-8' and 8-10' couplings of resveratrol*

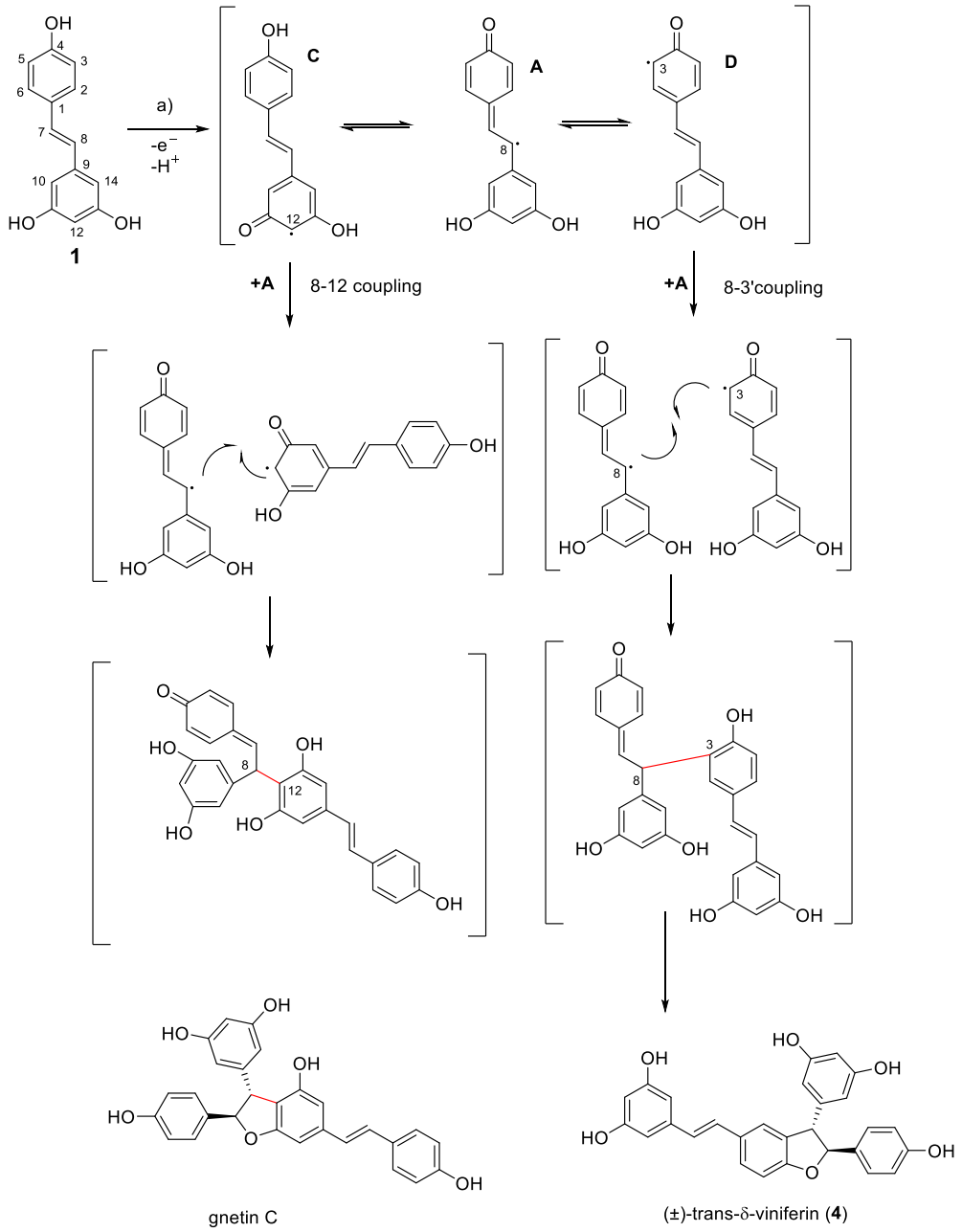

Scheme 1.3. *Proposed mechanisms of 8-12' and 8-3' couplings of resveratrol*

The 8-10’ coupling is the most common connectivity among resveratrol natural derivatives (Attar-ur-Rahman 2002) (Scheme 1.2) and, through an oxa-conjugate addition or a vinilogous Friedel-Crafts reaction of the *para*-quinone methide, takes to the formation of ε-viniferin (Scheme 1.2), found in both enantiomeric forms depending on the plant family (Keylor et al. 2015).

The 8-8’ coupling leads to the formation of the proposed dimeric intermediate bearing two *para*-quinone methides and two vicinal stereogenic centers, which undergo double Friedel-Crafts cyclizations to form the [3.3.0] byciclic core of pallidol (Scheme 1.2) (Keylor et al. 2015).

The 3-8’ coupling yields *δ*-viniferin (Breuil et al. 1998), which is the most common product resulting from the oxidation of resveratrol with inorganic reagents and enzymes such laccases and peroxidases (Scheme 1.3) (Keylor et al. 2015).

In a similar fashion manner, dimers can undergo oligomerization in presence of other molecules of resveratrol. However, unlike dimers, which are almost exclusively generated by an oxidative radical coupling, the higher order oligomers may derive either from an oxidative coupling or an intramolecular Friedel-Crafts cyclization. Notably, the majority of oligomers derive from convergent processes of dimerization of dimers and trimers. Usually, oligomerization is the result of intermolecular radical couplings and intramolecular Friedel-Crafts cyclization (Keylor et al. 2015).

Interestingly, a majority of resveratrol derivatives are isolated as optically active compounds, suggesting that the radical coupling is mediated by some chiral entity, but so far there is no evidence about this observation (Keylor et al. 2015). In 1997, *Fi*DIR1 was isolated as a protein able to dimerize coniferyl alcohol regiospecifically and enantioselectively (Davin et al. 1997). *Fi*DIR1 is a “dirigent” protein, without any oxidase activity on its own, but able to trap and guide the phenoxyl radical of coniferyl alcohol faster than the background rate of self-dimerization (Kim et al. 2015). The structural similarity of

resveratrol oligomers with lignans suggested the presence of similar proteins to guide the regiospecific and enantioselective couplings of resveratrol (Pezet et al. 2004; Pickel et al. 2010). So far, no cellular components have been identified as the actual responsible for the stereoselective biosynthesis of resveratrol oligomers (Keylor et al. 2015).

The oligomers can undergo further modifications, besides Friedel-Crafts cyclizations and oxidative couplings. The so called “viniferins” (i.e. α-viniferin, δ-viniferin, ε-viniferin, Figure 1.7, Scheme 1.2 and 1.3), discovered in the leaves and in the stem tissues of *Vitis vinifera*, are characterized by a 2,3-dihydrobenzofuran core. In 1999, from the corks of *Vitis vinifera* “Kyohou”, the benzofuran derivatives of ε-viniferin, viniferifuran or dehydro-ε-viniferin, was isolated (Ito et al. 1999) (Figure 1.8). Interestingly, 2,3-substituted benzofuran derivatives represent a large number of natural products endowed with multiple biological activities, such as anticancer, antimicrobial, immunomodulatory, antioxidant and anti-inflammatory properties (Khanam and Shamsuzzaman 2015; Naik et al. 2015; Chand et al. 2017; Miao et al. 2019). Dehydro-ε-viniferin was found to inhibit the Spleen tyrosinase kinase (Syk) (Jiang et al. 2014), modulating anti-inflammatory effects related to autoimmune disorders. Moreover, in a recent work, viniferifuran and other oligostilbenoids bearing a benzofuran core (i.e. dehydroampelopsin B, anigopressin A, dehydro-δ-viniferin, and resveratrol-piceatannol hybrid) were found to block the virulence factor T3SS in *Y. pseudotuberculosis* and *P. aeruginosa* (Sundin et al. 2020) (Figure 1.8).

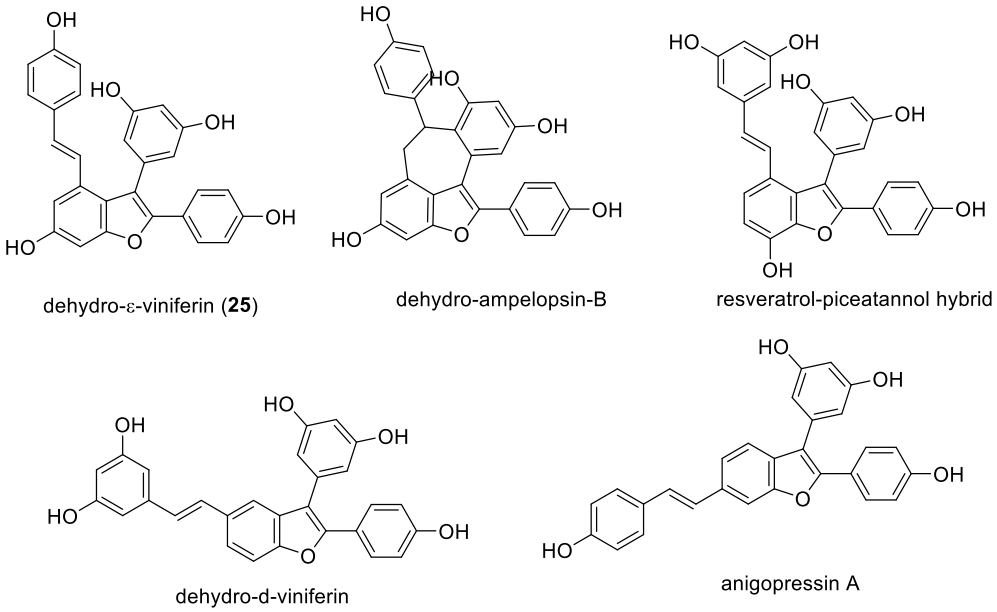

Figure 1.8. *Oligostilbenoids with a benzofuran scaffold*

Thanks to their three-dimensional structures and to the presence of stereogenic centers, oligomers should be more prone than resveratrol and its monomeric analogues to specifically and stereoselectively interact with biological targets, such as an enzyme or a receptor. Unfortunately, these compounds are found in nature as complex mixtures of stereo- and regio-isomers. Therefore, strenuous extraction and purification procedures are needed for their isolation, identification and biological evaluation. This results in limited biological studies of these intriguing molecular structures, due to low availability of sufficient amounts of resveratrol oligomers to perform biological tests.

1.1.3.3. Therapeutic potential of stilbenoids

As a result of the great interest in resveratrol, exploded with the so-called French Paradox, stilbenoids have attracted the attention of several scientists, who studied their several biological activitites, such as antioxidant, antidiabetic, antimicrobial, anticancer and antinflammatory and immunomodulatory properties (Akinwumi et al. 2018).

1.1.3.3.1. Antioxidant activity

Oxygen is essential for all life, but at the same time it can be deleterious to all aerobic organisms (oxygen paradox), due to the radical nature of molecular oxygen (O_2) bearing two unpaired electrons, which lead to the formation of reactive oxygen species (ROS) (Tadros and Vij 2018). ROS include superoxide anion ($O_2^{\bullet -}$), hydroxyl radical ($HO^{\bullet}$), hydrogen peroxide (H_2O_2), peroxyl radical $ROO^{\bullet}$ and singlet oxygen ($^1O_2$), nitric oxide (NO). These molecules play a beneficial role at low concentrations, since they are produced by normal aerobic metabolism, for example in response to noxia and as stimulus to mitogenic response (He and Yan 2013). However, an overproduction of ROS results in oxidative stress (OS), because the endogenous antioxidant cellular species are not able anymore to defend cell structure against ROS damage to all types of macromolecules (DNA, lipids, aminoacids and carbohydrates). This damage may cause or contribute to a wide variety of pathologies, such as neurodegenerative and cardiovascular diseases, cancer, and diabetes (Valko et al. 2007; Tadros and Vij 2018).

Polyphenols can act as antioxidants through different mechanisms. Their action can be due to their capability of chelating metal ions (Fe and Cu), necessary to the formation of hydroxyl radicals, or to their inhibition of enzymes involved in the formation of ROS, such as xanthine oxidase and protein kinase C. However, the scavenging activity is the most relevant property that contribute to the polyphenols antioxidant power. Through the hydrogen atom transfer (HAT) mechanism, a phenol ring can donate a hydrogen atom to a radical species ($R^{\bullet}$), becoming a free radical itself (ArO•), stabilized by the electron delocalization throughout the aromatic ring (Mustafa et al. 2020). The number and the position of other hydroxy groups on the polyphenolic, involved in hydrogen bonds and in the electronic delocalization, affects the bond dissociation energy (BDE), measuring the chemical bond strength: the weaker the O-H bond is, the easier the H-atom transfer will be (He and Yan 2013). Alternatively, through a single electron transfer (SET), a polyphenol ArOH can transfer a single electron to a free radical $R^{\bullet}$ with

formation of the stable radical ArOH•+. In this case, the antioxidant efficacy is determined by the ionization potential (IP) of ArOH: the lower PI is, the easier electron transfer is and the more efficient antioxidant activity is (Quideau et al. 2011) (Figure 1.9).

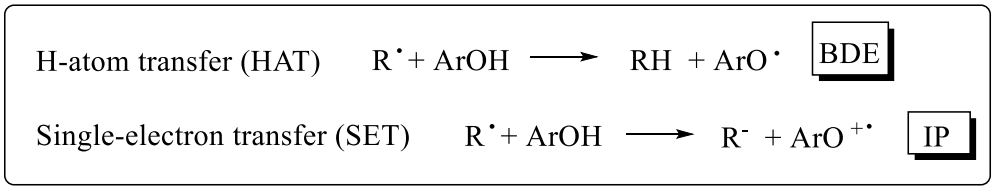

Figure 1.9. *Mechanisms of scavenging activity of polyphenols, BDE (bond dissociation energy) and IP (ionization potential)*

In stilbenoids, the number and position of hydroxy groups highly affects their antixodiant potency. The *para*-hydroxy group of resveratrol, thanks to its more acidic nature, is more effective than *meta* hydroxy groups in the peroxyl radical scavenging activity, exploiting the HAT mechanism. In addition, the *trans* double bond was demonstrated to contribute to the antioxidant activity, since the *cis* isomer and the derivative with a saturated bond were found to be less effective than resveratrol. Furthermore, partial or complete methylation of hydroxy groups causes a decrease or loss of the antioxidant potency (He and Yan 2013).

1.1.3.2.2. Anti-inflammatory activity

Inflammation, along with ROS production, is the physiological response to tissue injury and pathogens invasion. Immune cells (macrophages, leukocytes, neutrophils, and mast cells) recognize cell damage or pathogen-associated molecular patterns (PAMPs), and release a variety of inflammatory mediators, including cytokines (i.e. TNFα, interleukins), histamine, nitric oxide, leukotrienes and prostaglandins. Chronic inflammation can lead to aging, and severe diseases, such as asthma, arthritis, cardiovascular disorders, neurodegeneration, and cancer. Inflammatory mediators activate numerous transcription factors, such as NF-κB, NFAT (nuclear factor of activated T-

cells), Nrf2 (nuclear factor erythroid 2-related factor 2), AP-1 (activator protein1), regulated through mitogen-activated protein kinases (MAPKs). Moreover, several enzymes, such as IKK (I kappa B kinase), iNOS (inducibile nitric oxide synthase), COX-2 (cyclooxygenase) and 5-LOX (lipoxygenase) (Newton and Dixit 2012) are activated. Stilbenoids have been extensively used in folk medicine to treat inflammatory-related disorders, such as stomachache, hepatitis, arthritis, skin inflammation (Dvorakova and Landa 2017). About the anti-inflammatory activity of resveratrol, there are more than 2000 research articles. It was found to inhibit COX-2, NF-κB nuclear translocation and transcriptional activity, MAPKs, AP-1 protein expression, STAT-1 (signal transducer and activator of transcription) activity and phosphorylation, cytokines and matrix metallopeptidases production. Conversely, resveratrol activates SIRT1 (Dvorakova and Landa 2017), a human NAD-dependent deacetylase, able to modulate several factors promoting cell survival, delaying cell apoptosis and involved in cell damage repair. Piceatannol, pterostilbene and other monomeric stilbenes were demonstrated to affect almost identical targets (COX-2, AP-1, iNOS, NF-κB, TNFα, various interleukins, MAPKs phosphorylation). An additional *ortho*-hydroxy group to the resveratrol structure (piceatannol) was shown to highly enhance the antioxidant and the anti-inflammatory activity, due to the ability to form semiquinone radicals. The presence of hydroxy group at the *para* position seems to play a crucial role in the anti-inflammatory activity, whereas derivatives with additional hydroxy groups at the *meta* position showed decreased potency. Eventually, completely methoxylated derivatives lose their activity. On the other hand, studies on oligostilbenoids are scarce or mainly evaluating the compounds as complex mixtures from plant extracts (Jayaprakash et al. 2020).

1.1.3.2.3. Chemopreventive and anticancer activity

Resveratrol was largely studied for its chemopreventive and anticancer effects, exerted by its antioxidant activity and through the inhibition of tumor-

associated macrophages (TAMs, a subset of macrophages activated by cancel cells to stimulate the production of inflammatory cytokines), VEGF pathway, fibrosis, and the pro-inflammatory IL-6 (Berretta et al. 2020; Talib et al. 2020). Moreover, stilbenoids may prevent the initiation process, blocking pro-carcinogens by inhibition of specific isoforms of cytochrome P450 enzymes, and resveratrol was found to induce phase II metabolism of carcinogens, promoting their elimination from the body (Chang et al. 2000; Chun et al. 2009). Resveratrol, pterostilbene and piceatannol were demonstrated to induce apoptosis, prevent proliferation, cause cell cycle arrest and inhibit angiogenesis in several cancer types, such as breast, prostate, pancreatic, liver and colonrectal cancer (Kita et al. 2012; Kosuru et al. 2016; Pavan et al. 2016). In addition, the capability of piceatannol to inhibit the matrix metallopeptidase (MMP)-9 reduced prostate and breast cancer cells metastasis (Jayasooriya et al. 2012). Gnetol was shown to exert anti-cancer activity inhibiting histone deacetylases and cytochrome enzymes CYP2C9 and CYP3A4 (Remsberg et al. 2015; Akinwumi et al. 2018). The oligomers hopeaphenol (Figure 1.10), hemsleyanol D, and (+)-α-viniferin (Figure 1.7) caused apoptosis of melanoma cells, by selectively arresting cell cycle at the G1 phase (Moriyama et al. 2016). The oligostilbene suffruticosol D (Figure 1.10), isolated from *P. suffruticosa* seeds, exerted its anticancer activity in lung cancer cells by causing oxidative stress, inducing apoptosis, decreasing mithocondrial membrane potential, reducing cell motility and interfering with the NF-κB pathway (Almosnid et al. 2016; Shen et al. 2017).

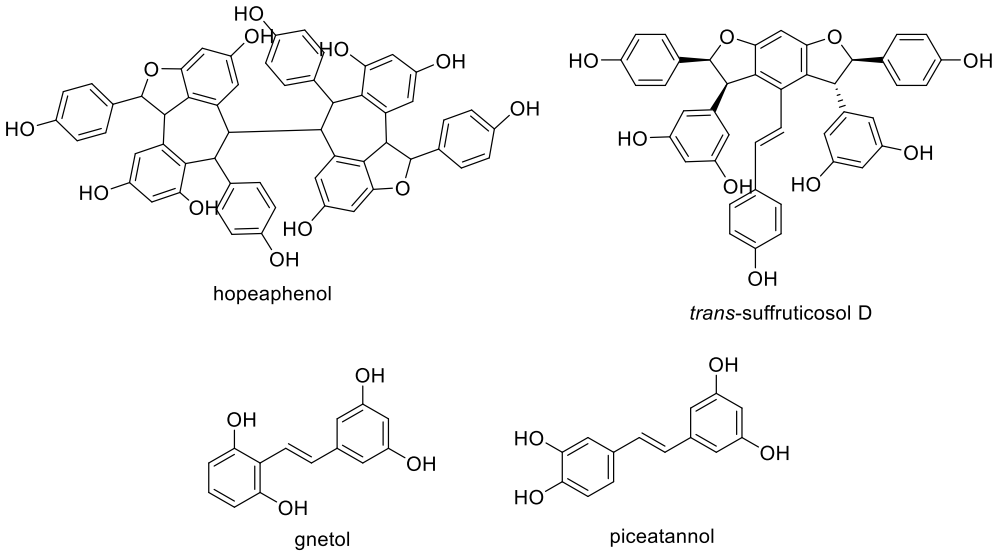

Figure 1.10 *Stilbenoids endowed with anticancer activity*

1.1.3.2.4 Antidiabetic activity

Diabetes mellitus (DM) indicates a group of metabolic disorders characterized by high blood glucose levels due to absent or inadequate pancreatic insulin secretion, with or without impairment of insulin action (Katzung 2018, chaps. 41-Pancreatic hormones and antidiabetic drugs). This pathologic condition leads to increased risk to develop several serious life-threatening health problems, such as cardiovascular, renal and hepatic diseases, resulting in high medical care costs and reduced life expectancy. Diabetes has become the most common serious metabolic disease worldwide, with 451 million people diagnosed of diabetes in 2017, expected to increase to 693 millions by 2045 (Cho et al. 2018; Zheng et al. 2018). Among the several beneficial effects on human health attributed to polyphenols, these compounds have been shown to manage and prevent type 2 diabetes, by directly modulating key enzymes of glucose and lipid metabolism (Cao et al. 2019). Resveratrol was demonstrated to exert antidiabetic effects through multiple mechanisms

resulting in a significant therapeutic effect in the whole organism (Oyenihi et al. 2016). In particular, resveratrol has been reported to target several proteins, including phosphodiesterases, adenylyl cyclases, kinases, sirtuins, transcription factors, cytokines, thus modulating different pathways involved in the antidiabetic effect of resveratrol (Öztürk et al. 2017; Cao et al. 2019). Pterostilbene increases glucokinase activity and skeletal muscle uptake, and protects pancreatic beta cells against oxidative stress and apoptosis. Despite the promising results of the monomeric compounds, the studies on the oligostilbenoids are still limited. However, the broad spectrum of bioactivities and the different potencies attributed to resveratrol may be partially, or even mainly, due to its products of oxidation, including the naturally-occurring oligomeric stilbenoids, which can elicit specific effects of their original precursor and, thanks to their three-dimensional structures, be more prone than resveratrol to specifically interact with macromolecular targets, such as regulatory proteins, receptors and enzymes.

1.1.3.2.5. Antimicrobial activity

Multidrug antibiotic resistance is dramatically increasing, due to overuse and disuse of antimicrobial agents in humans as well as in livestock and poultry, and antibiotic resistant infections are expected to cause 10 million deaths per year by 2050 (Pasberg-Gauhl 2014; Aidara-Kane et al. 2018; Domalaon et al. 2018; Wright et al. 2018). In addition, pathogenic microorganisms, such as *Listeria monocytogenes*, *Salmonella enterica*, *Staphylococcus aureus*, can easily contaminate food and drinks becoming responsible for foodborne infections, which are a big concern for human health (Kirk et al. 2015; Ma et al. 2018). In this scenario, stilbenoids, phytoalexins expressed by plants in response to microbial and fungal infections and stress factors, represent an interesting class of potential antimicrobials (Mattio et al. 2020). In a recent review, Vestergaard *et al* (Vestergaard and Ingmer 2019) described the multiple targets involved in the antibacterial activity of resveratrol. Resveratrol can bind to ATP synthase, reducing cellular energy and inhibiting cell

proliferation. Moreover, it was found to suppress the gene encoding for the filamentous temperature sensitive protein (FtsZ), fundamental in bacterial cell division. Thanks to its *para* hydroxy group and to the extensive electron conjugation conferred from the olefinic bridge, resveratrol can cleave DNA, by the formation of a complex DNA-resveratrol-Cu complex (Ma et al. 2018). Resveratrol, along with piceatannol and pterotilbene, was also demonstrated to interfere with quorum sensing (QS) and to have antivirulence properties, such as inhibition of biofilm formation and motility, and reduction of toxins expression (Sheng et al. 2015; Nijampatnam et al. 2018; Tang et al. 2019a; Vestergaard and Ingmer 2019). Studies on other monomeric stilbenoids, including piceatannol, pterostilbene, pinostilbene and oxyresveratrol (Figures 1.7-1.8-1.10-1.11), highlighted again the importance of the number and relative position of hydroxy groups. In particular, *ortho*-dihydroxy groups on ring B and methoxy groups on ring A (see *trans*-resveratrol formula, Figure 1.7, pag 24) enhanced the antibacterial activity on *S. aureus* (Cai et al. 2006; Zakova et al. 2018). In addition, the prenylation was found to positively affect the antimicrobial potency (Araya-Cloutier et al. 2017; de Bruijn et al. 2018). Oligostilbenoids, such as ε-viniferin (Figure 1.8), α-viniferin, and vitisin A (Figure 1.11) showed promising results in different studies, with also antibiofilm activity (Yim et al. 2010; Cho et al. 2013; Sahidin et al. 2017; Yadav et al. 2019). δ-Viniferin (Scheme 1.3) was shown to exert its antimicrobial activity on Gram-positive bacteria by downregulation of ABC transporters involved in cell division, and by inhibition of DNA gyrase (Mora-Pale et al. 2015). (-)-Hopeaphenol (Figure 1.10) and a series of resveratrol dimers bearing a benzofuran core (Figure 1.8) were found to act as antivirulence compounds, by inhibition of the T3SS (type III secretion system) in Gram-negative pathogens (Zetterström et al. 2013; Sundin et al. 2020). However, systematic studies of stilbenoids as antimicrobials are quite scarce and usually focused on the evaluation of plant extracts as complex mixtures of molecules and not aimed at understanding the contribute of single pure molecules. Therefore, there is a lack of knowledge about the mechanisms of

action and the molecular features relevant to the antimicrobial activity. Even though natural stilbenoids have been reported to act mainly on Gram-positive bacteria, some studies led to the identification of modified natural stilbenoids with increased antibacterial activity, on both antibiotic-resistant species and on Gram-negative strains. This highlights the potential of the stilbenoid scaffold in the antimicrobial research field (Chanawanno et al. 2010; Wan et al. 2017; Zhou et al. 2018; Rezaei-Seresht et al. 2019; Tang et al. 2019b).

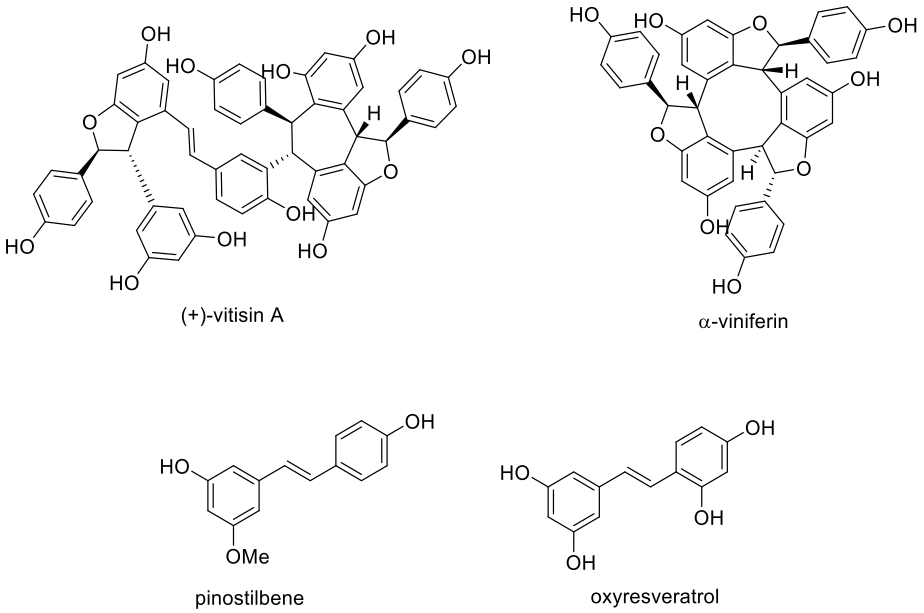

Figure 1.11. *Stilbenoids endowed with antimicrobial activity*

1.4. Bibliography

Adesanya SA, Nia R, Martin MT, Boukamcha N, Montagnac A, Pais M (1999) Stilbene derivatives from *Cissus quadrangularis*. J Nat Prod 62:1694–1695. https://doi.org/10.1021/np9902744

Aidara-Kane A, Angulo FJ, Conly JM, Minato Y, Silbergeld EK, McEwen SA, Collignon PJ (2018) World Health Organization (WHO) guidelines on use of medically important antimicrobials in food-producing animals. Antimicrob Resist Infect Control 7:1–8. https://doi.org/10.1186/s13756-017-0294-9

Akinwumi BC, Bordun KAM, Anderson HD (2018) Biological activities of stilbenoids. Int J Mol Sci 19:1–25. https://doi.org/10.3390/ijms19030792

Almosnid NM, Gao Y, He C, Park SY, Altman E (2016) In vitro antitumor effects of two novel oligostilbenes, cis- and trans-suffruticosol D, isolated from *Paeonia suffruticosa* seeds. Int J Oncol 48:646–656. https://doi.org/10.3892/ijo.2015.3269

Araya-Cloutier C, den Besten HMW, Aisyah S, Gruppen H, Vincken JP (2017) The position of prenylation of isoflavonoids and stilbenoids from legumes (Fabaceae) modulates the antimicrobial activity against Gram positive pathogens. Food Chem 226:193–201. https://doi.org/10.1016/j.foodchem.2017.01.026

Arichi H, Kimura Y, Okuda H, Baba K, Kozawa M, Arichi S (1982) Effects of Stilbene Components of the Roots of *Polygonum cuspidatum* SIEB. et ZUCC. on Lipid Metabolism. Chem Pharm Bull 30:1766–1770

Attar-ur-Rahman (ed) (2002) Studies in Natural Products Chemistry

Berretta M, Bignucolo A, Di Francia R, Comello F, Facchini G, Ceccarelli M, Iaffaioli RV, Quagliariello V, Maurea N (2020) Resveratrol in cancer patients: From bench to bedside. Int J Mol Sci 21:1–22. https://doi.org/10.3390/ijms21082945

Brandvold KR, Weaver JM, Whidbey C, Wright AT (2019) A continuous fluorescence assay for simple quantification of bile salt hydrolase activity in the gut microbiome. Sci Rep 9:1359. https://doi.org/10.1038/s41598-018-37656-7

Breuil A-C, Adrian M, Pirio N, Meunier P, Bessis R, Jeandet P (1998) Metabolism of Stilbene Phytoalexins by Botrytis cinerea : 1. Characterization of a Resveratrol Dehydrodimer. Tetrahedron Lett 39:537–540. https://doi.org/10.1016/S0040-4039(97)10622-0

Cai YZ, Sun M, Xing J, Quiong L, Harold C (2006) Structure-radical scavenging activity relationships of phenolic compounds from traditional

Chinese medicinal plants. Life Sci 78:2872–2888. https://doi.org/10.1016/j.lfs.2005.11.004

Cao H, Ou J, Chen L, Zhang Y, Szkudelski T, Delmas D, Daglia M, Xiao J (2019) Dietary polyphenols and type 2 diabetes: Human Study and Clinical Trial. Crit Rev Food Sci Nutr 59:3371–3379. https://doi.org/10.1080/10408398.2018.1492900

Ceremuga TE, Johnson LA, Adams-Henderson JM, McCall S, Johnson D (2013) Investigation of the anxiolytic effects of xanthohumol, a component of *humulus lupulus* (Hops), in the male sprague-dawley rat. AANA J 81:193–198

Chanawanno K, Chantrapromma S, Anantapong T, Kanjana-Opas A, Fun HK (2010) Synthesis, structure and in vitro antibacterial activities of new hybrid disinfectants quaternary ammonium compounds: Pyridinium and quinolinium stilbene benzenesulfonates. Eur J Med Chem 45:4199–4208. https://doi.org/10.1016/j.ejmech.2010.06.014

Chand K, Rajeshwari, Hiremathad A, Singh M, Santos MA Keri R (2017) A review on antioxidant potential of bioactive heterocycle benzofuran: Natural and synthetic derivatives. Pharmacol Reports 69:281–295. https://doi.org/10.1016/j.pharep.2016.11.007

Chang TKH, Lee WBK, Ko HH (2000) Trans-resveratrol modulates the catalytic activity and mRNA expression of the procarcinogen-activating human cytochrome P450 1B1. Can J Physiol Pharmacol 78:874–881. https://doi.org/10.1139/y00-067

Cho HS, Lee JH, Ryu SY, Joo SW, Cho MH, Lee J (2013) Inhibition of *Pseudomonas aeruginosa* and *Escherichia coli* O157:H7 Biofilm formation by plant metabolite ε-viniferin. J Agric Food Chem 61:7120–7126. https://doi.org/10.1021/jf4009313

Cho NH, Shaw JE, Karuranga S, Huang Y, da Rocha Fernandes JD, Ohlrogge AW, Malanda B (2018) IDF Diabetes Atlas: Global estimates of diabetes prevalence for 2017 and projections for 2045. Diabetes Res Clin Pract 138:271–281. https://doi.org/10.1016/j.diabres.2018.02.023

Chong J, Poutaraud A, Hugueney P (2009) Metabolism and roles of stilbenes in plants. Plant Sci 177:143–155. https://doi.org/10.1016/j.plantsci.2009.05.012

Chun YJ, Oh YK, Kim BJ, Kim D, Kim SS, Choi HK, Kim MY (2009) Potent inhibition of human cytochrome P450 1B1 by tetramethoxystilbene. Toxicol Lett 189:84–89. https://doi.org/10.1016/j.toxlet.2009.05.005

Cueva C, Gil-Sánchez I, Ayuda-Durán B, Gonzalez-Manzano S, Gonzalez-Paramàs AM, Santos-Buelga C, Bartolomé B, Moreno-Arribas MV (2017) An integrated view of the effects of wine polyphenols and their relevant

metabolites on gut and host health. Molecules 22:1–15. https://doi.org/10.3390/molecules22010099

Cutrim CS, Cortez MAS (2018) A review on polyphenols: Classification, beneficial effects and their application in dairy products. Int J Dairy Technol 71:564–578. https://doi.org/10.1111/1471-0307.12515

Davin LB, Wang H Bin, Crowell AL, Bedgar DL, Martin DM, Sarkanen S, Lewis NG (1997) Stereoselective bimolecular phenoxy radical coupling by an auxiliary (dirigent) protein without an active center. Science (80-) 275:362–366. https://doi.org/10.1126/science.275.5298.362

de Bruijn WJC, Araya-Cloutier C, Bijlsma J, de Swart A, Sanders MG, de Waard P, Gruppen H, Vincken JP (2018) Antibacterial prenylated stilbenoids from peanut (Arachis hypogaea). Phytochem Lett 28:13–18. https://doi.org/10.1016/j.phytol.2018.09.004

de La Rosa LA, Alvarez-Parrilla E, Gonzalez-Aguilarez GA (2010) Fruit and Vegetable Phytochemicals, 1th Editio

Domalaon R, Idowu T, Zhanel GG, Schweizer F (2018) Antibiotic hybrids: The next generation of agents and adjuvants against gram-negative pathogens? Clin Microbiol Rev 31:1–45. https://doi.org/10.1128/CMR.00077-17

Ducrot PH, Kollmann A, Bala AE, Majira A, Kerhoas L, Delorme R, Einhorn J (1998) Cyphostemmins A-B, two new antifungal oligostilbenes from Cyphostemma crotalarioides (Vitaceae). Tetrahedron Lett 39:9655–9658. https://doi.org/10.1016/S0040-4039(98)02207-2

Dvorakova M, Landa P (2017) Anti-inflammatory activity of natural stilbenoids: A review. Pharmacol Res 124:126–145. https://doi.org/10.1016/j.phrs.2017.08.002

Eswara P (2016) Antioxidants Market by Type (Natural (Vitamin A, Vitamin B, Vitamin C, and Rosemary Extract), Synthetic (Butylated Hydroxyanisole, Butylated Hydroxytoluene, and Others) - Global Opportunity Analysis and Industry Forecast, 2014-2022. https://www.alliedmarketresearch.com/anti-oxidants-market

Frankel EN, Kanner J, German JB, Parks E, Kinsella JE (1993) Inhibition of oxidation of human low-density lipoprotein by phenolic substances in red wine. Lancet 341:454–457. https://doi.org/10.1016/0140-6736(93)90206-V

Fuchs D, Chambless LE (2007) Is the cardioprotective effect of alcohol real ? 41:1999–2002. https://doi.org/10.1016/j.alcohol.2007.05.004

Giacosa A, Barale R, Bavaresco L, Faliva MA, Gerbi V, La Vecchia C, Negri E, Opizzi A, Perna S, Pezzotti M, Rondanelli M (2016) Mediterranean

Way of Drinking and Longevity. Crit Rev Food Sci Nutr 56:635–640. https://doi.org/10.1080/10408398.2012.747484

Guo J, Nikolic D, Chadwick LR, Pauli GF, van Breemen RB (2006) Identification of human hepatic cytochrome P450 enzymes involved in the metabolism of 8-prenylnaringenin and isoxanthohumol from hops (*Humulus lupulus* L.). Drug Metab Dispos 34:1152–1159. https://doi.org/10.1124/dmd.105.008250

Han X, Shen T, Lou H (2007) Dietary Polyphenols and Their Biological Significance. Int J m 8:950–988. https://doi.org/10.3390/i8090950

Haslam E, Cai Y (1994) Plant Polyphenols (Vegetable Tannins*) : Gallic Acid Metabolism. Nat Prod Res 11:41–66. https://doi.org/0.1039/NP9941100041

He S, Yan X (2013) From Resveratrol to Its Derivatives: New Sources of Natural Antioxidant. Curr Med Chem 20:1005–1017. https://doi.org/10.2174/0929867311320080004

Huang KS, Lin M, Cheng GF (2001) Anti-inflammatory tetramers of resveratrol from the roots of Vitis amurensis and the conformations of the seven-membered ring in some oligostilbenes. Phytochemistry 58:357–362. https://doi.org/10.1016/S0031-9422(01)00224-2

Ito J, Takaya Y, Oshima Y, Niwa M (1999) New oligostilbenes having a benzofuran from *Vitis vinifera* “Kyohou.” Tetrahedron 55:2529–2544. https://doi.org/10.1016/S0040-4020(99)00039-3

Jayaprakash JS, Gowda D V., Kulkarni PK (2020) Therapeutic application of resveratrol in human diseases. Int J Res Pharm Sci 11:1447–1456. https://doi.org/10.26452/ijrps.v11i2.2017

Jayasooriya RGPT, Lee YG, Kang CH, Lee KT, Choi YH, Park SY, Hwang JK, Kim GY (2012) Piceatannol inhibits MMP-9-dependent invasion of tumor necrosis factor-α-stimulated DU145 cells by suppressing the Akt-mediated nuclear factor-κB pathway. Oncol Lett 5:341–347. https://doi.org/10.3892/ol.2012.968

Jiang CH, Sun TL, Xiang DX, Wei SS, Li WQ (2018) Anticancer activity and mechanism of xanthohumol: A prenylated flavonoid from hops (*Humulus lupulus* L.). Front Pharmacol 9:530. https://doi.org/10.3389/fphar.2018.00530

Jiang M, Liu R, Chen Y, Zheng Q, Fan S, Liu P (2014) A combined experimental and computational study of Vam3, a derivative of resveratrol, and syk interaction. Int J Mol Sci 15:17188–17203. https://doi.org/10.3390/ijms150917188

Jung HA, Yokozawa T, Kim BW, Jung JH, Choi JS (2010) Selective inhibition

of prenylated flavonoids from Sophora flavescens against BACE1 and cholinesterases. Am J Chin Med 38:415–429. https://doi.org/10.1142/S0192415X10007944

Katzung BG (2018) Basic & Clinical Pharmacology, 14th edn.

Keylor MH, Matsuura BS, Stephenson CRJ (2015) Chemistry and Biology of Resveratrol-Derived Natural Products. Chem Rev 115:8976–9027. https://doi.org/10.1021/cr500689b

Khanam H, Shamsuzzaman (2015) Bioactive Benzofuran derivatives: A review. Eur J Med Chem 97:483–504. https://doi.org/10.1016/j.ejmech.2014.11.039

Kim H, Seo K-H, Yokoyama W (2020) Chemistry of Pterostilbene and Its Metabolic Effects. J Agric Food Chem 68:12836–12841. https://doi.org/10.1021/acs.jafc.0c00070

Kim KW, Smith CA, Daily MD, Cort JR, Davin LB, Lewis NG (2015) Trimeric structure of (+)-pinoresinol-forming dirigent protein at 1.95 A˚ resolution with three isolated active sites. J Biol Chem 290:1308–1318. https://doi.org/10.1074/jbc.M114.611780

Kinsella G (1992) Changes in life expectancy 1900-1990. Am J Clin Nutr 55:1196S-1202S. https://doi.org/10.1093/ajcn/55.6.1196S

Kirk MD, Pires SM, Black RE, Caipo M, Crump JA, Devleesschauwer B, Dopfer D, Fazil A, Fischer-Walker CL, Hald T, Hall AJ, Keddy KH, Lake RJ, Lanata CF, Torgerson PR, Havelaar AH, Angulo FJ (2015) World Health Organization Estimates of the Global and Regional Disease Burden of 22 Foodborne Bacterial , Protozoal , and Viral Diseases , 2010 : A Data Synthesis. PLOS Med 12:1–21. https://doi.org/10.1371/journal.pmed.1001921

Kita Y, Miura Y, Yagasaki K (2012) Antiproliferative and anti-invasive effect of Piceatannol, a polyphenol present in grapes and wine, against hepatoma AH109A cells. J Biomed Biotechnol ID 672416. https://doi.org/10.1155/2012/672416

Kosuru R, Rai U, Prakash S, Singh A, Singh S (2016) Promising therapeutic potential of pterostilbene and its mechanistic insight based on preclinical evidence. Eur J Pharmacol 789:229–243. https://doi.org/10.1016/j.ejphar.2016.07.046

Langcake P (1981) Disease resistance of Vitis spp. and the production of the stress metabolites resveratrol, ε-viniferin, α-viniferin and pterostilbene. Physiol Plant Pathol 18:213–226. https://doi.org/10.1016/s0048-4059(81)80043-4

Langcake P, Pryce RJ (1976) The production of resveratrol by *Vitis vinifera*

and other members of the Vitaceae as a response to infection or injury. Physiol Plant Pathol 9:77–86. https://doi.org/10.1016/0048-4059(76)90077-1

Lattanzio V, Kroon PA, Quideau S, Treutter D (2008) Recent Advances in Polyphenol Research, Volume 1 (2008, Wiley-Blackwell)

Legette LL, Karnpracha C, Reed RL, Choi J, Bobe G, Christensen JM, Rodriguez-Proteau R, Purnell JQ, Stevens JF (2014) Human pharmacokinetics of xanthohumol, an antihyperglycemic flavonoid from hops. Mol Nutr Food Res 58:248–255. https://doi.org/10.1002/mnfr.201300333

Legette LL, Ma L, Reed RL, Miranda CL, Christensen JM, Rodriguez-Proteau R, Stevens JF (2012) Pharmacokinetics of xanthohumol and metabolites in rats after oral and intravenous administration. Mol Nutr Food Res 56:466–474. https://doi.org/10.1002/mnfr.201100554

Legette LL, Moreno Luna AY, Reed RL, Miranda CL, Bobe G, Rodriguez-Proteau, Stevens JF (2013) Xanthohumol lowers body weight and fasting plasma glucose in obese male Zucker fa/fa rats. Phytochemistry 91:236–241. https://doi.org/10.1016/j.phytochem.2012.04.018

Lin W-S, Leland JV, Ho C-T, Pan M-H (2020) Occurrence, Bioavailability, Anti-inflammatory, and Anticancer Effects of Pterostilbene. J Agric Food Chem 68:12788–12799. https://doi.org/10.1021/acs.jafc.9b07860

Lins AP, Ribeiro MNDS, Gottlieb OR, Gottlieb HE (1982) Gnetins: Resveratrol oligomers from Gnetum species. J Nat Prod 45:754–761. https://doi.org/10.1021/np50024a022

Liu M, Hansen PE, Wang G, Qiu L, Dong L, Dong J, Yin H, Qian Z, Yang M, Miao J (2015) Pharmacological profile of xanthohumol, a prenylated flavonoid from hops (*Humulus lupulus)*. Molecules 20:754–779. https://doi.org/10.3390/molecules20010754

Lu D, Zhao W, Zhu K, Zhao S (2012) Relevant Enzymes, Genes and Regulation Mechanisms in Biosynthesis Pathway of Stilbenes. Open J Med Chem 2:15–23. https://doi.org/10.4236/ojmc.2012.22003

Ma DSL, Tan LTH, Chan KG, Yap WH, Pusparajah P, Chuah L-H, Ming LC, Khan TM, Lee L-H, Goh B-H (2018) Resveratrol-potential antibacterial agent against foodborne pathogens. Front Pharmacol 9:1–16. https://doi.org/10.3389/fphar.2018.00102

Mattio LM, Catinella G, Dallavalle S, Pinto A (2020) Stilbenoids: A natural arsenal against bacterial pathogens. Antibiotics 9:1–40. https://doi.org/10.3390/antibiotics9060336

Meissner O, Häberlein H (2006) Influence of xanthohumol on the binding

behavior of $GABA_A$ receptors and their lateral mobility at hippocampal neurons. Planta Med 72:656–658. https://doi.org/10.1055/s-2006-931609

Miao YH, Hu YH, Yang J, Liu T, Sun J, Wang X-J (2019) Natural source, bioactivity and synthesis of benzofuran derivatives. RSC Adv 9:27510–27540. https://doi.org/10.1039/c9ra04917g

Mirabelli M, Chiefari E, Arcidiacono B, Corigliano DM, Brunetti FS, Maggisano VM, Russo D, Foti DP, Brunetti A (2020) Mediterranean Diet Nutrients to Turn the Tide against Insulin Resistance and Related Diseases. Nutrients 12:1–37. https://doi.org/10.3390/nu12041066

Miranda CL, Elias VD, Hay JJ, Choi J, Reed RL, Stevens JF (2016) Xanthohumol improves dysfunctional glucose and lipid metabolism in diet-induced obese C57BL/6J mice. Arch Biochem Biophys 599:22–30. https://doi.org/10.1016/j.abb.2016.03.008

Miranda CL, Johnson LA, De Montgolfier O, Elias VD, Ullrich LS, Hay JJ, Paraiso IL, Choi J, Reed RL, Revel JS, Kioussi C, Bobe G, Iwaniec UT, Turner RT, Katzenellenbogen BS, Katzenellenbogen JA, Blakemore PR, Gombart AF, Maier CS, Raber J, Stevens JF (2018) Non-estrogenic Xanthohumol Derivatives Mitigate Insulin Resistance and Cognitive Impairment in High-Fat Diet-induced Obese Mice. Sci Rep 8:1–17. https://doi.org/10.1038/s41598-017-18992-6

Miranda CL, Maier CS, Stevens JF (2012) Flavonoids. eLS John Wiley Sons, Ltd Chichester 1–13. https://doi.org/10.1002/9780470015902.a0003068.pub2

Mora-Pale M, Bhan N, Masuko S, James P, Wood J, McCallum S, Linhardt RJ, Dordick JS, Koffas M (2015) Antimicrobial mechanism of resveratrol-trans-dihydrodimer produced from peroxidase-catalyzed oxidation of resveratrol. Biotechnol Bioeng 112:2417–2428. https://doi.org/10.1002/bit.25686

Moriyama H, Moriyama M, Ninomiya K, Morikawa T, Hayakawa T (2016) Inhibitory effects of oligostilbenoids from the bark of *Shorea roxburghii* on malignant melanoma cell growth: Implications for novel topical anticancer candidates. Biol Pharm Bull 39:1675–1682. https://doi.org/10.1248/bpb.b16-00420

Mustafa SK, Oyouni AAWA, Aljohani MMH, Ayaz Ahmad M (2020) Polyphenols more than an antioxidant: Role and scope. J Pure Appl Microbiol 14:47–61. https://doi.org/10.22207/JPAM.14.1.08

Naik R, Harmalkar DS, Xu X, Jang X, Kyeong L (2015) Bioactive benzofuran derivatives: Moracins A-Z in medicinal chemistry. Eur J Med Chem 90:379–393. https://doi.org/10.1016/j.ejmech.2014.11.047

Nandurkar D, Manohar M, Gowda D V. (2020) Recent review on role of resveratrol in diabetes and its complication. Int J Res Pharm Sci 11:1692–1700. https://doi.org/10.26452/IJRPS.V11I2.2069

Negrão R, Costa R, Duarte D, Gomes TT, Mendanha M, Moura L, Vasques L, Azevedo I, Soares R (2010) Angiogenesis and inflammation signaling are targets of beer polyphenols on vascular cells. J Cell Biochem 111:1270–1279. https://doi.org/10.1002/jcb.22850

Negrão R, Incio J, Lopes R, Azevedo I Soares R (2007) Evidence for the Effects of Xanthohumol in Disrupting Angiogenic, but not Stable Vessels. Int J Biomed Sci 3:279–86

Newton K, Dixit VM (2012) Signaling in innate immunity and inflammation

Niesen DB, Hessler C, Seeram NP (2013) Beyond resveratrol: A review of natural stilbenoids identified from 2009-2013. J Berry Res 3:181–196. https://doi.org/10.3233/JBR-130062

Nijampatnam B, Zhang H, Cai X, Michalek SM, Wu H, Velu SE (2018) Inhibition of *Streptococcus mutans* Biofilms by the Natural Stilbene Piceatannol Through the Inhibition of Glucosyltransferases. ACS Omega 3:8378–8385. https://doi.org/10.1021/acsomega.8b00367

Oshima Y, Ueno Y, Hisamichi K, Takeshita M (1993) Ampelopsins F and G, novel bridged plant oligostilbenes from *Ampelopsis brevipedunculata* var. hancei roots (vitaceae). Tetrahedron 49:5801–5804. https://doi.org/10.1016/S0040-4020(01)87946-1

Oyenihi OR, Oyenihi AB, Adeyanju AA, Oguntibeju OO (2016) Antidiabetic Effects of Resveratrol: The Way Forward in Its Clinical Utility. J Diabetes Res ID 9737483. https://doi.org/10.1155/2016/9737483

Öztürk E, Arslan AKK, Yerer MB, Bishayee A (2017) Resveratrol and diabetes: A critical review of clinical studies. Biomed Pharmacother 95:230–234. https://doi.org/10.1016/j.biopha.2017.08.070

Panche AN, Diwan AD, Chandra SR (2016) Flavonoids: An overview. J Nutr Sci 5:. https://doi.org/10.1017/jns.2016.41

Paraiso IL, Plagmann LS, Yang L, Zielke R, Gombart AF, Maier CS, Sikora A, Blakemore PR, Stevens JF (2019) Reductive Metabolism of Xanthohumol and 8-Prenylnaringenin by the Intestinal Bacterium *Eubacterium ramulus*. Mol Nutr Food Res 63:1–8. https://doi.org/10.1002/mnfr.201800923

Paraiso IL, Revel JS, Choi J, Miranda CL, Lak P, Kioussi C, Bobe G, Gombart AF, Raber J, Maier CS, Stevens JF (2020) Targeting the Liver-Brain Axis with Hop-Derived Flavonoids Improves Lipid Metabolism and Cognitive Performance in Mice. Mol Nutr Food Res 64:1–10.

https://doi.org/10.1002/mnfr.202000341

Pasberg-Gauhl C (2014) A need for new generation antibiotics against MRSA resistant bacteria. Drug Discov Today Technol 11:109–116. https://doi.org/10.1016/j.ddtec.2014.04.001

Pavan AR, da Silva GDB, Jornada DH, Chiba DE, dos Santos Fernandes GF, Chin CM, dos Santos JL (2016) Unraveling the anticancer effect of curcumin and resveratrol. Nutrients 8:. https://doi.org/10.3390/nu8110628

Pecyna P, Wargula J, Murias M, Kucinska M (2020) More than resveratrol: New insights into stilbene-based compounds. Biomolecules 10:1–40. https://doi.org/10.3390/biom10081111

Pezet R, Gindro K, Viret O, Spring JL (2004) Glycosylation and oxidative dimerization of resveratrol are respectively associated to sensitivity and resistance of grapevine cultivars to downy mildew. Physiol Mol Plant Pathol 65:297–303. https://doi.org/10.1016/j.pmpp.2005.03.002

Pickel B, Constantin MA, Pfannstiel J, Conrad J, Beifuss U, Schaller A (2010) An enantiocomplementary dirigent protein for the enantioselective lacease-catalyzed oxidative coupling of phenols. Angew Chemie - Int Ed 49:202–204. https://doi.org/10.1002/anie.200904622

Piotrowska H, Kucinska M, Murias M (2012) Biological activity of piceatannol: Leaving the shadow of resveratrol. Mutat Res - Rev Mutat Res 750:60–82. https://doi.org/10.1016/j.mrrev.2011.11.001

Possemiers S, Heyerick A, Robbens V, De Keukeleire D, Verstraete W (2005) Activation of proestrogens from hops (*Humulus lupulus* L.) by intestinal microbiota; conversion of isoxanthohumol into 8-prenylnaringenin. J Agric Food Chem 53:6281–6288. https://doi.org/10.1021/jf0509714

Power FB, Tutin F, Rogerson H (1913) The Constituents of Hops. J Chem Soc 103:1267–1292. https://doi.org/10.1039/CT9130301267

Quideau S, Deffieux D, Douat-Casassus C, Pouységu L (2011) Plant polyphenols: Chemical properties, biological activities, and synthesis. Angew Chemie - Int Ed 50:586–621. https://doi.org/10.1002/anie.201000044

Remsberg CM, Martinez SE, Akinwumi BC, Anderson HD, Takemoto JK, Sayre CL, Davies NM (2015) Preclinical Pharmacokinetics and Pharmacodynamics and Content Analysis of Gnetol in Foodstuffs. Phyther Res 29:1168–1179. https://doi.org/10.1002/ptr.5363

Rezaei-Seresht E, Salimi A, Mahdavi B (2019) Synthesis, antioxidant and antibacterial activity of azo dye-stilbene hybrid compounds. Pigment Resin Technol 48:84–88. https://doi.org/10.1108/PRT-01-2018-0005

Richard JL, Cambien F, Ducimetiere P (1981) Epidemiologic characteristics of coronary disease in France. Nouv Presse Med 10:1111–1114

Rimm EB, Klatsky A, Grobbee D, Stampfer MJ (1996) Review of moderate alcohol consumption and reduced risk of coronary heart disease : is the effect due to beer, wine, or spirits? Br Med J 312:1–6. https://doi.org/10.1136/bmj.312.7033.731

Rivière C, Pawlus AD, Mérillon JM (2012) Natural stilbenoids: Distribution in the plant kingdom and chemotaxonomic interest in Vitaceae. Nat Prod Rep 29:1317–1333. https://doi.org/10.1039/c2np20049j

Rosa GP, Seca AML, Barreto MDC, Pinto DCGA (2017) Chalcone: A Valuable Scaffold Upgrading by Green Methods. ACS Sustain Chem Eng 5:7467–7480. https://doi.org/10.1021/acssuschemeng.7b01687

Sahidin I, Wahyuni W, Malaka MH, Imran I (2017) Antibacterial and cytotoxic potencies of stilbene oligomers from stem barks of baoti (*Dryobalanops lanceolata*) growing in Kendari, Indonesia. Asian J Pharm Clin Res 10:139–143. https://doi.org/10.22159/ajpcr.2017.v10i8.18664

Shen J, Zhou Q, Li P, Wang Z, Liu S, He C, Zhang C, Xiao P (2017) Update on phytochemistry and pharmacology of naturally occurring resveratrol oligomers. Molecules 22:1–26. https://doi.org/10.3390/molecules22122050

Sheng JY, Chen TT, Tan XJ, Chen T, Jia A-Q (2015) The quorum-sensing inhibiting effects of stilbenoids and their potential structure-activity relationship. Bioorganic Med Chem Lett 25:5217–5220. https://doi.org/10.1016/j.bmcl.2015.09.064

Siemann EH, Creasy LL (1992) Conoentration of the Phytoalexin Resveratrol in Wine. Am J Enol Vitic 43:49–52

Singh A, Yau YF, Leung KS, El-Nezami H, Lee JCY (2020) Interaction of polyphenols as antioxidant and anti-inflammatory compounds in brain–liver–gut axis. Antioxidants 9:1–20. https://doi.org/10.3390/antiox9080669

Stevens JF, Page JE (2004) Xanthohumol and related prenylflavonoids from hops and beer: To your good health! Phytochemistry 65:1317–1330. https://doi.org/10.1016/j.phytochem.2004.04.025

Sundin C, Zetterström CE, Vo DD, Brkljaca R, Urban S, Elofsson M (2020) Exploring resveratrol dimers as virulence blocking agents – Attenuation of type III secretion in *Yersinia pseudotuberculosis* and *Pseudomonas aeruginosa*. Sci Rep 10:1–11. https://doi.org/10.1038/s41598-020-58872-0

Swain T, Bate-Smith EC (1962) Comparative Biochemistry. Academic Press,

New York

Tadros NN, Vij SC (2018) The oxidant paradox. Elsevier Inc.

Talib WH, Alsayed AR, Farhan F, Al Kury LT (2020) Resveratrol and Tumor Microenvironment: Mechanistic Basis and Therapeutic Targets. Molecules 25:1–25. https://doi.org/10.3390/molecules25184282

Tang F, Li L, Meng XM, Li B, Wang CQ, Wang SQ, Wang TL, Tian YM (2019a) Inhibition of alpha-hemolysin expression by resveratrol attenuates Staphylococcus aureus virulence. Microb Pathog 127:85–90. https://doi.org/10.1016/j.micpath.2018.11.027

Tang KW, Yang SC, Tseng CH (2019b) Design, synthesis, and anti-bacterial evaluation of triazolyl-pterostilbene derivatives. Int J Mol Sci 20:. https://doi.org/10.3390/ijms20184564

Tauchen J, Huml L, Rimpelova S, Jurášek M (2020) Flavonoids and related members of the aromatic polyketide group in human health and disease: Do they really work? Molecules 25:3–31. https://doi.org/10.3390/molecules25173846

Torretta E, Barbacini P, Al-Daghri NM, Gelfi C (2019) Sphingolipids in obesity and correlated comorbidities: The contribution of gender, age and environment. Int J Mol Sci 20:. https://doi.org/10.3390/ijms20235901

Tronina T, Popłonski J, Bartmanska A (2020) Flavonoids as Phytoestrogenic Components of Hops and Beer. Molecules 25:1–21. https://doi.org/10.3390/molecules25184201

Tsao R (2010) Chemistry and biochemistry of dietary polyphenols. Nutrients 2:1231–1246. https://doi.org/10.3390/nu2121231

Valko M, Leibfritz D, Moncol J, Cronin MTD, Mazur M, Telser J (2007) Free radicals and antioxidants in normal physiological functions and human disease. Int J Biochem Cell Biol 39:44–84. https://doi.org/10.1016/j.biocel.2006.07.001

Vanhoecke B, Derycke L, Van Marck V, Depypere H, De Keukeleire D, Bracke M (2005) Antiinvasive effect of xanthohumol , a prenylated chalcone present in hops (*Humulus lupulus* L .) and beer. Int J Cancer 895:889–895. https://doi.org/10.1002/ijc.21249

Vestergaard M, Ingmer H (2019) Antibacterial and antifungal properties of resveratrol. Int J Antimicrob Agents 53:716–723. https://doi.org/10.1016/j.ijantimicag.2019.02.015

Viola K, Kopf S, Rarova L, Jarukamjorn K, Kretschy N, Teichmann M, Vonach C, Atanasov AG, Giessrigl B, Huttary N, Raab I, Krieger S, Strnad M, de Martin R, Saiko P, Szekeres T, Knasmuller S, Dirsch VM, Jager W,

Grusch M, Dolznig H, Mikulits W, Krupitza G (2013) Xanthohumol attenuates tumour cell-mediated breaching of the lymphendothelial barrier and prevents intravasation and metastasis. Arch Toxicol 87:1301–1312. https://doi.org/10.1007/s00204-013-1028-2

Wan M, Hua L, Zeng Y, Jiao P, Xie D, Tong Z, Wu G, Zhou Y, Tang Q, Mo F (2017) Synthesis and properties of novel stilbene-twelve alkyl quaternary ammonium salts as antibacterial optical whitening agents. Cellulose 24:3209–3218. https://doi.org/10.1007/s10570-017-1323-9

Weiskirchen S, Weiskirchen R (2016) Resveratrol: How Much Wine Do You Have to Drink to Stay Healthy? Adv Nutr An Int Rev J 7:706–718. https://doi.org/10.3945/an.115.011627

White T (1957) Tannins—their occurrence and significance. J Sci Food Agric 8:377–385. https://doi.org/10.1002/jsfa.2740080702

WHO (2018) Cancer. https://www.who.int/news-room/fact-sheets/detail/cancer

Wiciński M, Domanowska A, Wódkiewicz E, Malinowski B (2020a) Neuroprotective properties of resveratrol and its derivatives—influence on potential mechanisms leading to the development of alzheimer's disease. Int J Mol Sci 21:1–17. https://doi.org/10.3390/ijms21082749

Wiciński M, Gębalski J, Mazurek E, Podhorecka M, Sniegocki M, Szychta P, Sawicka E, Malinowski B (2020b) The influence of polyphenol compounds on human gastrointestinal tract microbiota. Nutrients 12:1–14. https://doi.org/10.3390/nu12020350

Williamson G (2017) The role of polyphenols in modern nutrition. Nutr Bull 42:226–235. https://doi.org/10.1111/nbu.12278

Wojtunik-Kulesza K, Oniszczuk A, Oniszczuk T, Combrzynski M, Nowakowska D, Matwijczuk A (2020) Influence of in vitro digestion on composition, bioaccessibility and antioxidant activity of food polyphenols—a non-systematic review. Nutrients 12:1401. https://doi.org/10.3390/nu12051401

Wright L, Rao S, Thomas N, Boulos RA, Prestidge AP (2018) Ramizol® encapsulation into extended release PLGA micro- and nanoparticle systems for subcutaneous and intramuscular administration: in vitro and in vivo evaluation. Drug Dev Ind Pharm 44:1451–1457. https://doi.org/10.1080/03639045.2018.1459676

Xu H, Li X, Adams H, Kubena K, Guo S (2019) Etiology of metabolic syndrome and dietary intervention. Int J Mol Sci 20:1–19. https://doi.org/10.3390/ijms20010128

Yadav MK, Mailar K, Masagalli JN, Chae SW, Song JJ, Choi WJ (2019)

Ruthenium Chloride-Induced Oxidative Cyclization of Trans-Resveratrol to (±)-ε-Viniferin and Antimicrobial and Antibiofilm Activity against *Streptococcus pneumoniae*. Front Pharmacol 10:1–15. https://doi.org/10.3389/fphar.2019.00890

Yen TL, Hsu CK, Lu WJ, Hsieh CY, Hsiao G, Chou DS, Wu GJ, Sheu JR (2012) Neuroprotective effects of xanthohumol, a prenylated flavonoid from hops (*humulus lupulus*), in ischemic stroke of rats. J Agric Food Chem 60:1937–1944. https://doi.org/10.1021/jf204909p

Yim NH, Ha DT, Trung TN, Kim JP, Lee SM, Na MK, Jung H, Kim HS, Bae KH (2010) The antimicrobial activity of compounds from the leaf and stem of Vitis amurensis against two oral pathogens. Bioorganic Med Chem Lett 20:1165–1168. https://doi.org/10.1016/j.bmcl.2009.12.020

Ying ZX, Li HY, Chao G, Lei Z ,Yue Q, Gong C (2014) Progress in Research of Nutrition and Life Expectancy. 27:155–161. https://doi.org/10.3967/bes2014.036

Young S, Lee I, Moon A (2013) Chemico-Biological Interactions 2-Hydroxychalcone and xanthohumol inhibit invasion of triple negative breast cancer cells. Chem Biol Interact 203:565–572. https://doi.org/10.1016/j.cbi.2013.03.012

Zakova T, Rondevaldova J, Bernardos A, Landa P, Kokoska L (2018) The relationship between structure and in vitro antistaphylococcal effect of plant-derived stilbenes. Acta Microbiol Immunol Hung 65:467–476. https://doi.org/10.1556/030.65.2018.040

Zamzow DR, Elias V, Legette LL, Choi J, Stevens JF, Magnusson KR (2014) Xanthohumol improved cognitive flexibility in young mice. Behav Brain Res 275:1–10. https://doi.org/10.1016/j.bbr.2014.08.045

Zanoli P, Zavatti M (2008) Pharmacognostic and pharmacological profile of Humulus lupulus L. J Ethnopharmacol 116:383–396. https://doi.org/10.1016/j.jep.2008.01.011

Zetterström CE, Hasselgren J, Salin O, Davis RA, Quinn RJ, Sundin C, Eloffson M (2013) The resveratrol tetramer (-)-hopeaphenol inhibits type III secretion in the gram-negative pathogens *Yersinia pseudotuberculosis* and *Pseudomonas aeruginosa*. PLoS One 8:1–12. https://doi.org/10.1371/journal.pone.0081969

Zheng Y, Ley SH, Hu FB (2018) Global aetiology and epidemiology of type 2 diabetes mellitus and its complications. Nat Rev Endocrinol 14:88–98. https://doi.org/10.1038/nrendo.2017.151

Zhou C, Chia GWN, Ho JCS, Seviour T, Sailov T, Liedberg B, Kjelleberg S, Hinks J, Bazan GC (2018) Informed Molecular Design of Conjugated Oligoelectrolytes To Increase Cell Affinity and Antimicrobial Activity.

Angew Chemie - Int Ed 57:8069–8072. https://doi.org/10.1002/anie.201803103

2. AIM OF THE THESIS

Polyphenols have raised the interest of several scientists thanks to their several beneficial effects on human health. *In vitro* and *in vivo* studies have revealed the activity of polyphenols in numerous biological pathways, involved in cardiovascular, neurodegenerative diseases, diabetes, and cancer. Despite of intensive scientific research, the mechanisms of action of this huge class of molecules in the human body remain still largely mysterious. Moreover, these compounds suffer from low oral bioavailability, due to poor water-solubility and intensive intestinal and hepatic metabolism. This is of particular interest, since metabolites may actually mediate the effect of polyphenols and be the actual responsible for the beneficial effects of the ingested molecules in humans. Noteworthy, the intestinal microbiota is well known to play a crucial role in the conversion of polyphenolic structures into their metabolites, likely affecting both beneficial and toxic effects of dietary polyphenols. Therefore, further and in-depth studies on this class of compounds are required to delineate their pharmacodynamics and investigate the influence of the metabolism on their bioactivity.

The aim of my PhD project was to investigate the molecular features of dietary polyphenols fundamental for their bioactivity and to study the metabolites of this class of compounds.

In particular, a part of my project dealt with the development of biocatalytic and synthetic strategies to obtain natural-resveratrol derivatives, stilbenoids, in order to perform systematic studies on their antidiabetic and antimicrobial activity. As reported in the introduction, the number of scientific studies on resveratrol is outstanding. However, in the last years, the interest in resveratrol-derived compounds and in particular in its oligomers, has highly increased in order to explain the poor bioavailability and the incomplete understanding of the mechanisms of action of resveratrol *in vivo*, which have severely limited its therapeutic use. Moreover, oligomers are intriguing

molecules because of their three-dimensional structures, which could have higher probability to selectively interact with a biological target, with respect to the simple planar structure of resveratrol. Compared with resveratrol, systematic studies on its monomeric analogues and in particular on its oligomers are quite scarce, and often focused on complex mixtures deriving from plant extracts. This is mainly due to the strenuous processes required for their isolation and purification from natural sources.

In this scenario, the development of versatile synthetic strategies to selectively produce pure compounds and to generate new analogues for structure-activity-relationship (SAR) studies is instrumental to overcome the limitations imposed by material scarcity. Moreover, design and synthesis of new analogues to perform SAR studies would allow the identification of the molecular features involved in the interaction with the biological targets and obtain novel chemical entities with improved pharmacodynamic and pharmacokinetic characteristics with respect to the natural precursors.

In particular, the first aim was to access to substantial amounts of a small collection of natural stilbenoids for their biological evaluation, through the development of efficient biocatalytic and synthetic procedures. Since several studies have shown the antidiabetic effects of resveratrol, we planned to test the obtained compounds as inhibitors of key enzymes involved in carbohydrate metabolism.

As we highlighted in the introduction, stilbenoids are natural phytoalexins produced by plants as means of protection against pathogens infections and other stress factors. Hence, we planned to evaluate the derivatives obtained against bacterial pathogens, which constitute a serious threat to public health, with the increasing spread of bacterial strains resistant to current antibiotics.

Successively, SAR studies on the most active compounds were planned to evaluate the molecular features relevant to the antimicrobial activity. Finally, further efforts were made for the development of synthetic procedures to

modify the scaffold of the natural derivatives in order to access a series of modified-stilbenoids, which could be active on Gram-negative bacteria.

Another part of the project focused on the prenylflavonoid xanthohumol (XN), endowed with promising bioactivities, as reported in the introduction. However, the beneficial properties of this compound can be affected by its metabolism. In particular, one of xanthohumol metabolites, 8-prenylnaringenin (8-PN) was recognized as a potent phytoestrogen, which raised concerns on the use of XN in dietary supplements and functional foods. Recent *in vitro* studies have also demonstrated that gut microbial enzymes can convert XN in dihydroxanthohumol (DXN) and desmethyldihydroxanthohumol (DMX), avoiding the formation of the phytoestrogen 8-PN. Therefore, we were interested in identifying and quantifying XN metabolites in humans, which could be important to understand how XN metabolites can affect the bioactivity of the natural precursor and to study the interaction of XN with gut microbiota. Indeed, finding differences in XN metabolites among different subjects would reflect inter-individual differences in microbiota composition, and consequently, differences in metabolic profiles.

Attempting to find the biological targets of XN, other aim of this PhD thesis was to develop a synthetic strategy to build a XN chemical probe, without affecting the chemical properties of the natural compound. In this regard, the objective was to develop an approach to selectively functionalize the prenyl chain of XN, maintaining unaltered the other parts of the molecule.

3. DISCUSSION AND RESULTS

3.1. SYNTHESIS OF NATURAL STILBENOIDS AND ANALOGUES FOR THEIR EVALUTATION AS α-AMYLASE INHIBITORS AND ANTIMICROBIALS

ABSTRACT: To improve the current understanding of the biological activities of stilbenoids, efficient synthetic and biocatalytic procedures were developed in order to obtain a series of resveratrol-derived monomers and dimers as single molecules. The compounds obtained were evaluated as inhibitors of α-amylase, relevant enzyme in the glucose metabolism, and as antimicrobials. Dimeric stilbenoids, in particular viniferin isomers, resulted to inhibit pancreatic α-amylase, more efficiently than the reference drug acarbose. Racemic mixtures of viniferins were more active than the respective isolated pure enantiomers, showing a synergism in the interaction with the target. On the other hand, studies on the antimicrobial activity revealed the dimers δ-viniferin, viniferifuran, and dehydro-δ-viniferin as promising antibacterial agents on Gram-positive foodborne bacteria. Investigation of the mechanism of action of dehydro-δ-viniferin showed its ability to damage cell membrane of *Listeria monocytogenes* and to disrupt the membrane potential.

3.1.1. Synthesis of monomeric and dimeric stilbenoid derivatives

3.1.1.1. Introduction

Besides the huge amount of literature regarding resveratrol, stilbenoids studies have been mainly focused on the evaluation of plant extracts as complex mixtures of molecules and not aimed at understanding the contribute of single pure molecules. Indeed, the isolation of pure stilbenoids by extraction procedures and purification processes from natural sources are quite strenuous and provide just low amounts of single compounds, making difficult their evaluation in biological models. Therefore, obtaining these compounds from chemical effective syntheses would allow to access to substantial

amounts of compounds for their biological evaluations, overcoming the limitations due to material scarcity and isolation difficulties.

3.1.1.2. Materials and Methods

Procedures for the synthesis, isolation, and characterization data for the various stilbenoids obtained are described in the experimental part 3.1.4.

Chiral HPLC analyses were performed using a Kromasil 5-AmyCoat column (4.6 mm i.d. × 250 mm, Nouryon Separation Products, Bohus, Sweden), fitted to a Jasco PU-980 pump and a Jasco UV-975 detector. Runs were carried out in 60/40 (v/v) hexane/iPrOH + 0.1% TFA at a flow rate of 1 mL min-1, monitoring the eluate at 280 nm. Preparative chiral HPLC was performed with a Kromasil 5-AmyCoat column (21.2 i.d. × 250 mm), fitted to a 1525 Extended Flow Binary HPLC pump and a Waters 2489 UV/Vis detector (both from Waters, Milan, Italy). The solvent was 60/40 (v/v) hexane/iPrOH + 0.1% TFA, at a flow rate of 15 mL min-1, monitoring the eluate at 280 nm.

3.1.1.3. Results and discussion

By chemoenzymatic and synthetic approaches, a series of monomers and dimers of resveratrol were efficiently obtained (Figure 3.1).

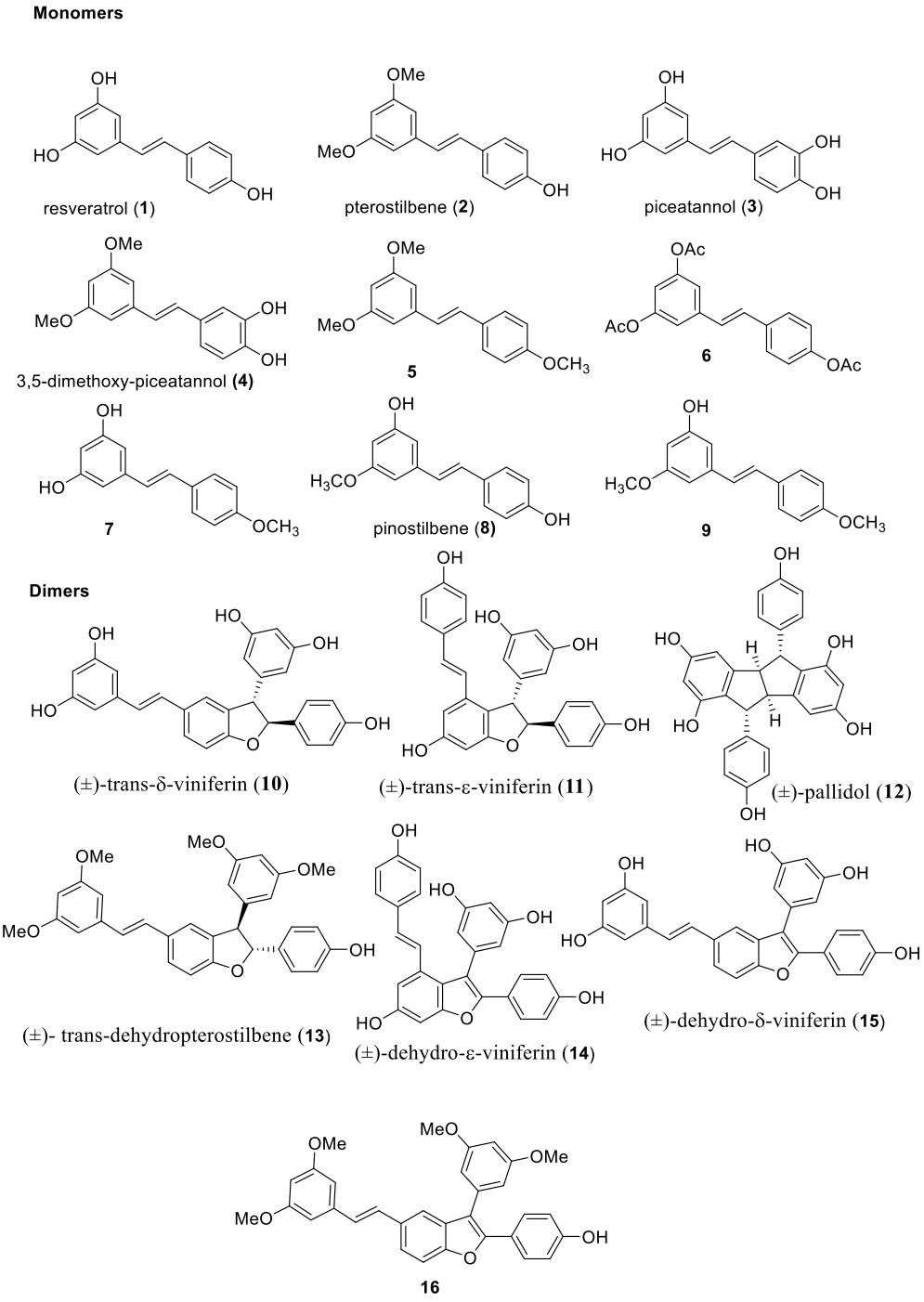

Figure 3.1. *Structures of stilbenoid monomers and dimers synthesized*

Firstly, we wanted to perform SAR studies on resveratrol monomers, investigating how the number and position of hydroxy, methoxy and acetoxy groups could contribute to the biological activity. Both resveratrol (**1**) and pterostilbene (**2**) were commercially available at low cost. For the preparation of piceatannol (**3**), different attempts were tried. We performed a regioselective oxydation of resveratrol with iodoxybenzoic acid (IBX) in MeOH at - 78°C and subsequent reduction of the intermediate *o*-quinone by $Na_2S_2O_4$, but we obtained only inseparable complex mixtures. Therefore, we perfomed the same reaction on pterostilbene, and using optimized conditions (DMF solvent at room temperature for 1h, Table 3.1), we finally succeeded in obtaining the desired product in 25% yield. Noteworthy, using $NaBH_4$ as reductive agent in place of $Na_2S_2O_4$, we obtained 3,5-dimethoxypiceatannol in 62% yield. However, the demethylation gave piceatannol in only 20% yield. The intermediate **4** was used for the synthesis of the tetramethylated compound **17** through Williamson reaction (Scheme 3.1).

Table 3.1. *Conditions for the regioselective oxidation of pterostilbene (**2**) with IBX*

Solvent	Reducing agent	Yield
DMSO	$Na_2S_2O_4$	15%
DMF	$Na_2S_2O_4$	25%
DMF	$NaBH_4$	62%

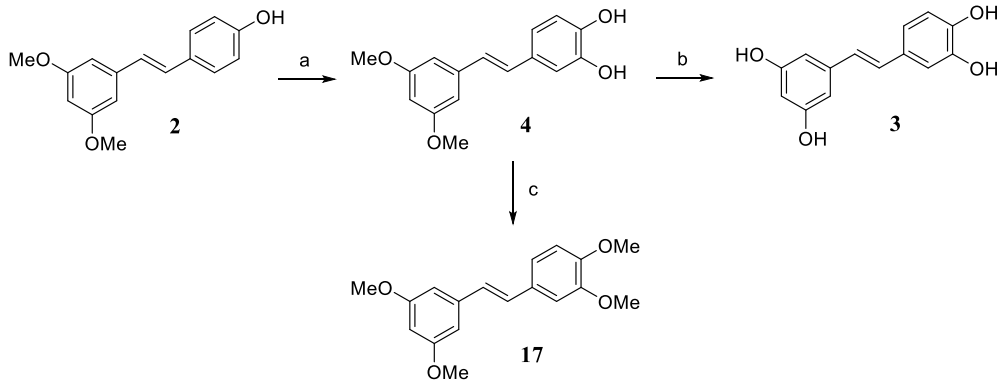

Scheme 3.1. a) 1) IBX, DMF, rt, 80 min 2) $NaBH_4$ MeOH 0°C, 62%; b) BBr_3, DCM, -35°C to rt, N_2, 22h, 20% c) CH_3I, K_2CO_3, acetone, rt, N_2, 70%

Alternatively (Scheme 3.2), attempting to obtain a precursor of piceatannol bearing protective groups more easily removable than methoxy groups, we started from compound **6**, which was selectively deacetylated on the *para* position by lipase *Candida Antarctica* to give 3,5-di-*O*-acyl resveratrol (**18**) in 81% yield (Bernini et al. 2009). Using the optimized conditions developed for the synthesis of the intermediate **4**, the regioselective oxidation with IBX and $NaBH_4$ gave 3,5-di-*O*-acyl piceatannol (**19**) in 42% yield. Removal of the two acyl groups was more tricky than expected. Indeed, catechols are not stable in basic conditions due to the high acidity of the *ortho* hydroxy groups and the tendency to form *o*-quinone derivatives, which can easily undergo polymerization processes, for example via aryloxy radical couplings (Yang et al. 2014). After several attempts (Table 3.2), following a procedure by Lang *et al* (Lang et al. 2008) for the deprotection of *di*-acetylated catechols, we obtained piceatannol in 81% yield. The procedure was based on the use of hydrazine monohydrate, whose reducing power avoided the potential formation of reactive *o*-quinones. Moreover, this approach did not require strong basic conditions.

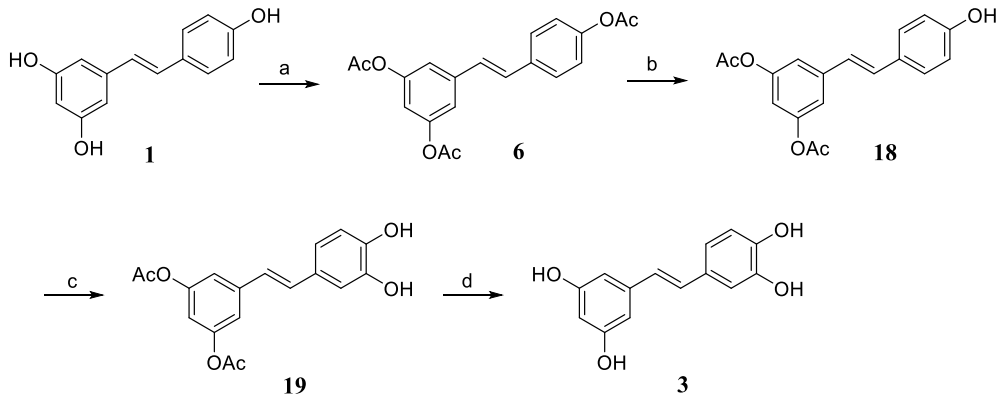

Scheme 3.2. a) Ac_2O, TEA, CH_2Cl_2, rt, overnight, 92% b) CAL-B, toluene/*n*-BuOH, 40°C, 6h, 81%; c) IBX, DMF, rt, 80 min, 42%; d) NH_2NH_2, MeOH, rt, 30 min, 81%.

*Table 1 Deacetylation conditions for intermediate **19***

Reaction conditions		Yield
K_2CO_3	H_2O 2:1 MeOH	NR
HCl 15%	EtOH	10%
NaOH	THF 1:1 H_2O	47%
NH_4OAc sol.25%	MeOH 7h	75%
NH_2NH_2 H_2O	MeOH 7h	81%

NR = No Reaction

Differently methylated monomers of resveratrol were also obtained. The use of K_2CO_3 and CH_3I (9 eq) at room temperature overnight provided permethylated resveratrol, whereas partial methylation of resveratrol with 2 eq of K_2CO_3 and CH_3I for 4h at reflux resulted in the formation of the monomethylated resveratrol derivatives **7** and **8**, and in an inseparable mixture of pterostilbene (**20**) and its regioisomer **9**.

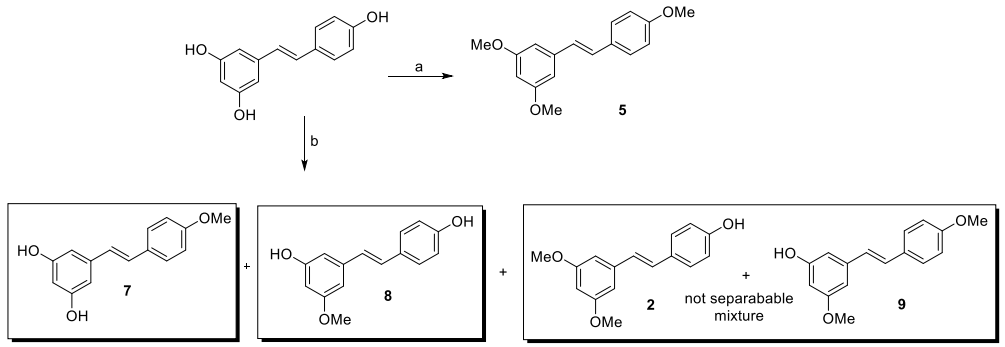

Scheme 3.3. a) K_2CO_3, CH_3I, acetone, rt, N_2, overnight, 81%; b) K_2CO_3, CH_3I, acetone, N_2, reflux, 4h, 16% of **8**, 12% of **7**, 35% **9+2**

Therefore, to obtain the pure regioisomer **9**, we applied the synthetic approach of Mattarei *et al*. (Mattarei et al. 2015). Resveratrol was protected as tri(*t*-butyldimethylsilyl)ether **20** in 95% yield, and then selectively deprotected at the *meta* and *para* positions by KF (1 eq) at - 15°C for 6h. The obtained derivative **21** was dimethylated and deprotected to afford compound **9** in 40% yield, over two steps.

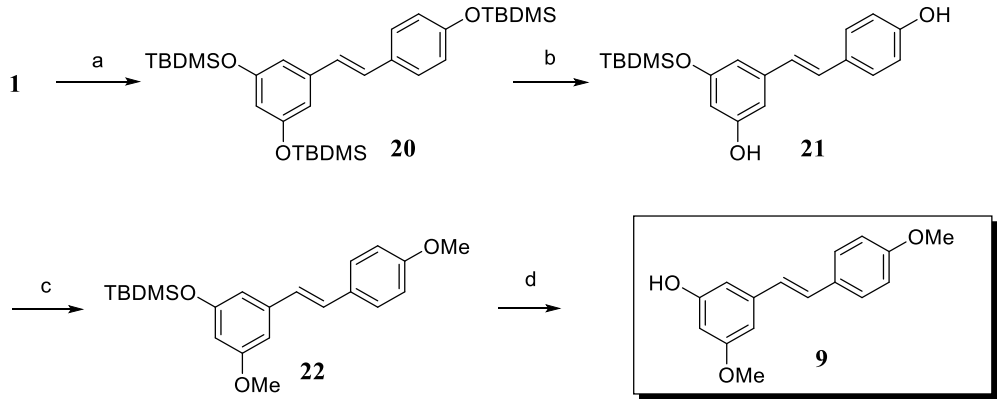

Scheme 3.4. a) TBDMSCl, DIPEA, DMF, -20°C to rt, N_2, overnight 95%; b) KF, -15°C, N_2, THF/MeOH 1:1, 6h; 56%; c) CH_3I, K_2CO_3, acetone, N_2, rt, 6h, 40%; d) KF, MeOH/THF 1:1, rt, N_2, overnight, 100%

We then focused on the synthesis of resveratrol dimers, which derive by oxidative radical couplings (see introduction). Performing biomimetic synthetic strategies, we were able to obtain the desired dimers **10 - 16** in substantial amounts (even on a gram scale) for their systematic biological evaluation.

Biomimetic syntheses aim at mimicking and reproducing reactions occurring in biological systems (De La Torre and Sierra 2003). This approach has been used to validate biosynthetic hypotheses and it represents an efficient strategy to obtain complex natural products (Keylor et al. 2015). In order to mimic the oxidative couplings of resveratrol, simple and biomimetic approaches rely on metal-oxidizing chemical reagents and enzymes to produce radical and carbocationic intermediates (Scheme 3.5) (Quideau et al. 2011; Velu et al. 2012; Keylor et al. 2015).

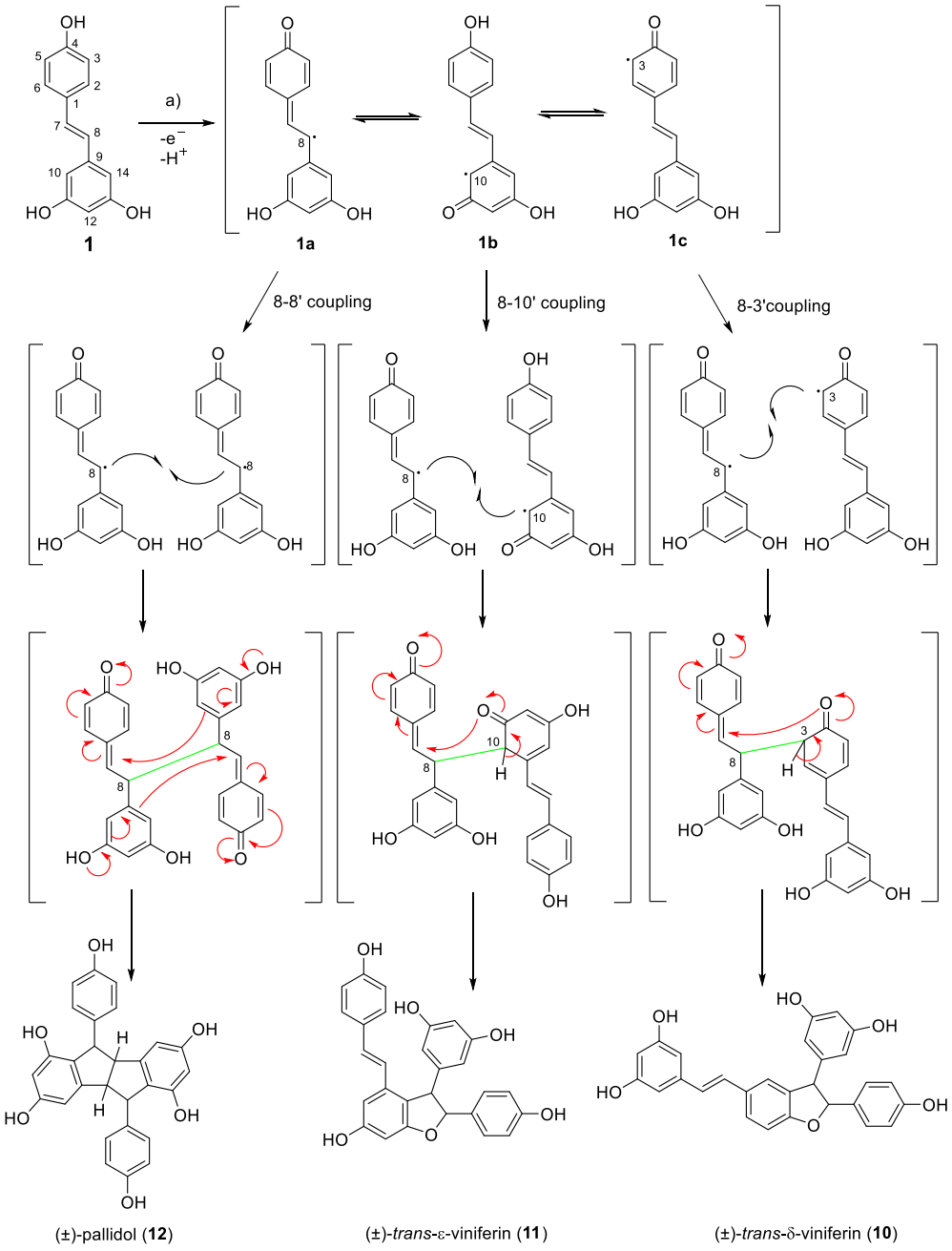

Scheme 3.5. *Proposed mechanism of resveratrol dimerization for the formation of dimers **10-12** (modified* (Velu et al. 2012)

Following the procedure of Li *et al.* (Li et al. 2012), treatment of resveratrol with horseradish peroxidase (HRP) (1 mg/mL solution) and H_2O_2 (30% solution) in a mixture of acetone/aqueous buffer 1:1 (v/v) provided *trans*-δ-viniferin (**10**) and pallidol (**12**). Noteworthy, enzymatic activity is highly dependent on the environmental pH (Vulfson et al. 2001). Indeed, the use of citrate buffer (pH 5) provided selectively *trans*-δ-viniferin in 49% yield, while the basic conditions with phosphate buffer (pH 8) led to the formation of pallidol as main product (21% yield), with minor amounts of *trans*-δ-viniferin (10%). On the other hand, *trans*-ε-viniferin (**11**) was obtained in 15% yield by treatment of resveratrol with the electron oxidant Fe^{3+} (as $FeCl_3 \cdot 6H_2O$) in a mixture MeOH/H_2O 1:1 (v/v) (Lindgren et al. 2016). Regardless of whether oxidation is enzymatic or metal-catalyzed (Li et al. 2012), the dimerization process starts from formation of a phenoxyl radical by loss of a proton and electron. Thanks to the high conjugation of the stilbenoid nucleus, the resulting radical species are stabilized in position 8 - radical quinone methide (**1a**) - or in position 3 and 10 - semiquinone radicals (**1b**-**1c**) (Scheme 3.9a). Subsequent radical coupling between **1a**+**1a** (8-8' coupling) **1a**+**1b** (8-10'coupling) and **1a**+**1c** (8-3' coupling) leads to the formation of very reactive *p*-quinone intermediates, which readily undergo intramolecular Friedel-Craft cyclization, giving respectively pallidol (**12**), *trans*-ε-viniferin (**11**) and *trans*-δ-viniferin (**10**) (Scheme 3.5).

Following the synthetic procedure developed by Beneventi *et al.* (Beneventi et al. 2015), the racemic structures of (±)-*trans*-ε-viniferin and (±)-*trans*-δ-viniferin were converted into the corresponding benzofuran derivatives **14** and **15**, respectively (Scheme 3.6). Intermediates **23** and **24** were smoothly obtained with Ac_2O and TEA in DCM from the corresponding viniferins. Their treatment with 2,3-dichloro-5,6-dicyano-1,4-benzoquinone (DDQ) (20 eq) at reflux for 48 hours resulted in their oxidative dehydrogenation, which was followed by deprotection of the hydroxy groups by KOH in MeOH at 0°C to give the natural *trans*-dehydro-ε-viniferin, known also as viniferifuran, and its

regioisomer *trans*-dehydro-δ-viniferin in 55% and 70% overall yield, respectively. Finally, pterostilbene was treated with HRP and H_2O_2 at pH 5 (citrate buffer) to afford pterostilbene-*trans*-dihydrodimer. The acetylation of its free phenolic moiety, followed by oxidative dehydrogenation with DDQ and final deprotection, afforded the corresponding benzofuran (Scheme 3.6).

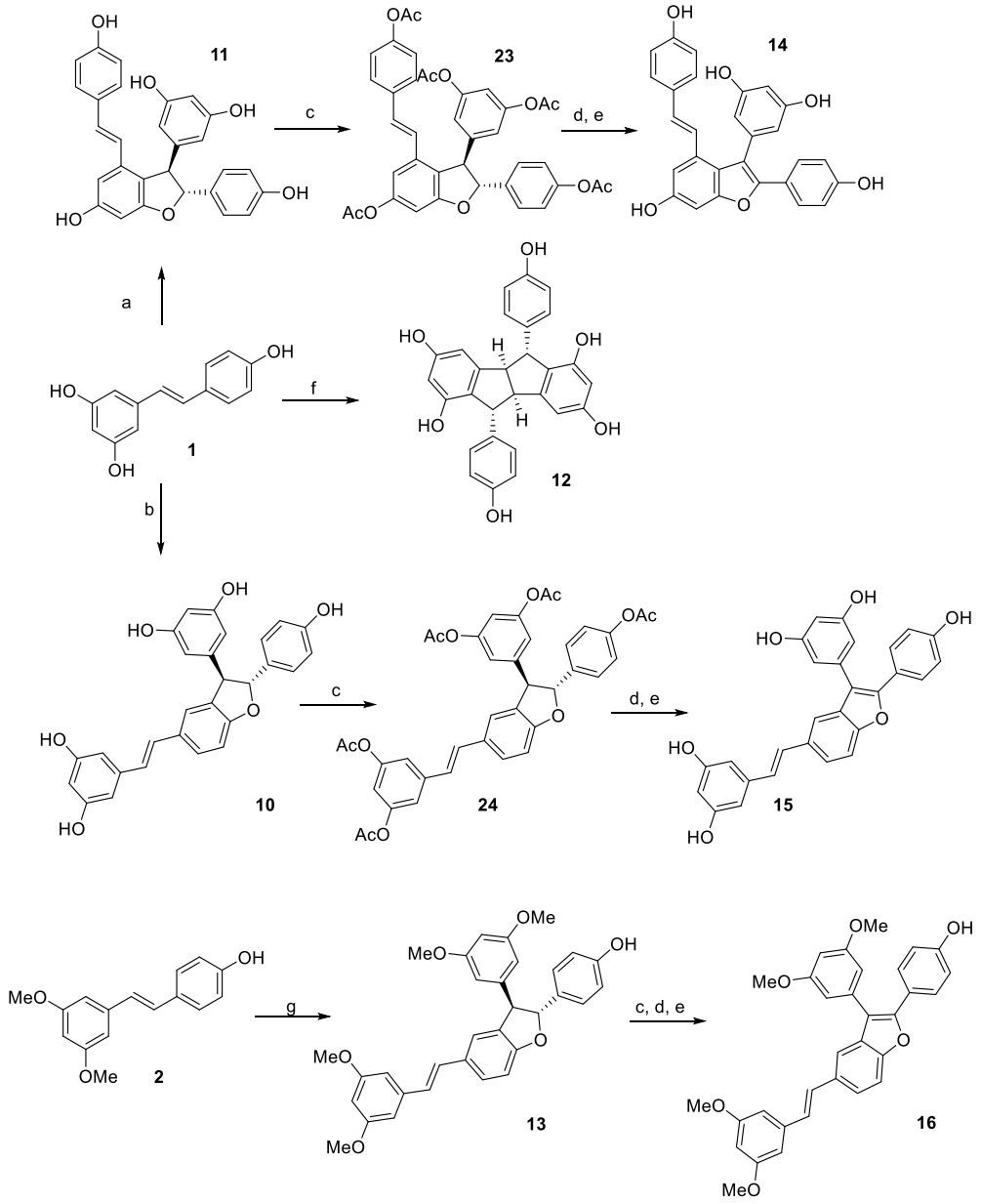

Scheme 3.6. a) $FeCl_3 \cdot 6H_2O$, MeOH/H_2O 1:1, 15%; b) i) HRP, 30 min, 40°C, acetone: citrate buffer pH 5 1:1; ii) H_2O_2, 90 min, 40°C, overall yield 49%; c) Ac_2O, TEA, DCM, rt, overnight, 90-92%; d) DDQ, DCM, reflux, 48h, 60-84%; e) KOH, MeOH, 1h, 0°C, 55-70%; f) 1) HRP, 30 min, 40°C, acetone/ phosphate buffer pH 8 1:1; 21%; 2) H_2O_2, 90 min, 40°C overall yield 21%; g) i)HRP, 30 min, 40°C, acetone/citrate buffer pH 5 1:1; ii) H_2O_2, 15 min, 40°C, 60%

Eventually, the enantiomers of both (±)-*trans*-δ-viniferin (**10**) and (±)-*trans*-ε-viniferin (**11**) were separated by preparative chiral HPLC (Figure 3.2 and 3.3).

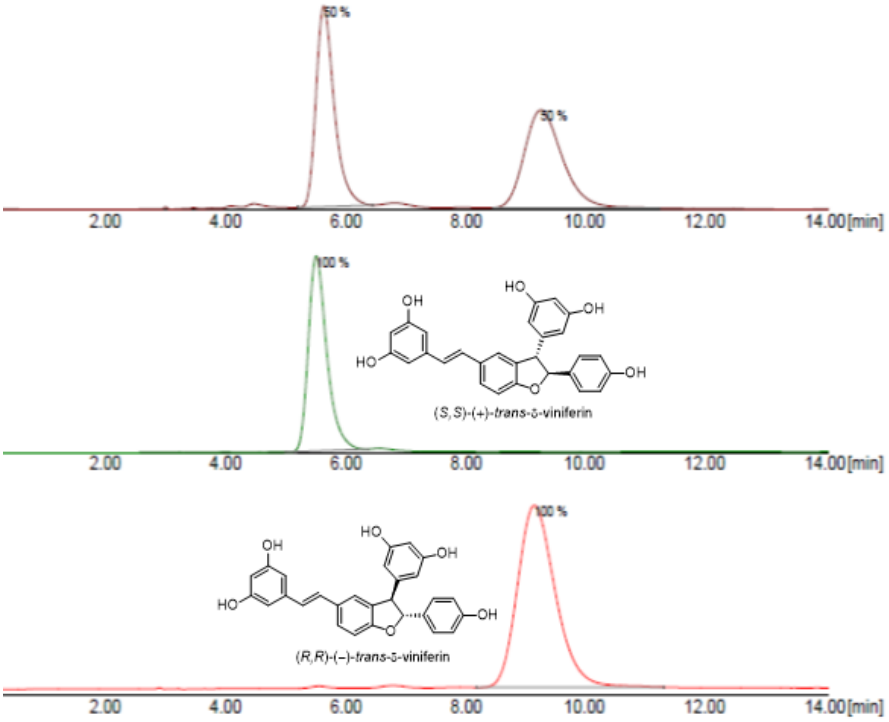

Figure 3.2. *Chromatogram of the separation of two enantiomers of (±)-trans-δ-viniferin (**12**)*

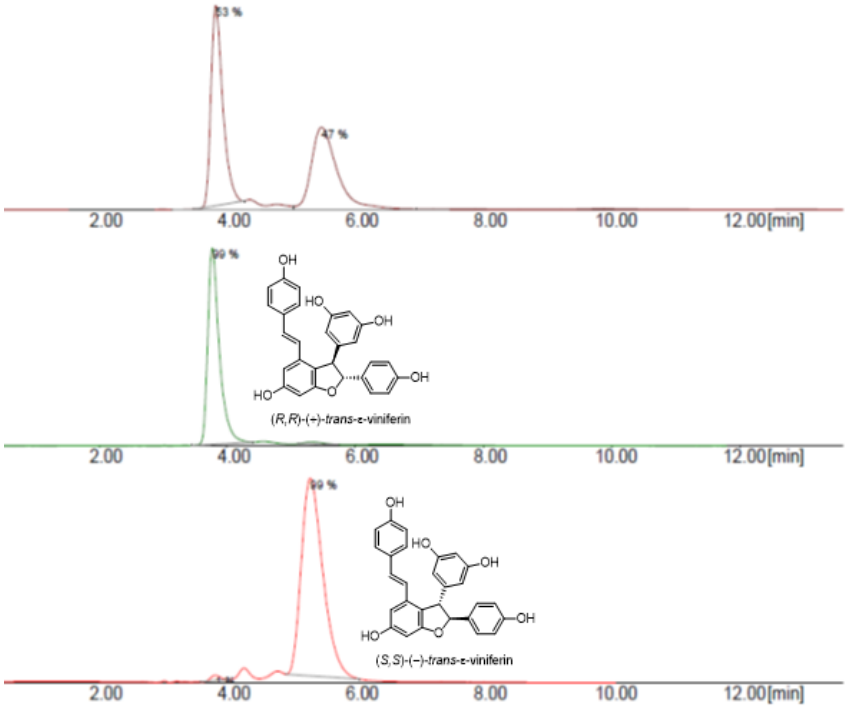

Figure 3.3 *Chromatogram of the separation of two enantiomers of (±)-trans-ε-viniferin (**11**)*

3.1.2. Inhibition of pancreatic α-amylase

3.1.2.1. Introduction

Diabetes mellitus (DM) represents a group of metabolic disorders characterized by high blood glucose levels derived from an inadequate pancreatic insulin secretion (Katzung 2018, chaps. 41-Pancreatic hormones and antidiabetic drugs). There are different classes of drugs to control blood glucose levels: 1) hypoglycaemic drugs acting on liver, muscle and adipose tissues (biguanides and thiazolidinediones); 2) insulin secretagogues, which stimulate insulin secretion by binding the sulfonylurea receptor (sulfonylureas, meglitinides, D-phenylalanine derivatives); 3) molecules mimicking or prolonging the effect of incretins, gut hormones that amplify the glucose-induced insulin secretion (GLP-1 receptor agonists or dipeptidyl peptidase [DPP-4] inhibitors); 4) agents inhibiting the glucose reabsorption system in the

kindey; 5) inhibitors of enzymes involved in the cleavage of polysaccharides to obtain simple sugars and in their absorption (Katzung 2018, chaps. 41-Pancreatic hormones and antidiabetic drugs).

Pancreatic α-amylase is an endo-hydrolase catalyzing the cleavage of 1,4-glucosidic bonds in starch, glycogen, maltodextrins and maltooligosaccharides. Then, the simpler sugars deriving from the activity of the pancreatic α-amylase are converted into glucose for intestinal absorption by other enzymes, like the brush border α-glucosidase. Therefore, α-amylase is a suitable target in type 2 diabetes treatment, since its inhibition results in low bioavailability of oligosaccharides and absorbable sugars, and consequently, in low postprandial hyperglycaemia (Tundis et al. 2010). α-Amylase inhibitors, such as acarbose and voglibose, cause competitive and reversible inhibition of the enzyme, but their use is associated with gastrointestinal side effects, such as diarrhoea, flatulence and abdominal pain (Fujisawa et al. 2005).

Polyphenols have been shown to manage and prevent type 2 diabetes by directly modulating key enzymes of glucose and lipid metabolism (Cao et al. 2019). In this wide class of molecules, stilbenoids have attracted the interest of scientists (Akinwumi et al. 2018) and resveratrol, the most studied stilbenoid, was demonstrated to exert antidiabetic effects through multiple mechanisms resulting in a significant therapeutic effect in the whole organism (Oyenihi et al. 2016)(Öztürk et al. 2017; Cao et al. 2019).

However, the broad spectrum of bioactivities and the different potencies attributed to resveratrol may be partially, or even mainly, due to its products of oxidation, including the naturally-occurring dimeric and more complex stilbenoids, which can elicit specific effects of their original precursor. Moreover, “in vivo” the biological environment may further favour oxidation and dimerization processes of the monomeric resveratrol, leading to resveratrol oligomers.

Therefore, we decided to test resveratrol and its natural monomeric and dimeric derivatives as inhibitors of the pancreatic α-amylase, key enzyme in the glucose metabolism. In order to perform a systematic study of the mechanistic and molecular characteristics involved in these specific interactions, the compounds were tested as single molecules. This approach allowed to identify the molecular features relevant to the activity, but also to avoid the possible effects of competition among different chemical species present in the natural extracts, usually used as model of study. Moreover, the possibility to assay pure compounds as single chemical entities allowed the investigation at known concentrations of possible synergies among the individual species under investigation, as well as synergies of combinations with synthetic drugs.

3.1.2.2. Material and methods

Enzymatic Inhibition

Porcine pancreatic α-amylase [EC 3.2.1.1] was from Sigma-Aldrich (Milan, Italy). Activity was monitored by using the K-AMYLSD kit from Megazyme (Bray, Ireland), with modifications. An aliquot of α-amylase (0.03 mL, 0.1 μM in 50 mM phosphate buffer, pH 6.8) was added to 0.120 mL of 50 mM phosphate buffer, pH 6.8, in a microtiter plate well. The investigated compounds where then added as methanolic solutions (0.03 mL) of appropriate concentration. The reaction was started by adding 0.02 mL of the substrate solution provided with the kit, resulting in a final concentration of 0.4 μM substrate. The kit-provided substrate solution also contained an excess of thermostable bacterial α-glucosidase that is required for the release of the *p*-nitrophenolate anion from the *p*-nitrophenyl glucosides produced by the activity of α-amylase on the chemically modified maltoheptaoside. At appropriate times, the reaction was stopped by adding 0.1 mL of 0.2 M Na_2CO_3, and the absorbance was read in a microplate reader set at 405 nm. Blanks were prepared in the absence of the pancreatic α-amylase. Controls were otherwise complete reaction mixtures, containing 15% MeOH (v/v), but

no bioactive species. Acarbose (from a stock solution in methanol) was used as the reference inhibitor. A minimum of three independent replications was carried out for each assay.

Computational Procedures

All the computational procedures were carried out with a Schrödinger Maestro BioLuminate v. 2019-01 (http://schrodinger.com) with the OPLS3e force field, as previously described (Guidi et al. 2018). The crystallographic structure of the pig pancreatic alpha amylase was downloaded from RCSB PDB (id: 1HX0) and was checked, fixed, and relaxed through the Protein Preparation Wizard. The *trans*-viniferin species and enantiomeric form database was sketched and prepared with the LigPrep, carefully checking the stereocenters. Molecular docking was carried out through the Glide Ligand Docking with a standard precision (SP) according to a well-established protocol (Omo et al. 2019). The active site was identified through the Site Map tool and confirmed according to the annotations of the UniProt pig pancreatic alpha amylase entry (AMYP_PIG). The prime MM-GBSA was run in order to estimate the binding energy of the (*S*, *S*)-*trans*-δ-viniferin to the active site of the pig pancreatic alpha amylase in the presence and absence of (*R*, *R*)-*trans*-δ-viniferin.

Statistical Analysis

The analysis of variance on the enzymatic inhibition data was performed adopting the least significant difference (LSD). Data were processed by using the Statgraphics XV, version 15.1.02 (StatPoint, Warrenton, VA, USA). The appropriate non-linear regression routines in SigmaPlot (rev. 10, Jandel Scientific, San Rafael, CA, USA) were used for graphical and numerical analysis of the inhibition data.

3.1.2.3. Discussion and results

A series of representative natural monomers and dimers (Figure 3.4), obtained as described in the previous section (3.1.1), were tested as inhibitors of α-amylase, using acarbose as reference drug.

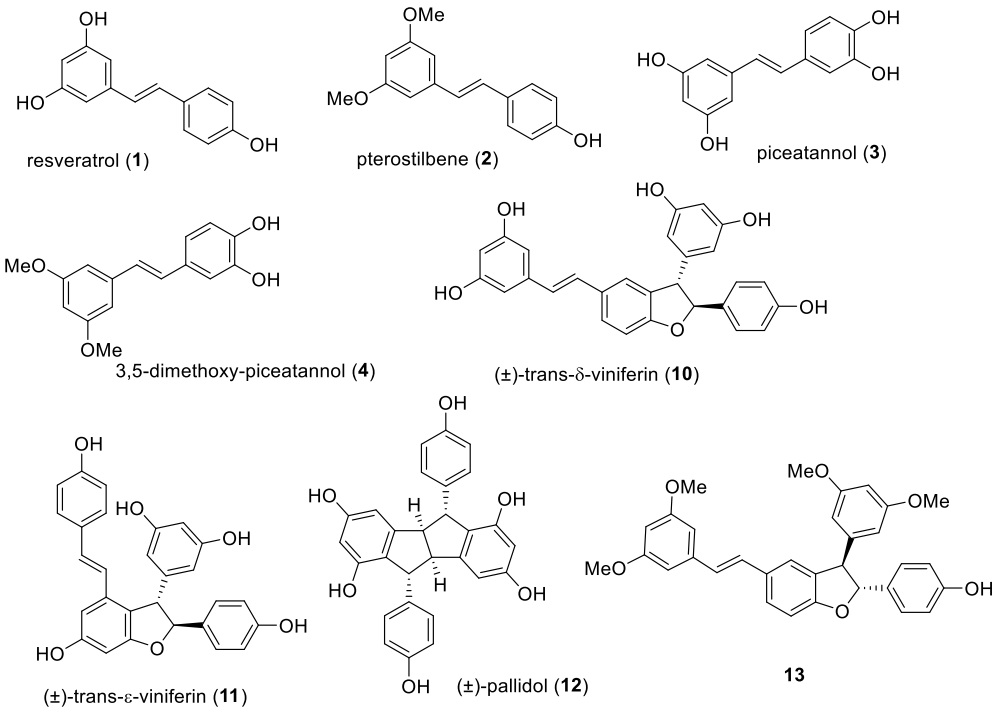

Figure 3.4. *Structures of stilbenoids tested on pancreatic α-amylase*

The assay for the evaluation of the enzymatic inhibition consisted in a two-step procedure. In a first step, α-amylase cleaved a modified *p*-nitrophenyl-α-D-maltoheptaoside, releasing products that might be substrates of an excess of α-glucosidase present in the assay mixture. The release of *p*-nitrophenolate was quantified by spectrophotometry to calculate the percentage of inhibition of the enzyme. The data obtained were compared with control runs (all including 15% MeOH, since MeOH was used as solvent for the stock solutions of compounds tested). None of the compounds investigated showed relevant inhibitory activity on α-glucosidase, at the concentrations used in the assay.

A preliminary screening (Figure 3.5) showed that the four monomers and pallidol, at a 10 mM final concentration, exerted a modest inhibitory activity (21-45%) on pancreatic α-amylase, compared to the reference drug acarbose (86% inhibition, at a 1 mM final concentration). On the contrary, the racemic dimers (±)-*trans*-δ-viniferin (5) and (±)-*trans*-ε-viniferin showed an inhibitory capacity of about ~ 90%, comparable with that observed with a 1 mM acarbose. Noteworthy, pterostilbene and its dimer **8** reduced the enzyme activity of only 21% and 28% respectively, highlighting the importance of free hydroxy groups in the interaction with the enzyme.

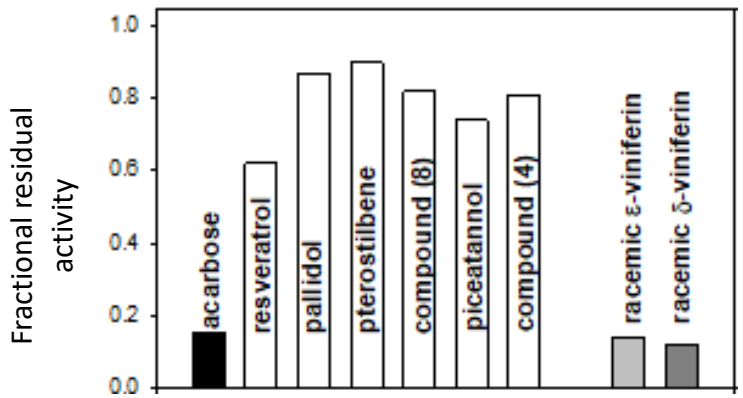

Figure 3.5. *Inhibition of the pancreatic α-amylase by the various compounds presented in Figure 3.4, each at 10 mM final concentration. The effect of a 1 mM acarbose is shown for comparison.*

From the results showed in Figure 3.5, it was evident that the racemic (±)-*trans*-δ-viniferin (**10**) and (±)-*trans*-ε-viniferin (**11**) were the most potent inhibitors of the pancreatic α-amylase. This finding prompted us to investigate whether the activity of the racemic viniferins was correlated with their geometrical features.

Therefore, we evaluated the activity of the pure enantiomers of (±)-*trans*-δ-viniferin (**10**) and (±)-*trans*-ε-viniferin (**11**), comparing it with that of the racemic forms, at a 1 mM concentration. A 1 mM acarbose was used again as reference drug. Figure 3.6 shows that the pure enantiomers with the (*R*, *R*) absolute configuration were more active than the corresponding (*S*, *S*)

enantiomers, revealing that the spatial orientation of substituents on the 2,3-dihydrobenzofuran ring could play a key role in the interaction with the enzyme.

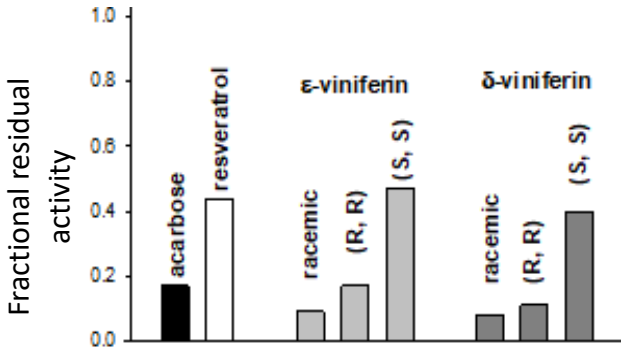

Figure 3.6. *Residual enzyme activity in the presence of viniferin isomers, of their purified enantiomeric forms, and of their racemic forms. Final concentration of each inhibitor species (including acarbose and resveratrol) was 1 mM.*

Surprisingly, the racemic forms of both viniferins were more potent inhibitors than their respective pure enantiomers, at the same concentration. To explain this finding, the compounds were tested at different concentrations ranging from 0 to 0.1 mM (Figure 3.7) for inhibition studies. In these experiments, purified enantiomers were compared with their equimolar mixtures in order to avoid errors due to the presence of impuritites that could have been part of the original racemic forms, simulating the simultaneous presence of the racemic forms of each viniferin. The comparative analysis showed in Figure 3.7 highlights the higher inhibition of *trans*-δ-viniferin compared with that of *trans*-ε-viniferin, and shows the different ability of the pure enantiomers and their equimolar racemic forms in the inhibitory activity of α-amylase. These experiments confirmed the higher inhibitory efficacy of the “simulated” racemic forms with respect to their respective pure enantiomers, at equivalent total concentrations.

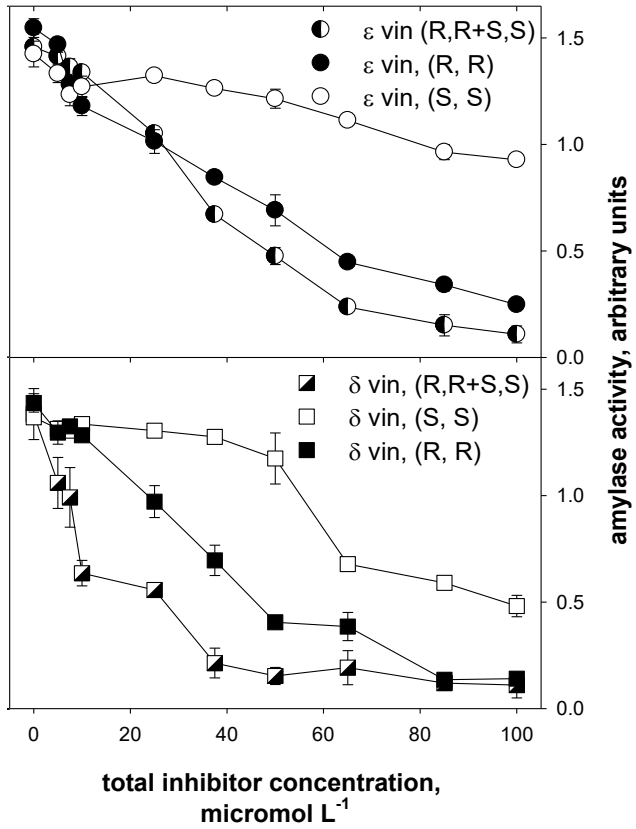

Figure 3.7. *Concentration dependence of the α-amylase inhibition by purified enantiomeric forms of trans-δ-viniferin and trans-ε-viniferin, and by equimolar mixtures of their purified enantiomers simulating the presence of a racemic form of each species.*

The higher efficacy of the enantiomeric mixtures was particularly significant for *trans*-δ-viniferin, suggesting that the two enantiomers could bind the target protein on multiple and non-equivalent sites. Figure 3.8 reports the analysis of inhibitory binding of *trans*-δ-viniferin (**10**) through the Hill equation, showing a facilitated binding of the (*S*, *S*) enantiomer at high concentrations. The markedly sigmoidal shape of the curve observed for the binding of the (*S*, *S*) enantiomer was characterized by a Hill cooperativity coefficient (n^H) of ~ 4 and a relatively high average value of K_i^{app} (58 μM). Conversely, n^H values of (*R*, *R*) enantiomers were close to 1 (n^H = 1.5, K_i^{app} = 43 μM), whereas the equimolar racemic mixtures showed n^H and K_i^{app} values of 1.2 and 12 μM, respectively.

Confirming the presence of different biding sites for the enantiomeric forms of *trans*-δ-viniferin, these cooperative effects suggested that the occupation of a binding site could facilitate a further binding of other binding sites on the target protein, not necessarily close to regions involved in inhibitory effects. This finding could explain the higher inhibitory efficacy of the racemic mixtures with respect to pure enantiomers. We postulated a synergic behaviour of enantiomers, implying that sequential binding of a “low affinity” enantiomer to the enzyme bound on the active site by the “high affinity” enantiomer could lead to a strong reduction of the apparent dissociation constant (K_i^{app}) of the high-affinity enantiomer, consequently increasing its inhibitory activity. In other words, when both enantiomers bind the target enzyme, one of them remains locked into the α-amylase active site with increased inhibitory ability.

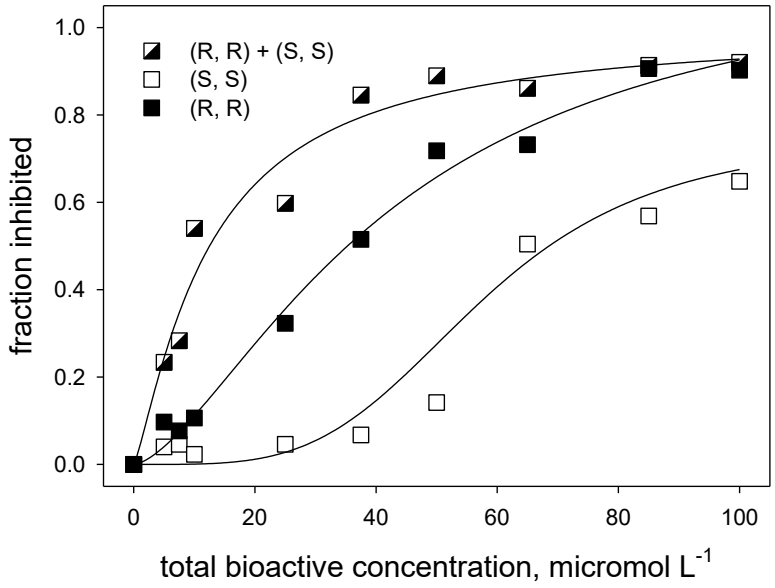

Figure 3.8. *Hill plot for the inhibition of α-amylase by different enantiomeric forms of trans-δ-viniferin* ***10****. Lines are the best fit to experimental data, obtained by using a 3-parameters Hill equation (y=a*x^n^H^/([K~i~]^n^H^+x^n^H^).*

Molecular docking studies were carried out to support our interpretation of the data obtained from the enzymatic assays. In Figure 3.9, the top-scoring

binding pose for each enantiomeric species of both *trans*-δ-viniferin **10** and *trans*-ε-viniferin **11** in the α-amylase active site are reported, whereas Figure 3.10 shows the detailed molecular interactions of each chemical species with the aminoacids of the enzyme. As reported in Table 3.2, the binding free energy values derived from the molecular docking confirmed that the all the chemical species can be accomodated in the α-amylase binding site, even if with different affinities. In particular, the docking scores are consistent with the efficacy of individual species determined in the enzymatic assays reported above.

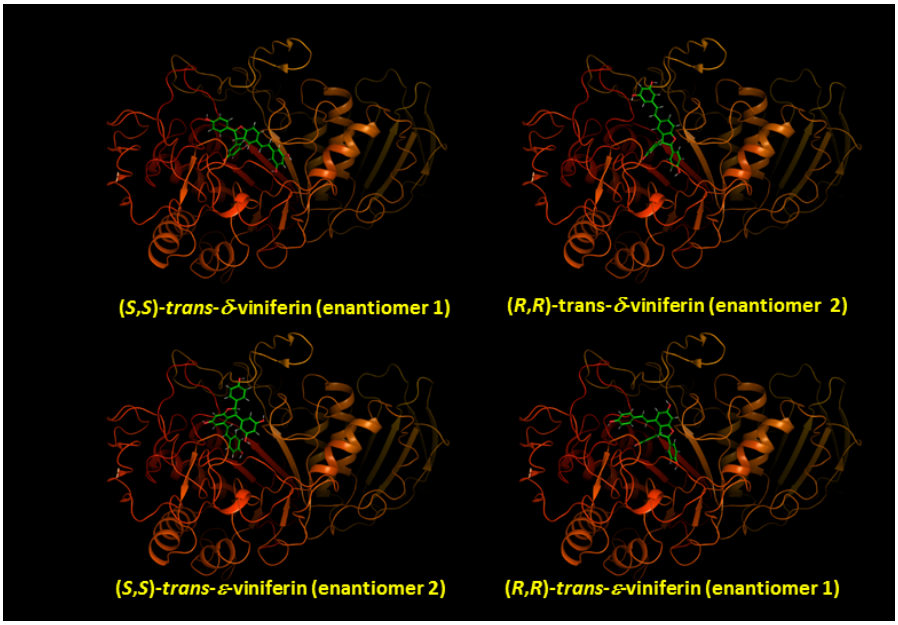

Figure 3.9. *Top-scoring binding poses between the pig pancreatic α-amylase and the enantiomeric forms of the trans-viniferin species in the protein active site: A, (S, S)-trans-δ-viniferin; B, (R, R)-trans-δ-viniferin;C), (S, S)-trans-ε-viniferin; D, (R, R)-trans-ε-viniferin.*

Docking studies (Figure 3.9 and 3.10 and Table 3.2) revealed the importance of the hydroxy groups in the interaction with the target, explaining the inactivity of the derivatives with methoxy groups in place of free phenolic functions, both

in the enzymatic assays and in the virtual screening, even at concentrations orders of magnitude higher than those of viniferins.

However, not all polyphenols resulted to be active with the same potency, since every compound endowed with high inhibitory efficacy was found to interact with specific different aminoacids of the protein, as shown in Figure 3.10. Indeed, as expected by their different overall geometry, the two viniferins isomers demonstrated different specific interactors with a different nature of the interactions. More interestingly, also the enantiomers of each *trans*-viniferin were found to have a completely different set of amino acid residues of the enzyme as interactors for structurally similar portions of the molecule, as a result of the different spatial arrangement of the phenolic rings at their stereogenic centers.

Overall, the most efficient inhibitors are shown in Figure 3.9 and Figure 3.10 to have a specific binding mode. Considering the computational data highlighting the specificity of the binding, and the efficacy of each stilbenoid in the enzymatic assay, it seemed that the most potent inhibitors of this study (with K_i^{app} values ranging from 10 to 20 μM) did not just behave as "hydrophobic plugs", having limited access to the active site of the enzyme.

On the other hand, computational data showed also that α-amylase can accommodate compounds with significantly different geometrical features. In binding the arrangements proposed here, the active site showed an interior pocket, close both to the active site and to the surface of the protein, able to accommodate large and hydrophilic species, such as the bulky substituted phenols on the 2,3-dihydrobenzofuran ring of the viniferins.

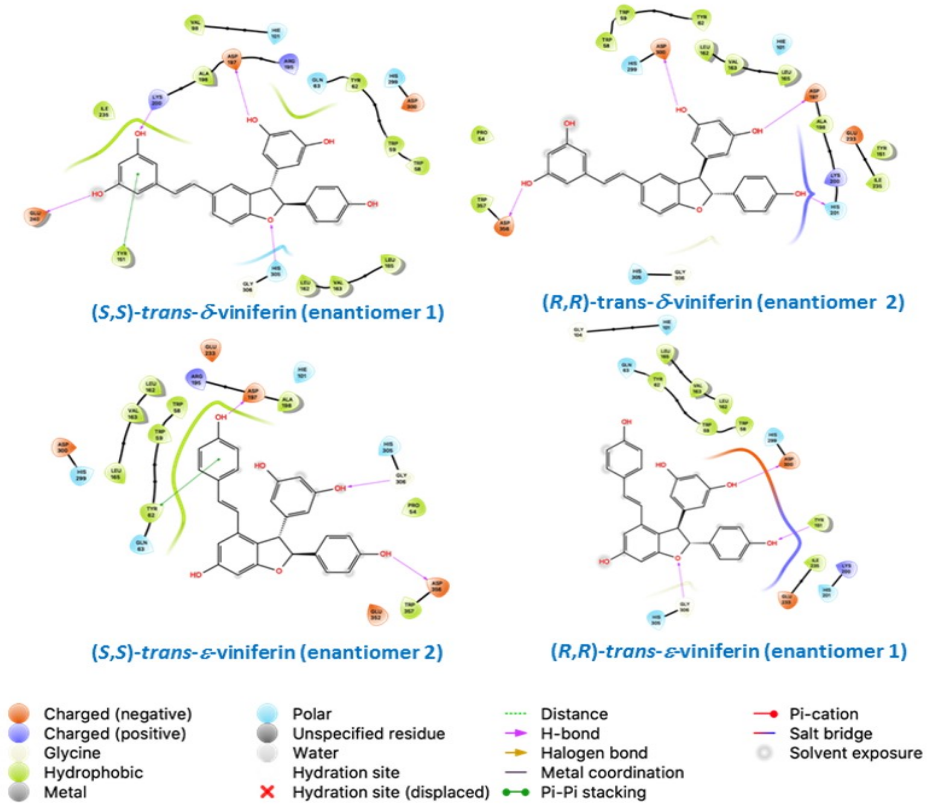

Figure 3.10. *Ligand interaction diagram for the molecular docking top-scoring complexes between the pig pancreatic α-amylase and various enantiomeric forms for the trans-viniferins isomers in the protein active site. Interactions are recapitulated in the figure legend.*

Table 3.2 Docking score of top scoring complexes between pig pancreatic α-amylase and various resveratrol-derived compounds.

Absolute configuration	Compound ID	Docking score (kcal/mol)
(*S*,*S*)-(+)	**10**	-8.144
(*S*,*S*)-(–)	**11**	-7.341
(*R*,*R*)-(–)	**10**	-6.908
(*R*,*R*)-(–)	**13**	-6.849
-	**4**	-6.427
-	**3**	-6.312
-	**1**	-6.041
(*S*,*S*)-(+)	**13**	-5.934
(*R*,*R*)-(+)	**11**	-5.851

Molecular modelling was also carried out to rationalize the “racemic effect” discussed with the results obtained by the inhibition studies. The modelling approach took into consideration the minimum energy mode of simultaneous

binding of different enantiomers of *trans*-δ-viniferin to the pancreatic α-amylase. In the model obtained (Figure 3.11), (*S*, *S*)-*trans*-δ-viniferin resulted to have higher affinity for the enzymatic active site. The (*R*, *R*)-enantiomer binding to a more external binding site, enhancing the stability of the complex of the enzyme with (*S*, *S*)-*trans*-δ-viniferin, has been demonstrated to be thermodynamically feasible. Therefore, the different enantiomers can bind simultaneously the enzyme in different sites, causing an overall increase of the inhibitory activity.

The changes in the inhibitory capacity experimentally observed (Figure 3.7) and analyzed in terms of cooperativity through the Hill plot (Figure 3.8) were in agreement with the molecular docking calculations, followed by MM, showing the change in the binding free energy calculated through the MM-GBSA approach (namely, -66.54 kcal/mol for (*S*, *S*)-*trans*-δ-viniferin in the binding site with externally bound (*R*, *R*)-*trans*-δ-viniferin versus -44.58 kcal/mol for (*S*, *S*)-trans-δ-viniferin in the active site by itself; corresponding to a ΔΔG of 21.96 kcal/mol).

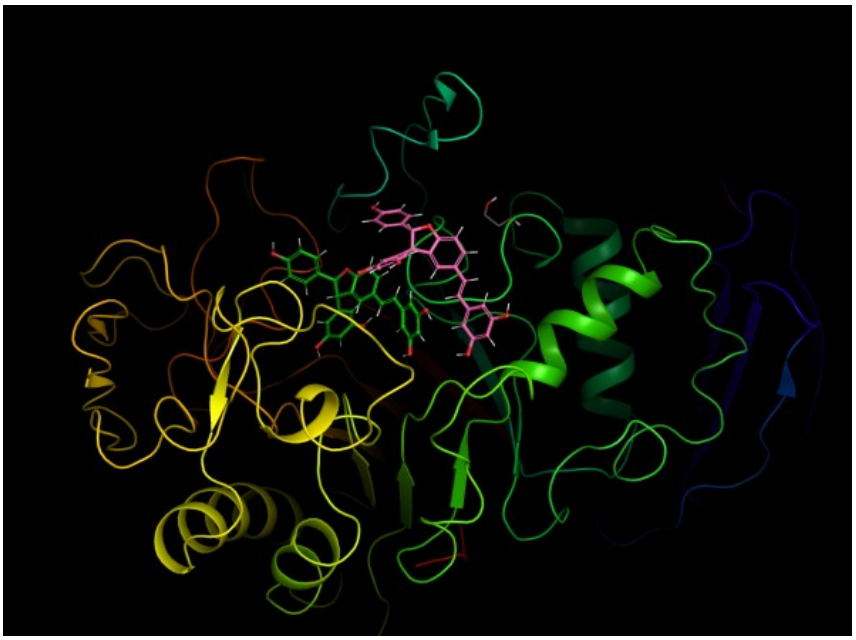

Figure 3.11. *Top scoring pose of (R, R)-trans-δ-viniferin to the pig pancreatic alpha amylase with (S, S)-trans-δ-viniferin already bound to its active site*

In conclusion, some dimeric stilbenoids, in particular the naturally occurring *trans*-δ-viniferin and *trans*-ε-viniferin, may be more efficacious than the reference drug acarbose in the inhibition of the pancreatic α-amylase (Figure 3.6). The geometric features of each viniferin affected their affinity with the enzyme and consequently their efficacy. These results were very exciting, in particular if we take into account the fact that intestinal concentrations of dimers could be higher than expected for a given food based only on their composition. Regarding this observation, it is worth reminding that dimeric stilbenoids can derive from simple metabolic transformations of their monomeric precursors, usually found in higher amounts than oligomers in common foods and beverages. Noteworthy, viniferins have been reported to account for up to 20% of the total content of stilbenoids in wine (Vitrac et al. 2005). However, despite of the availability of extraction procedures for the selective recovery of viniferins from food byproducts, usually viniferins are

recovered as complex mixtures of isomers (Navarro et al. 2018; Kosović et al. 2020).

Surprisingly, the racemic mixtures of both *trans*-δ-viniferin and *trans*-ε-viniferin were found to have higher inhibitory activity than their respective pure enantiomers. This finding was rationalized by molecular docking studies, which provided thermodynamics-based evidence for the different activity of the compounds tested in this work, as well as mechanistic explanation for the synergistic behaviour of the racemic mixtures of the *trans*-viniferins. To the best of our knowledge, this is the first time that chemically pure species were used to analyse in details the geometric and structural features involved in synergistic effects that have been observed in several reported protein-phenolics interactions (Akkarachiyasit et al. 2010; Parizad et al. 2019).

3.1.3. Evaluation of antimicrobial activity

3.1.3.1. Introduction

Foodborne diseases caused by pathogenic microorganisms, such as *Listeria monocytogenes*, *Salmonella enterica*, *Staphylococcus aureus*, which can easily contaminate food and drinks, represent a global health concern (Ma et al. 2018). More severe and less responsive to treatments infections are dramatically spreading because of drug resistance, a natural phenomenon greatly accelerated by overuse and misuse of antibiotics. Stilbenoids, expressed by plants in response to pathogens invasion and stress factors, represent a promising class of potential antimicrobials (Akinwumi et al. 2018). Besides many studies on resveratrol, its poor bioavailability and the resulting difficulty to understand the mechanism of action moved the attention to resveratrol-derived compounds, which can derive from its metabolism in humans and in nature and so be the actual responsible for the activity attributed to resveratrol (Keylor et al. 2015).

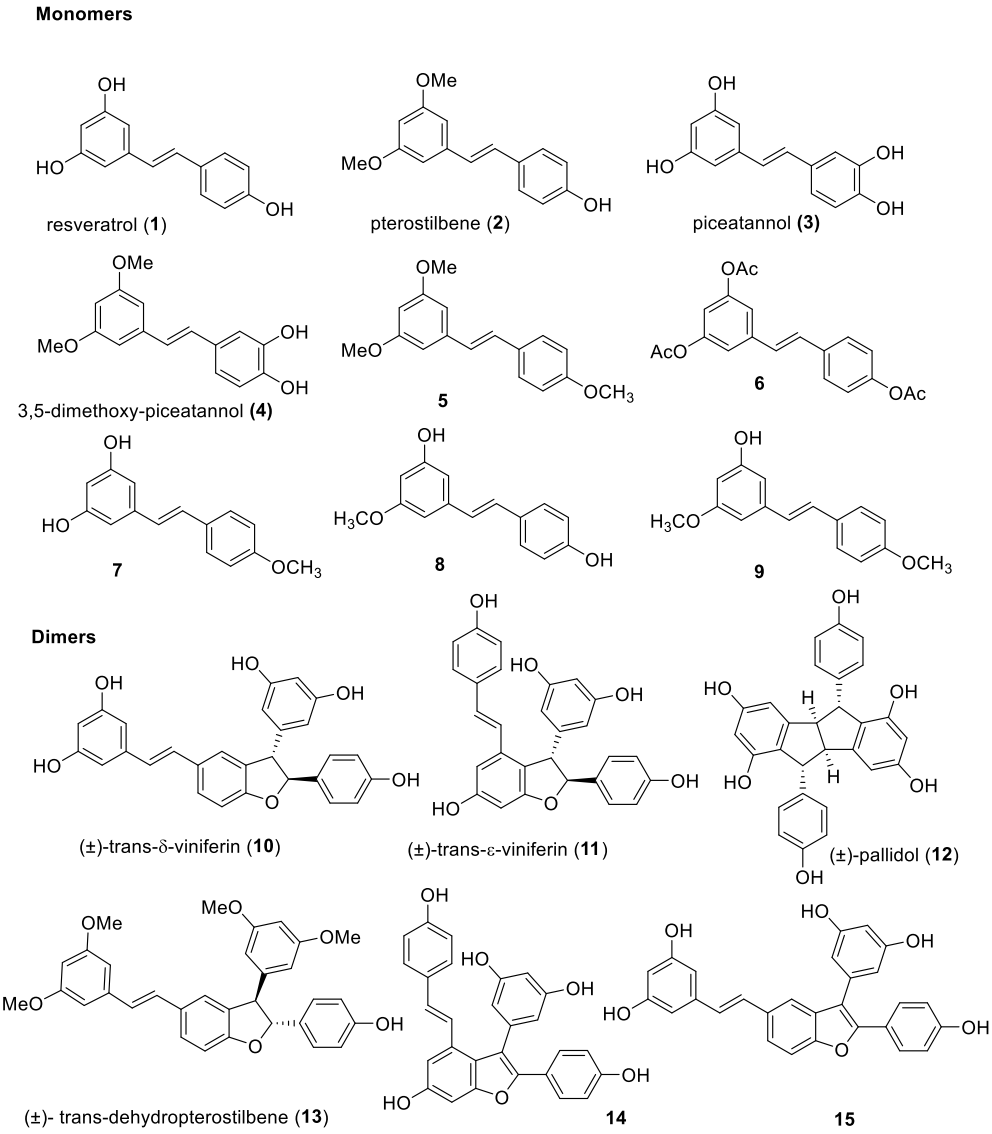

Figure 3.12. *Stilbenoids tested as antimicrobials*

3.1.3.2. Material and methods

Evaluation of the minimal concentration (MIC) and minimal bactericidal concentration (MBC) of polyphenols against gram-positive and gram-negative bacteria.

The molecules were tested on the gram-positive bacteria *Listeria monocytogenes* Scott A, *Staphylococcus aureus* ATCC 25923, *Enterococcus*

faecium DSM 20477, *Enterococcus faecalis* DSM 20478, and *Bacillus cereus* DSM 9378, and on the gram-negative bacteria *Pseudomonas aeruginosa* ATCC 27853, *Escherichia coli* DSM 682, *E. coli* DSM 8579, *Salmonella enterica* DSM 9386, and *Proteus hauseri* DSM 30118. The antibacterial activity was determined using the standard microdilution method for drug susceptibility testing (Diseases 2003). The strains were cultivated aerobically in tryptic soy broth (TSB, Sigma Aldrich, Italy) for 24 h at 30–37 °C, except *E. faecium* DSM 20477 and *E. faecalis* DSM 20478, which were cultivated in microaerophilic conditions for 24 h at 30 °C. The test was carried out in 96-well plates in a final volume of 200 µl in the presence of 10 increasing concentrations of each antimicrobial, ranging from 1 up to 512 µg/ml. The molecules were resuspended in dimethyl sulfoxide (DMSO, Sigma Aldrich, Italy) at a concentration of 4.096 mg/mL and then diluted 1:2 in sterile broth. The inoculum was prepared by diluting the cell suspension from an overnight culture in sterile TSB to obtain a turbidity equivalent to the McFarland 0.5 standard. Then, plates were incubated for 24 h at 30–37 °C. All plates included at least one well as a positive growth control (TSB with and without DMSO 12.5% v/v and the inoculum) and a negative growth control (TSB without inoculum), to exclude any microbial contamination. Chlorhexidine was used as reference biocide for its broad spectrum of activity against Gram positive and Gram negative bacteria and its known ability to disrupt the bacterial cell membrane. The MIC is the lowest concentration of the antimicrobial that completely inhibits growth. In addition, we determined the MBC for each molecule tested. After shaking the 96-well plate to resuspend the cell pellet, MBC determination was performed by subculturing 10 µL from each well where no visible microbial growth occurred. After 48 h of incubation, the antimicrobial dilutions yielding three colonies or less were scored as the MBC for the starting inocula of 105 CFU/mL. The experiments were performed in triplicate. The MIC and MBC experiments were performed according to the CLSI (Clinical and Laboratory Standards Institute) methods for dilution

antimicrobial susceptibility tests for aerobic bacteria (approved standard, Wayne, PA, USA: CLSI; 2009).

Measurement of cFSE fluorescence cell leakage

To evaluate whether membrane damage was due to cell leakage of intracellular components, microbial cells from an overnight culture were washed and diluted in sterile filtered (0.22 µm) phosphate-buffered saline (PBS) (NaCl 8 g/L; KCl 0.2 g/L; Na_2HPO_4 1.44 g/L; KH_2PO_4 0.24 g/L; pH 7.4) to a final concentration of 3 × 109 cells per mL. The cell suspension was supplemented with 4 µM cFDASE (Sigma-Aldrich), which is a precursor molecule of cFSE (Arioli et al. 2010). Then, the cell suspension was exposed to each compound (100 µg/mL) or to chlorhexidine (100 µg/mL) (Sigma-Aldrich) at 30–37 °C (according to the optimum temperature of growth). As a control, the cFSE-labeled cell suspension was also exposed to a volume of DMSO equal to that used for all tested molecules. After 30 min of incubation, 1 mL of sample was used to measure cFSE fluorescence cell leakage. The sample was centrifuged (13000 rpm, 2 min), and the cell-free supernatant was transferred to a 96-microtiter plate for the measurement of cFSE fluorescence in a Victor 3 fluo- rometer (PerkinElmer) (Arioli et al. 2010; Kaduskar et al. 2017)32,33. The fluorescence data were calculated as the average of three independent assays and expressed as arbitrary units of fluorescence ± standard deviation (SD).

Flow cytometry to assess the viability and membrane potential of *L. monocytogenes* ScottA after exposure to compound **15** and chlorhexidine

A cell suspension in PBS (3 × 109 cells per mL) from an overnight culture of *L. monocytogenes* ScottA was exposed to 10 or 100 µg/mL of compound **15** or chlorhexidine for 30 min at 37 °C. As a control, we maintained cells in PBS with or without 2.4% DMSO (v/v) to simulate the same amount of DMSO used when the cells were treated with antimicrobials. Then, the viability of the cells was evaluated by flow cytometry with double staining with 20 µM SYTO™ 24

(Thermo Scientific, Italy) and 2 µM propidium iodide (PI) (Sigma, Italy), according to ISO 19344 (2015). The effect of the treatment on the membrane potential was evaluated by staining cells with 3,3′-dimethyloxacarbocyanine iodide ($DiOC_2$). After incubation, the cells were stained with 30 µM $DiOC_2$ (ThermoFisher Scientific, Milan, Italy) at 37 °C for 15 min in the dark. As a positive control, cells were previously incubated with 100 µM gramicidin A, an exogenous ion channel forming agent, inducing a decrease in the membrane potential and depolarization of the cells (Liou et al. 2015). The dye $DiOC_2$ has green fluorescence, and a redshift occurs when the dye self-associates in the cytosol when the membrane potential is large. A decrease in membrane potential leads to an increase in green fluorescence and a decrease in the ratio of green/red fluorescence (Mora-Pale et al. 2015). Stained samples were analyzed by a C6 Plus flow cytometer (BD Biosciences, Milan Italy) with thresholds FSC-H 4000 and SSC-H 1000. Green and red fluorescence were detected in the FL1 (excitation 488 nm, emission filter 530/30) and FL3 (excitation 488 nm, emission filter 670 LP) channels, respectively. In addition, to evaluate cell culturability, samples were subjected to a standard plate count on TSA (Sigma, Italy). Plates were incubated at 37 °C for 24–48 h under aerobic conditions.

Transmission electron microscopy (TEM)

Cell suspensions of *L. monocytogenes* Scott A (3 × 109 cells/ mL) in PBS (0.1 M, pH 7.2, control) or exposed to DMSO (control), chlorhexidine (10 or 100 µg/mL) and tested compound (10 or 100 µg/mL) were investigated at the ultrastructural level by TEM (Incecco et al. 2018). After 30 min incubation at 37 °C, cell suspensions were centrifuged at 10,000 × g for 10 min, and the pellets were fixed at 4 °C for 2 h with a solution containing 2% glutaraldehyde and 2% paraformaldehyde in 0.1 M sodium cacodylate solution buffered at pH 7.2 (Agar Scientific, Stansted, UK). Fixed cells were washed twice with sodium cacodylate solution and then suspended in 100 µL of low temperature gelling agarose (2% w/v in water, melted at 35–40 °C) (VWR, Milan, Italy). The

suspension was layered onto a microscope slide, allowed to set and then cut into 1 mm^3 cubes. The cubes were incubated in the fixative solution for 1 h at 4 °C, then washed twice with sodium cacodylate buffer and postfixed in osmium tetroxide (EMS, Hatfield, USA) (1% in water, w/v) for 2 h. Samples were dehydrated in a series of ethanol solutions for 15 min (25, 50, 75, 90, 95 and 100%), embedded in Spurr resin (EMS, Hatfield, USA), and finally cured at 60 °C for 24 h. Ultrathin sections, 60 nm thick, were cut and stained with uranyl acetate and lead citrate (EMS, Hatfield, USA), both 0.2% in water (w/v). Sections were examined with a LEO912ab transmission electron microscope (Zeiss, Germany) at 100 kV, and digital images were acquired with an Esivision CCD-BM/1k system.

3.1.3.3. Results and Discussion

Monomeric and dimeric stilbenoids (**1**-**15**) were tested against the foodborne pathogens *S. aureus* ATCC 25923 and *P. aeuriginosa* ATCC 27853, as representatives of Gram-positive and Gram-negative bacteria, respectively. Among the monomeric derivatives, only pterostilbene (**2**) and its regioisomer (**9**) showed an interesting antimicrobial activity on *S. aureus* (MIC values of 4 and 64 µg/mL, respectively) (Table 3.3). Notably, the MIC of pterostilbene was about 128-fold lower than that of resveratrol (512 µg/mL). Against *P. aeruginosa*, compounds **3, 7, 8** and **9** showed MIC values of 64-128 µg/mL (Table 3.3), confirming previous observations on the reduced susceptibility of Gram-negative bacteria towards these compounds (Ma et al. 2018; Mattio et al. 2020).

Table 3.2. *MIC and MBC values of compounds tested on S. aureus (ATCC 25923) and P.aeruginosa ATCC 27853*

Compound	*S. aureus* ATCC 25923		*P. aeruginosa* ATCC 27853	
	MIC (µg/mL)	MBC (µg/mL)	MIC (µg/mL)	MBC (µg/mL)
1	512	>512	>512	>512
2	4	128	512	512
3	>512	>512	128	>512
4	128	512	512	>512
5	>512	>512	>512	>512
6	>512	>512	>512	>512
7	256	>512	64	>512
8	512	>512	64	>512
9	64	512	128	256
10	16	512	256	>512
11	512	>512	256	>512
12	64	>512	>512	>512
13	>512	>512	>512	>512
14	16	>512	128	>512
15	2	16	128	>512

Dimers were also tested, and compounds **10, 12, 14** and **15** showed a significant activity against the Gram-positive *S. aureus*, with MIC values of 16, 64, 16 and 2 µg/mL, respectively, much lower than MIC value of resveratrol. However, also the dimers showed a modest activity on the Gram-negative bacterium *P. aeuriginosa.* Nevertheless, the high MBC values (> 512 µg/mL) for most of the tested compounds on both *S. aureus* and *P. aeuruginosa* revealed a prevailing growth inhibitory effect rather than bactericidal effect on both Gram-positive and Gram-negative bacteria. Only compound **15** showed a bactericidal effect on *S. aureus* at low concentrations (MBC value of 16 µg/mL).

Based on the obtained results, the most promising compounds (monomers **2** and **9** and dimers **10, 14, 15**) were selected for further investigation studies. Using the bioactive biocide chlorhexidine as positive control, the selected compounds were tested against a panel of foodborne pathogens, five gram-positive strains (*L. monocytogenes* ScottA, *S. aureus* ATCC 25923, *E.*

faecium DSM 20477, *E. faecalis* DSM 20478, and *B. cereus* DSM 9378), and four gram-negative strains (*P. aeruginosa* ATCC 27853, *E. coli* DSM 682, *E. coli* DSM 8579, *S. enterica* DSM 9386, and *Proteus hauseri* DSM 30118) (Table 3.4)

Table 3.3 *Minimal inhibitory concentration (MIC) and minimal bactericidal concentration (MBC) values of selected monomers **2**, **9** and dimers **10**, **14**, **15** against Gram-positive and Gram-negative bacteria*

Bacteria	MIC (MBC) µg/mL					
	14	**15**	**10**	**9**	**2**	**Chlorhexidine**
Gram-positive						
L. monocytogenes Scott A	16 (>512)	2 (16)	16 (128)	256 (512)	64 (128)	8 (32)
S. aureus ATCC 25923	16 (>512)	2 (16)	16 (512)	64 (512)	4 (128)	32 (128)
E. faecium DSM 20477	8 (>512)	2 (32)	8 (512)	4 (512)	32 (512)	4 (128)
E. faecalis DSM 20478	8 (512)	4 (64)	16 (512)	128 (512)	32 (128)	8 (128)
B. cereus DSM 9378	4 (128)	1 (16)	4 (256)	8 (>512)	16 (512)	8 (16)
Gram-negative						
P. aeruginosa ATCC 27853	128 (>512)	256 (512)	256 (>512)	128 (256)	512 (512)	32 (64)
E. coli DSM 682	256 (>512)	512 (>512)	256 (>512)	512 (>512)	512 (>512)	32 (64)
E. coli DSM 8579	256 (>512)	512 (>512)	256 (512)	256 (>512)	512 (>512)	32 (32)
S. enterica DSM 9386	256 (>512)	512 (>512)	256 (512)	256 (>512)	512 (>512)	32 (32)
P. hauseri DSM 30118	256 (>512)	512 (512)	256 (512)	256 (>512)	256 (>512)	32 (32)

The MIC and MBC values confirmed a higher susceptibility of Gram-positive bacteria towards the selected compounds (Table 3.4). In particular, the dimers resulted to be more potent than pterostilbene (MIC value of 4-64 μg/mL) with MIC values of 4-16 μg/mL for both dimers **10** and **14** and 1-4 μg/mL for compound **15**. Compound **9**, showing a MIC value range of 4-256 μg/mL, was more species-dependent and less effective than its regioisomer pterostilbene **2**. The MBC values of dimers **10** and **14** and pterostilbene were comparable (128-512 μg/mL), whereas compound **15** confirmed its bactericidal effect at lower concentrations (16-64 μg/mL) in comparison to the other stilbenoids. Conversely, all compounds were less effective on all Gram-negative strains tested (MIC and MBC values ranging from 128 to 512 μg/mL, and ≥ 512 μg/mL), confirming the reduced susceptibility of Gram-negative bacteria towards stilbenoid compounds. On the contrary, the positive control chlorhexidine was efficient at low concentrations against both Gram-positive and Gram-negative strains (MIC 4-32 μg/mL, MBC 16-128 μg/mL) (Table 3.4).

Based on literature studies (Wu et al. 2016; Chibane et al. 2019), the stilbenoid compounds were postulated to interact with the bacterial cell membrane through the hydroxy groups. Indeed, it was reported that accumulation of phenolics in the cell membrane could result in alterations of the membrane structure and provoke loss of intracellular components, leading to cell death (Wu et al. 2016). Therefore, membrane damage of Gram-positive bacteria was investigated, upon exposure of cells to the active compounds. The membrane-permeable dye cFDASE (carboxyfluorescein diacetate *N*-succinimidyl ester) was used as stain for Gram-positive bacterial cells. Inside the cell, intracellular esterases cleave cFDASE to yield the fluorescent 5(6)-carboxyfluorescein succinimidyl ester (cFSE) molecules that conjugate to the aliphatic amine portions of the intracellular proteins. The cFSE-labeled starving cells were incubated with 100 μg/mL of the selected compounds (**2, 9, 10, 14, 15** and chlorhexidine) for 30 min at 30–37 °C, and the leakage of cFSE fluorescence outside the cells, indicating membrane damage, was

monitored by cytofluorometry (Arioli et al. 2010; Kaduskar et al. 2017). Pterostilbene **2**, its regioisomer **9,** and dimer **15** were able to cause a significant ($P < 0.001$) release of cSFE in all Gram-positive bacteria tested, with dimer **15** and chlorhexidine resulting the most potent compounds (Figure 3.13). Trying to rationalize the lower damage induced by monomers **2** and **9** with respect to the damage caused by dimer **15**, we analysed the physicochemical properties of the tested compounds, calculating the topological polar surface area, logP and other relevant descriptors of molecular shape and geometry (Table 3.5). As a matter of fact, the relative position of hydroxy groups on the phenol ring has been reported to affect the antibacterial potency of polyphenols (Liou et al. 2015; Zakova et al. 2018; Chibane et al. 2019; Singh et al. 2019). The obtained data showed that the capability to enter the membrane bilayer and interact with phospholipids depends on an appropriate balance between lipophilicity and properly oriented functional groups for the most convenient interaction with cell membrane components.

From these findings, the molecules tested were assumed to disrupt the phospholipid bilayer, as chlorhexidine, which is known to act on the bacterial plasma membrane (Komljenović et al. 2010). Therefore, the mechanism of action of compound **15** was further investigated.

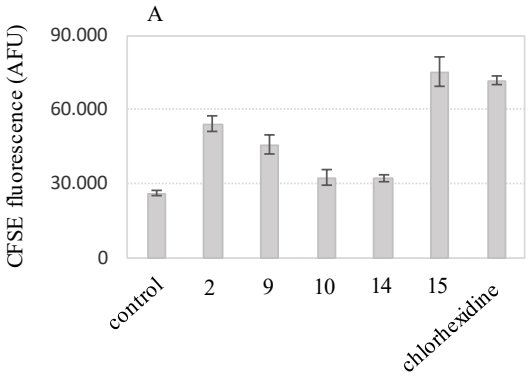
A
CFSE fluorescence (AFU)
90.000
60.000
30.000
0
control
2
9
10
14
15
chlorhexidine

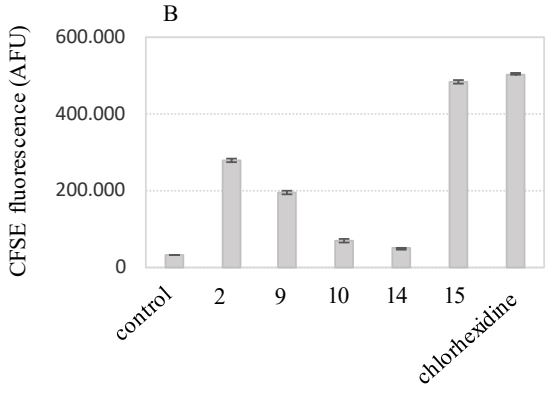
B
CFSE fluorescence (AFU)
600.000
400.000
200.000
0
control
2
9
10
14
15
chlorhexidine

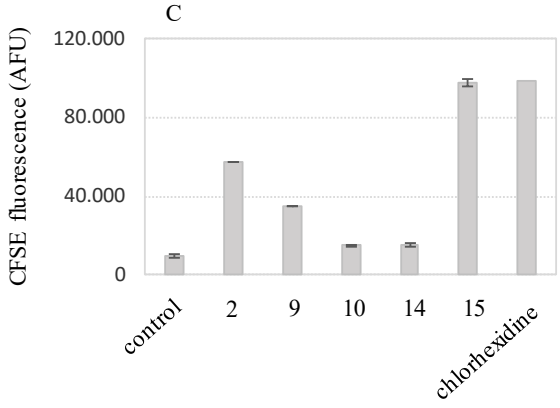
C
CFSE fluorescence (AFU)
120.000
80.000
40.000
0
control
2
9
10
14
15
chlorhexidine

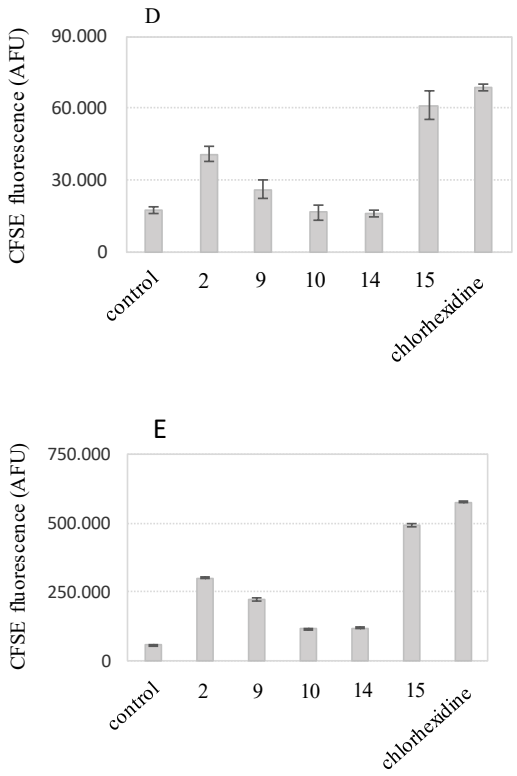

Figure 3.13. *Leakage of cFSE fluorescence outside the Gram-positive cells due to membrane damages after exposure to 100 µg/ml of each compounds for 1 h at 30–37 °C. A) B. cereus DSM 9378. B) S. aureus ATCC 25923. C) L. monocytogenes Scott A. D) E. faecium DSM 20477. E) E. faecalis DSM 20478. Data are means of three replicates; standard deviation is shown as error bars. In the same chart, different letters indicate statistically significant differences between groups (p < 0.001).*

Table 3.4 *Structural properties and geometries of compounds **1-15**. Values were calculated from www.chemicalize.org*

cpd	Topological polar surface area Å²	Highest acidic pKa	logP	logD	Min projection area Å²	Max projection area Å²	Solvent accessible surface area Å²
1	60.69	8.49	3.40	3.37	29.68	78.08	419.53
2	38.69	9.00	3.69	3.68	39.57	88.22	532.81
9	38.69	8.88	3.69	3.68	38.99	89.06	533.15
7	121.38	9.07	5.31	5.31	73.59	113.90	589.24
8	66.38	9.47	6.54	6.54	84.55	144.05	898.40
10	110.38	8.50	5.96	5.93	75.63	125.61	676.71
11	110.38	8.51	5.96	5.93	80.57	119.41	628.00
14	114.29	7.91	6.17	6.05	60.19	127.71	621.49
15	114.29	8.43	6.17	6.13	59.13	129.20	674.77

L. monocytogenes, responsible for listeriosis and considered as a cause of major foodborne diseases (Ferreira and Domingues 2016; Lee 2020), was selected for the evaluation of the effects of compound **15** on cell viability, culturability and membrane potential.

Starving *L. monocytogenes* ScottA cells were incubated for 30 min at 37°C with compound **15** and chlorhexidine at concentrations of 10 or 100 µg/mL. The results obtained (Figure 3.14a, b) showed that exposure to a concentration of 100 µg/mL of either compound **15** and chlorhexidine caused a 95% reduction of cell viability, whereas a lower concentration of the tested compounds (10 µg/mL) decreased the viable population (Active Fluorescent Unit, AFU) of 22% and 30% with compound 15 and chlorhexidine, respectively (Figure 3.14a).

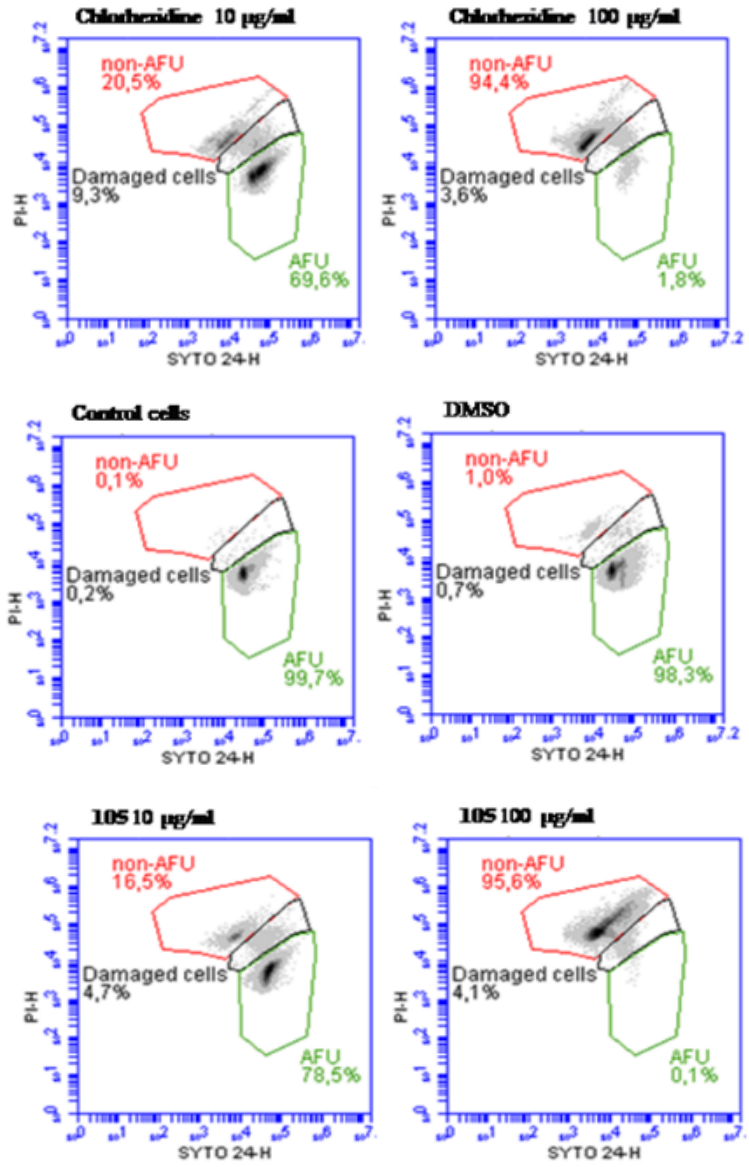

Figure 3.14a. *Dot plot of cell viability determined by flow cytometry. Cell suspensions were stained with SYTO™ 24 and PI just after exposure to either* ***15*** *or chlorhexidine, for 30 min at 37 °C. Green gate: AFU (considered as live cells); dark gate: damaged cells; red gate: non-AFU (considered as dead cells). Inoculum was 9.0 ± 0.20 log10 AFU L. monocytogenes cells. Control cells were incubated in PBS; cells exposed to DMSO served as treatment control.*

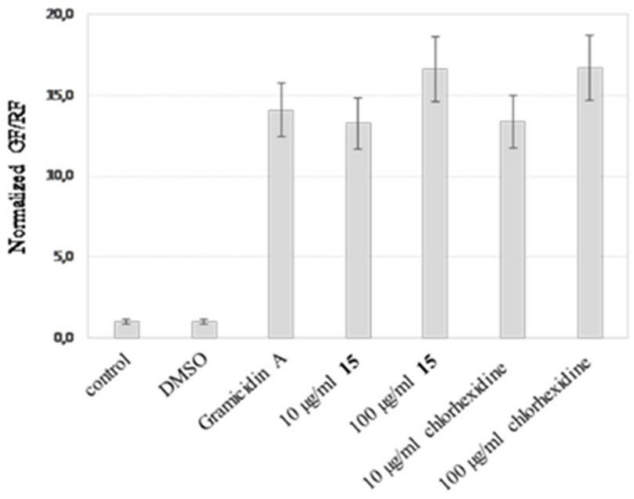

Figure 3.14b. *Effect of* ***15*** *and chlorhexidine exposure on membrane potential of L. monocytogenes ScottA cells. The membrane potential is reported as normalized green/red fluorescence (GF/RF). Fluorescence was measured by flow cytometry and GF/RF ratio considers the fluorescence of 30000 events. Gramicidin A used as standard molecule inducing membrane depolarization. Data are means of three replicates; standard deviation is shown as error bars. In the same chart, different letters indicate statistically significant differences between groups ($p < 0.001$).*

Conversely, the cell culturability after exposure to 10 µg/mL of either compound **15** and chlorhexidine was 2.5-log lower than expected, and no culturable cells were detected after esposure to 100 µg/mL concentrations of two compounds, though cell viability was not completed depleted (Table 3.6). The discrepancy between culturability and viability data could derive from the viable-but-not-culturable (VBNC) state, usually induced by environmental conditions, such as starvation, low temperature, decreased oxygen levels, pH variations, and antibiotic exposure. These stress conditions create a subpopulation of bacteria, which transiently lose their capability to grow on an ordinary medium, maintaining their metabolic activity (functionally viable). This phenomenon supports the survival of foodborne pathogens in food processing plants (Ayrapetyan et al. 2018).

Table 3.6. *Confronting culturability (as Log CFU/ml) and viability (as Log AFU/ml) of L. monocytogenes ScottA cells exposed to compound 15 or chlorhexidine.*

	Culturability as Log CFU/ml	**Viability as Log AFU/ml**
Control	8.98 ± 0.31	9.15 ± 0.05
DMSO	9.08 ± 0.26	9.19 ± 0.10
15 **10 µg/mL**	6.42 ± 0.28	8.89 ± 0.11
15 **100 µg/mL**	< 1	6.01 ± 0.15
chlorhexidine 10 µg/mL	6.60 ± 0.35	8.83 ± 0.12
chlorhexidine 100 µg/mL	< 1	7.39 ± 0.08

To better understand the mechanism of action of compound **15**, the cell membrane potential was measured, by staining cells with the fluorescent dye 3,3-diethyloxacarbocyanine iodide ($DiOC_2$) (Mora-Pale et al. 2015). The ion channel forming agent gramicidin A, known to cause membrane permeabilization and dissipation of the electrochemical gradient across the cell membrane (Liou et al. 2015), was used as positive control. The dye $DiOC_2$ has green fluorescence, but its self-association in the cytosol, due to a large potential membrane, results in a redshift. Therefore, observed reduction of red fluorescence reveals the disruption of cell membrane potential hampering the internalization of the stain. The green fluorescence/red fluorescence ratio (GF/RF) of cells exposed to compound **15** and chlorhexidine increased about 15-fold, demonstrating complete cell membrane potential depletion, irrespective of the antimicrobial concentrations. Cells exposed to DMSO or maintained in PBS did not show any significant differences ($P < 0.001$), demonstrating that the solvent was not toxic to the cells, and compound **15** and chlorhexidine were the actual responsible for membrane potential dissipation (Figure 3.14b).

To achieve direct evidence of the cell membrane damage, transmission electron microscopy (TEM) analysis was performed on ultrafin sections of resin-embedded samples of *L. monocytogenes* exposed to compound **15** and chlorhexidine. Control cells, either in PBS and DMSO, showed an evenly distributed cytoplasm within a continuous and smooth cell wall and cell membrane (Figure 3.15 a, b), whereas cells exposed to compound **15** (100

μg/mL) resulted in important modifications (Figure 3.15 c, d). Indeed, in all treated cells, several clumps and few spots likely corresponding to cytoplasm-depleted areas appeared in place of an even cytoplasm distribution. Furthermore, in presence of compound **15**, in the proximity of the most deeply damaged cells, free cytoplasm was observed, as revealed by interruptions in either the cell wall or the cell membrane. Black spots were also found within a few cells, possibly indicating more extensive cytoplasm clumping or fixative accumulation (Figure 3.15 d). Notably, a 100 μg/mL concentration of chlorhexidine caused only subtler damage to *L. monocytogenes* (Figure 3.15 e, f). Indeed, the wall did not show any ruptures but an increased roughness, as compared to controls, with accordingly no cytoplasmic material leakage out of the cells. Cell damage caused by chlorhexidine is indicated by the presence of defined spots lacking cytoplasm within the cell.

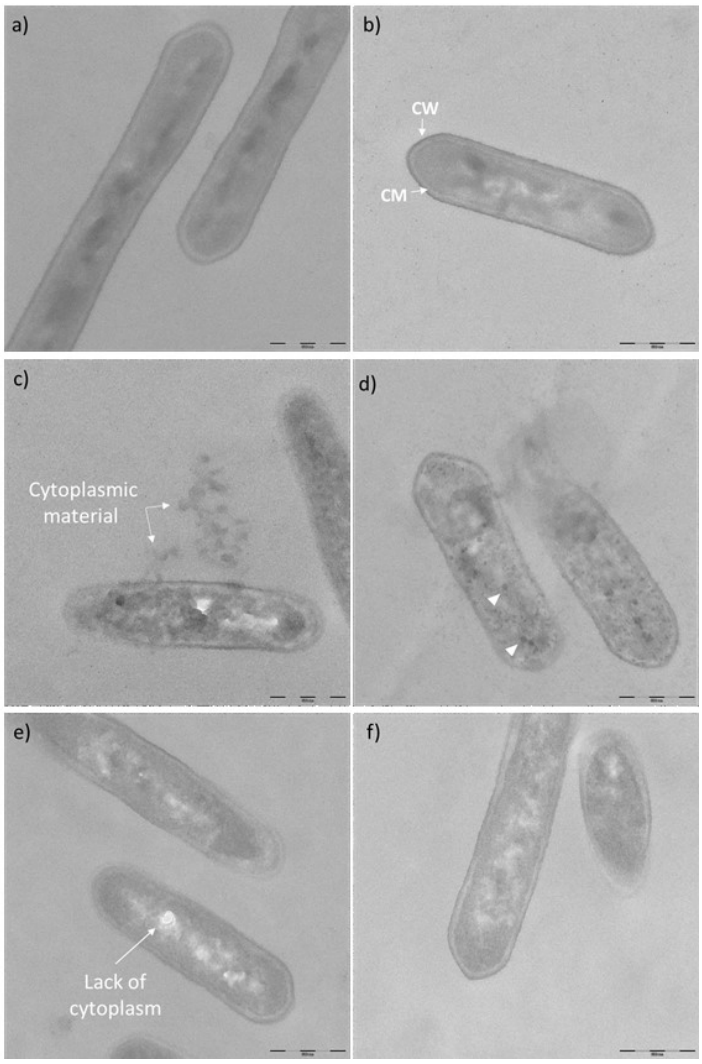

Figure 3.15. TEM micrographs of *L. monocytogenes* Scott A suspended in either PBS (**a**) or exposed to DMSO (**b**), 15 (**c**,d) or chlorhexidine (**e**,**f**). Intact cell wall (CW) and cell membrane (CM) were present in control samples (**a**,**b**). Cell wall or cell membrane interruptions (arrows) were visible in 15 exposed cells (**c**). Bar is 500 nm.

In conclusion, a set of resveratrol-derived monomers (compounds **1-9**) and dimers (compound **10-15**) were tested as single molecules against *S. aureus* ATCC 25923 and *P. aeruginosa* ATCC 27853, as representative Gram-positive and Gram-negative strains, respectively (Table 3.3). Pterostilbene resulted to be more active than resveratrol against *S. aureus*, confirming previous studies (Yang et al. 2017). Depending on the tested strains and

experimental conditions (inoculum size, medium), resveratrol has been shown to exert antibacterial activity on foodborne pathogens with a high range of MIC values, from 16.5 to 300 µg/mL on Gram-positive bacteria, and from 0.625 to 521 µg/mL on Gram-negative bacteria (Bostanghadiri et al. 2017; Ma et al. 2018; Vestergaard and Ingmer 2019). The strain used in our study was poorly sensitive towards resveratrol (MIC value ≥ 512 µg/mL). On the other hand, pterostilbene was reported to exert higher antimicrobial activity, in particular against Gram-positive strains (25 µg/mL) rather than against Gram-negative strains (100 µg/mL) (Singh et al. 2019).

Out of the nine monomers tested, only pterostilbene and its regioisomer **9** were active on gram-positive bacteria, whereas, among dimers, compounds **10, 14** and **15** showed high antibacterial activity with MIC values ranging from 2 to 16 µg/mL on *S. aureus*. All compounds were considerably less active on gram-negative bacteria.

The most active molecules (compound **2, 9, 10, 14** and **15**) were tested against nine foodborne pathogens, including both Gram positive and Gram negative strains. Pterostilbene showed a good bacteriostatic activity with MIC values of 4-64 µg/mL, but higher concentrations were needed for the bactericidal effect (MBC values from 128 to 512 µg/mL). Similar results were obtained for compounds **9**, **10** and **14** (MIC 4–128 µg/mL; MBC 128 to >512 µg/mL), confirming previous results obtained for compound **9** and **10** on foodborne pathogens (Mora-Pale et al. 2015). The most active compound dehydro-δ-viniferin **15** demonstrated also a bactericidal effect at low concentrations (MBC 16-64 µg/mL), besides high bacteriostatic activity (MIC values of 1-4 µg/mL). None of the molecules showed relevant antibacterial activity on Gram-negative strains. Indeed, in the literature, polyphenols have been reported to exert poor activity on Gram-negative strains, protected by their complex outer membrane in addition to their rigid cell wall of polysaccharides (Fernández and Hancock 2012; Araya-Cloutier et al. 2018). Moreover, Gram-negative bacterial double membrane presents an efficient

efflux pumps system for antimicrobials with a broad substrate specificity, allowing the extrusion of xenobiotics across the whole cell envelope (Blair et al. 2015).

Investigation of the mechanism of action by cytofluorimetry assay and TEM analysis revealed that dehydro-δ-viniferin was able to damage the cytoplasmic membrane of *L. monocytogenes*, causing membrane depolarization, loss of membrane integrity, and severe morphological changes. To the best of our knowledge, this was the first time that membrane depolarization has been reported as the initial event in the antibacterial activity. However, other mechanisms on intracellular targets may be involved in the bactericidal activity of dehydro-δ-viniferin.

Studies of combinations of the most active derivatives with known antibiotics hold promise for future investigation (Nøhr-Meldgaard et al. 2018).

3.1.4. Experimental section

3.1.4.1. General information

All chemicals were provided by supplier and used without further purification unless otherwise stated. All reagents and solvents were of reagent grade or were purified by standard methods before use. All reactions requiring anhydrous conditions were performed under nitrogen or argon atmosphere with Schlenk-type oven-dired and/or flame-dried glassware. Melting points were determined on a model B-540 Büchi apparatus and are uncorrected. Optical rotation determinations were carried out using a Jasco P-1010 spectropolarimeter (Jasco Europe, Cremella, Italy), coupled with a Haake N3-B thermostat. NMR data were acquired using a Varian Mercury-300 MHz spectrometer (Varian, Palo Alto, CA, USA), Bruker AV600. Chemical shifts (δ values) and coupling constants (J values) are given in ppm and Hz, respectively. Isolation and purification of the compounds were performed by flash column chromatography on silica gel 60 (230–400 mesh). The analytical thin-layer chromatography (TLC) was conducted on Supelco TLC plates (silica gel 60 F254, aluminum foil). Substances were detected with a UV-light source (λ = 254 or 365 nm) or stained with 10% phosphomolybdic acid solution (10.0 g phosphomolybdic acid in 100 mL of abs. ethanol), or with ninhydrin solution (1.5 g ninhydrin, 3.0 mL acetic acid in 100 mL of abs. ethanol), or with 2,4-dinitrophenylhydrazine solution (12 g 2,4-dinitrophenylhydrazine, 60 mL conc sulfuric acid, 80 mL water in 200 mL of 95% ethanol), or with potassium permanganate solution (1.5 g $KMnO_4$, 10 g K_2CO_3, 1.25 mL 10% NaOH in 200 mL of water).

3.1.4.2. Experimental procedures

(*E*)-3-(4-hydroxystyryl)-5-methoxyphenol (7) and (*E*)-5-(4-methoxystyryl) benzene-1,3-diol (8)

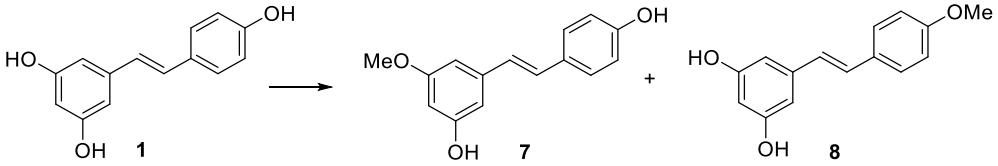

To a solution of resveratrol (**1**) (1 g, 4.88 mmol) in dry acetone (20 mL) at room temperature, under nitrogen atmosphere, K_2CO_3 (1.2 g, 8.76 mmol, 2 eq) was added, followed by the dropwise addition of CH_3I (818 µl, 13.14 mmol, 3 eq). The mixture was stirred overnight. Then, the solvent was evaporated, the residue diluted with AcOEt and washed with H_2O. The aqueous phase was extracted with AcOEt (3 x 20 mL). The combined organic layers were washed with brine (20 mL), dried over anhydrous Na_2SO_4 and concentrated under reduced pressure. The residue was purified by FC (DCM/AcOEt 95:5) to obtain **7** (white solid, 12% yield) and **8** (white solid, 15% yield). Analytical data were in accordance with literature report (Polunin and Schmalz 2004; Lee et al. 2010)

Compound 7

M.p.: 117-118°C

R_f: 0.41 (DCM/AcOEt 92:8)

^{1}H NMR (300 MHz, DMSO-d_6) δ (ppm): 7.42 – 7.34 (m, 2H), 7.02 (d, *J* = 16.3 Hz, 1H), 6.86 (d, *J* = 16.3 Hz, 1H), 6.77 – 6.71 (m, 2H), 6.55 (dd, J_1 = 2.3, J_2 = 1.4 Hz, 1H), 6.51 (t, *J* = 1.8 Hz, 1H), 6.20 (t, *J* = 2.2 Hz, 1H), 3.71 (s, 3H).
^{13}C NMR (75 MHz, C*D*Cl$_3$) δ (ppm): 162.5, 159.7, 158.4, 141.3, 130.3, 129.9, 129.8, 128.9 (x2C), 116.5 (x2C), 106.6, 104.4, 101.4, 55.6 from (Polunin and Schmalz 2004)

Compound 8

M.p.: 176-178°C

R_f: 0.29 (DCM/AcOEt 92:8)

^{1}H NMR (300 MHz, DMSO-d_6) δ (ppm): 9.19 (s, 2H), 7.54 – 7.47 (m, 2H), 7.01 – 6.82 (m, 4H), 6.39 (d, *J* = 2.1 Hz, 2H), 6.11 (t, *J* = 2.1 Hz, 1H), 3.75 (s, 3H). **^{13}C NMR (75 MHz, Acetone-d_6)** δ (ppm): 160.1, 159.2 (x2C), 140.5, 130.7, 128.8, 128.5 (x2C), 127.4, 114.8 (x2C), 105.8 (x2C), 102.9, 55.8 from (Lee et al. 2010).

(*E*)-1,3-dimethoxy-5-(4-methoxystyryl)benzene (5)

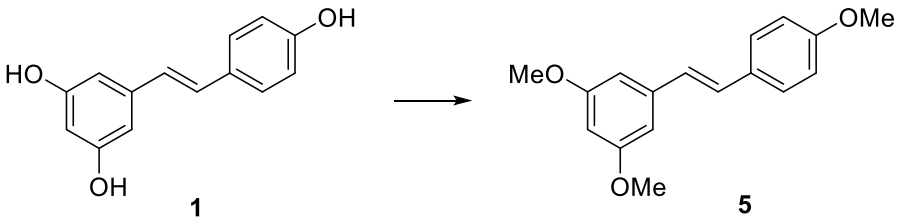

To a solution of **1** (500 mg, 2.19 mmol) in dry acetone (10 mL), at room temperature, under nitrogen atmosphere, was added K_2CO_3 (2.725 g, 19.7 mmol, 9 eq). After 10 minutes stirring was added CH_3I (1.23 mL, 19.7 mmol, 9 eq) dropwise. The mixture was stirred overnight. Then the solvent was evaporated, the residue was quenched with a saturated solution of NH_4Cl (15 mL) and H_2O (10 mL). The aqueous phase was extracted with AcOEt (3 x 20 mL). The combined organic layers were washed with H_2O (20 mL), brine (20 mL), dried over anhydrous Na_2SO_4, and concentrated under reduced pressure. The residue was purified by FC (Cyclohexane/AcOEt 8:2) to afford the desired product as white solid, in 81% yield. Analytical data were in accordance with literature report (Polunin and Schmalz 2004).

M.p.: 55-57°C

R_f: 0.45 (Cyclohexane/AcOEt 8:2)

^{1}H NMR (300 MHz, $CDCl_3$) δ (ppm): 7.48 – 7.41 (m, 2H), 7.04 (d, *J* = 16.2 Hz, 1H), 6.94 – 6.86 (m, 4H), 6.65 (d, *J* = 2.2 Hz, 2H), 6.38 (t, *J* = 2.3 Hz, 1H), 3.83 (s, 9H)

^{13}C NMR (75 MHz, Chloroform-*d*) δ (ppm): 160.9 (x2C), 159.3, 139.6, 129.8, 128.7, 127.8 (x2C), 126.5, 114.1 (x2C), 104.2 (x2C), 99.5, 55.3 (x2C), 55.2

(*E*)-4-[3,5-Bis(*tert*-butyldimethylsilyloxy)styryl](*tert*-butyldimethylsilyloxy) benzene (20)

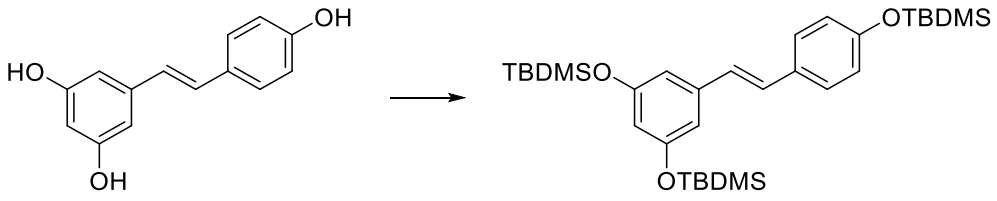

1 **20**

To a solution of **1** (500 mg, 2.19 mmol) in anhydrous DMF (15 mL) at -20°C under nitrogen atmosphere, a solution of TBDMSCl (1.32 g, 8.76 mmol, 4 eq) in anhydrous DMF (5 mL) and DIPEA (1.5 mL, 8.76 mmol, 4 eq) were added. The reaction mixture was allowed to warm to room temperature. After 16 h the resulting reaction mixture was diluted with AcOEt (70 mL) and washed with a mixture HCl 0,1 N/brine 1:1 (5 x 30 mL). The organic layer was dried over anhydrous Na_2SO_4, and concentrated under reduced pressure. The residue was purified by FC (DCM/cyclohexane 3:7) to obtain the desired product as white sticky solid in 95% yield. Analytical data were in accordance with literature report (Mattarei et al. 2015).

R_f: 0.7 (Cyclohexane/DCM 8:2)

^{1}H NMR (300 MHz, C*D*Cl$_3$) δ (ppm): 7.41 – 7.35 (m, 2H), 6.96 (d, *J* = 16.2 Hz, 1H), 6.87 – 6.80 (m, 4H), 6.60 (d, *J* = 2.2 Hz, 2H), 6.24 (t, *J* = 2.2 Hz, 1H), 1.00 (d, *J* = 1.1 Hz, 27H), 0.22 (d, *J* = 1.1 Hz, 18H).

^{13}C NMR (75 MHz, C*D*Cl$_3$) δ (ppm): 156.8 (x2C), 155.6, 139.6, 130.8, 128.6 (x2C), 127.8, 126.9, 120.5 (x2C), 111.7, 111.4 (x2C), 25.9, 25.8 (x2C), 18.4 (x9C), -4.2 (x6C) (Mattarei et al. 2015)

(*E*)-3-(*tert*-butyldimethylsilyloxy)-5-(4-hydroxystyryl)phenol (21)

20 **21**

To a solution of **20** (600 mg, 1.05 mmol) in dry THF (12 mL) was added a solution of KF (61 mg, 1.05 mmol, 1.0 eq) in MeOH (12 mL) at −15 °C, under nitrogen atmosphere, and the mixture was vigorously stirred for 6 h. The resulting reaction mixture was concentrated by rotary evaporation, then diluted with AcOEt and washed with 50% brine (2×30 mL). The organic layer was dried over anhydrous Na_2SO_4 and concentrated under reduced pressure. The resulting crude product was purified by FC (DCM/acetone 95:5) to afford the desired product as white solid in 56% yield. Analytical data were in accordance with literature report (Mattarei et al. 2015)

M.p.: 62-63°C

R_f: 0.39 (DCM/acetone 95:5)

^{1}H NMR (300 MHz, C*D*Cl$_3$) δ (ppm): 7.43 – 7.38 (m, 2H), 6.98 (d, *J* = 16.3 Hz, 1H), 6.89 – 6.79 (m, 3H), 6.58 (d, *J* = 2.1 Hz, 2H), 6.27 (t, *J* = 2.1 Hz, 1H), 1.00 (s, 9H), 0.23 (s, 6H).

^{13}C NMR (75 MHz, C*D*Cl$_3$) δ (ppm): 157.2, 156.7, 155.4, 140.0, 130.3 (x2C), 128.8, 128.2, 126.4, 115.8 (x2C), 111.3, 106.8, 106.5, 25.82, 18.35 (x3C), -4.2 (x2C) from (Mattarei et al. 2015).

3-(*tert*-butyldimethylsilyloxy)-4′,5-dimethoxystilbene (**22**)

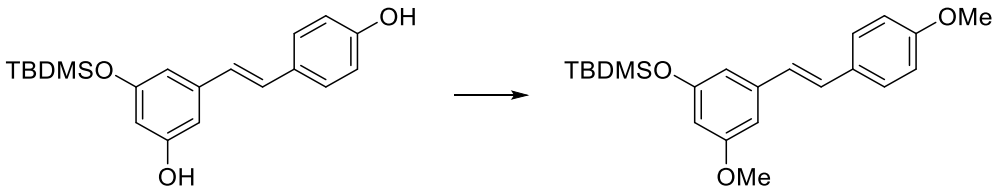

21 **22**

To a solution of **21** (109 mg, 0.318 mmol) in dry acetone (1.5 mL) at room temperature, under nitrogen atmsphere, was added K_2CO_3 (264 mg, 1.91 mmol, 6 eq). After 10 minutes stirring, CH_3I (118 µL, 1.91 mmol, 6 eq) was added dropwise, and the solution was stirred overnight. Then, the solvent was evaporated, the residue was quenched with a saturated solution of NH_4Cl. The aqueous phase was extracted with AcOEt (3 x 10 mL). The combined organic layers were washed with H_2O (20 mL), brine (20 mL), dried over anhydrous Na_2SO_4, and concentrated under reduced pressure. The residue was purified by FC (Cyclohexane/DCM 7:3) to afford the desired product as a colourless oil in 38% yield. Analytical data were in accordance with literature report (Pettit et al. 2002).

Rf: 0.31 (Cyclohexane/DCM 7:3)

^{1}H NMR (300 MHz, C*D*Cl$_3$) δ (ppm): 7.49 – 7.42 (m, 2H), 7.02 (d, *J* = 16.3 Hz, 1H), 6.94 – 6.85 (m, 3H), 6.69 – 6.66 (m, 1H), 6.60 (dd, *J* = 2.1, 1.4 Hz, 1H), 6.32 (t, *J* = 2.2 Hz, 1H), 3.84 (s, 3H), 3.82 (s, 3H), 1.01 (s, 9H), 0.24 (s, 6H).
^{13}C NMR (75 MHz, C*D*Cl$_3$) δ (ppm): 160.8, 159.4, 156.9, 139.6, 130.0 (x2C), 128.5, 127.8, 126.6, 114.1 (x2C), 110.9, 104.8 (x2C), 55.3 (x2C), 25.7, 14.1 (x3C), -4.4 (x2C).

(E)-3-methoxy-5-(4-methoxystyryl)phenol (**9**)

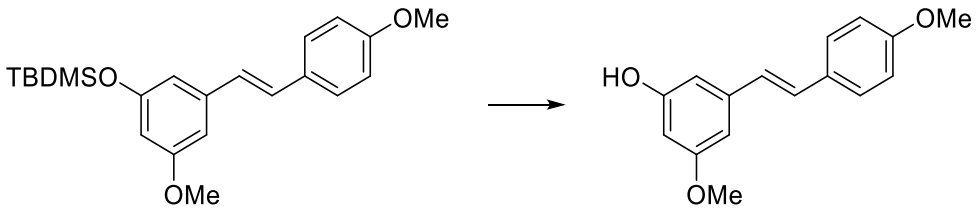

22 **9**

To a solution of **22** (28 mg, 0.0756 mmol) in dry MeOH (1 mL) was added dropwise a solution of KF (26 mg, 0.453 mmol, 6 eq) in a mixture MeOH/THF 2:1 (1.5 mL) at room temperature. The mixture was stirred under nitrogen atmosphere overnight. Solvents were evaporated and the resulting residue was diluted with AcOEt and washed with 50% brine (2×30 mL). The organic layer was dried over anhydrous Na_2SO_4 and concentrated under reduced pressure. The crude was purified by FC (cyclohexane/AcOEt 7:3) to give the product as white solid in quantitative yield. Analytical data were in accordance with literature report (Li et al. 2010)

M.p.: 115-117°C

R_f: 0.29 (cyclohexane/AcOEt 7:3)

^{1}H NMR (300 MHz, C*D*Cl$_3$) δ (ppm): 7.47 – 7.41 (m, 2H), 7.02 (d, *J* = 16.3 Hz, 1H), 6.94 – 6.83 (m, 3H), 6.66 – 6.62 (m, 1H), 6.58 (dd, J_1 = 2.2, J_2 = 1.4 Hz, 1H), 6.32 (t, *J* = 2.2 Hz, 1H), 3.84 (s, 3H), 3.82 (s, 3H).
^{13}C NMR (100MHz, DMSO-*d*$_6$) δ: 160.6, 159.0, 158.6, 139.3, 129.6 (x2C), 128.0, 127.8, 126.4, 114.1 (x2C), 106.0, 102.6,100.6, 55.1, 55.0 from (Li et al. 2010).

1-Hydroxy-1,2-benziodoxol-3(1H)-one 1-Oxide (IBX)

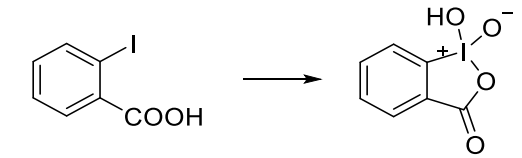

2-iodobenzoic acid IBX

2-Iodobenzoic acid (1 g, 4.032 mmol) was added in one portion to a solution of oxone (7.45 g, 12.096 mmol, 3 eq) in deionized water (40 mL). The reaction mixture was warmed to 70°C and mechanically stirred at this temperature for 1.15 h. The white suspension obtained was then cooled to 5 °C and left at this temperature for 1 h with slow stirring. The mixture was filtered through a sintered-glass funnel, and the solid was repeatedly rinsed with water (6 × 10 mL) and acetone (2 × 10 mL). The white, crystalline solid was left to dry under vacuum. The product was obtained as a white powder in 64% yield. Analytical data were in accordance with literature report (Giuffredi et al. 2009). Mother and washing liquors were treated with solid Na_2SO_3 (1.5 g, 12.096 mmol, 3 eq) and neutralized with NaOH (1 M) before disposal.

M.p.: dec. T>230°C

^{1}H NMR (300 MHz, DMSO-d_6) δ (ppm): 8.13 (dd, J_1 = 8.0, J_2 = 1.1 Hz, 1H), 8.04 – 7.93 (m, 2H), 7.82 (td, J_1 = 7.3, J_2 = 1.1 Hz, 1H).
^{13}C NMR (75 MHz, DMSO-d_6) δ (ppm): 168.4, 147.4, 133.8, 132.3, 131.3, 131.0, 125.

(*E*)-4-(3,5-dimethoxystyryl)benzene-1,2-diol (4)

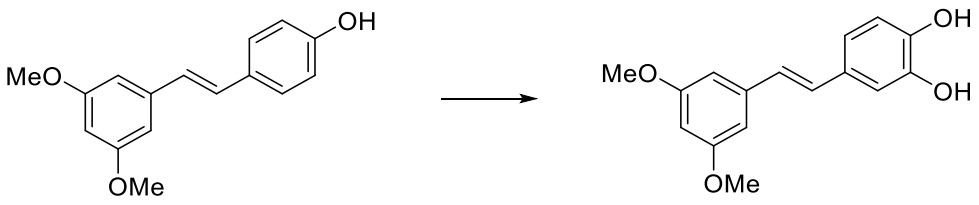

2 **4**

To the solution of **2** (50 mg, 0.195 mmol, 1 eq) in DMF (2.6 mL) at room temperature, under nitrogen, IBX (64 mg, 0.290 mmol, 1.5 eq) was added and the reaction was stirred for 90 minutes. Then, a solution of $NaBH_4$ (18 mg, 0.49 mmol, 2.5 eq) in MeOH (0.5 mL) was added at 0°C and the mixture was stirred for 5 minutes. The reaction was quenched with aq 2N HCl at 0°C (pH 1-2). The aqueous phase was extracted with AcOEt (4 x 10 mL). The combined organic layers were washed with aq 5% $NaHCO_3$ 5% (15 mL), a mixture water/brine 1:1 (3 x 15 mL), dried over anhydrous Na_2SO_4 and concentrated under reduced pressure. The residue was purified by FC (Cyclohexane/AcOEt 7:3) to afford the desired product as a pale yellow solid in 62% yield. Analytical data were in accordance with literature report (Lee et al. 2010)

M.p.: 112-115°C

R_f: 0.28 (Cyclohexane/AcOEt 7:3)

^{1}H NMR (300 MHz, acetone-d_6) δ (ppm): 7.05 (s, 1H) 6.95 (d, *J* = 15.3 Hz, 1H), 6.94 (d, *J* = 8.1 Hz, 1H), 6.84 (d, *J* = 15.9 Hz, 1H), 6.83 (d, *J* = 8.1 Hz, 1H), 6.62 (d, *J* = 1.8 Hz, 2H), 6.37 (d, *J* = 2.4 Hz, 1H), 5.39 (br s, 2H), 3.82 (s, 6H)

^{13}C NMR (75 MHz, acetone-d_6) δ (ppm): 161.0 (x2C), 143.9, 143.7, 139.7, 130.9, 128.9, 127.1, 120.4, 115.7, 113.2, 104.6 (x2C), 99.9, 55.7 (x2C).

(*E*)-4-(3,5-dimethoxystyryl)-1,2-dimethoxybenzene (**17**)

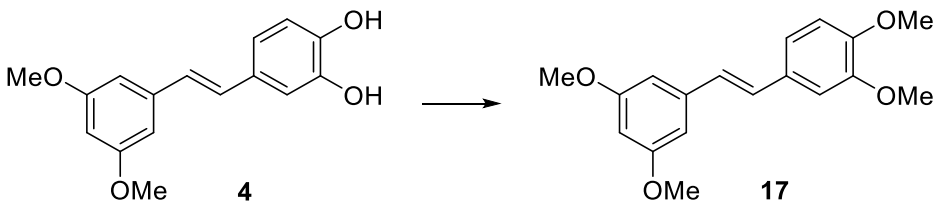

To a solution of **4** (30 mg, 0.1098 mmol) in dry acetone (1 mL) at room temperature, under nitrogen atmosphere, was added K_2CO_3 (91 mg, 0.6586

mmol, 6 eq), followed by the dropwise addition of CH_3I (41 µL, 0,6586 mmol, 6 eq). The mixture was stirred overnight. Then, the solvent was evaporated under reduced pressure, and the residue was diluted with a saturated aq solution of NH_4Cl. The aqueous phase was extracted with AcOEt (4 x 10 mL) and the combined organic layers were washed with brine, dried over anhydrous Na_2SO_4 and concentrated under reduced pressure. The residue was purified by FC (cyclohexane/AcOEt 8:2) to afford the desired product as a yellowish solid in 70% yield. Analytical data were in accordance with literature report (Shibutani et al. 2004)

M.p.: 66-67°C

R_f: 0.45 (Cyclohexane/AcOEt 7:3)

^{1}H NMR (300 MHz, C*D*Cl$_3$) δ (ppm): 7.08-6.84 (m, 5H), 6.66 (d, *J* = 2.3Hz 2H), 6.39 (t, *J* = 2.3 Hz, 1H), 3.95 (s, 3H), 3.90 (s, 3H), 3.83 (s, 6H).
^{13}C NMR (75 MHz, C*D*Cl$_3$) δ (ppm): 162.1 (x2C), 150.6, 150.5, 140.8, 131.1, 129.9, 127.4, 120.9, 112.7, 110.3, 105.0 (x2C), 100.3, 56.1 (x2C), 55.6 (x2C).

(*E*)-5-(4-acetoxystyryl)-1,3-phenylene diacetate (**6**)

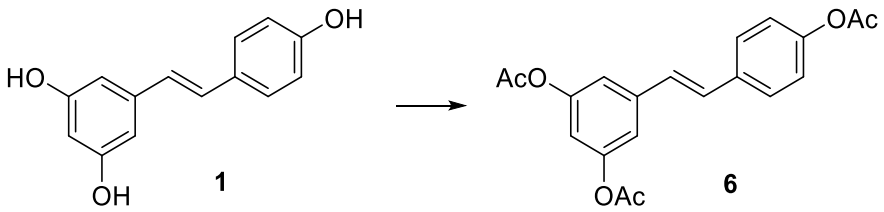

To the suspension of **1** (1 g, 4.38 mmol) in dry DCM (14 mL), Ac_2O (1.5 mL, 15.26 mmol, 3.5 eq) and TEA (5 mL, 35.75 mmol, 8.2 eq) were added and the mixture was stirred at room temperature overnight. The reaction mixture was washed with aq 5% $NaHCO_3$ and the aqueous phase was extracted with DCM (2 x 15 mL). The combined organic phases were washed with water (3 x 30 mL), brine (30 mL), dried over anhydrous Na_2SO_4, and concentrated under

reduced pressure. The residue was purified by FC (cyclohexane/AcOEt 6:4) to afford the product as a white solid in 92% yield. Analytical data were in agreement with literature report (Biasutto et al. 2009)

M.p.: 110-112 °C

R_f: 0.40 (Cyclohexane/AcOEt 7:3)

^{1}H NMR (300 MHz, C*D*Cl$_3$) δ (ppm): 7.51 – 7.46 (m, 2H), 7.13 – 7.03 (m, 6H), 6.96 (d, *J* = 16.3 Hz, 1H), 6.82 (t, *J* = 2.1 Hz, 1H), 2.31 (s, 9H).
^{13}C NMR: (75 MHz, DMSO-*d*$_6$) δ (ppm): 169.1 (x2C), 168.9, 151.1 (x2C), 150.2, 139.3, 134.2, 129.4(x2C), 127.6, 126.7, 122.1 (x2C), 117.1 (x2C), 114.9, 20.8 (x2C), 20.7.

(*E*)-5-(4-hydroxystyryl)-1,3-phenylene diacetate (18)

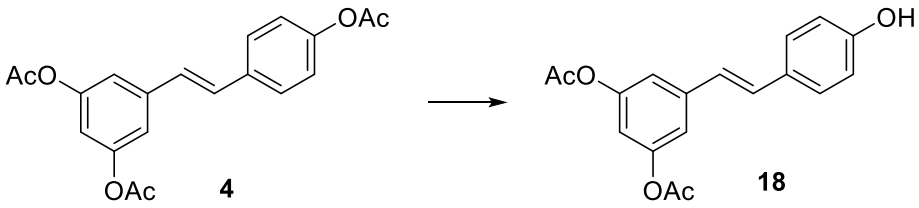

To a solution of **4** (400 mg, 1.13 mmol) in toluene (40 mL) and *n*-BuOH (1.6 mL, 17.5 mmol, 15.5 eq) at 40°C, *Candida Antarctica* lipase (400 mg) was added and the mixture was stirred (400 rpm) at the same temperature for 6 hours. The reaction was cooled to room temperature, quenched by filtering off the enzyme and the filtrate was evaporated *in vacuo*. The residue was purified by FC (DCM/AcOEt 95:5) to give the desired product as a white solid in 81% yield.

M.p.: 146-147°C

R_f: 0.55 (DCM/AcOEt 95:5)

^{1}H NMR: (300 MHz, Acetone-d_6) δ (ppm): 7.52 – 7.43 (m, 2H), 7.23 (d, *J* = 16.4, 1H), 7.20 (d, *J* = 2.1, 2H), 7.04 (d, *J* = 16.4, 1H), 6.90 – 6.82 (m, 2H), 2.28 (s, 3H).

^{13}C NMR: (75 MHz, Acetone-d_6) δ (ppm): 168.6 (x2C), 157.7, 151.71 (x2C), 140.2, 130.4, 128.2 (x2), 123.9 (x2C), 116.5 (x2C), 115.6 (x2C), 114.2, 20.1 (x2C).

(*E*)-5-(3,4-dihydroxystyryl)-1,3-phenylene diacetate (**19**)

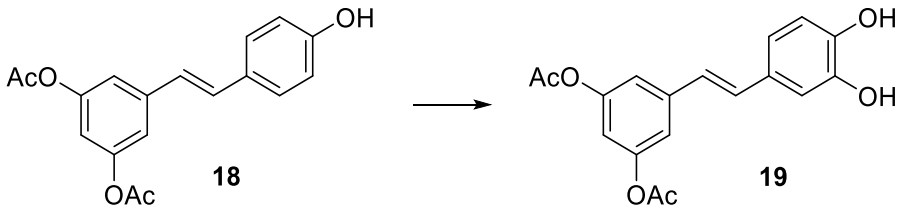

To the solution of **18** (50 mg, 0.152 mmol) in dry DMF (2 mL) at room temperature, under nitrogen atmosphere, IBX (64 mg, 0.29 mmol, 1.5 eq) was added and the reaction was stirred for 90 minutes. Then, a solution of $NaBH_4$ (15 mg, 0.38 mmol, 2.5 eq) in MeOH (0.5 mL) was added at 0°C and the mixture was stirred for 5 minutes. A chromatic change of the solution from red to yellowish was observed. Then, the reaction was quenched with aq 2N HCl at 0°C until pH 1-2. The aqueous phase was extracted with AcOEt (4 x 10 mL). The combined organic layers were washed with aq 5% $NaHCO_3$ 5% (15 mL), and a mixture of water/brine 1:1 (3 x 15 mL), dried over anhydrous Na2SO4, and concentrated under reduced pressure. The residue was purified by FC (DCM/AcOEt 95:5) to afford the desired product as a yellowish oil in 42% yield. Analytical data were in accordance with literature report (Bernini et al. 2009).

R_f: 0.38 (DCM/AcOEt 95:5)

^{1}H NMR: (300 MHz, acetone-d_6) δ (ppm): 7.20-6.80 (m, 8H), 2.27 (s, 6H).

^{13}C NMR: (75 MHz, acetone-d_6) δ (ppm): 170.0 (x2C), 151.2 (x2C), 144.2

(x2C), 140.4, 130.3, 129.7, 123.9, 120.1, 116.9 (x2C), 115.3, 113.6, 113.1, 21.1 (x2C).

(*E*)-4-(3,5-dihydroxystyryl)benzene-1,2-diol (Piceatannol) (**3**)

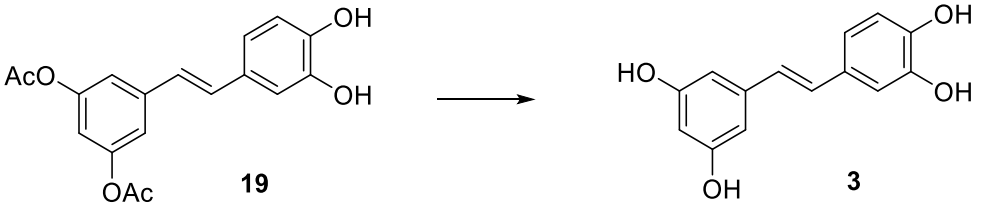

To the solution of **19** (93 mg, 0.28 mmol, 1 eq) in MeOH at room temperature, under nitrogen atmosphere, $NH_2NH_2 \cdot H_2O$ (55 µL, 1.13 mmol, 4 eq) was added and the reaction was stirred for 20 minutes. The solvent was evaporated, and the residue was diluted with AcOEt and acidified with aq 2N HCl under nitrogen until pH 1-2. The aqueous phase was extracted with AcOEt (4 x 10 mL). The combined organic layers were washed with brine (20 mL), dried over anhydrous Na_2SO_4, and concentrated under reduced pressure. The crude was purified by FC (DCM/MeOH 9:1) to afford the desired product as a white solid in 81% yield. Analytical data were in accordance with literature report (Han et al. 2009)

M.p.: 228-229°C

R_f: 0.31 (DCM/MeOH 9:1)

^{1}H NMR (300 MHz, acetone-d_6) δ (ppm): 8.15 (broad s, 4H,) 7.10 (d, *J* = 1.8 Hz,1H), 6.95 (d, *J* = 16.5 Hz, 1H), 6.90 (dd, J_1 = 8.4, J_2 = 1.8 Hz, 1H), 6.83 (d, J = 9.0 Hz, 1H), 6.82 (d, J = 16.2 Hz, 1H), 6.57 (d, J =1.8 Hz, 2H), 6.31 (t, J = 2.1 Hz, 1H).

^{13}C NMR (75 MHz, acetone-d_6) δ (ppm): 158.6 (x2C), 145.3, 145.2, 140.2, 130.0, 128.8, 126.2, 119.5, 115.7, 113.2, 105.2 (x2C), 102.1.

(*E*)-5-((±)-2-(3-(3,5-dihydroxyphenyl)-2-(4-hydroxyphenyl)-2,3-dihydrobenzofuran-5-yl)vinyl)benzene-1,3-diol (δ-viniferin)- (±)-10

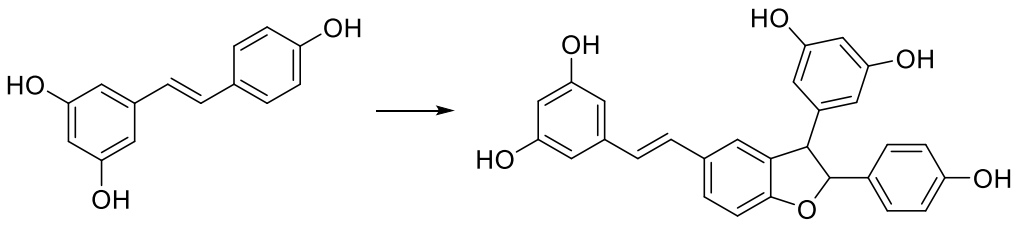

1 (±)-**10**

To a solution of **1** (1g, 4.38 mmol, 1 eq) in a mixture acetone/citrate buffer (pH 5) 1:1 (43.8 mL) was added a solution of HRP (1.75 mL, 1 mg/mL aqueous solution) at 40°C and the resulting mixture stirred for 30 minutes. Then, H_2O_2 30% (0.66 mL) was added and the mixture was stirred at the same temperature for 1h. Acetone was evaporated and the aqueous layer was extracted with AcOEt (3 x 50 mL). The combined organic layers were washed with brine, dried over anhydrous Na_2SO_4, and concentrated under reduced pressure. The residue was purified by flash column chromatography (DCM/MeOH 9:1) to give the desired product as a yellow amorphous solid in 48% yield. Analytical data were in agreement with the literature report (Pezet et al. 2003)

R_f: 0.25 (DCM/MeOH 9:1)

^{1}H NMR (300 MHz, CD_3OD) δ (ppm): 7.40 – 7.33 (m, 1H), 7.20 – 7.13 (m, 3H), 6.97 (d, *J* = 16.3 Hz, 1H), 6.87 – 6.74 (m, 4H), 6.42 (d, *J* = 2.2 Hz, 2H), 6.19 (t, *J* = 2.2 Hz, 1H), 6.14 (t, *J* = 2.2 Hz, 1H), 6.12 (d, *J* = 2.2 Hz, 2H), 5.38 (d, *J* = 8.4 Hz, 1H), 4.40 (d, *J* = 8.4 Hz, 1H).

^{13}C NMR (100 MHz, CD_3OD) δ (ppm): 161.0, 160.0 (x2C), 159.7 (x2C), 158.8, 145.4, 141.2, 132.9, 132.4 (x2C), 129.4, 128.7 (x3C), 127.5, 124.2, 116.3 (x2C), 110.4, 107.7 (x2C), 105.8 (x2C), 102.7, 102.5, 94.9, 58.0.

5-((*E*)-2-((2*S*,3*S*)-3-(3,5-dihydroxyphenyl)-2-(4-hydroxyphenyl)-2,3-dihydrobenzofuran-5-yl)vinyl)benzene-1,3-diol-(*S*,*S*)-(+)-4

5-((*E*)-2-((2*R*,3*R*)-3-(3,5-dihydroxyphenyl)-2-(4-hydroxyphenyl)-2,3-dihydrobenzofuran-5-yl)vinyl)benzene-1,3-diol-(*R*,*R*)-(–)-4

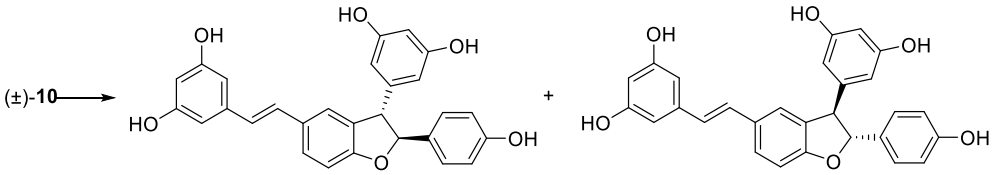

(2S,3S)-(+)-**10** (2*R*,3*R*)-(–)-**10**

The separation of the two enantiomers (*S*,*S*)-(+)-**4** and (*R*,*R*)-(–)-**4** was carried out by HPLC-UV using a chiral column (Kromasil-5 Ami Coat, 250×21.2 mm, λ = 280 nm) and an isocratic elution (hexane: iPrOH 70:30 + 0.1% TFA, rate flow 15 mL/min^{-1}).

(2*S*,3*S*)-(+)-**4**, t_R= 6.3 min $[\alpha]_D$= +38 (*c* 0.5, MeOH)

(2*R*,3*R*)-(–)**4**, t_R= 8.4 min; $[\alpha]_D$= –34 (*c* 0.5, MeOH)

(*E*)-5-((±)-6-hydroxy-2-(4-hydroxyphenyl)-4-(4-hydroxystyryl)-2,3-dihydrobenzofuran-3-yl)benzene-1,3-diol (*trans*-ε-viniferin)-(±)-11

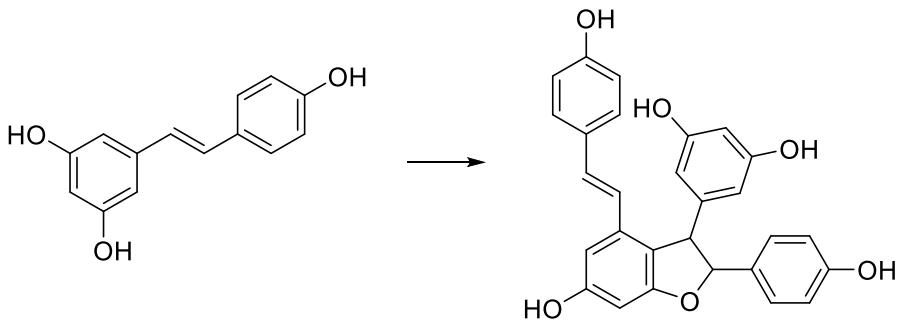

1 (±)-**11**

To a solution of **1** (2 g, 8.76 mmol, 1 eq) in MeOH (20 mL) a solution of $FeCl_3 \cdot 6H_2O$ (2.39 g, 8.85 mmol, 1.01 eq) in water (20 mL) was added dropwise. The mixture was stirred at room temperature for 48 hours. MeOH was evaporated and the residue was diluted with water (30 mL) and extracted with AcOEt (4 x 50 mL). The combined organic layers were dried over anhydrous Na_2SO_4, and concentrated under reduced pressure. The residue was purified by FC (cyclohexane/acetone 3:2) and a mixture of (±)-**5** and *cis*-analogue was obtained. A further purification by reverse phase column chromatography (H_2O/MeOH 2:3) gave the desired product as a light green amorphous solid in 15% yield. Analytical data were in agreement with those reported in literature (Vo and Elofsson 2016)

R_f: 0.30 (cyclohexane/acetone 3:2) - 0.42 (H_2O/MeOH 2:3)

^{1}H NMR (300 MHz, C*D*$_3$O*D*) δ (ppm): 7.18 – 7.11 (m, 2H), 7.07 – 7.01 (m, 2H), 6.86 – 6.73 (m, 3H), 6.64 (dd, *J* = 8.7, 2.1 Hz, 3H), 6.56 (d, *J* = 16.3 Hz, 1H), 6.25 (d, *J* = 2.1 Hz, 1H), 6.20 – 6.14 (m, 3H), 5.36 (d, *J* = 6.6 Hz, 1H), 4.34 (d, *J* = 6.6 Hz, 1H).

^{13}C NMR (100 MHz, C*D*$_3$O*D*) δ (ppm): 162.8, 160.1, 159.8, 159.7, 158.5, 158.4, 147.4, 137.0, 136.9, 133.9, 130.5, 130.4, 128.8, 128.2, 123.8, 123.7, 120.1, 116.4 (x2C), 116.3 (x2C), 107.5 (x2C), 104.4, 102.2, 96.9, 94.9, 58.3.

5-((2*R*,3*R*)-6-hydroxy-2-(4-hydroxyphenyl)-4-((*E*)-4-hydroxystyryl)-2,3-dihydrobenzofuran-3-yl)benzene-1,3-diol (2*R*,3*R*)-(+)-11

5-((2*S*,3*S*)-6-hydroxy-2-(4-hydroxyphenyl)-4-((*E*)-4-hydroxystyryl)-2,3-dihydrobenzofuran-3-yl)benzene-1,3-diol (2*S*,3*S*)-(–)-11

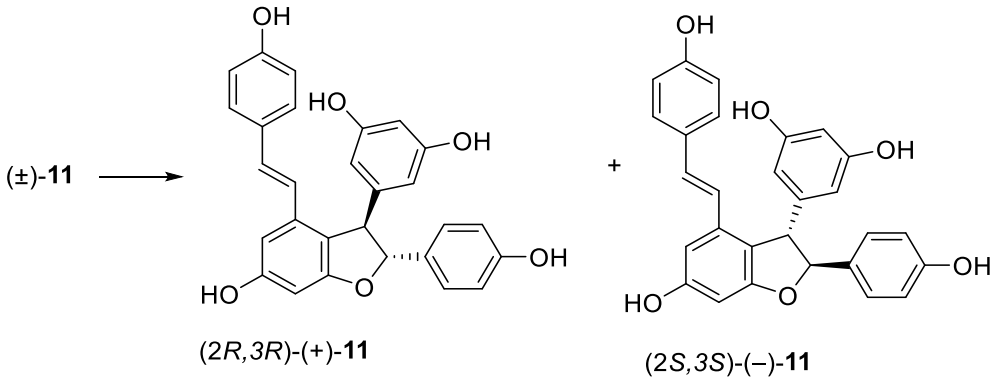

(2*R,3R*)-(+)-**11** (2*S,3S*)-(–)-**11**

The separation of the two enantiomers (2*R*,3*R*)-(+)-**5** and (2*S*,3*S*)-(–)-**5** was carried out by HPLC-UV using a chiral column (Kromasil-5 Ami Coat, 250×21.2 mm, λ=280nm) and an isocratic elution (hexane: iPrOH 60:40 + 0.1% TFA, rate flow 15 mL/min^{-1}).

(2*R*,3*R*)-(+)-**5**, t_R= 4 min $[\alpha]_D$= –29 (*c* 0.3, MeOH)

(2*S*,3*S*)-(–)-**5**, t_R= 6 min $[\alpha]_D$= +30 (*c* 0.3, MeOH)

(±)-5,10-bis(4-hydroxyphenyl)-4b,5,9b,10-tetrahydroindeno[2,1-a]indene-1,3,6,8-tetraol (pallidol) (±)-**12**

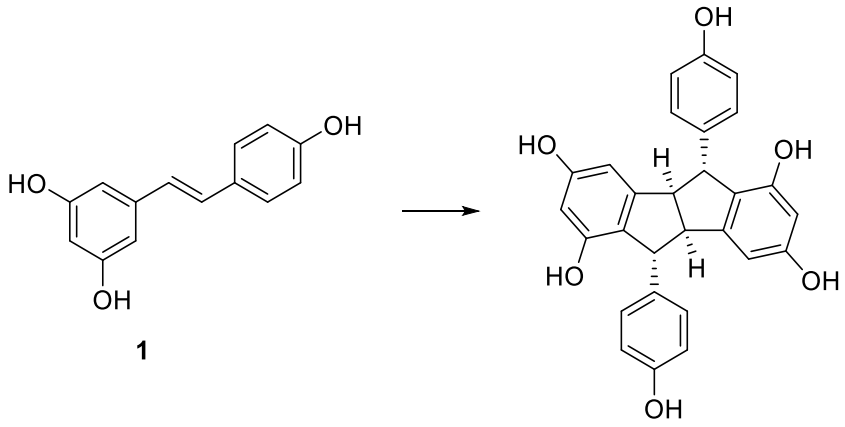

To a solution of **1** (1 g, 4.38 mmol, 1 eq) in a mixture of acetone/phosphate buffer (pH 8) 1:1 (43.8 mL), a solution of HRP (1.75 mL, 1 mg/mL aqueous solution) was added at 40°C and the resulting mixture was stirred for 30 minutes. Then, H_2O_2 30% (0.66 mL) was added and the mixture was stirred at the same temperature for 1h. Acetone was evaporated and the aqueous layer was extracted with AcOEt (3 x 50 mL). The combined organic layers were washed with brine, dried over anhydrous Na_2SO_4, and concentrated under reduced pressure. The residue was purified by flash column chromatography (DCM/MeOH 85:15) to give the desired product as brown solid in 21% yield. Analytical data were in agreement with those reported in literature (Snyder et al. 2009)

M.p.: dec. T>296°C

R_f: 0.15 (DCM/MeOH 9:1)

^{1}H NMR (300 MHz, C*D*$_3$O*D*) δ (ppm): 6.99 – 6.87 (m, 4H), 6.73 – 6.59 (m, 4H), 6.52 (d, *J* = 2.1 Hz, 2H), 6.10 (d, *J* = 2.1 Hz, 2H), 4.46 (s, 2H), 3.72 (s, 2H).

^{13}C NMR (**75 MHz, Acetone-*d*$_6$)** δ (ppm): 159.3 (x2C), 156.3 (x2C), 155.3 (x2C), 150.3 (x2C), 137.7 (x2C), 129.0 (x4C), 123.2 (x2C), 115.8 (x4C), 103.3 (x2C), 102.5 (x2C), 60.5 (x2C), 53.9 (x2C).

(*E*)-4-((±)-3-(3,5-dimethoxyphenyl)-5-(3,5-dimethoxystyryl)-2,3-dihydrobenzofuran-2-yl)phenol (±)-**13**

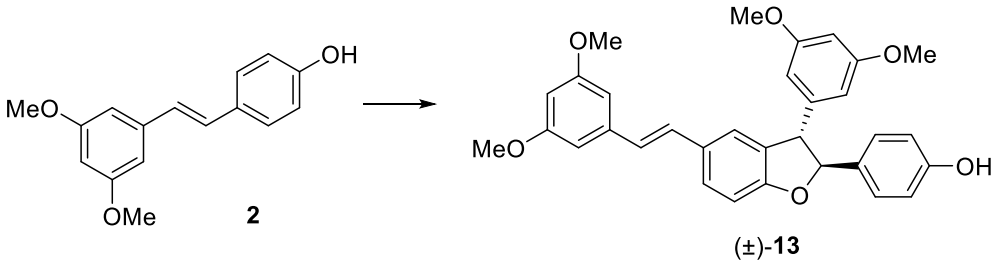

To a solution of **2** (100 mg, 0.39 mmol, 1 eq) in a mixture of acetone/citrate buffer (pH 5) 1:1 (3.8 mL), a solution of HRP (160 µl, 1 mg/mL aqueous solution) was added at 40°C and stirred for 30 minutes. Then H_2O_2 30% (59 µl, 0.573 mmol, 1.47 eq) was added and the mixture was stirred at the same temperature for 15 min. Then, acetone was evaporated and the aqueous layer was extracted with AcOEt (3 x 50 mL). The combined organic layers were washed with brine, dried over anhydrous Na_2SO_4 and concentrated under reduced pressure. The residue was purified by FC (cyclohexane/AcOEt 7:3) to give the desired product as a white amorphous solid in 61% yield. Analytical data were in agreement with those reported in literature (Velu et al. 2008)

R_f: 0.2 (cyclohexane/AcOEt 3:1)

^{1}H NMR (300 MHz, C*D*Cl$_3$) δ (ppm): 7.37 (dd, J_1 = 8.3, J_2 = 0.8 Hz, 1H), 7.24 – 7.19 (m, 3H), 7.02 (d, J = 16.2 Hz, 1H), 6.92 (d, J = 8.3 Hz, 1H), 6.88 – 6.78 (m, 3H), 6.62 (d, J = 2.3 Hz, 2H), 6.41 (t, J = 2.2 Hz, 1H), 6.36 (t, J = 2.2 Hz, 1H) 6.34 (d, J = 2.2 Hz, 2H), 5.51 (d, J = 8.4 Hz, 1H), 4.48 (d, J = 8.4 Hz, 1H), 3.81 (s, 6H), 3.75 (s, 6H).

^{13}C NMR (75 MHz, C*D*Cl$_3$) δ (ppm): 161.2 (x2C), 161.0 (x2C), 159.8, 156.0, 144.0, 139.8, 132.6, 132.3, 132.1, 130.9, 130.8, 129.1, 128.8, 128.0, 127.6, 126.3, 123.2, 115.6 (x2C), 109.8, 106.5 (x2C), 104.3 (x2C), 99.8, 57.9 (x2C), 55.5 (x2C).

(*E*)-5-((±)-6-acetoxy-2-(4-acetoxyphenyl)-4-(4-acetoxystyryl)-2,3-dihydrobenzofuran-3-yl)-1,3-phenylene diacetate-(±)-23

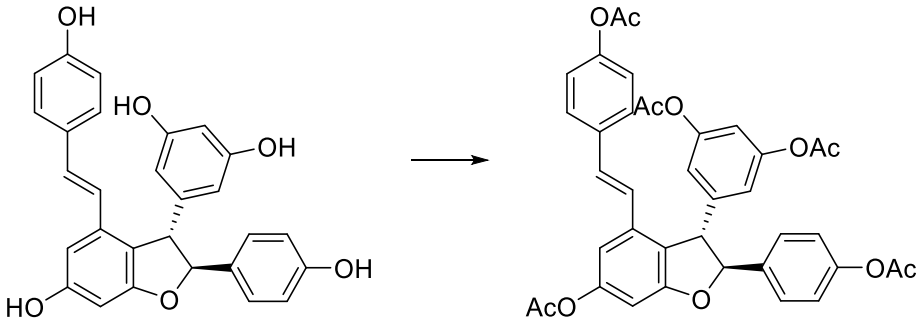

(±)-**11** (±)-**23**

To a solution of (±)-**11** (140 mg, 0.31 mmol, 1 eq) in DMSO (0.8 mL) and DCM (19.8 mL) at room temperature, Ac_2O (0.19 mL, 2 mmol, 6.6 eq) and TEA (0.63 mL, 4.56 mmol, 14.7 eq) were added and the mixture was stirred overnight. Solvent was evaporated and the residue was diluted with AcOEt (10 mL) and washed with $NaHCO_3$ 5% solution (10 mL). The aqueous phase was extracted with AcOEt (2 x 10 mL). The combined organic layers were washed with water (20 mL), dried over anhydrous Na_2SO_4, and concentrated under reduced pressure. The residue was purified by FC (cyclohexane/AcOEt 3:2) to afford the desired product as a white solid in 92% yield. Analytical data were in agreement with those reported in literature (Houillé et al. 2014)

M.p.: 78°C

R_f: 0.35 (cyclohexane/AcOEt 3:2)

^{1}H NMR (300 MHz, C*D*Cl$_3$) δ (ppm): 7.37 – 7.30 (m, 2H), 7.21 – 7.15 (m, 2H), 7.14 – 7.07 (m, 3H), 7.02 – 6.94 (m, 3H), 6.90 (t, *J* = 2.2 Hz, 1H), 6.86 (d, *J* = 2.2 Hz, 3H), 6.65 (d, *J* = 2.0 Hz, 1H), 6.54 (d, *J* = 16.2 Hz, 1H), 5.61 (d, *J* = 6.8 Hz, 1H), 4.60 (d, *J* = 6.9 Hz, 1H), 2.34 (s, 3H), 2.31 (s, 3H), 2.28 (s, 3H), 2.27 (s, 6H).

^{13}C NMR (75 MHz, C*D*Cl$_3$) δ (ppm): 169.5, 169.5 (x2C), 168.8 (x2C), 161.0, 152.2 (x2C), 151.8, 150.8, 150.5, 144.5, 138.1, 135.4, 134.5, 130.5, 127.9 (x2C), 126.8 (x2C), 124.2, 124.0, 122.1 (x2C), 121.9 (x2C), 118.7 (x2C), 114.9, 110.8, 103.0, 92.8, 56.8, 21.3 (x4C), 21.2.

(*E*)-5-((±)-2-(2-(4-acetoxyphenyl)-3-(3,5-diacetoxyphenyl)-2,3-dihydrobenzofuran-5-yl)vinyl)-1,3-phenylene diacetate (±)-**24**

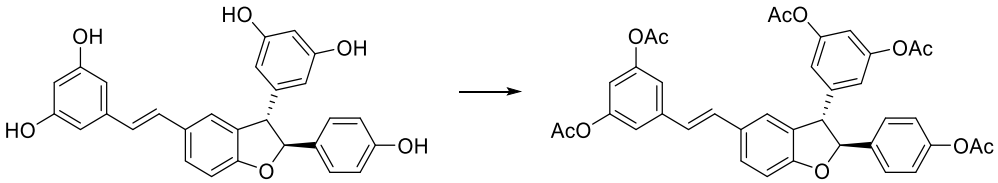

(±)-**10** (±)-**24**

To a solution of (±)-**10** (100 mg, 0.22 mmol, 1 eq) in DMSO (1.5 mL) and DCM (12 mL) at rt, Ac_2O (0.14 mL, 1.45 mmol, 6.6 eq) and TEA (0.45 mL, 3.2 mmol, 14.7 eq) were added and the mixture was stirred at room temperature overnight. Solvent was evaporated and the residue was diluted with AcOEt (10 mL) and washed with aq 5 %$NaHCO_3$ 5% (10 mL). The aqueous phase was extracted with AcOEt (2 x10 mL). The combined organic layers were washed with water (20 mL), dried over anhydrous Na_2SO_4 and concentrated under reduced pressure. The residue was purified by FC (cyclohexane/AcOEt 3:2) to afford the desired product in 90% yield as pale yellow oil. Analytical data were in agreement with those reported in literature (Soldi et al. 2014)

R_f: 0.32 (cyclohexane/AcOEt 3:2)

^{1}H NMR (300 MHz, C*D*Cl$_3$) δ (ppm): 7.39 – 7.31 (m, 3H), 7.20 (s, 1H), 7.13 – 7.08 (m, 2H), 7.07 (d, *J* = 2.1 Hz, 2H), 7.01 (d, *J* = 16.3 Hz, 1H), 6.97 – 6.87 (m, 3H), 6.82 (d, *J* = 2.2 Hz, 2H), 6.77 (t, *J* = 2.1 Hz, 1H), 5.55 (d, *J* = 8.0 Hz, 1H), 4.54 (d, *J* = 8.0 Hz, 1H), 2.30 (s, 3H), 2.29 (s, 6H), 2.27 (s, 6H).
^{13}C NMR (75 MHz, C*D*Cl$_3$) δ (ppm): 169.4, 169.0 (x2C), 168.9 (x2C), 159.9, 151.4 (x2C), 151.2 (x2C), 150.6, 143.7, 139.9, 137.7, 130.7, 130.2, 129.7 (x2C), 128.5, 126.9, 124.9, 123.4, 121.9 (x2C), 118.8 (x2C), 116.6 (x2C), 114.8, 113.9, 110.0, 92.4, 57.3, 21.1 (x5C).

(*E*)-5-(6-acetoxy-2-(4-acetoxyphenyl)-4-(4-acetoxystyryl)benzofuran-3-yl)-1,3-phenylene diacetate (**25**)

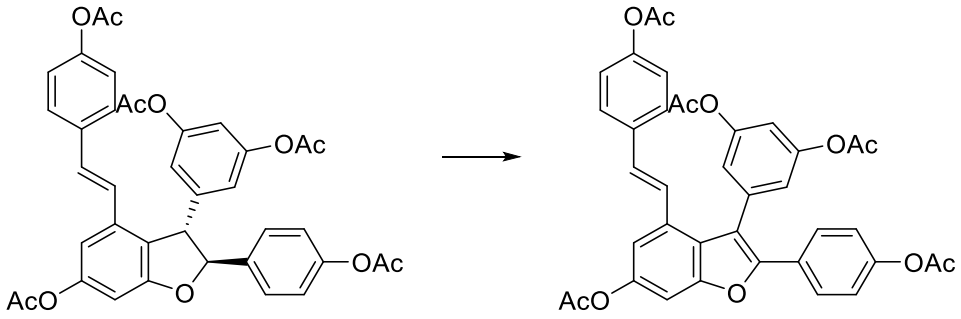

(±)-**23** **25**

To a solution of (±)-**23** (38 mg, 0.057 mmol, 1 eq) in DCM (5 mL) at room temperature was added DDQ (260 mg, 1.14 mmol, 20 eq). The mixture was stirred under reflux for 48 hours. The mixture was cooled to room temperature, then filtered on a celite pad and concentrated under reduced pressure. The residue was purified by FC (cyclohexane/AcOEt 7:3) to give the desired product as brownish sticky solid in 84% yield.

R_f: 0.3 (cyclohexane/AcOEt 3:2)

^{1}H NMR (300 MHz, C*D*Cl$_3$) δ (ppm): 7.60 – 7.54 (m, 2H),7.25 – 7.22 (m, 2H), 7.14 – 7.09 (m, 4H), 7.08 – 7.02 (m, 2H), 7.02 – 6.98 (m, 2H), 6.90 (d, *J* = 1.7 Hz, 1H), 2.38 (s, 3H), 2.29 (m, 6H), 2.25 (s, 6H).

(*E*)-5-(2-(2-(4-acetoxyphenyl)-3-(3,5-diacetoxyphenyl)benzofuran-5-yl)vinyl)-1,3-phenylene diacetate (**26**)

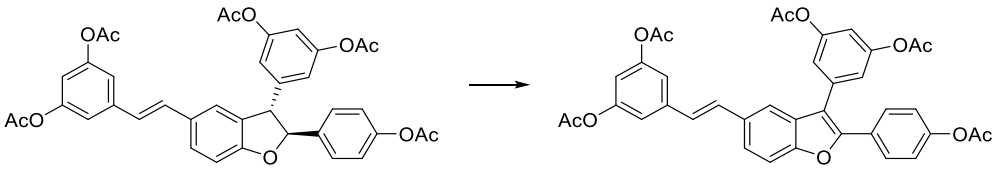

(±)-**24** **26**

To a solution of (±)-**26** (130 mg, 0.195 mmol, 1 eq) in DCM (10 mL) at room temperature was added DDQ (888 mg, 3.9 mmol, 20 eq). The mixture was stirred under reflux for 48 hours. The mixture was cooled to room temperature, then filtered on a celite pad and concentrated under reduced pressure. The residue was purified by FC (cyclohexane/AcOEt 7:3) to give the desired product in 60% yield, as white sticky solid.

R*f*: 0.28 (cyclohexane/AcOEt 7:3)

^{1}H NMR (300 MHz, C*D*Cl$_3$) δ (ppm): δ 7.76 – 7.71 (m, 2H), 7.62 (d, *J* = 1.3 Hz, 1H), 7.53 – 7.51 (m, 2H), 7.17 – 7.09 (m, 7H), 7.07 (d, *J* = 7.7 Hz, 1H), 7.03 (t, *J* = 2.1 Hz, 1H), 6.81 (t, *J* = 2.1 Hz, 1H), 2.31 (s, 15H).

^{13}C NMR (300 MHz, C*D*Cl$_3$) δ (ppm): 169.3, 169.1 (x2C), 168.9 (x2C), 153.9, 151.6, 151.3 (x2C), 150.9, 150.8, 139.8, 134.3, 132.3, 130.7, 130.1, 128.2 (x2C), 127.5 (x2C), 126.2, 123.9, 121.9 (x2C), 120.3, 118.1 (x2C), 116.8 (x2C), 115.7, 115.0, 114.1, 111.5, 21.2 (x5C).

(*E*)-5-(6-hydroxy-2-(4-hydroxyphenyl)-4-(4-hydroxystyryl)benzofuran-3-yl)benzene-1,3-diol-(dehydro-ε-viniferin) (**14**)

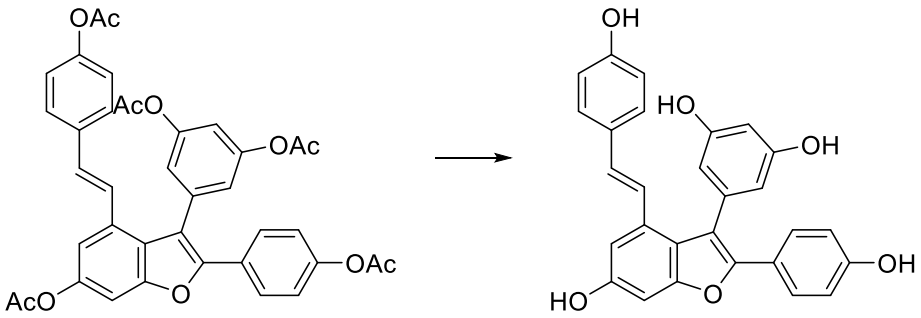

25 **14**

To the suspension of **25** (32 mg, 0.048 mmol, 1 eq) in MeOH at 0°C was added KOH 85% (32 mg, 0.48 mmol, 10 eq). The mixture was stirred at 0°C for 90 minutes and then acidified with aq 0.1M HCl until pH 1. MeOH was evaporated and the residue was diluted with water (5 mL), extracted with AcOEt (3 x 10 mL). The combined organic phases were washed with water (10 mL), brine (10 mL), dried over anhydrous Na_2SO_4 and concentrated under reduced pressure. The residue was purified by FC (cyclohexane/acetone 1:1) to afford the desired product in 55% yield, as yellow amorphous solid. Analytical data were in agreement with those reported in literature (Vo and Elofsson 2016)

R_f: 0.3 (cyclohexane/acetone 3:2)

^{1}H NMR (300 MHz, CD_3OD) δ (ppm): 7.45 – 7.40 (m, 2H), 7.01 – 6.92 (m, 4H), 6.85 (d, *J* = 16.3 Hz, 1H), 6.81 (d, *J* = 2.0 Hz, 1H), 6.72 – 6.68 (m, 2H), 6.68 – 6.63 (m, 2H), 6.48 (t, *J* = 2.0 Hz, 1H), 6.41 (d, *J* = 2.0 Hz, 2H).
^{13}C NMR (75 MHz, CD_3OD) δ (ppm): 160.7 (x2C), 158.5, 158.2, 156.6, 156.4, 150.6, 138.7, 133.3, 130.7, 129.3, 128.8 (x2C), 128.5 (x2C), 123.9, 123.3, 122.5, 117.4 (x2C), 116.4 (x2C), 116.2, 110.2, 107.4 (x2C), 103.1, 97.4**.**

(E)-5-(2-(3-(3,5-dihydroxyphenyl)-2-(4-hydroxyphenyl)benzofuran-5-yl)vinyl)benzene-1,3-diol-(dehydro-δ-viniferin)- (15)

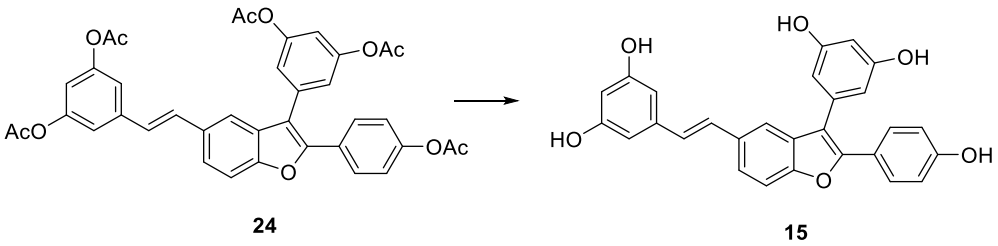

24 **15**

To the suspension of **24** (76 mg, 0.115 mmol, 1 eq) in MeOH at 0°C was added KOH 85% (76 mg, 1.15 mmol, 10 eq). The mixture was stirred at 0°C for 90 minutes and then acidified with aq 0.1M HCl until pH 1. MeOH was evaporated and residue was diluted with water (5 mL), extracted with AcOEt (3 x 10 mL). The combined organic phases were washed with water (10 mL), brine (10 mL), dried over anhydrous Na_2SO_4, and concentrated under reduced pressure. The residue was purified by FC (cyclohexane/acetone 1:1) to afford the desired product as a yellow amorphous solid in 70% yield. Analytical data were in agreement with those reported in literature (Beneventi et al. 2015)

R_f: 0.25 (DCM/MeOH 9:1)

^{1}H NMR (300 MHz, Acetone-d_6) δ (ppm): 7.65 (d, *J* = 1.3, 1H), 7.63 – 7.51 (m, 4H), 7.24 (d, *J* = 16.3 Hz, 1H), 7.06 (d, *J* = 16.3 Hz, 1H), 6.91 – 6.84 (m, 2H), 6.60 (d, *J* = 2.2 Hz, 2H), 6.52 (d, *J* = 2.2 Hz, 2H), 6.45 (t, *J* = 2.2 Hz, 1H), 6.30 (t, *J* = 2.2 Hz, 1H).

^{13}C NMR (150 MHz, DMSO-d_6): δ (ppm): 159.5 (x2C), 158.9 (x2C), 158.6, 153.1, 151.3, 133.0, 128.8 (x2C), 128.7, 128.3, 123.6, 117.9 (x2C), 116.0, 115.8, 111.6, 107.8 (x2C), 105.1 (x2C), 102.6, 102.4.

4-((2S,3S)-3-(3,5-dimethoxyphenyl)-5-((E)-3,5-dimethoxystyryl)-2,3-dihydrobenzofuran-2-yl)phenyl acetate (27)

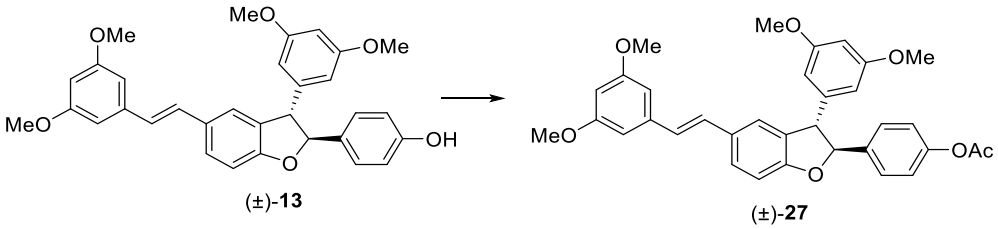

To a solution of **13** (300 mg, 0.587 mmol, 1 eq) in dry DCM (3.5 mL), TEA (245 µL, 1.761 mmol, 3 eq) and Ac_2O (83 µL, 0.881 mmol, 1.5 eq) were added and the resulting solution was stirred overnight. The reaction mixture was diluted with DCM (5 mL) and washed with water (10 mL). The aqueous layer was extracted with DCM (2x 15 mL). The combined organic layers were washed with aq 1M HCl (3 x 20 mL), aq 5% $NaHCO_3$ (40 mL), brine (40 mL), dried over anhydrous Na_2SO_4, filtered and evaporated. The product was obtained as a white sticky solid in 95% yield and was used as such for the next step.

R_f: 0.40 (CHX/AcOEt 7:3)

(E)-4-(3-(3,5-dimethoxyphenyl)-5-(3,5-dimethoxystyryl)benzofuran-2-yl)phenyl acetate - 28

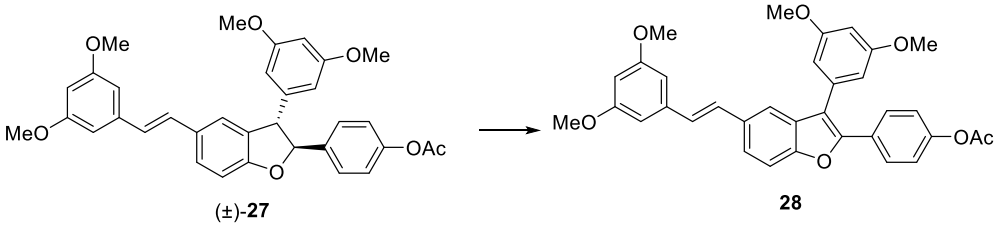

To the suspension of **27** (280 mg, 0.507 mmol, 1 eq) in toluene (35 mL), DDQ (2.3 g, 10.133 mmol, 20 eq) was added and the mixture was stirred at 40°C for 48 h. The solvent was evaporated, and the residue was partitioned

between DCM and water. The red aqueous phase was extracted with DCM three times. The combined organic phases were washed with aq $NaHCO_3$ 5% three times. The combined aquoues layers were extracted with DCM twice. The collected organic phases were dried over anhydrous Na_2SO_4, filtered and evaporated. The crude was used as such for the next step.

R_f: 0.51 (CHX/AcOEt 6:4)

^{1}H NMR (300 MHz, C*D*Cl$_3$) δ (ppm): 7.75 – 7.66 (m, 2H), 7.58 (d, *J* = 1.3 Hz, 1H), 7.53 – 7.51 (m, 2H), 7.17 (d, *J* = 16.2 Hz, 1H), 7.10 – 7.04 (m, 2H), 7.00 (d, *J* = 16.2 Hz, 1H), 6.67 (d, *J* = 2.3 Hz, 2H), 6.65 (d, *J* = 2.3 Hz, 2H), 6.56 (t, *J* = 2.3 Hz, 1H), 6.39 (t, *J* = 2.3 Hz, 1H), 3.83 (s, 3H), 3.80 (s, 3H), 2.30 (s, 3H).

(E)-4-(3-(3,5-dimethoxyphenyl)-5-(3,5-dimethoxystyryl)benzofuran-2-yl)phenol - 16

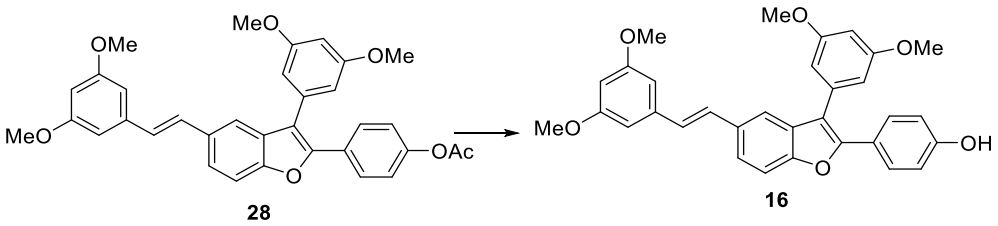

Compound **28** (280 mg, 0.507 mmol, 1 eq) was dissolved in THF (4 mL) and MeOH (8mL). At 0°C KOH 85% (101 mg, 1.521 mmol, 3 eq) was added and the mixture was stirred at the same temperature for 1h. The reaction mixture was quenched with aq 0.1 N HCl (20 mL). Organic solvents were evaporated and the acqueous phase was extracted with AcOEt three times. The combined organic layers were dried over anhydrous Na_2SO_4, filtered and evaporated. The residue was purified on silica gel by column chromatography, using as eluent CHX/AcOEt 7:3 to afford the desired product as foamy white solid in 93% yield over two steps.

R_f: 0.34 (CHX/AcOEt 7:3)

M.p.: 173-175°C

^{1}H NMR (600 MHz, C*D*Cl$_3$) δ (ppm): 7.63 – 7.55 (m, 3H), 7.51 (s, 2H), 7.18 (d, *J* = 16.2 Hz, 1H), 6.83 – 6.80 (2H, m), 6.68 (d, *J* = 2.2 Hz, 2H), 6.67 (d, *J* = 2.2 Hz, 2H), 6.55 ((t, *J* = 2.2 Hz, 1H), 6.40 (t, *J* = 2.2 Hz, 1H), 3.84 (s, 6H), 3.81 (s, 6H).

^{13}C NMR (150 MHz, C*D*Cl$_3$) δ (ppm): 161.3 (x2C), 160.9 (x3C), 155.9, 153.6, 151.3, 139.6, 134.8, 132.4, 130.8, 129.5, 128.7 (x2C), 127.5, 123.3, 123.1, 117.9, 116.0, 115.4 (x2C), 111.1, 107.7 (x2C), 104.4 (x2C), 99.9, 55.5 (x2C), 55.4 (x2C).

3.1.5. Bibliography

Akinwumi BC, Bordun KAM, Anderson HD (2018) Biological activities of stilbenoids. Int J Mol Sci 19:1–25. https://doi.org/10.3390/ijms19030792

Akkarachiyasit S, Charoenlertkul P, Yibchok-Anun S, Adisakwattana S (2010) Inhibitory activities of cyanidin and its glycosides and synergistic effect with acarbose against intestinal α-glucosidase and pancreatic α-amylase. Int J Mol Sci 11:3387–3396. https://doi.org/10.3390/ijms11093387

Araya-Cloutier C, Vincken JP, van Ederen R, den Besten HMW (2018) Rapid membrane permeabilization of *Listeria monocytogenes* and *Escherichia coli* induced by antibacterial prenylated phenolic compounds from legumes. Food Chem 240:147–155. https://doi.org/10.1016/j.foodchem.2017.07.074

Arioli S, Ragg E, Scaglioni L, Fessas D, Signorelli M, Karp M, Daffonchio D, De Noni I, Mulas L, Oggioni M, Guglielmetti S, Mora D (2010) Alkalizing reactions streamline cellular metabolism in acidogenic microorganisms. PLoS One 5:. https://doi.org/10.1371/journal.pone.0015520

Ayrapetyan M, Williams T, Oliver JD (2018) Relationship between the Viable but Nonculturable State and Antibiotic Persister Cells. J Bacteriol 200:e00249-18. https://doi.org/10.1128/JB.00249-18

Beneventi E, Conte S, Cramarossa MR, Riva S, Forti L (2015) Chemo-enzymatic synthesis of new resveratrol-related dimers containing the benzo[b]furan framework and evaluation of their radical scavenger activities. Tetrahedron 71:3052–3058. https://doi.org/10.1016/j.tet.2014.11.012

Bernini R, Barontini M, Spatafora C (2009) New lipophilic piceatannol derivatives exhibiting antioxidant activity prepared by aromatic hydroxylation with 2-iodoxybenzoic acid (IBX). Molecules 14:4669–4681. https://doi.org/10.3390/molecules14114669

Biasutto L, Marotta E, Mattarei A, Beltramello S, Caliceti P, Salmaso S, Bernkop-Schnurch A, Garbisa S, Zoratti M, Paradisi C (2009) Absorption and metabolism of resveratrol carboxyesters and methanesulfonate by explanted rat intestinal segments. Cell Physiol Biochem 24:557–566. https://doi.org/10.1159/000257512

Blair JMA, Webber MA, Baylay AJ, Ognolu DO, Piddock LJV (2015) Molecular mechanisms of antibiotic resistance. Nat Rev Microbiol 13:42–51. https://doi.org/10.1038/nrmicro3380

Bostanghadiri N, Pormohammad A, Chirani AS, Pouriran R, Erfanimanesh S, Hashemi A (2017) Comprehensive review on the antimicrobial potency

of the plant polyphenol Resveratrol. Biomed Pharmacother 95:1588–1595. https://doi.org/10.1016/j.biopha.2017.09.084

Cao H, Ou J, Chen L, Zhang Y, Szkudelski, Delmas D, Daglia M, Xiao J (2019) Dietary polyphenols and type 2 diabetes: Human Study and Clinical Trial. Crit Rev Food Sci Nutr 59:3371–3379. https://doi.org/10.1080/10408398.2018.1492900

Chibane BL, Degraeve P, Ferhout H, Bouajila J, Oulahal N (2019) Plant antimicrobial polyphenols as potential natural food preservatives. J Sci Food Agric 99:1457–1474. https://doi.org/10.1002/jsfa.9357

De La Torre MC, Sierra MA (2003) Comments on Recent Achievements in Biomimetic Organic Synthesis. Angew Chemie - Int Ed 43:160–181. https://doi.org/10.1002/anie.200200545

European Committee for Antimicrobial Susceptibility Testing (EUCAST) of the European SOciety of Clinical Microbiology and Infectious Diseases (ESCMID) (2003) Determination of minimum inhibitory concentrations (MICs) of antibacterial agents by broth dilution. Clin Microbiol Infect 9:1–7. https://doi.org/10.1046/j.1469-0691.2003.00790.x

Fernández L, Hancock REW (2012) Adaptive and mutational resistance: Role of porins and efflux pumps in drug resistance. Clin Microbiol Rev 25:661–681. https://doi.org/10.1128/CMR.00043-12

Ferreira S, Domingues F (2016) The antimicrobial action of resveratrol against Listeria monocytogenes in food-based models and its antibiofilm properties. J Sci Food Agric 96:4531–4535. https://doi.org/10.1002/jsfa.7669

Fujisawa T, Ikegami H, Inoue K, Kawabata Y, Ogihara T (2005) Effect of two α-glucosidase inhibitors, voglibose and acarbose, on postprandial hyperglycemia correlates with subjective abdominal symptoms. Metabolism 54:387–390. https://doi.org/10.1016/j.metabol.2004.10.004

Giuffredi GT, Purser S, Sawicki M, Thompson A, Gouverneur V (2009) Asymmetric de novo synthesis of fluorinated D-glucitol and D-mannitol analogues. Tetrahedron Asymmetry 20:910–920. https://doi.org/10.1016/j.tetasy.2009.03.001

Guidi B, Planchestainer M, Contente ML, Laurenzi T, Eberini I, Gourlay LJ, Romano D, Paradisi F, Molinari F (2018) Strategic single point mutation yields a solvent- and salt-stable transaminase from *Virgibacillus* sp . in soluble form. Sci Rep 8:ID 16441. https://doi.org/10.1038/s41598-018-34434-3

Han SY, Lee HS, Choi DH, Hwang JW, Yang DM, Jun JG (2009) Efficient total synthesis of piceatannol via (*E*)-selective wittig-horner reaction. Synth Commun 39:1425–1432. https://doi.org/10.1080/00397910802528944

Houillé B, Papon N, Boudesocque L, Bourdeaud E, Besseau S, Courdavault V, Enguehard-Gueiffier C, Delanoue G, Guérin L, Bouchara JP, Clastre M, Giglioli-Guivarc'h N, Guillard J, Lanoue A (2014) Antifungal activity of resveratrol derivatives against *Candida Species*. J Nat Prod 77:1658–1662. https://doi.org/10.1021/np5002576

D'Incecco P, Pellegrino L, Hogenboom JA, Cocconcelli PS, Bassi D (2018) The late blowing defect of hard cheeses : Behaviour of cells and spores of Clostridium tyrobutyricum throughout the cheese manufacturing and ripening. LWT - Food Sci Technol 87:134–141. https://doi.org/10.1016/j.lwt.2017.08.083

Kaduskar RD, Della Scala G, Al Jabri ZJH, Arioli S, Musso L, Oggioni MR; Dallavalle S, Mora D (2017) Promysalin is a salicylate-containing antimicrobial with a cell-membrane-disrupting mechanism of action on Gram-positive bacteria. Sci Rep 7:1–11. https://doi.org/10.1038/s41598-017-07567-0

Katzung BG (2018) Basic & Clinical Pharmacology, 14th edn.

Keylor MH, Matsuura BS, Stephenson CRJ (2015) Chemistry and Biology of Resveratrol-Derived Natural Products. Chem Rev 115:8976–9027. https://doi.org/10.1021/cr500689b

Komljenović I, Marquardt D, Harroun TA, Sternin E (2010) Location of chlorhexidine in DMPC model membranes: A neutron diffraction study. Chem Phys Lipids 163:480–487. https://doi.org/10.1016/j.chemphyslip.2010.03.007

Kosović E, Topiař M, Cuřínová P, Sajfrtová M (2020) Stability testing of resveratrol and viniferin obtained from *Vitis vinifera* L. by various extraction methods considering the industrial viewpoint. Sci Rep 10:1–9. https://doi.org/10.1038/s41598-020-62603-w

Lang M, Mühlbauer A, Jägers E, Steglich W (2008) Studies on the biosynthesis of bovilactone-4,4 and related fungal meroterpenoids. European J Org Chem 3544–3551. https://doi.org/10.1002/ejoc.200800232

Lee HS, Lee BW, Kim MR, Jun JG (2010) Syntheses of resveratrol and its hydroxylated derivatives as radical scavenger and tyrosinase inhibitor. Bull Korean Chem Soc 31:971–975. https://doi.org/10.5012/bkcs.2010.31.04.971

Lee S (2020) Bacteriocins of *Listeria monocytogenes* and Their Potential as a Virulence Factor. Toxins (Basel) 12:1–13. https://doi.org/10.3390/toxins12020103

Li C, Lu J, Xu X, Hu R, Pan Y (2012) PH-switched HRP-catalyzed dimerization of resveratrol: A selective biomimetic synthesis. Green Chem 14:3281–

3284. https://doi.org/10.1039/c2gc36288k

Li W, He X, Shi W, Jia H, Zhong B (2010) Pan-PPAR agonists based on the resveratrol scaffold: Biological evaluation and docking studies. ChemMedChem 5:1977–1982. https://doi.org/10.1002/cmdc.201000360

Lindgren AEG, Öberg CT, Hillgren JM, Elofsson M (2016) Total synthesis of the resveratrol oligomers (±)-Ampelopsin B and (±)-σ-Viniferin. European J Org Chem 2016:426–429. https://doi.org/10.1002/ejoc.201501486

Liou JW, Hung YJ, Yang CH, Chen YC (2015) The antimicrobial activity of gramicidin a is associated with hydroxyl radical formation. PLoS One 10:5–7. https://doi.org/10.1371/journal.pone.0117065

Ma DSL, Tan LTH, Chan KG, Yap WH, Pusparajah P, Chuah LH, Ming LC, Khan TM, Lee LH, Goh BH (2018) Resveratrol-potential antibacterial agent against foodborne pathogens. Front Pharmacol 9:1–16. https://doi.org/10.3389/fphar.2018.00102

Mattarei A, Biasutto L, Romio M, Zoratti M, Paradisi C (2015) Synthesis of resveratrol sulfates : turning a nightmare into a dream. Tetrahedron 71:3100–3106. https://doi.org/10.1016/j.tet.2014.09.063

Mattio LM, Catinella G, Dallavalle S, Pinto A (2020) Stilbenoids: A natural arsenal against bacterial pathogens. Antibiotics 9:1–40. https://doi.org/10.3390/antibiotics9060336

Mora-Pale M, Bhan N, Masuko S, James P, Wood J, McCallum S, Linhardt R, Dordick J, Koffas MAG (2015) Antimicrobial mechanism of resveratrol-trans-dihydrodimer produced from peroxidase-catalyzed oxidation of resveratrol. Biotechnol Bioeng 112:2417–2428. https://doi.org/10.1002/bit.25686

Navarro G, Martínez Pinilla E, Ortiz R, Noé V, Ciudad CJ, Franco R (2018) Resveratrol and Related Stilbenoids, Nutraceutical/Dietary Complements with Health-Promoting Actions: Industrial Production, Safety, and the Search for Mode of Action. Compr Rev Food Sci Food Saf 17:808–826. https://doi.org/10.1111/1541-4337.12359

Nøhr-Meldgaard K, Ovsepian A, Ingmer H, Vestergaard M (2018) Resveratrol enhances the efficacy of aminoglycosides against Staphylococcus aureus. Int J Antimicrob Agents 52:390–396. https://doi.org/10.1016/j.ijantimicag.2018.06.005

Dell'Omo G, Crescenti D, Vantaggiato C, Parravicini C, Borroni AP, Rizzi N, Garofalo M, Pinto A, Recordati C, Scanziani E, Bassi FB, Pruneri G, Conti P, Eberini I, Maggi A, Ciana P (2019) Inhibition of SIRT1 deacetylase and p53 activation uncouples the anti-in fl ammatory and chemopreventive actions of NSAIDs. Br J Cancer 120:537–546. https://doi.org/10.1038/s41416-018-0372-7

Oyenihi OR, Oyenihi AB, Adeyanju AA, Oguntibeju OO (2016) Antidiabetic Effects of Resveratrol: The Way Forward in Its Clinical Utility. J Diabetes Res ID 9737483. https://doi.org/10.1155/2016/9737483

Öztürk E, Arslan AKK, Yerer MB, Bishayee A (2017) Resveratrol and diabetes: A critical review of clinical studies. Biomed Pharmacother 95:230–234. https://doi.org/10.1016/j.biopha.2017.08.070

Parizad PA, Capraro J, Scarafoni A, Bonomi F, Blandino M, Marengo M, Giordano D, Carpen A, Iametti S (2019) The Bio-Functional Properties of Pigmented Cereals may Involve Synergies among Different Bioactive Species. Plant Foods Hum Nutr 74:128–134. https://doi.org/10.1007/s11130-019-0715-4

Pettit GR, Grealish MP, Jung MK, Hamel E, Pettit RK, Chapuis JC, Schmidt JM (2002) Antineoplastic agents. 465. Structural modification of resveratrol: Sodium resverastatin phosphate. J Med Chem 45:2534–2542. https://doi.org/10.1021/jm010119y

Pezet R, Perret C, Jean-Denis JB, Perret C, Jean-Denis BJ, Tabacchi R, Gindro K, Viret O (2003) δ-Viniferin, a resveratrol dehydrodimer: One of the major stilbenes synthesized by stressed grapevine leaves. J Agric Food Chem 51:5488–5492. https://doi.org/10.1021/jf030227o

Polunin KE, Schmalz HG (2004) Application of chromium-arene complexes in the organic synthesis. Efficient synthesis of stilbene phytoalexins. Russ J Coord Chem Khimiya 30:252–261. https://doi.org/10.1023/B:RUCO.0000022800.70211.7d

Quideau S, Deffieux D, Douat-Casassus C, Pouységu L (2011) Plant polyphenols: Chemical properties, biological activities, and synthesis. Angew Chemie - Int Ed 50:586–621. https://doi.org/10.1002/anie.201000044

Shibutani S, Samejima M, Doi S (2004) Effects of stilbenes from bark of Picea glehnii (Sieb. et Zucc) and their related compounds against feeding behaviour of Reticulitermes speratus (Kolbe). J Wood Sci 50:439–444. https://doi.org/10.1007/s10086-003-0583-1

Singh D, Mendonsa R, Koli M, Subramanian M, Nayak SK (2019) Antibacterial activity of resveratrol structural analogues: A mechanistic evaluation of the structure-activity relationship. Toxicol Appl Pharmacol 367:23–32. https://doi.org/10.1016/j.taap.2019.01.025

Snyder SA, Breazzano SP, Ross AG, Lin Y, Zografos A (2009) Total synthesis of diverse carbogenic complexity within the resveratrol class from a common building block. J Am Chem Soc 131:1753–1765. https://doi.org/10.1021/ja806183r

Soldi C, Lamb KN, Squitieri RA, Gonzalez-Lopez M, Di Maso MJ, Shaw JT

(2014) Enantioselective intramolecular C-H insertion reactions of donor-donor metal carbenoids. J Am Chem Soc 136:15142–15145. https://doi.org/10.1021/ja508586t

Tundis R, Loizzo MR, Menichini F (2010) Natural Products as Alpha-Amylase and Alpha-Glucosidase Inhibitors and their Hypoglycaemic Potential in the Treatment of Diabetes: An Update. Mini-Reviews Med Chem 10:315–331. https://doi.org/10.2174/138955710791331007

Velu S, Thomas N, Weber JF (2012) Strategies and methods for the syntheses of natural oligomeric stilbenoids and analogues. Curr Org Chem 605–662

Velu SS, Buniyamin I, Ching LK, Feroz F, Noorbatcha I, Gee LC, Awang K, Wahab IA, Weber JFF (2008) Regio- and stereoselective biomimetic synthesis of oligostilbenoid dimers from resveratrol analogues: Influence of the solvent, oxidant, and substitution. Chem - A Eur J 14:11376–11384. https://doi.org/10.1002/chem.200801575

Vestergaard M, Ingmer H (2019) Antibacterial and antifungal properties of resveratrol. Int J Antimicrob Agents 53:716–723. https://doi.org/10.1016/j.ijantimicag.2019.02.015

Vitrac X, Bornet A, Vanderlinde R, Valls J, Richard T, Delaunay JC, Merillon JM, Teissédre PL (2005) Determination of stilbenes (δ-viniferin, *trans*-astringin, *trans*-piceid, cis- and *trans*-resveratrol, ε-viniferin) in Brazilian wines. J Agric Food Chem 53:5664–5669. https://doi.org/10.1021/jf050122g

Vo DD, Elofsson M (2016) Total Synthesis of Viniferifuran, Resveratrol-Piceatannol Hybrid, Anigopreissin A and Analogues – Investigation of Demethylation Strategies. Adv Synth Catal 358:4085–4092. https://doi.org/10.1002/adsc.201601089

Vulfson EN, Halling PJ, Holland HL (2001) Enzymes in Nonaqueous Solvents, Methods and Protocols. Nat Prod Rep 18:579–582. https://doi.org/10.1039/b105988m

Wu Y, Bai J, Zhong K, Huang Y, Qi H, Jiang Y, Gao H (2016) Antibacterial activity and membrane-disruptive mechanism of 3-*p*-*trans*-coumaroyl-2-hydroxyquinic acid, a novel phenolic compound from pine needles of Cedrus deodara, against Staphylococcus aureus. Molecules 21:1084. https://doi.org/10.3390/molecules21081084

Yang J, Cohen Stuart MA, Kamperman M (2014) Jack of all trades: Versatile catechol crosslinking mechanisms. Chem Soc Rev 43:8271–8298. https://doi.org/10.1039/c4cs00185k

Yang SC, Tseng CH, Wang PW, Lu PL, Weng YH, Yen FL, Fang JY (2017) Pterostilbene, a methoxylated resveratrol derivative, efficiently

eradicates planktonic, biofilm, and intracellular MRSA by topical application. Front Microbiol 8:1103. https://doi.org/10.3389/fmicb.2017.01103

Zakova T, Rondevaldova J, Bernardos A, Landa P, Kokoska L (2018) The relationship between structure and in vitro antistaphylococcal effect of plant-derived stilbenes. Acta Microbiol Immunol Hung 65:467–476. https://doi.org/10.1556/030.65.2018.040

3.2. SAR STUDIES ON DEHYDRO-δ- AND DEHYDRO-ε-VINIFERIN FOR ANTIMICROBIAL ACTIVITY AGAINST THE FOODBORNE PATHOGEN *L. MONOCYTOGENES*

ABSTRACT: From the studies on the antimicrobial activity on resveratrol-derived monomers and dimers against a panel of foodborne pathogens, dehydro-δ-viniferin (**15**) and dehydro-ε-viniferin (**14**) resulted to be promising antibacterial agents against Gram-positive strains. In order to identify the structural elements relevant to the antimicrobial potency on the foodborne pathogen *L. monocytogenes* Scott A, as representative of Gram-positive microorganisms, a series of simplified analogues of dehydro-δ-viniferin and dehydro-ε-viniferin was designed and synthesized. By systematically removing the aromatic moieties of the parent precursors, we could elucidate the most relevant structural features involved in the antibacterial activity. While removal of every phenolic moiety from dehydro-δ-viniferin scaffold resulted in significant loss of activity, the structural simplification of dehydro-ε-viniferin (MIC 16 μg/mL, MBC > 512 μg/mL) led to the analogue **34** with improved antimicrobial potency (MIC 8 μg/mL, MBC > 64 μg/mL). Moreover, the compounds were tested for their cytotoxicity.

3.2.1. Introduction

To elucidate the relevant molecular features of the most active dimers relevant to the antibacterial activity on the foodborne pathogen *L. monocytogenes*, a series of simplified analogues of dehydro-δ-viniferin (**15**) and dehydro-ε-viniferin (**16**) was designed and synthesized. Both dehydro-δ-viniferin and dehydro-ε-viniferin consist of a benzofuran core bearing two phenol rings at the position 2 and 3 and a third phenol ring linked by an olefin bridge at position 5 or 4, respectively. To shed light on the minimal structural features crucial to the antimicrobial activity, the moieties linked to the benzofuran core (groups A, B, and C) were systematically removed to give compounds **29**-**31** as simplified analogues of dehydro- δ-viniferin (**15**), and compounds **32**-**34**, as simplified analogues of dehydro-ε-viniferin (**14**) (Figure 3.16). Furthermore,

we designed three representative methoxylated analogues (**35**-**37**). All compounds obtained were tested against *L. monocytogenes* Scott A.

Looking at the literature, we found that benzofuran derivatives have attracted the interest of several researcher, since these heterocyclic compounds are present in a large number of bioactive natural compounds, endowed with anticancer, antimicrobial, immunomodulatory, antioxidant and anti-inflammatory properties (Khanam and Shamsuzzaman 2015; Naik et al. 2015; Chand et al. 2017; Miao et al. 2019). Moreover, in the last years, the benzofuran motif has appeared as a pharmacophore of choice for the design of new antimicrobial agents, and numerous results have revealed the great potential of benzofuran-containing compounds in this research field (Hiremathad et al. 2015; Elsherif et al. 2020).

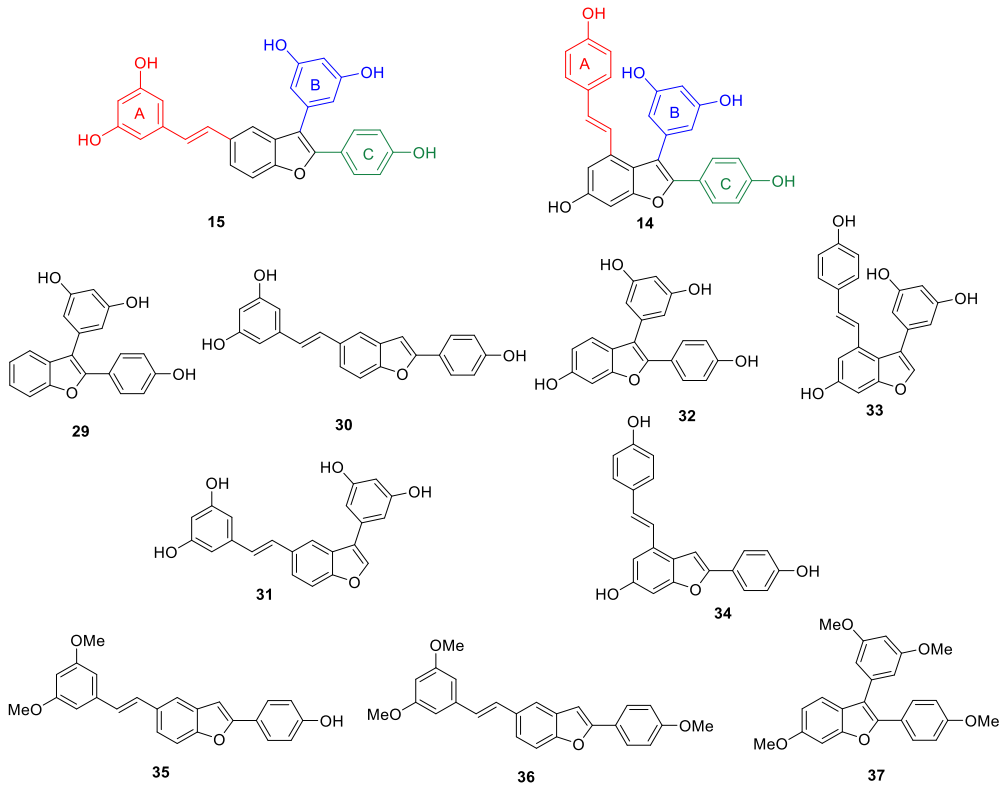

Figure 3.16. *Structures of compounds* ***14*** *and* ***15*** *and of the simplified analogues* ***29***-***37****.*

3.2.2. Material and methods

3.2.2.1. Chemical synthesis

Procedures for the synthesis, isolation, and characterization data for the various compounds obtained are detailed in the experimental section 3.2.4.

3.2.2.2. Evaluation of MIC and MBC

MIC and MBC values of compounds were evaluate on *L. monocytogenes*, as described in section 3.1.3.2.

3.2.2.3. Cytotoxicity on Human Skin Normal WS1 Fibroblast Cells

The normal human skin WS1 fibroblast cells (ATCC CRL-1502) were cultured in Eagle's Minimum Essential Medium plus 10% fetal bovine serum at 37 ◦C and 5% CO2. Cytotoxic potency was assessed by a growth inhibition assay (CellTiter 96® AQueous One Solution Cell Proliferation Assay MTS, Promega). The cells were seeded in a 96-well plate, and 24 h later were exposed to the compounds (concentration range 1−200 μM). After 48 h of exposure, 20 μL of 3-(4,5-dimethylthiazol-2-yl)-5-(3-carboxymethoxyphenyl)-2-(4-sulfophenyl)-2H-tetrazolium salt was added to each well. The absorbance was measured using a FLUOstar OPTIMA plate reader (BMG Labtech GmbH, Offenburg, Germany) at 492 nm after 4 h of incubation at 37 ◦C in 5% CO2. The IC50 was defined as the drug concentration causing 50% cell growth inhibition, determined by the dose−response curves. Experiments were performed in triplicate.

3.2.3. Results and discussions

The synthesis of the designed compounds required the development of different synthetic strategies depending on the nature of the benzofuran substitution pattern (Figure 3.16).

Firstly, we focused on the synthesis of the simplified analogues of dehydro-δ-viniferin (compounds **29**-**31**). Following the synthetic approach by Markina *et al.* (Markina et al. 2013) to obtain 2-aryl substituted benzofuran rings, we

performed a Cu-catalyzed tandem Sonogashira coupling-cyclization reaction, starting from 2-iodophenol (**38**) and 1-ethynilanisole (**39**). Then, iodination of compound **40** with *N*-iodosuccinimide (NIS), in presence of *p*-toluensulfonic acid, gave compound **41** in 74% yield (Yao et al. 2014). Subsequent Suzuki coupling of **41** with (3,5-dimethoxyphenyl)boronic acid and deprotection of the phenolic functions with BBr_3 yield the 2,3-substituted benzofuran **29** (Scheme 3.7).

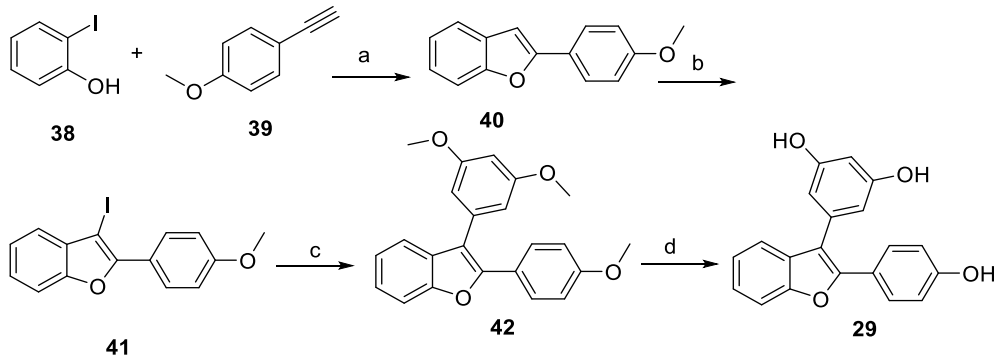

Scheme 3.7. Reagents and conditions: a) i) $PdCl_2(PPh_3)_2$ (5% mol), CuI (3% mol), TEA/THF 1:1, N_2, 40 °C, 40 min; ii) ACN, 100 °C, 90 min, 50%; b) NIS, *p*-TsOH, ACN, N_2, overnight, 74%; c) (3,5-dimethoxyphenyl)boronic acid, K_2CO_3, $PdCl_2$(dppf)·DCM, THF/H_2O 1:1, MW, 70 °C, 30 min, 83%; d) BBr_3, DCM, 0 °C to rt, overnight, 61%.

The Cu-catalyzed tandem Sonogashira coupling cyclization was applied also to the synthesis of compound **30** (Scheme 3.8). In this case, the iodophenol should bear a functional group enabling the installation of the styryl moiety on position 5 of the benzofuran ring. Therefore, compound **43** was reacted with **39** to yield compound **44**, which was converted into the corresponding aldehyde **45** by reduction with $LiAlH_4$, followed by the oxidation of the obtained alcohol with Dess-Martin periodinane (DMP). Following a procedure described by Vo and Elofsson (Vo and Elofsson 2016), a Wittig-Horner olefination with diethyl-(3,5-dimethoxyphenyl)phosphonate under microwave irradiation afforded the desired compound **36** in 76% yield. Unfortunately, the final deprotection of all phenol groups resulted to be very troublesome. In previous works, stilbenoids demethylation was achieved by BBr_3 in DCM (Kraus and Gupta 2009; Miliovsky et al. 2013). However, when we applied

standard conditions to **36**, surprisingly we observed the selective demethylation of the *para*-hydroxy group of the ring at the 2 position of the benzofuran core to afford **35** in 60% yield. When we used more equivalents of BBr_3 or increased the temperature and time of reaction, we obtained only degradation products. Indeed, stilbenoids, because of the olefinic bridge, have been described to lead to the formation of dimers and polymers in presence of a variety of acids, including BBr_3, through the formation of carbocations at the α position of the electron-rich aromatic rings (Li and Ferreira 2003; Velu et al. 2012). Therefore, we applied the alternative approach employed by Vo *et al.* (Vo and Elofsson 2016), who also faced the demethylation problem with stilbenoid compounds by using boron trichloride/tetra-*n*-butylammonium iodide (BCl_3/TBAI). This alternative method allowed to obtain the fully demethylated derivative **30**, though preparative HPLC was necessary to separate it from the side product deriving from the partial halogenation of the double bond.

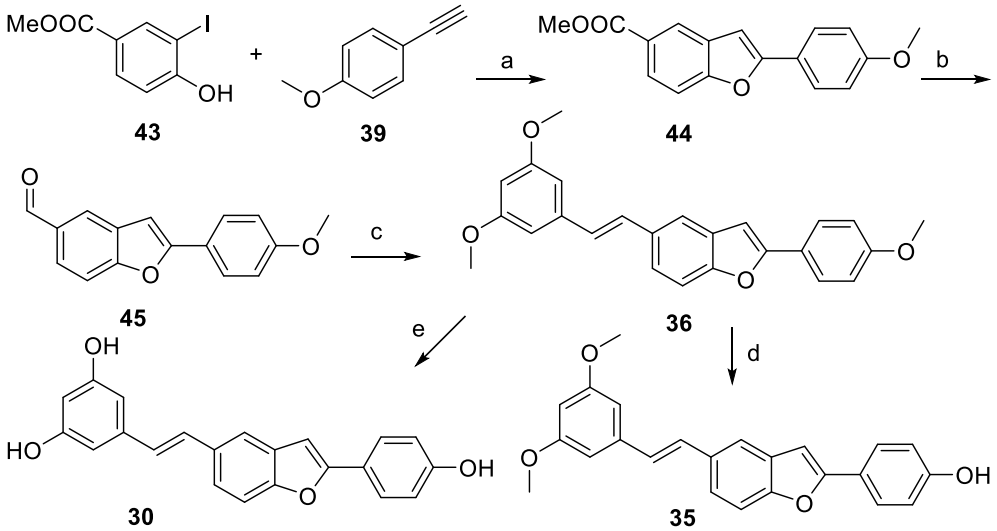

Scheme 3.8. Reagents and conditions: a) i) $PdCl_2(PPh_3)_2$ (5% mol), CuI (3% mol), TEA/THF 1:1, N_2, 40 °C, 40 min; ii) ACN, 100 °C, 90 min, 62%; b) i) $LiAlH_4$, THF, N_2, 0 °C, 10 min, 77%; ii) DMP, DCM, 0 °C 15 min, rt, 90 min, 85%; c) diethyl (3,5-dimethoxyphenyl)phosphonate, NaH, THF, MW, 120 °C, 30 min, 76%; d) BBr_3, DCM, 0 °C to rt, overnight, 60%; e) BCl_3, TBAI, DCM, N_2, 0 °C to rt, 6h, 35%.

A completely different synthetic approach was applied for the synthesis of compound **31**, functionalized on position 3 and 5 (Scheme 3.9). We synthesized the benzofuran core from compound **46** by alkylation with bromoacetaldehyde dimethylacetale and subsequent cyclohydration of **47** with Amberlyst-15, following a procedure described by Liu *et al.* (Liu et al. 2016). A bromine was selectively introduced at the position 3 of the obtained benzofuran core by bromination of **48**, followed by treatment with KOH in MeOH, following a protocol of Saitoh *et al* (Saitoh et al. 2009). Suzuki coupling reaction of compound **50** with (3,5-dimethoxyphenyl)boronic acid afforded compound **51**, which was converted into aldehyde **52** by reduction with $LiAlH_4$ and DMP oxidation. Compound **53** was obtained by Wittig-Horner olefination with diethyl(3,5-dimethoxyphenyl)phosphonate, under microwave irradiation at 120°C for 30 minutes. The deprotection of the stilbenoid compounds resulted again troublesome. After several attempts, compound **31** was obtained in 14% yield by reaction with BBr_3 and purification by flash chromatography.

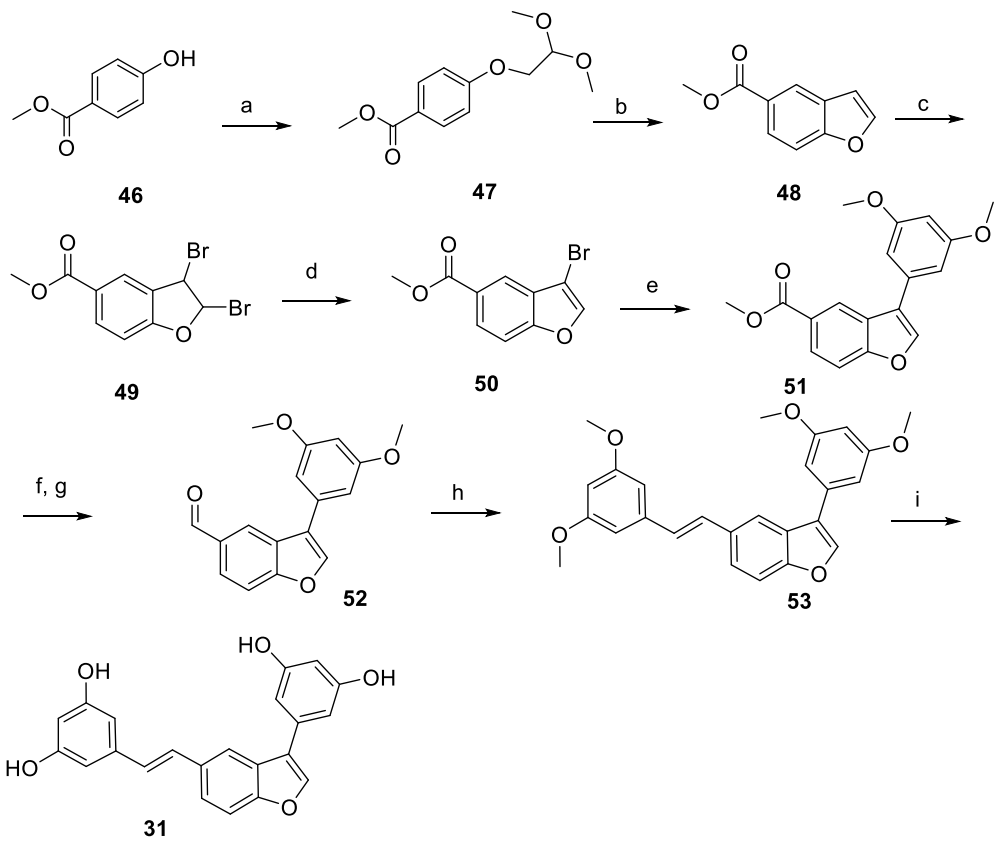

Scheme 3.9. Reagents and conditions: a) 2-bromo-1,1-dimethoxyethane, Cs_2CO_3, MeCN, reflux, 3 days, 61%; b) amberlyst-15, toluene, reflux, 6h, 51%; c) Br_2, DCM, 0 °C to rt, 75 min, 82%; d) KOH, MeOH, THF, 0 °C, 20 min, 82%; e) (3,5-dimethoxyphenyl)boronic acid, $Pd(PPh_3)_4$, Na_2CO_3, DME:H_2O 5:1, 80 °C, overnight, 74%; f) $LiAlH_4$, THF, 0 °C, 10 min, 97%; g) DMP, DCM, 0 °C to rt, 90 min, 78%; h) diethyl (3,5-dimethoxyphenyl)phosphonate, NaH, THF, MW, 120 °C, 30 min, 80%; i) BBr_3, DCM, 0 °C to rt, overnight, 14%.

Then, we focused on the synthesis of the simplified analogues of dehydro-ε-viniferin. In this case, we applied a mild procedure by Kim and Choi (Kim and Choi 2009) to construct the 3-arylbenzofuran rings by a intramolecular Friedel-Craft acylation of an *α*-aryloxyketone, followed by dehydration, catalysed by $Bi(OTf)_3$. Interestingly, we could use this approach only for the 3-aryl substituted benzofuran rings of dehydro-ε-viniferin. Indeed, in our hands, the reaction worked in presence of electron-releasing groups on the 5 position of the *α*-aryloxyketone, likely activating the *para* position for the intramolecular Friedel-Craft acylation. When the same reaction was performed on

unsubstituted *α*-aryloxyketones or bearing electron-withdrawing groups, no reaction was observed (Scheme 3.10, Table 3), and thus we could not apply this approach to the synthesis of dehydro-δ-viniferin simplified derivatives, lacking the hydroxy group on position 6 of the benzofuran core.

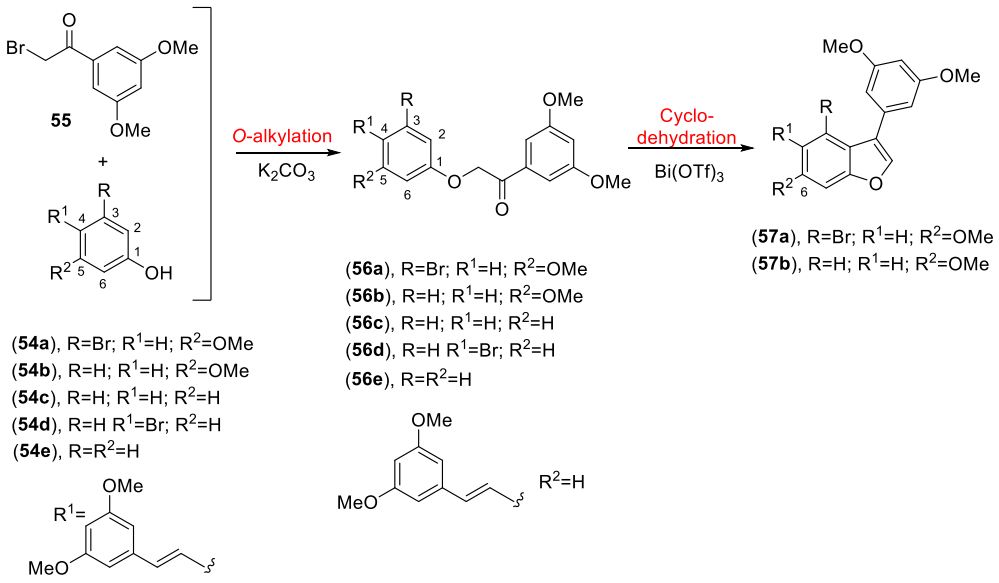

Scheme 3.10. Cyclodehydration of α-aryloxyketones

Table 3.7. O-alkylation and cyclodehydration yields of differently substituted phenols

54	O-alkylation Yields	**56**	Cyclo-dehydratation Yield
(**a**)	89%	(**a**)	83%
(***b***)	90%	(***b***)	85%
(**c**)	95%	(**c**)	NR
(**d**)	83%	(**d**)	NR
(**e**)	51%	(**e**)	NR

NR = No Reaction

Following this protocol we were able to obtain both compounds **32** and **33** starting from 3,5-dimethoxyacetophenone, which was treated with $CuBr_2$ to give selectively the corresponding α-bromo ketone **55** (King and Ostrum

1964). Reaction with *m*-methoxyphenol yield compound **56b**, which was subjected to the intramolecular Friedel-acylation followed by dehydration to afford regioselectively the desired benzofuran **57b** in 43% yield. Direct arylation of the C-2 position of the benzofuran ring **57b** by $Pd(OAc)_2$ and $P(Cy)\cdot HBF_4$, following a procedure by Lindgren *et al* (Lindgren et al. 2016), allowed the formation of compound **37**, which was demethylated with BBr_3 to afford compound **32** in 52% yield (Scheme 3.11).

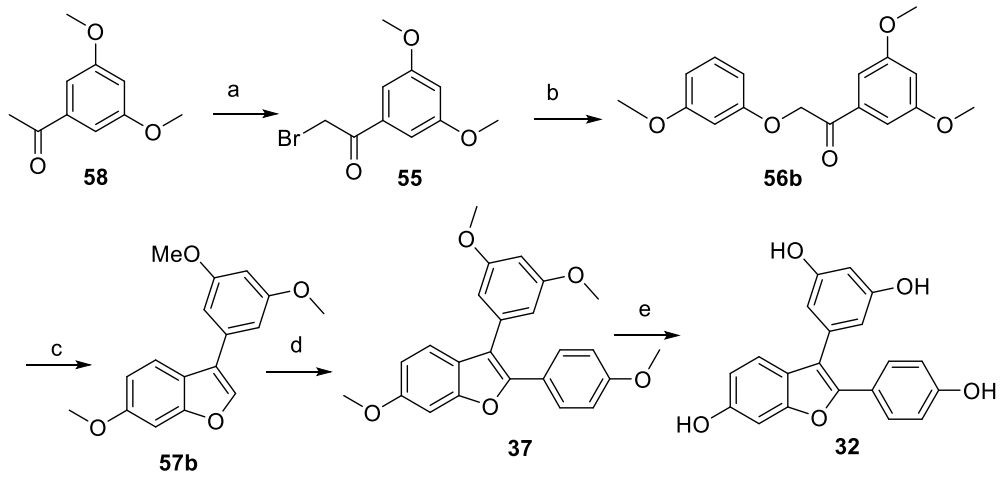

Scheme 3.11. Reagents and conditions: a) $CuBr_2$, EtOAc:$CHCl_3$, reflux, overnight, 67%; b) *m*-methoxyphenol, K_2CO_3, acetone, N_2, reflux, 2h, 90%; c) $Bi(OTf)_3$, DCM, N_2, reflux, overnight, 43%; d) *p*-methoxybromobenzene, $Pd(OAc)_2$, PCy_3HBF_4, K_2CO_3, pivalic acid, DMA, N_2, 100 °C, 20h, 80%; e) BBr_3, DCM, -78 °C to rt, overnight, 52%;

Following the same synthetic approach for the construction of the benzofuran core, the *α*-bromoketone **55** was reacted with 3-bromo-5-methoxyphenol to afford **56a**. The intermediate **56a** was demethylated before introducing the styryl moiety at the position 4, in order to avoid the troublesome deprotection of the derivative bearing the styryl double bond, sensititve to the demethylating reagents, as reported above. Conversely, deprotection of compound **56a** with BBr_3 proceeded smoothly to yield compound **57a** in 91% yield. Eventually, a Heck reaction with *p*-hydroxystyrene afforded the desired benzofuran **33** in 80% yield (Scheme 3.12).

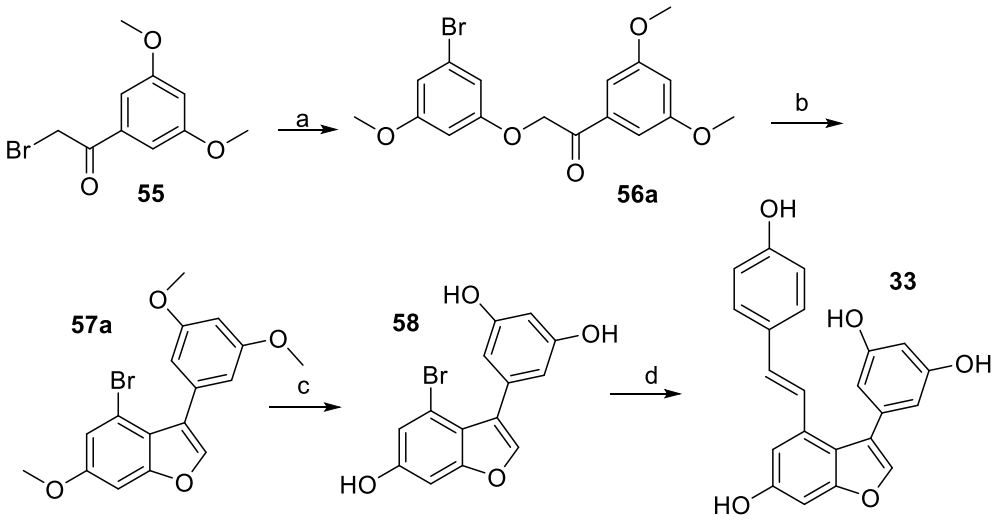

Scheme 3.12. Reagents and conditions: a) 3-Br-5-methoxyphenol, K_2CO_3, acetone, N_2, reflux, 2h, 89%; b) $Bi(OTf)_3$, DCM, N_2, reflux, overnight, 83%; c) BBr_3, DCM, -78 °C to rt, overnight, 91%; d) *p*-hydroxystyrene, $Pd(OAc)_2$, TEA, dppp, DMF, N_2, 120 °C, 20h, 80%.

For the synthesis of the last simplified analogue of dehydro-ε-viniferin, compound **34**, we started from methyl-3,5-dihydroxybenzoate **59**, which was monomethylated following a procedure by Iino (Iino et al. 2009). Then, we applied the same approach used for compound **31** (Scheme 3.9). Therefore, compound **60** was alkylated with 2-bromo-1,1-dimethoxyethane and subsequent dehydration with Amberlyst-15 afforded benzofuran **62**. A regioselective bromination with *N*-bromosuccinimide (NBS) at reflux in 1,2-dichloroethane afforded compound **63** as the only isomer (Liu et al. 2016). Suzuki coupling, followed by conversion into the corresponding aldehyde, as described before, gave compound **65**, which underwent Wittig-Horner olefination to yield compound **66**. Final deprotection of methoxy groups with BBr_3 afforded the simplified compound **34** (Scheme 3.13).

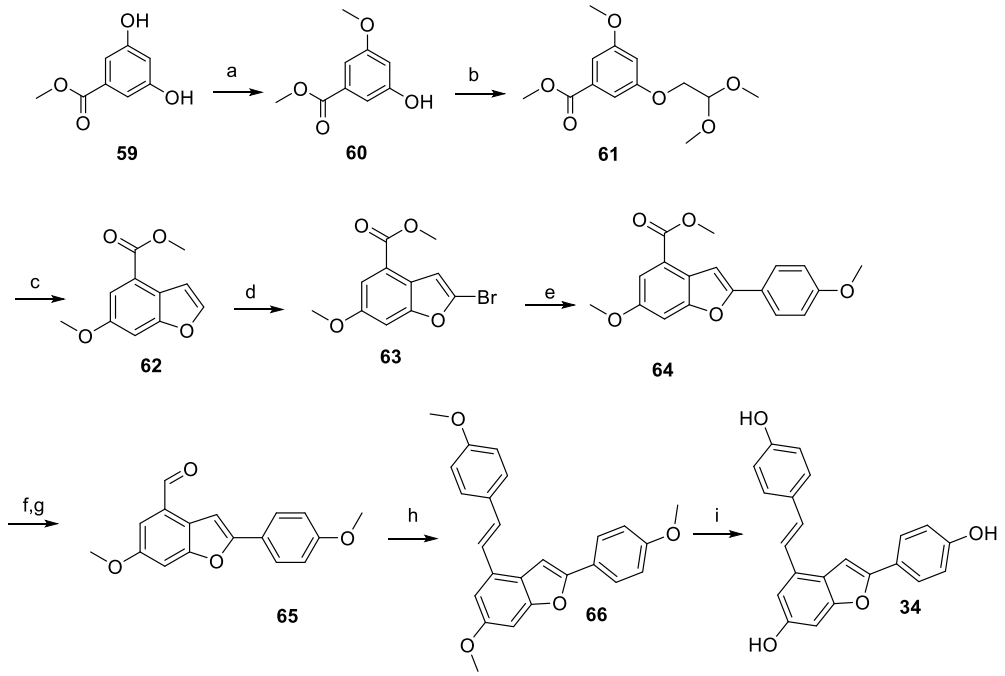

Scheme 3.13. Reagents and conditions: a) K_2CO_3, CH_3I, DMF, rt, 45h, 35%; b) 2-bromo-1,1-dimethoxyethane, Cs_2CO_3, CH_3CN, reflux, 72h, 67%; c) Amberlyst-15, C_6H_5Cl, 120 °C, 3h, 63%; d) NBS, DMF cat., $ClCH_2CH_2Cl$, 75 °C, 3h, 80%; e) (4-methoxyphenyl)boronic acid, $Pd(PPh_3)_4$, K_2CO_3, DMF, 70 °C, overnight, 91%; f) $LiAlH_4$, DCM, 0 °C, 10 min., 89%; g) DMP, DCM, 0 °C to rt, 90 min, 97%; h) diethyl (4-methoxybenzyl)phosphonate, NaH, dry THF, 120 °C - MW, 30 min, 54%; i) BBr_3, 0 °C to rt, 6h, 24%.

The compounds obtained were tested against the foodborne pathogen *L. monocytogenes* Scott A, which was demonstrated to be one of the most sensitive species to the stilbenoids tested in the previous screening (Section 3.1.3). The values of MIC and MBC (Table 3.8) confirmed that dehydro-δ-viniferin (**15**) (MIC 2 µg/mL, MBC 16 µg/mL) was more active than its regioisomer dehydro-ε-viniferin (MIC 16 µg/mL, MBC > 512 µg/mL). Overall, the removal of one of the phenolic rings from the benzofuran core negatively affected the antimicrobial activity of the simplified analogues of both dehydro-δ-viniferin and dehydro-ε-viniferin.

The simplified analogues of dehydro-δ-viniferin **29**, **30**, and **31**, derived from the selective removal of the aromatic rings in positions 5, 3, and 2,

respectively, of the benzofuran core showed a loss of activity compared to the original precursor. In particular, compound **30**, lacking the ring B, showed a dramatic decrease of the antimicrobial potency (MIC 256 μg/mL, MBC > 512 μg/mL). From these findings, we supposed that all three phenolic portions A, B, and C were important and likely synergic for the antimicrobial activity of dehydro-δ-viniferin.

Conversely, the removal of ring B resulting in compound **34**, a simplified analogue of dehydro-ε-viniferin, showed increased antimicrobial potency compared to its natural precursor, with MIC and MBC values of 8 and 64 μg/mL, respectively. On the other hand, compounds **32** and **33**, deriving from the selective removal of the moieties C and A, respectively, were four-fold less active (only in terms of MIC) than the parent compound (MIC 64 μg/mL vs. 16 μg/mL). Notably, compound **34** bears three phenolic portions with a spatial orientation similar to that of dehydro-δ-viniferin. Moreover, it is interesting to notice that the introduction of a hydroxy group on the benzofuran skeleton of compound **29** (**32** vs. **29**) resulted in a four-fold decrease of the activity (MIC 64 μg/mL, MBC >512 μg/mL vs. MIC 16 μg/mL, MBC 64 μg/mL). All compounds bearing methoxy groups in place of hydroxy functions were inactive (compounds **35**-**37**).

Noteworthy, compound **35** and pterostilbene (**2**) differ only in the length of the spacer (the benzofuran core) connecting the two substituted rings. The significant drop of activity of compound **35** (MIC and MBC values > 512 μg/mL) compared with that of pterostilbene (MIC 64 μg/mL, MBC 128 μg/mL) suggested that the antimicrobial efficacy could be affected not only by the spatial orientation, but also by the distance between the substituted rings.

In order to evaluate the potential toxicity of the compounds on healthy human cells, the synthesized molecules were tested on normal skin fibroblast WS1 cells to investigate their antiproliferative effect, calculated as IC_{50} (the concentration of compound causing 50% cell growth inhibition) (Table 3.8). Resveratrol showed the best value of IC_{50} (> 200 μM), in contrast to the other

compounds with IC_{50} values ranging from 33 to > 100 μM. The ratio between the cytotoxic concentrations and the MIC values showed that dehydro-δ-viniferin (**15**) has the best profile of selectivity, with an IC_{50} value ~ 10 fold higher than the lowest concentration of bacterial growth inhibition. Furthermore, compound **29**, **31**, and **34** were cytotoxic at a concentration two-fold higher than their MIC values.

Table 3.8. Antimicrobial activity of synthesized compounds against L. monocytogenes Scott A[a] and cytotoxic activity on WS1[b]

Compound	*L. monocytogenes* Scott A	*L. monocytogenes* Scott A	WS1
	MIC (MBC) μg/mL [a]	MIC (μM) [a]	IC_{50} (μM) [b]
Resveratrol (1)	200 (—) [c]	876	>200
Pterostilbene (2)	64 (128)	250	57±10
15 dehydro-δ-viniferin	2 (16)	4.42	37.0±1.4
14 dehydro-ε-viniferin	16 (> 512)	35.4	33.0±1.4
29	16 (64)	50.3	98.7±1.8
30	256 (> 512)	743	97.8±3.0
31	16 (64)	44.4	96.8±4.5
32	64 (> 512)	191	98.5±2.0
33	64 (> 512)	178	85.0±4.6
34	8 (64)	23.2	45.0±1.2
35	> 512 (> 512)	1370	95.0±2.3
36	>256 (> 256)	662	>100
37	>256 (> 256)	656	>100
Chlorhexidine	8 (32)	15.8	-

[a]MIC is the minimal inhibitory concentration inhibiting the growth; MBC (in brackets) is the minimal bactericidal concentration. [b] IC_{50} is defined as the concentration of compound causing 50% cell growth inhibition. Twenty-four hours after seeding, cells were exposed for 48 h to the compounds and cytotoxicity was measured using MTS assay. Data represent mean values ± SD of three independent experiments. [c] *L. monocytogenes* LMG 16,779 (Ferreira and Domingues 2016).

In conclusion, the results showed that the shape and the geometry of the molecules play a key role in the antimicrobial activity, confirming that the

relative position of hydroxy groups on polyphenolic compounds highly affected the antibacterial potency (Wu et al. 2016; Singh et al. 2019) and the interaction with the bacterial cell membrane (Chibane et al. 2019). In particular, the results obtained identified dehydro-δ-viniferin (**15**) and compound **34** as the most promising scaffolds for further developments as nature-inspired antimicrobials against foodborne pathogens.

3.2.4. Experimental section

3.2.4.1. General information

See chapter 3.1.4.1 for General information.

3.2.4.2. Experimental procedures

2-(4-methoxyphenyl)benzofuran (40)

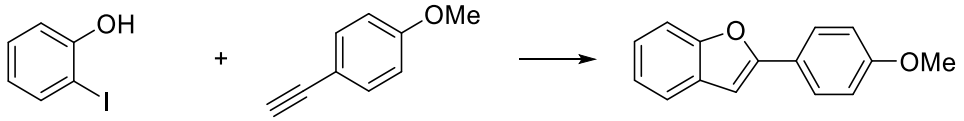

38 **39** **40**

A solution of 2-iodophenol **38** (0.45 mmol, 1 eq.), 1-ethynyl-4-methoxybenzene **39** (0.54 mmol, 1.2 eq.), CuI (0.013 mmol, 0.03 eq.) and $PdCl_2(PPh_3)_2$ (0.02 mmol, 0.05 eq.) in TEA (9.09 mmol, 20 eq.) and THF (1.2 mL) was degassed and heated to 40 °C under N_2 for 40 min. After addition of ACN (2.4 mL) the reaction mixture was heated to 100 °C for 90 min. Then, it was allowed to cool to room temperature and concentrated under reduced pressure. The residue was purified by flash chromatography (FC) with CHX/EtOAc (98:2) as eluent to give the desired product. Yield: 50%, white solid. Spectral data were in accordance with literature report (Jaseer et al. 2010).

M.p.: 148-150 °C.

R_f: 0.3 (cyclohexane/AcOEt 98:2)

^{1}H NMR: (300 MHz, C*D*Cl$_3$) δ (ppm): 7.85-7.78 (m, 2H), 7.59-7.49 (m, 2H); 7.31-7.19 (m, 2H), 7.02- 6.96 (m, 2H), 6.90 (d, *J* = 0.9 Hz, 1H), 3.87 (s, 3H).
^{13}C NMR: (75 MHz, C*D*Cl$_3$) δ (ppm): 160.1, 156.2, 154.8, 129.6, 126.5 (x2C), 123.9, 123.5, 123.0, 120.7, 114.4 (x2C), 111.1, 99.8, 55.5.

3-Iodo-2-(4-methoxyphenyl)benzofuran (41)

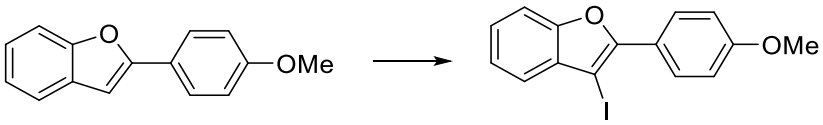

40 **41**

To the suspension of **40** (0.22 mmol, 1 eq.) in CH_3CN (6.7 mL) *N*-iodosuccinimide (0.22 mmol, 1 eq.) and *p*-toluensulfonic acid (0.22 mmol, 1 eq.) were added. The reaction mixture was stirred overnight under nitrogen atmosphere at room temperature. Then, the resulting brownish mixture was diluted with EtOAc (20 mL), washed with aq saturated $NaHCO_3$ (20 mL), 10% aq saturated $Na_2S_2O_3$ (20 mL), and brine (20 mL). The organic layer was dried over anhydrous Na_2SO_4 and concentrated under reduced pressure. The residue was purified by FC with CHX/AcOEt (99:1) as eluent to give the desired product. Yield: 74%, white solid. Spectral data were in accordance with literature report (Yao et al. 2014).

M.p.: 59-61 °C

R_f: 0.25 (cyclohexane/AcOEt 99:1)

^{1}H NMR (300 MHz, C*D*Cl$_3$) δ (ppm): 8.10 (d, *J* = 8.8 Hz, 2H), 7.45 - 7.39 (m, 2H), 7.31 - 7.28 (m, 2H), 6.99 (d, *J* = 8.0 Hz, 2H), 3.84 (s, 3H).
^{13}C NMR (75 MHz, C*D*Cl$_3$) δ (ppm): 160.5, 153.9, 153.4, 132.8, 129.2 (x2C), 125.4, 123.6, 122.8, 121.7, 114.1 (x2C), 111.2, 59.7, 55.5.

(3,5-dimethoxyphenyl)boronic acid

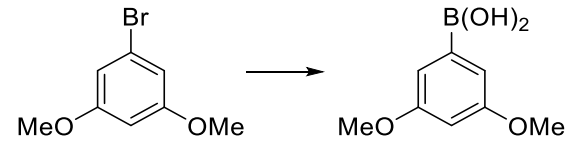

1-bromo-3,5-dimethoxybenzene **(3,5-dimethoxyphenyl) boronic acid**

To the solution of 1-bromo-3,5-dimethoxybenzene (1g, 4.606 mmol, 1 eq) in dry THF (22 mL) at -78°C, *n*-BuLi 1.6 M in hexane (3.46 mL, 5.527 mmol, 1.2 eq) was added dropwise and the mixture was stirred at -78°C for 1h. Then, trimethylborate (1.54 mL, 13.818 mmol, 3 eq) was added in one portion and the reaction mixture was stirred for 30 min at - 78°C, and then at room temperature for 4h. The reaction mixture was quenched with aq saturated NH_4Cl (100 mL) and aq 2M HCl (10 mL). The aqueous layer was extracted with DCM (3 x 80 mL). The combined organic layers were washed with brine, dried over anhydrous Na_2SO_4, filtered, and evaporated. The crude was washed and triturated with hexane (4 x 15 mL) to give the product as a white solid. Analytical data were in agreement with literature (Elbert et al. 2017).

M.p.: 203°C

R_f: 0.42 (CHX/AcOEt 1:1)

^{1}H-NMR (300 MHz, DMSO-*d*$_6$) δ (ppm): 8.02 (s, 2H), 6.95 (d, 2H, *J* = 2.3 Hz), 6.51 (t, 1H, J = 2.3 Hz), 3.73 (s, 6H).
^{13}C-NMR (75 MHz, DMSO-*d*$_6$) δ (ppm): 160.8 (x2C), 112.3, 103.3, 55.9 (x2C).

3-(3,5-dimethoxyphenyl)-2-(4-methoxyphenyl)benzofuran (42)

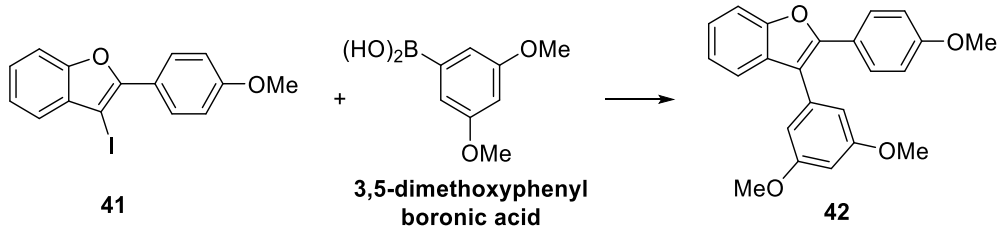

41 **3,5-dimethoxyphenyl boronic acid** **42**

A mixture of **41** (0.04 mmol, 1 eq.), (3,5-dimethoxyphenyl)boronic acid (0.06 mmol, 1.4 eq.), K_2CO_3 (0.13 mmol, 3 eq.), $PdCl_2(dppf)\cdot DCM$ (0.0021 mmol, 0.05 eq.) in a mixture THF/H_2O 1:1 previously degassed, was heated at 70 °C for 30 min, under microwave irradiation. After cooling down, the mixture was diluted with EtOAc and washed with H_2O. The aqueous phase was extracted with EtOAc. The combined organic phases was washed with brine, dried over anhydrous Na_2SO_4 and concentrated under reduced pressure. The residue was purified by FC with CHX/EtOAc 93:7 as eluent. Yield: 83%, light brown amorphous solid.

R_f: 0.15 (cyclohexane/AcOEt 99:1)

^{1}H NMR (300 MHz, C*D*Cl$_3$) δ (ppm): 7.69 – 7.62 (m, 2H), 7.56 – 7.50 (m, 2H), 7.34 – 7.28 (m, 1H), 7.26 – 7.20 (m, 1H), 6.91 – 6.84 (m, 2H), 6.66 (d, *J* = 2.3 Hz, 2H), 6.52 (t, *J* = 2.3 Hz, 1H), 3.83 (s, 3H), 3.79 (s, 6H).

5-(2-(4-hydroxyphenyl)benzofuran-3-yl)benzene-1,3-diol (29)

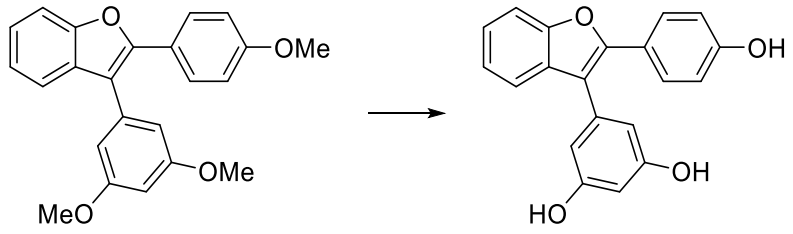

42 **29**

To a solution of **42** (0.11 mmol, 1 eq.) in dry DCM (1.3 mL), under nitrogen atmosphere, at 0°C a 1M BBr_3 solution in DCM (0.33 mmol, 2.9 eq.) was added dropwise. Then mixture was allowed to warm to room temperature. After 16 h the reaction solution was quenched at 0°C with a cold saturated solution of $NaHCO_3$ (0 °C), concentrated under reduced pressure and diluted with H_2O. The aqueous phase was extracted with EtOAc for three times. The combined organic phases were dried over anhydrous Na_2SO_4, and concentrated under reduced pressure. The residue was purified by FC with DCM/MeOH (95:5) as eluent to give the desired product as a light brown amorphous solid. Yield: 61%.

R_f: 0.45 (DCM/MeOH 95:5)

^{1}H NMR: (300 MHz, CD_3OD) δ (ppm): 7.56 – 7.51 (m, 2H), 7.50 – 7.41 (m, 2H), 7.31 – 7.16 (m, 2H), 6.79 – 6.73 (m, 2H), 6.40 (d, *J* = 2.2 Hz, 2H), 6.31 (t, *J* = 2.2 Hz, 1H).

^{13}C NMR (75 MHz, CD_3OD) δ (ppm): 158.7 (×2), 157.7, 153.7, 150.7, 134.7, 130.2, 128.3 (×2), 123.7, 122.4, 121.9, 119.2, 115.4, 114.8 (×2), 110.2, 107.7 (×2), 101.5.

Methyl 2-(4-methoxyphenyl)benzofuran-5-carboxylate (44)

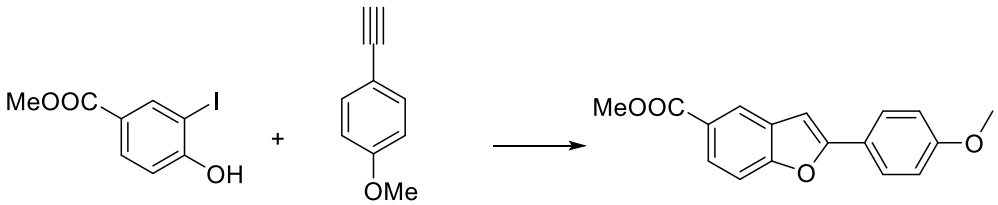

To a solution of methyl 4-hydroxy-3-iodobenzoate **43** (0.36 mmol, 1 eq.) in dry THF (0.95 mL) and dry TEA (1 mL, 7.19 mmol, 20 eq.), 1-ethynyl-4-methoxybenzene **39** (0.43 mmol, 1.2 eq.), CuI (0.01 mmol, 0.03 eq.) and $PdCl_2(PPh_3)_2$ (0.02 mmol, 0.05 eq.) were added under nitrogen atmosphere.

The mixture was degassed and heated at 40 °C for 40 min. Then CH_3CN (1.9 mL) was added and the resulting mixture was heated at 100 °C for 90 min. The reaction mixture was allowed to cool to room temperature, washed twice with H_2O and concentred under reduced pressure. The residue was purified by FC with CHX/EtOAc (95:5) as eluent to give the desired product as a white sticky solid. Yield: 62%. Spectral data were in accordance with literature report (Wang et al. 2015).

R_f: 0.42 (CHX/DCM 1:1)

^{1}H NMR (300 MHz, C*D*Cl$_3$) δ (ppm): 8.28 (d, *J*=1.8 Hz, 1H), 7.98 (dd, J_1 =8.6 Hz, J_2 = 1.8 Hz, 1H), 7.80 (d, *J* = 8.9 Hz, 2H), 7.51 (d, *J* = 8.6 Hz, 1H), 6.99 (d, *J* = 8.9 Hz, 2H), 6.93 (d, *J* = 0.8 Hz, 1H), 3.94 (s, 3H), 3.87 (s, 3H).
^{13}C NMR (75 MHz, C*D*Cl$_3$) δ (ppm): 167.4, 160.3, 157.5, 157.3, 129.5, 126.6 (x2C), 125.6, 125.8, 122.9, 122.7, 114.3 (x2C), 110.8, 99.8, 55.4, 52.1.

2-(4-methoxyphenyl)benzofuran-5-carbaldehyde (45)

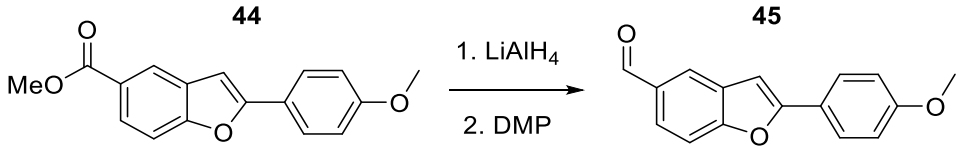

To the solution of compound **44** (0.99 mmol, 1 eq.) in dry THF (9.5 mL), under nitrogen atmpsphere, at 0 °C, 1M $LiAlH_4$ in THF (2.97 mmol, 3 eq.) was added dropwise. The mixture was stirred for 10 min at 0 °C, then was quenched with aq 1M HCl at 0 °C. The aqueous phase was extracted with EtOAc for three times. The combined organic phases were dried over anhydrous Na_2SO_4, filtered and concentrated under reduced pressure. The residue (0.82 mmol, 1 eq.) was dissolved in DCM (4.7 mL) and DMP (1.07 mmol, 1.3 eq.) was added at 0 °C. The mixture was stirred at room temperature for 2 h and the solvent was evaporated under reduced pressure. The residue was purified by FC with CHX/EtOAc (8:2) as eluent. Yield: 85%, white solid. Spectral data were in agreement with literature report (Vo and Elofsson 2016).

M.p.: 121 °C

R_f: 0.34 (CHX/AcOEt 85:15)

^{1}H NMR (300 MHz, Acetone-d_6) δ (ppm): 10.09 (s, 1H), 8.20 (dd, J_1 = 2.3 Hz, J_2 = 0.5 Hz, 1H), 7.92 (d, J = 9.2 Hz, 2H), 7.89 (dd, J_1 = 9.0, J_2= 2.0 Hz, 1H), 7.73 (d, J = 8.4 Hz, 1H), 7.32 (d, J = 0.8 Hz, 1H), 7.09 (d, J = 8.9 Hz, 2H), 3.88 (s, 3H).

^{13}C NMR (75 MHz, CDCl$_3$) δ (ppm): 191.8, 160.5, 158.1, 132.3, 130.1, 126.7 (x2C), 125.6, 123.5, 122.4, 114.4 (x2C), 111.6, 99.8, 55.4

(*E*)-5-(3,5-dimethoxystyryl)-2-(4-methoxyphenyl)benzofuran (36)

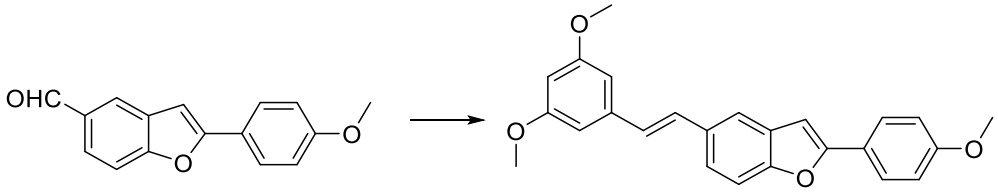

45 **36**

In a MW vial, compound **45** (0.55 mmol, 1 eq.) and diethyl (3,5-dimethoxybenzyl)phosphonate (0.83 mmol, 1.5 eq.) were solubilized in dry THF under nitrogen atmosphere. Then 60% NaH in mineral oil (1.66 mmol, 3 eq.) was added to the solution and the mixture was heated under microwave irradiation at 120 °C for 30 min. After cooling, the mixture was quenched by aq saturated NH_4Cl and the aqueous phase was extracted with EtOAc three times. The organic phases were washed with brine, dried over anhydrous Na_2SO_4, and concentrated under reduced pressure. The crude product was purified by FC with CHX/EtOAc (8:2) as eluent. Yield: 76%, light yellow solid.

M.p.: 169-171 °C

R_f: 0.41 (CHX/AcOEt 85:15)

^{1}H NMR (300 MHz, C*D*Cl$_3$) δ (ppm): 7.80 (d, *J*=8.8 Hz, 2H), 7.67 (s, 1H), 7.48 (d, *J* = 8.4 Hz, 1H), 7.44 (dd, J_1 = 8.6 Hz, J_2 = 1.6 Hz, 1H), 7.19 (d, *J*= 16.2 Hz, 1H), 7.03 (d, *J* = 15.7 Hz, 1H), 6.99 (d, *J* = 8.8 Hz, 2H), 6.88 (d, *J* = 0.5 Hz, 1H), 6.70 (d, *J* = 2.2 Hz, 2H), 6.40 (t, *J* = 2.2 Hz, 1H), 3.87 (s, 3H), 3.85 (s, 6H).

^{13}C NMR (75 MHz, C*D*Cl$_3$) δ (ppm): 161.0 (x2C), 160.1, 156.8, 154.6, 139.7, 132.3, 130.0, 129.6, 127.5, 126.4 (x2C), 123.2, 122.7, 118.6, 114.3 (x2C), 111.1, 104.5 (x2C), 99.7, 99.6, 55.3 (x2C).

(*E*)-4-(5-(3,5-dimethoxystyryl)benzofuran-2-yl)phenol (35)

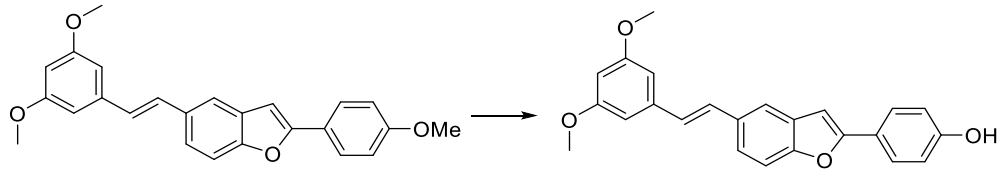

To a solution of **36** (0.12 mmol, 1 eq.) in dry DCM (1.3 mL), under nitrogen atmosphere at 0 °C, a 1M BBr_3 solution in DCM (0.34 mmol, 2.9 eq.) was added dropwise. The mixture was allowed to warm to room temperature. After 16 h the reaction was quenched with H_2O (0 °C) and concentrated under reduced pressure. The aqueous phase was extracted with EtOAc three times. The combined organic phases were dried over anhydrous Na_2SO_4, filtered and concentrated under reduced pressure. The residue was purified by FC with CHX/EtOAc (8:2) as eluent to give the desired product. Yield: 60%, pale yellow solid.

M.p.:194 – 195 °C

R_f: 0.23 (CHX/AcOEt 8:2)

^{1}H NMR: (300 MHz, Acetone-d_6) δ (ppm): 7.80 (d, *J* = 9.0 Hz, 2H), 7.78 (s, 1H), 7.55 (dd, J_1 = 2.3 Hz, J_2 = 0.9 Hz, 1H), 7.51 (d, *J* = 2.3 Hz, 1H), 7.36 (d,

J = 8.4 Hz, 1H), 7.17 (d, *J* = 15.0 Hz, 1H), 7.09 (d, *J* = 15.0 Hz, 1H), 6.98 (d, *J* = 9.0 Hz, 2H), 6.80 (d, *J* = 0.9 Hz, 2H), 6.41 (t, *J* = 2.3 Hz, 1H), 3.83 (s, 6H). **^{13}C NMR (75 MHz, Acetone-*d*$_6$)** δ (ppm): 161.2 (x2C), 158.3, 157.1, 154.4, 139.8, 132.7, 130.2, 129.3, 127.5, 126.5 (x2C), 122.7, 121.9, 118.6, 115.8 (x2C), 110.8, 104.3 (x2C), 99.5, 99.3, 54.7 (x2C).

(*E*)-5-(2-(2-(4-hydroxyphenyl)benzofuran-5-yl)vinyl)benzene-1,3-diol (30)

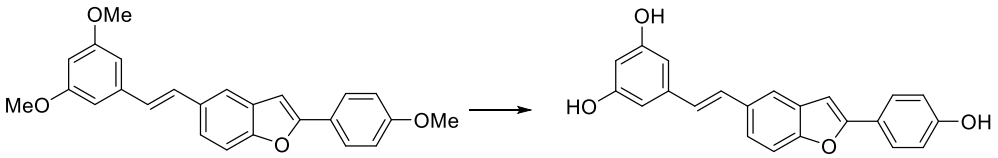

36 **30**

To a solution of compound **36** (0.08 mmol, 1 eq.) and TBAI (0.70 mmol, 9 eq.) in dry DCM (4.8 mL) 1M BCl_3 in DCM (0.70 mmol, 9 eq.) was added dropwise at 0 °C, under nitrogen atmosphere. The mixture was stirred at room temperature. After 6 h the reaction solution was quenched with H_2O at 0 °C and diluted with EtOAc. The organic phase was washed with aq 10% Na_2SO_3. The aqueous phase was extracted twice with EtOAc. The combined organic phases were washed with brine, dried over anhydrous Na_2SO_4, filtered and concentrated under reduced pressure. The residue was purified by FC with CHX/Acetone (6:4) as eluent. The product needed to be purified by preparative HPLC-UV. Chromatographic separation was performed using Kromasil 5 – AmyCoat (250 × 21.2 mm, λ = 220 nm) and an isocratic elution (hexane: *i*PrOH 60:40, rate flow 15 mL/min). Product **4**, t_R = 6.75 min. Yield: 35%, white sticky solid.

R_f: 0.35 (CHX/Acetone 6:4)

^{1}H NMR: (300 MHz, CD_3OD) δ (ppm): 7.80 (d, *J* = 9.0 Hz, 2H), 7.78 (s, 1H), 7.55 (dd, J_1 = 2.3 Hz, J_2 = 0.9 Hz, 1H), 7.51 (d, *J* = 2.3 Hz, 1H), 7.36 (d, *J* = 8.4 Hz, 1H), 7.17 (d, *J* = 15.0 Hz, 1H), 7.09 (d, *J* = 15.0 Hz, 1H), 6.98 (d, *J* = 9.0 Hz, 2H), 6.80 (d, *J* = 0.9 Hz, 2H), 6.41 (t, *J* = 2.3 Hz, 1H) 3.83 (s, 6H).

^{13}C NMR (75 MHz, C*D*$_3$O*D*) δ (ppm): 158.3 (x2C), 158.1, 157.1, 154.3, 139.7, 132.7, 130.1, 128.5, 127.4, 126.1 (x2C), 122.1, 121.9, 118.0, 115.3 (x2C), 110.4, 104.6 (x2C), 101.5, 98.7.

Methyl 4-(2,2-dimethoxyethoxy)benzoate (47)

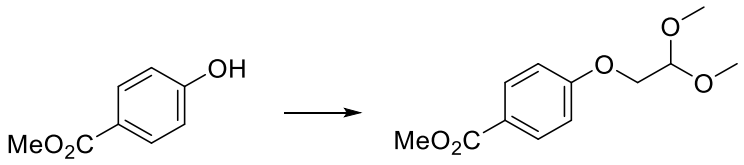

46 **47**

To a solution of methyl 4-hydroxybenzoate **46** (3.29 mmol, 1 eq.) in dry ACN under nitrogen atmosphere, 2-bromo-1,1-dimethoxyethane (4.98 mmol, 1.5 eq.) and Cs_2CO_3 (6.64 mmol, 2 eq.) were added. The mixture was stirred at reflux for three days. After cooling the reaction to room temperature, the solvent was evaporated under reduced pressure. The crude was diluted in EtOAc and washed with H_2O. The aqueous phase was extracted twice with EtOAc. The combined organic phases were dried over anhydrous Na_2SO_4 and concentrated under reduced pressure. The residue was purified by FC with CHX/DCM/EtOAc (10:2:1) as eluent. Yield: 61%, yellow oil.

R_f: 0.36 (CHX/AcOEt 8:2)

^{1}H NMR (300 MHz, C*D*Cl$_3$) δ (ppm): 8.0 (d, *J* = 9.2 Hz, 2H), 6.94 (d, *J* = 9.2 Hz, 2H), 4.73 (t, *J* = 5.2 Hz, 1H), 4.05 (d, *J* = 5.2 Hz, 2H), 3.88 (s, 3H), 3.46 (s, 6H).

^{13}C NMR (75 MHz, C*D*Cl$_3$) δ (ppm): 166.6, 162.1, 131.5 (x2C), 122.9, 114.1 (x2C), 101.9, 67.6, 54.2 (x2C), 51.8.

Methyl benzofuran-5-carboxylate (48)

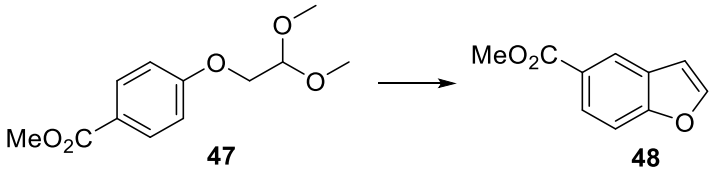

47 **48**

To a solution of compound **47** (1.55 mmol, 1 eq.) in toluene (22.8 mL), amberlyst-15 (10 wt%) was added. The mixture was refluxed for 6 h. After cooling, the mixture was filtered, and the solvent was evaporated under reduced pressure. The residue was purified by FC using CHX/EtOAc (8:2) as eluent. Yield: 51%, white solid. Analytical data were in accordance with literature report (Várela-Fernández et al. 2009).

M.p.: 69-70°C

R_f: 0.52 (CHX/AcOEt 9:1)

^{1}H NMR (300 MHz, C*D*Cl$_3$) δ (ppm): 8.35 (d, *J* = 1.8 Hz, 1H), 8.03 (dd, *J*= 8.7, 1.8 Hz, 1H), 7.69 (d, *J*= 2.2 Hz, 1H), 7.53 (dd, *J*= 8.7, 0.8 Hz, 1H), 6.84 (dd, J= 2.2, 0.8 Hz, 1H), 3.89 (s, 3H).
^{13}C NMR (75 MHz, C*D*Cl$_3$) δ (ppm): 167.2, 157.4, 146.2, 127.5, 126.0, 125.1, 123.7, 111.2, 107.1, 52.1.

Methyl 2,3-dibromo-2,3-dihydrobenzofuran-5-carboxylate (49)

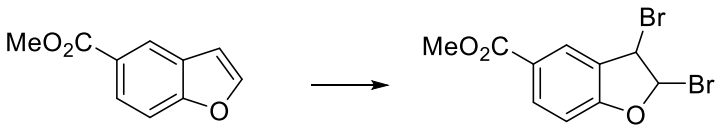

48 **49**

To a solution of compound **48** (0.79 mmol, 1 eq.) in dry DCM (0.6 mL) under N_2 at 0 °C, Br_2 (0.79 mmol, 1 eq.) was added dropwise and the mixture was

stirred at room temperature for 75 min. The solution was quenched with aq 1M Na_2SO_3. The aqueous phase was extracted with EtOAc three times. The combined organic phases were washed with brine, dried over anhydrous Na_2SO_4, filtered, and concentrated under reduced pressure. The residue was purified by FC with CHX/EtOAc (95:5) as eluent. Yield: 82%, white sticky solid.

R_f: 0.59 (CHX/AcOEt 9:1)

^{1}H NMR (300 MHz, C*D*Cl$_3$) δ (ppm): 8.23 (d, *J* = 1.9 Hz, 1H), 8.11 (dd, J_1 = 8.6 Hz, J_2 = 1.9 Hz, 1H), 7.10 (d, *J* = 8.6 Hz, 1H), 6.93 (s, 1H), 5.75 (s, 1H), 3.92 (s, 3H).

^{13}C NMR (75 MHz, C*D*Cl$_3$) δ (ppm): 165.8, 160.3, 133.7, 127.8, 126.8, 126.6, 112.3, 90.2, 52.3, 51.6.

Methyl 3-bromobenzofuran-5-carboxylate (50)

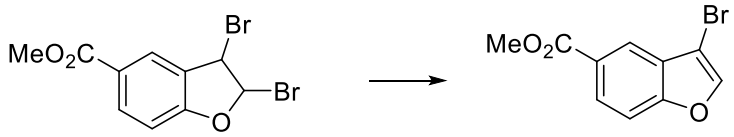

49 **50**

To a solution of compound **49** (0.56 mmol, 1 eq.) in dry THF (0.76 mL) at 0 °C KOH 85% (0.56 mmol, 1 eq.) and MeOH (152 µL) were added. The mixture was stirred for 20 min, and then diluted with EtOAc and washed with H_2O. The aqueous phase was extracted twice with EtOAc. The combined organic phases were washed with aq saturated $NaHCO_3$, dried over anhydrous Na_2SO_4, filtered and concentrated under reduced pressure. The residue was purified by FC with CHX/EtOAc (95:5) as eluent. Yield: 82%, white sticky solid.

R_f: 0.40 (CHX/AcOEt 95:5)

^{1}H NMR (300 MHz, C*D*Cl$_3$) δ (ppm): 8.30 (d, *J* = 1.8 Hz, 1H), 8.09 (dd, J_1 = 8.8 Hz, J_2 = 1.8 Hz, 1H), 7.72 (s, 1H), 7.53 (d, *J* = 8.8 Hz, 1H), 7.26 (s, 1H), 3.97 (s, 3H).

^{13}C NMR (75 MHz, C*D*Cl$_3$) δ (ppm): 166.7, 156.8, 143.9, 143.8, 127.1, 125.9, 122.3, 111.7, 98.4, 52.2.

Methyl 3-(3,5-dimethoxyphenyl)benzofuran-5-carboxylate (51).

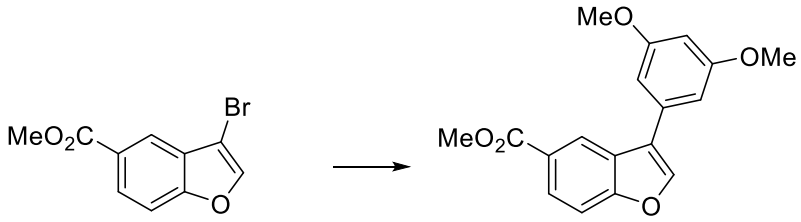

50 **51**

A solution of compound **50** (0.45 mmol, 1 eq.), 3,5-dimethoxyphenylboronic acid (0.50 mmol, 1.1 eq.) and Na_2CO_3 (1.0 mmol, 2.2 eq.) in a mixture DME/H_2O 5:1 was degassed for 30 min. Then, $Pd(PPh_3)_4$ (0.01 mmol, 0.03 eq.) was added and the mixture was degassed again. The reaction was heated at 80 °C overnight. After cooling, the mixture was quenched with water and the aqueous phase was extracted three times with EtOAc. The organic phases were washed with brine, dried over anhydrous Na_2SO_4 and concentrated. The crude was purified by FC with CHX/EtOAc 9:1 as eluent. Yield: 74%, white solid.

M.p.:101-103 °C.

R_f: 0.35 (CHX/AcOEt 9:1)

^{1}H NMR (300 MHz, C*D*Cl$_3$) δ (ppm): 8.56 (d, *J* = 1.7 Hz, 1H), 8.09 (dd, J_1 = 8.7 Hz, J_2 = 1.7 Hz, 1H), 7.84 (s, 1H), 7.57 (d, *J* = 8.7 Hz, 1H), 6.78 (d, *J* = 2.3 Hz, 2H), 6.52 (t, *J* = 2.3 Hz, 1H), 3.96 (s, 3H), 3.87 (s, 6H).

^{13}C NMR (75 MHz, C*D*Cl$_3$) δ (ppm): 166.2, 160.2, 159.3 (x2C), 143.0, 141.7, 136.2, 132.3, 130.9, 129.4, 128.7, 112.1, 104.5 (x2C), 99.9, 55.8 (x2C), 51.7.

(3-(3,5-dimethoxyphenyl)benzofuran-5-yl)methanol (67)

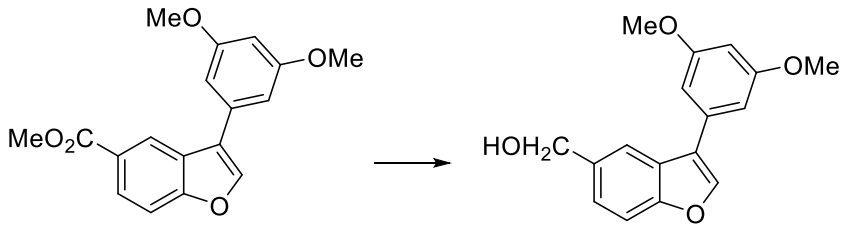

To a solution of compound **51** (0.23 mmol, 1 eq.) in dry THF, under nitrogen atmosphere, at 0°C was added $LiAlH_4$ 1M in THF (0.70 mmol, 3 eq.) dropwise. The mixture was stirred for 10 minutes at 0 °C, and then quenched with HCl 1M at 0°C. The aqueous phase was extracted with EtOAc for three times. The combined organic phases were dried over anhydrous Na_2SO_4, filtered, and concentrated under reduced pressure. Purification by FC using CHX/EtOAc (6:4) as eluent afforder the desired product as a brown sticky solid. Yield: 97%.

R_f: 0.21 (CHX/AcOEt 7:3)

^{1}H NMR (300 MHz, C*D*Cl$_3$) δ (ppm): 7.83 (d, *J* = 1.1 Hz, 1H), 7.80 (s, 1H), 7.53 (d, *J* = 8.5 Hz, 1H), 7.37 (dd, J_1 = 8.5, J_2 = 1.7 Hz, 1H), 6.78 (d, *J* = 2.3 Hz, 2H), 6.50 (t, *J* = 2.3 Hz, 1H), 4.80 (s, 2H), 3.86 (s, 6H).
^{13}C NMR (75 MHz, C*D*Cl$_3$) δ (ppm): 161.2 (x2C), 155.3, 142.0, 136.0, 133.7, 126.5, 124.2, 122.3, 119.1, 111.8, 105.8 (x2C), 99.3, 65.6, 55.4 (x2C).

3-(3,5-dimethoxyphenyl)benzofuran-5-carbaldehyde (52)

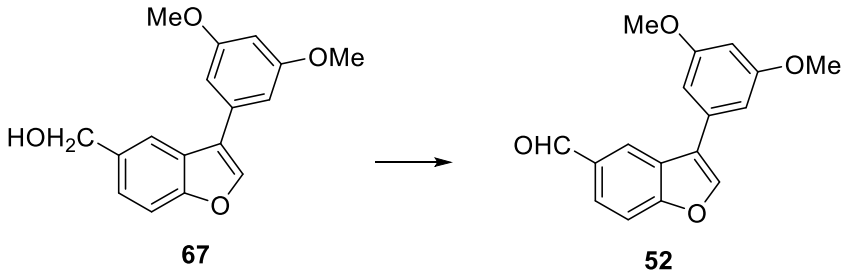

To a solution of compound **67** (0.21 mmol, 1 eq.) in dry DCM, DMP (0.27 mmol, 1.3 eq.) was added at 0 °C. The mixture was stirred at room temperature for 90 min. The solvent was evaporated under reduced pressure and the residue was purified by FC using as eluent CHX/EtOAc (8:2). Yield: 78%, yellow solid.

M.p.: 96 - 98 °C.

R_f: 0.48 (CHX/AcOEt 8:2)

^{1}H NMR (300 MHz, C*D*Cl$_3$) δ (ppm): 10.09 (s, 1H), 8.36 (d, *J* = 1.6 Hz, 1H), 7.93 (dd, J_1 = 8.6, J_2 = 1.6 Hz, 1H), 7.88 (s, 1H), 7.66 (d, *J* = 8.6 Hz, 1H), 6.53 (t, *J* = 2.3 Hz, 1H), 3.87 (s, 6H).
^{13}C NMR (75 MHz, C*D*Cl$_3$) δ (ppm): 191.6, 161.4 (x2C), 159.0, 143.0, 132.7, 132.4, 127.1, 125.9, 124.1, 123.0, 112.6, 105.9 (x2C), 99.7, 55.5 (x2C).

(*E*)-3-(3,5-dimethoxyphenyl)-5-(3,5-dimethoxystyryl)benzofuran (53)

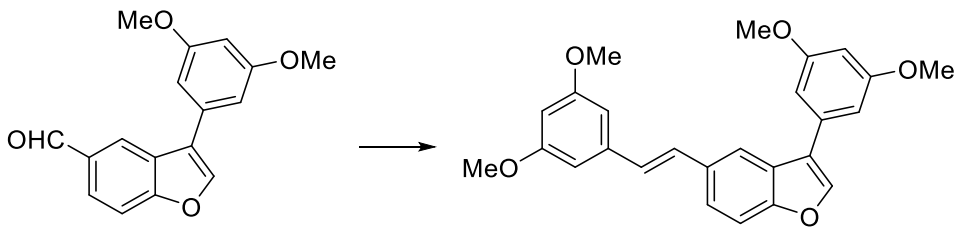

52 **53**

In a MW vial, compound **52** (0.15 mmol, 1 eq.) and diethyl (3,5-dimethoxybenzyl)phosphonate (0.22 mmol, 1.5 eq.) were solubilized in dry THF (2 mL) under nitrogen atmosphere, followed by the addition of 60% NaH in mineral oil (0.45 mmol, 3 eq.). The mixture was heated under microwave irradiation at 120 °C for 30 min. After cooling, the mixture was quenched with aq saturated NH_4Cl and the aqueous phase was extracted with EtOAc for three times. The organic phases were washed with brine, dried over anhydrous Na_2SO_4, and concentrated under reduced pressure. Purification by

FC with CHX/EtOAc (8:2) as eluent gave the title compound as a white sticky solid. Yield: 80%.

R_f: 0.43 (CHX/AcOEt 85:15)

^{1}H NMR (300 MHz, C*D*Cl$_3$) δ (ppm): 7.85 (d, *J* = 1.5 Hz, 1H), 7.77 (s, 1H), 7.53 (dd, J_1 = 8.6, J_2 = 1.5 Hz, 1H), 7.49 (d, *J* = 8.6 Hz, 1H), 6.92 (d, *J* = 16.3 Hz, 1H), 6.89 (d, *J* = 16.3 Hz, 1H), 6.65 (d, *J* = 2.2 Hz, 2H), 6.51 (d, *J* = 2.2 Hz, 2H), 6.40 (t, *J* = 2.2 Hz, 1H), 6.35 (t, *J* = 2.2 Hz, 1H), 3.87 (s, 6H), 3.82 (s, 6H).

^{13}C NMR (75 MHz, C*D*Cl$_3$) δ (ppm): 161.3 (x2C), 161.0 (x2C), 155.5, 142.1, 139.5, 132.6, 129.5, 127.9, 126.9, 123.2, 122.4, 118.8, 111.9, 110.0, 105.4 (x2C), 104.3 (x2C), 99.9, 99.3, 55.5 (x2C), 55.4 (x2C).

(*E*)-5-(2-(3-(3,5-dihydroxyphenyl)benzofuran-5-yl)vinyl)benzene-1,3-diol (31)

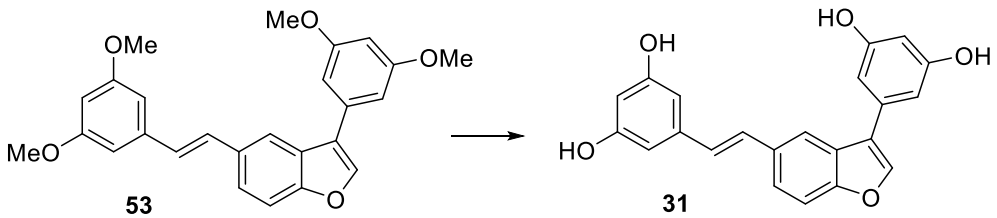

To a solution of compound **53** (0.11 mmol, 1 eq.) in dry DCM (7 mL) under nitrogen atmosphere a 1M BBr_3 solution in DCM (1.37 mmol, 12 eq.) was added dropwise at 0 °C. The mixture was stirred at room temperature for 9 h. The reaction was quenched with H_2O at 0 °C. The aqueous phase was extracted with EtOAc three times. The combined organic phases were dried over anhydrous Na_2SO_4, and concentrated under reduced pressure. The residue was purified by FC with DCM/MeOH (95:5) to give the desired product. Yield: 14%, light brown sticky solid.

R_f: 0.48 (DCM/MeOH 9:1)

^{1}H NMR (300 MHz, C*D*$_3$O*D*) δ (ppm): 7.93 (d, *J* = 1.5 Hz, 1H), 7.90 (s, 1H), 7.57 (dd, J_1 = 8.6, J_2 = 1.5 Hz, 1H), 7.49 (d, *J* = 8.6 Hz, 1H), 7.19 (d, *J* = 16.3 Hz, 1H), 7.00 (d, *J* = 16.3 Hz, 1H), 6.65 (d, *J* = 2.2 Hz, 2H), 6.51 (d, *J* = 2.2 Hz, 2H), 6.31 (t, *J* = 2.2 Hz, 1H), 6.19 (t, *J* = 2.2 Hz, 1H).
^{13}C NMR (150 MHz, C*D*$_3$O*D*) δ (ppm): 160.1 (x2C), 159.7 (x2C), 156.9, 143.4, 140.9, 134.8, 134.2, 129.7, 129.2, 128.0, 124.2, 123.6, 119.5, 112.7, 106.9 (x2C), 106.0 (x2C), 103.0, 102.8.

2-bromo-1-(3,5-dimethoxyphenyl)ethan-1-one (55)

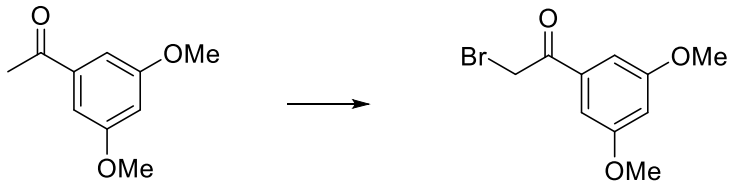

58 **55**

To a solution of 1-(3,5-dimethoxyphenyl)ethan-1-one **58** (11.09 mmol, 1 eq) in a mixture of EtOAc/$CHCl_3$ (1:1, v/v, 30 mL) $CuBr_2$ (22.19 mmol, 2 eq) was added. The mixture was stirred at reflux overnight. The green reaction mixture was cooled to room temperature and filtered on a celite pad using EtOAc to wash the filter. The solvent was evaporated under reduced pressure. The crude was purified by FC with CHX/DCM/EtOAc 10:1:0.5 as eluent. Yield: 67%; orange amorphous solid. Analitical data were in accordance with literature report (Lindgren et al. 2016)

R_f: 0.32 (cyclohexane/AcOEt/DCM 10:0.5:1)

^{1}H NMR (300 MHz, C*D*Cl$_3$) δ (ppm): 7.11 (d, 2H, *J*=2.3 Hz), 6.69 (t, 1H, *J*=2.3 Hz), 4.42 (s, 2H), 3.84 (s, 6H).
^{13}C NMR (75 MHz, C*D*Cl$_3$) δ (ppm): 191.2, 161.1 (x2C), 135.9, 106.8 (x2C), 106.3, 55.8 (x2C), 31.1.

1-(3,5-dimethoxyphenyl)-2-(3-methoxyphenoxy)ethan-1-one (56b)

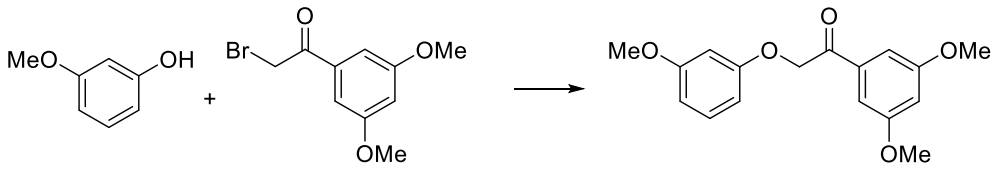

3-methoxyphenol **55** **56b**

A solution of **55** (1.15 mmol), 3-methoxyphenol (1.23 mmol, 1.1 eq) and K_2CO_3 (3.47 mmol, 3 eq) in dry acetone (3.2 mL) under nitrogen atmosphere was heated at reflux. After 2h, the reaction mixture was cooled to room temperature, concentrated under reduced pressure, diluted with EtOAc and washed with H_2O. The aqueous phase was extracted twice with EtOAc. The combined organic phases were washed with H_2O, dried over anhydrous Na_2SO_4 and concentrated under reduced pressure. The residue was purified by FC with CHX/AcOEt/DCM (10:1:2) as eluent. Yield: 90%, yellow-orange sticky solid. Analytical data were in accordance with literature report (Lindgren et al. 2016)

R_f: 0.32 (cyclohexane/AcOEt/DCM 10:1:2)

^{1}H NMR (300 MHz, C*D*Cl$_3$) δ 7.22 – 7.14 (m, 1H), 7.12 (d, *J* = 2.3 Hz 2H), 6.69 (t, *J* = 2.3 Hz, 1H), 6.58 – 6.49 (m, 3H), 5.23 (s, 2H), 3.84 (s, 6H), 3.78 (s, 3H).

^{13}C NMR (75 MHz, C*D*Cl$_3$) δ (ppm): 193.3, 161.4, 161.2 (x2C), 159.7, 136.2, 123.1, 111.1, 110.6, 106.3, 105.9 (x2C), 100.9, 70.8, 55.8 (x2C), 55.7.

3-(3,5-dimethoxyphenyl)-6-methoxybenzofuran (57b)

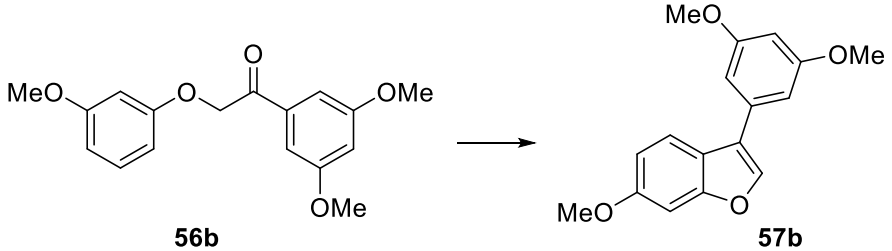

56b **57b**

To a solution of compound **56b** (0.33 mmol, 1 eq.) in dry DCM (3.9 mL) under nitrogen atmosphere $Bi(OTf)_3$ (0.07 mmol, 0.2 eq.) was added. The mixture was stirred at reflux overnight. After cooling, the mixture was filtered on a celite pad washing with DCM and then concentrated under reduced pressure. The crude was purified by FC (CHX/EtOAc from 9:1 to 7:3). Yield: 43%, white solid.

M.p. 87 °C.

R_f: 0.47 (cyclohexane:AcOEt 85:15)

^{1}H NMR (300 MHz, C*D*Cl$_3$) δ (ppm): 7.72 (s, 1H), 7.70 (d, *J* = 8.6 Hz, 1H), 7.07 (d, *J* = 2.3 Hz, 1H), 6.95 (dd, J_1 = 8.6, J_2 = 2.3 Hz, 1H), 6.78 (d, *J* = 2.3 Hz, 2H), 6.49 (t, *J* = 2.3 Hz, 1H), 3.88 (s, 3H), 3.86 (s, 6H).
^{13}C NMR (75 MHz, C*D*Cl$_3$) δ (ppm): 161.2 (x2C), 158.2, 156.8, 140.6, 134.0, 122.2, 120.6, 119.7, 112.1, 105.6 (x2C), 99.4, 96.2, 55.7, 55.4 (x2C).

3-(3,5-dimethoxyphenyl)-6-methoxy-2-(4-methoxyphenyl)benzofuran (37)

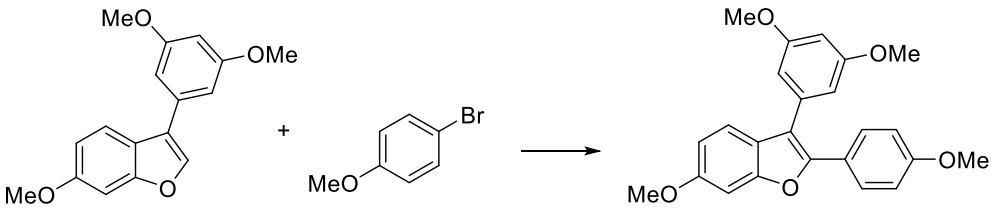

37 **1-bromo-4-methoxybenzene** **38**

A mixture of compound **37** (0.14 mmol, 1eq.), $Pd(OAc)_2$ (0.01 mmol, 0.1 eq.), 1-bromo-4-methoxybenzene (0.28 mmol, 2 eq.), $PCy_3 \cdot HBF_4$ (0.03 mmol, 0.2 eq.), K_2CO_3 (0.21 mmol, 1.5 eq.) and pivalic acid (0.42 mmol, 3 eq.) in DMA (0.6 mL) was degassed. Then, the reaction mixture was heated at 100 °C under stirring for 20 h. After cooling, the mixture was diluted with EtOAc, washed with H_2O and aq saturated $NaHCO_3$. The organic phase was dried over anhydrous Na_2SO_4 and concentrated under reduced pressure. FC was

used to purify the crude with CHX/AcOEt/DCM (from 10:0.1:1 to 9:1:2) as eluent. Yield: 80%, orange sticky solid.

R_f: 0.31 (cyclohexane/AcOEt/DCM 10:0.5:1)

^{1}H NMR (300 MHz, C*D*Cl$_3$) δ (ppm): 7.64 – 7.57 (m, 2H), 7.38 (d, *J* = 8.6 Hz, 1H), 7.08 (d, *J* = 2.2 Hz, 1H), 6.89 – 6.83 (m, 3H), 6.64 (d, *J* = 2.3 Hz, 2H), 6.50 (t, *J* = 2.3 Hz, 1H), 3.89 (s, 3H), 3.82 (s, 3H), 3.78 (s, 6H).
^{13}C NMR (75 MHz, C*D*Cl$_3$) δ (ppm): 161.2 (x2C), 159.5, 158.1, 154.7, 149.9, 135.1, 128.2 (x2C), 123.7, 123.5, 120.0, 115.8, 113.8 (x2C), 111.7, 107.6 (x2C), 99.8, 95.7, 55.8, 55.4 (x2C), 55.3.

3-bromo-5-methoxyphenol (54a)

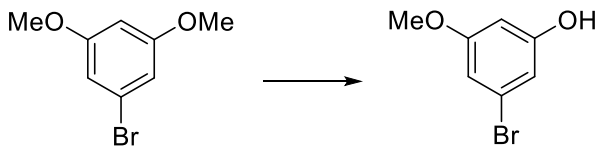

1-bromo-3,5-dimethoxybenzene → **54a**

To a solution of 1-bromo-3,5-dimethoxybenzene (1 g, 4.60 mmol) in dry DCM (3.2 mL) was added BBr_3 1M in DCM (1.52 mL, 1.52 mmol, 0.33 eq), at 0°C under nitrogen. The mixture was slowly warmed to room temperature. After 22 h the reaction mixture was quenched with MeOH under nitrogen atmosphere and concentrated under reduced pressure. The residue was purified by FC (cyclohexane/AcOEt 9:1) to give the desired product as yellow sticky solid in 58% yield. Analytical data were in accordance with literature report (Lindgren et al. 2016)

R_f: 0.2 (cyclohexane/AcOEt 9:1)

^{1}H NMR (300 MHz, C*D*Cl$_3$) δ (ppm): 6.63 (dd, J_1 = 2.2, J_2 = 1.5 Hz, 2H), 6.33 (t, *J* = 2.2 Hz, 1H), 3.77 (s, 3H).

^{13}C NMR (75 MHz, C*D*Cl$_3$) δ (ppm): 161.4, 157.1, 122.9, 111.5, 110.1, 100.9, 55.6.

2-(3-bromo-5-methoxyphenoxy)-1-(3,5-dimethoxyphenyl)ethan-1-one (56a)

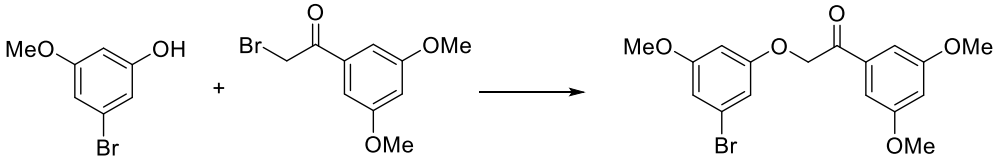

54a **55** **56a**

A mixture of compound **55** (2.46 mmol, 1 eq.), **55a** (2.46 mmol, 1 eq.) and K_2CO_3 (7.39 mmol, 3 eq) in dry acetone (7 mL) was stirred at reflux. After 2h, the mixture was cooled to room temperature, concentrated under reduced pressure, diluted with EtOAc and washed with H_2O. The aqueous phase was extracted again with EtOAc. The collected organic phases dried over anhydrous Na_2SO_4, filtered and concentrated. The crude was purified by FC (CHX/EtOAc from 9:1 to 8:2). Yellow solid, yield: 89%.

M.p.:106-108 °C.

R$_f$: 0.24 (cyclohexane/AcOEt/DCM 10:1:2)

^{1}H NMR (300 MHz, C*D*Cl$_3$) δ (ppm): 7.10 (d, *J* = 2.3 Hz, 2H), 6.70 (t, *J* = 2.1 Hz, 2H), 6.67 (dd, J_1 = 2.3, J_2 = 1.6 Hz, 1H), 6.45 (t, *J* = 2.3 Hz, 1H), 5.21 (s, 2H), 3.85 (s, 6H), 3.76 (s, 3H).

^{13}C NMR (75 MHz, C*D*Cl$_3$) δ (ppm): 193.3, 161.4, 161.2 (x2C), 159.7, 136.2, 123.1, 111.1, 110.6, 106.3, 105.9 (x2C), 100.9, 70.8, 55.8 (x2C), 55.7.

4-bromo-3-(3,5-dimethoxyphenyl)-6-methoxybenzofuran (57a)

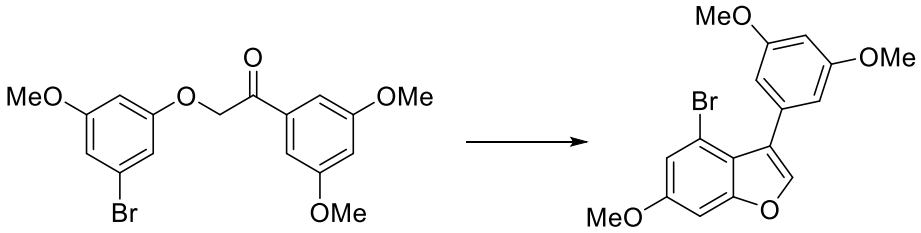

56a **57a**

To a solution of compound **56a** (0.33 mmol, 1 eq) in dry DCM (3.9 mL) under nitrogen atmosphere $Bi(OTf)_3$ (0.07 mmol,0.2 eq.) was added. The mixture was stirred at reflux overnight. After cooling, the mixture was filtered on a celite pad washing the filter with DCM. The filtrate was concentrated under reduced pressure, and the resulting residue was purified by FC (CHX/EtOAc from 9:1 to 7:3). Yield: 83%, white sticky solid. Analytical data were in agreement with literature report (Lindgren et al. 2016)

R_f: 0.49 (cyclohexane/AcOEt 9:1)

^{1}H NMR (300MHz, C*D*Cl$_3$) δ (ppm): 7.54 (s, 1H), 7.10 (d, *J* = 2.2 Hz, 1H), 7.03 (d, *J* = 2.2 Hz, 1H), 6.66 (d, *J* = 2.3 Hz, 2H), 6.51 (t, *J*= 2.3 Hz, 1H), 3.86 (s, 3H), 3.83 (s, 6H).

^{13}C NMR (75 MHz, C*D*Cl$_3$) δ (ppm): 160.1 (x2C), 158.3, 156.6, 142.5, 132.8, 123.2, 119.9, 116.6, 114.0, 109.1 (x2C), 100.2, 95.9, 56.1, 55.5 (x2C).

5-(4-bromo-6-hydroxybenzofuran-3-yl)benzene-1,3-diol (58)

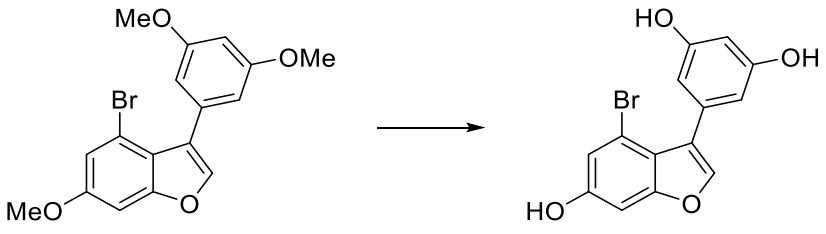

57a **58**

To a solution of **57a** (0.14 mmol, 1 eq.) in dry DCM (1.45 mL), under nitrogen atmosphere, at 0 °C, BBr_3 1M in DCM, (0.40 mmol, 3 eq.) was added dropwise. The reaction mixture was allowed to warm to room temperature. After 16 h, the reaction mixture was quenched with cold saturated aq $NaHCO_3$ (0°C), and the organic solvent was evaporated. The aqueous phase was extracted with EtOAc three times. The combined organic phases were dried over anhydrous Na_2SO_4, and concentrated under reduced pressure. The residue was purified by FC with DCM/MeOH (95:5) as eluent to give the desired product. Yield: 91%, light brown oil. Analytical data were in accordance with literature report (Lindgren et al. 2016).

R_f: 0.49 (DCM/MeOH 9:1)

^{1}H NMR (300 MHz, CD_3OD) δ (ppm): 7.54 (s, 1H), 6.95 (d, *J* = 2.0 Hz, 1H), 6.90 (d, *J* = 2.0 Hz, 1H), 6.39 (d, *J* = 2.2 Hz, 2H), 6.29 (t, *J* = 2.2 Hz, 1H).
^{13}C NMR (75 MHz, DMSO-d_6) δ (ppm): 157.6 (x2C), 156.2, 156.0, 142.4, 132.0, 122.6, 118.0, 116.6, 112.8, 108.9 (x2C), 101.9, 97.7.

5-(6 hydroxy-2-(4-hydroxyphenyl)benzofuran-3-yl)benzene-1,3-diol (32)

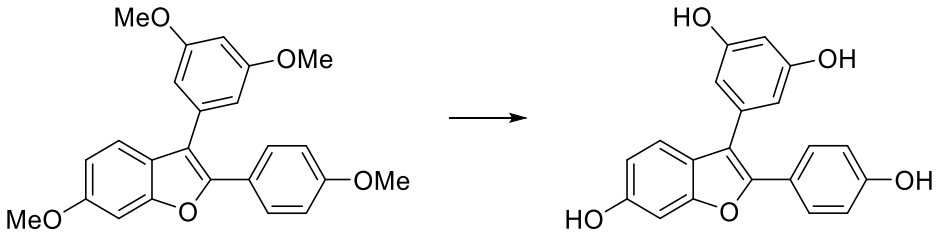

37 **32**

To a solution of **37** (0.12 mmol, 1 eq.) in dry DCM (1.2 mL), under nitrogen atmosphere, at 0°C, BBr_3 1M in DCM (0.45 mmol, 3.9 eq.) was added dropwise. The reaction mixture was allowed to warm to room temperature. After 16 h, the mixture was quenched with cold aq saturated $NaHCO_3$ (0°C), and the organic solvent was evaporated. The aqueous phase was extracted

with EtOAc three times. The combined organic phases were dried over anhydrous Na_2SO_4, and concentrated under reduced pressure. The residue was purified by FC using CHX/acetone (6:4) as eluent to give the desired product. Yield: 52%, light brown solid.

M.p.: 239-240°C.

R_f: 0.2 (cyclohexane/acetone 6:4)

^{1}H NMR (300 MHz, C*D*$_3$O*D*) δ (ppm): 7.50 – 7.43 (m, 2H), 7.24 (d, *J* = 8.6 Hz, 1H), 6.91 (d, *J* = 2.2 Hz, 1H), 6.77 – 6.70 (m, 3H), 6.38 (d, *J* = 2.2 Hz, 2H), 6.29 (t, *J* = 2.2 Hz, 1H).
^{13}C NMR (75 MHz, C*D*$_3$O*D*) δ (ppm): 158.6 (x2C), 157.2, 155.3, 154.7, 149.3, 135.1, 127.8 (x2C), 122.8, 122.3, 119.4, 115.4, 114.8 (x2C), 111.5, 107.7 (x2C), 101.3, 96.9.

(E)-5-(6-hydroxy-4-(4-hydroxystyryl)benzofuran-3-yl)benzene-1,3-diol (33)

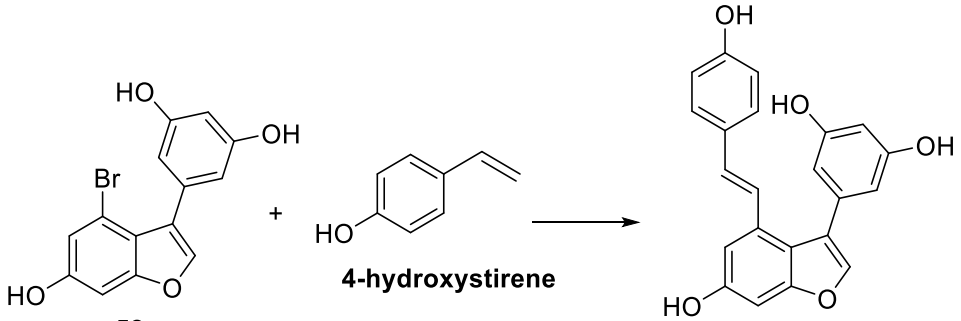

A mixture of compound **58** (0.45 mmol, 1eq.), 4-hydroxystirene (0.78 mmol, 1.5 eq.), 1,3-bis(diphenylphosphino)propane (dppp) (0.05 mmol, 0.1 eq.) and dry TEA (0.91 mmol, 2 eq.) in dry DMF (14.6 mL) was degassed. $Pd(OAc)_2$ (0.05 mmol, 0.1 eq.) was added to the mixture, and the reaction mixture was heated at 120 °C under stirring for 20 h. After cooling, DMF was evaporated,

and the residue was diluted with EtOAc, washed with H_2O and brine. The organic phase was dried over anhydrous Na_2SO_4 and concentrated under reduced pressure. The crude was purified by FC using CHX/Acetone 6:4 as eluent. Yield: 80%, light brown solid.

M.p.: 234-235°C.

R_f: 0.22 (cyclohexane/acetone 6:4)

^{1}H NMR (300 MHz, CD_3OD) δ (ppm): 7.50 (s, 1H), 7.20 (d, *J* = 16.3 Hz, 1H), 7.11 – 7.06 (m, 2H), 7.05 (d, *J* = 2.0 Hz, 1H), 6.91 (d, *J* = 16.3 Hz, 1H), 6.79 (d, *J* = 2.0 Hz, 1H), 6.70 – 6.64 (m, 2H), 6.43 (d, *J*= 2.2 Hz, 2H), 6.38 (t, *J*= 2.2 Hz, 1H).
^{13}C NMR (75 MHz, CD_3OD) δ (ppm): 158.2 (x2C), 156.9, 155.4, 140.4, 135.1, 132.2, 129.2, 128.4, 127.4 (x2C), 123.2, 122.4, 117.8, 114.9 (x2C), 110.0, 108.4 (x2C), 106.5, 101.4, 96.4.

Methyl 3-hydroxy-5-methoxybenzoate (60)

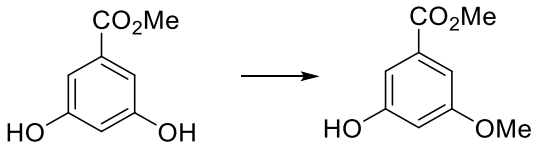

To a solution of 3,5-hydroxymethoxybenzoate **59** (5.94 mmol, 1 eq.) in dry DMF (7.5 mL) under hydrogen atmosphere, CH_3I (5.94 mmol, 1 eq.) and K_2CO_3 (8.92 mmol, 1.5 eq.) were added. The mixture was stirred at room temperature for 2 days. Then, the reaction was quenched with aq saturated NH_4Cl and the mixture was extracted with EtOAc three times. The collected organic phases were dried over anhydrous Na_2SO_4, and concentrated under reduced pressure. FC was used to purify the crude with CHX/EtOAc 7:3 as eluent. Yield: 35%, white solid. Analytical data were in accordance with literature report (Hoffmann and Pete 2001).

M.p.: 93-94°C

R_f: 0.43 (CHX/AcOEt 7:3)

^{1}H NMR (300 MHz, C*D*Cl$_3$) δ (ppm): 7.17 - 7.15 (m, 2H), 6.63 (t, *J*= 2.4 Hz, 1H), 5.52 (s, 1H), 3.91 (s, 3H), 3.82 (s, 3H).
^{13}C NMR (75 MHz, C*D*Cl$_3$) δ (ppm): 167.5, 160.7, 157.1, 131.6, 109.4, 107.1, 106.8, 55.5, 52.5.

Methyl 3-(2,2-dimethoxyethoxy)-5-methoxybenzoate (61)

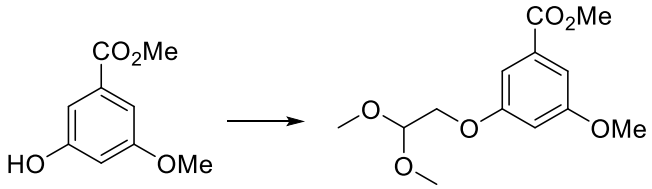

60 **61**

To a solution of compound **60** (2.74 mmol, 1 eq.) in dry ACN, under nitrogen atmosphere, 2-bromo-1,1-dimethoxyethane (4.18 mmol, 1.5 eq.) was added dropwise, followed by Cs_2CO_3 (5.54 mmol, 2 eq.). The mixture was refluxed for three days. After cooling, the solvent was evaporated under reduced pressure, and the residue was diluted with EtOAc and washed with H_2O. The aqueous phase was extracted with EtOAc and the collected organic phases were dried over anhydrous Na_2SO_4, and concentrated under reduced pressure. The residue was purified by FC with CHX/DCM/EtOAc (10:2:1) as eluent. Yield: 67%, yellow oil. Analytical data were in accordance with literature report (Liu et al. 2016)

R_f: 0.36 (CHX/AcOEt 8:2)

^{1}H NMR (300 MHz, C*D*Cl$_3$) δ (ppm): 7.20 (d, *J* = 2.3 Hz, 2H), 6.69 (t, *J* = 2.3 Hz, 1H), 4.72 (t, *J* = 5.2 Hz, 1H), 4.03 (d, *J* = 5.1 Hz, 3H), 3.90 (s, 3H), 3.82 (s, 3H), 3.46 (s, 6H).

^{13}C NMR (75 MHz, C*D*Cl$_3$) δ (ppm): 166.8, 160.8, 159.7, 132.2, 107.9, 107.7, 106.4, 102.1, 68.0, 55.7, 54.3 (x2C), 52.4.

Methyl 6-methoxybenzofuran-4-carboxylate (62)

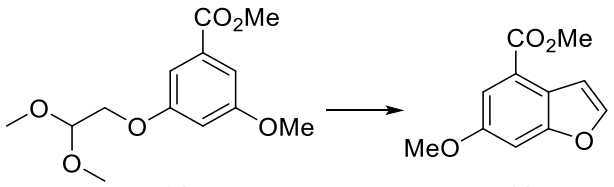

61 **62**

To a solution of compound **61** (0.37 mmol, 1 eq.) in chlorobenzene (3 mL) amberlyst-15 (10 wt%) was added. The mixture was heated at 120 °C for 4 h. After cooling, the mixture was filtered, and the solvent was evaporated under reduced pressure. The residue was purified by FC with CHX/EtOAc 9:1 as eluent. Yield: 63%, white solid. Analytical data were in accordance with literature report (Liu et al. 2016).

M.p.: 49-50°C

R_f: 0.42 (CHX/AcOEt 9:1)

^{1}H NMR (300 MHz, C*D*Cl$_3$) δ (ppm): 7.63 (d, *J* = 2.2 Hz, 1H), 7.60 (d, *J* = 2.2 Hz, 1H), 7.26 – 7.20 (m, 2H), 3.98 (s, 3H), 3.89 (s, 3H).
^{13}C NMR (300 MHz, C*D*Cl$_3$) δ (ppm): 166.8, 157.4, 156.4, 145.7, 122.8, 121.7, 113.4, 107.7, 101.5, 56.1, 52.2.

Methyl 2-bromo-6-methoxybenzofuran-4-carboxylate (63)

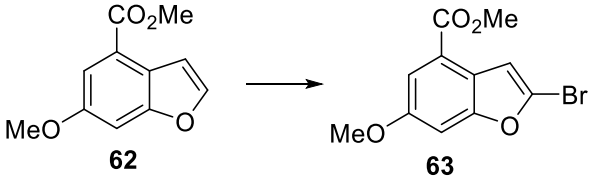

62 **63**

To a solution of compound **62** (0.23 mmol, 1 eq.) in 1,2 dichloroethane, *N*-bromosuccinimide (0.35 mmol, 1.5 eq) and a catalytic amount of DMF (12 µL) were added. The mixture was stirred at 70 °C for 4h. To quench the reaction, aq saturated $Na_2S_2O_3$ was added to the mixture and the aqueous phase was extracted with EtOAc three times. The organic phases were combined, dried over anhydrous Na_2SO_4, and concentrated under reduced pressure. The crude was purified by FC with CHX/EtOAc 95:5 as eluent. Yield: 80%, white solid. Analytical data were in agreement with literature report (Liu et al. 2016).

M.p.: 92-93°C

R_f: 0.42 (CHX/AcOEt 95:5)

^{1}H NMR (300 MHz, C*D*Cl$_3$) δ (ppm): 7.57 (d, *J* = 2.3 Hz, 1H), 7.22 (d, *J* = 0.9 Hz, 1H), 7.18 (dd, J_1 = 2.3, J_1 = 0.9 Hz, 1H), 3.97 (s, 3H), 3.88 (s, 3H).
^{13}C NMR (75 MHz, C*D*Cl$_3$) δ (ppm): 166.4, 157.3, 157.0, 128..8, 122.9, 122.0, 113.5, 109.5, 101.3, 56.3, 52.4.

Methyl 6-methoxy-2-(4-methoxyphenyl)benzofuran-4-carboxylate (64)

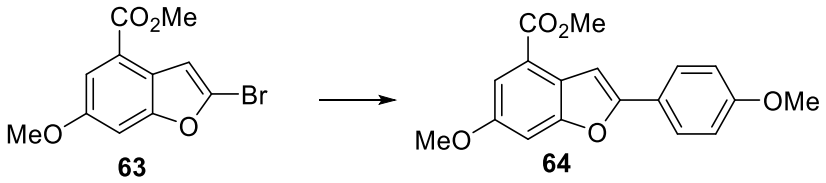

A solution of compound **63** (0.17 mmol, 1 eq.), 4-methoxyphenylboronic acid (0.35 mmol, 2 eq.), and K_2CO_3 (0.92 mmol, 5.3 eq.) was degassed for 30 min. Then, $Pd(PPh_3)_4$ (0.005 mmol, 0.03 eq.) was added and the mixture was degassed again. The reaction was heated at 70 °C overnight. After cooling, the mixture was quenched with water and the aqueous phase was extracted three times with EtOAc. The organic phases were washed with brine, dried over anhydrous Na_2SO_4, and concentrated. The crude was purified on FC with

CHX/EtOAc (9:1) as eluent. Yield: 91%, white solid. Analytical data were in agreement with literature report (Liu et al. 2016)

M.p.: 101-103 °C.

R_f: 0.25 (CHX/AcOEt 9:1)

^{1}H NMR (300 MHz, C*D*Cl$_3$) δ (ppm): 7.79 (d, *J* = 9.0 Hz, 2H), 7.56 (d, *J* = 2.3 Hz, 1H), 7.39 (d, *J* = 0.9 Hz, 1H), 7.25 (dd, J_1 = 2.3 Hz, J_2 = 0.9 Hz, 1H), 6.97 (d, *J* = 9.0 Hz, 2H), 4.00 (s, 3H), 3.90 (s, 3H), 3.87 (s, 3H).
^{13}C NMR (75 MHz, C*D*Cl$_3$) δ (ppm): 166.8, 160.1, 157.0, 156.7, 156.0, 126.4 (x2C), 124.0, 123.0, 121.7, 114.3 (x2C), 112.5, 101.4, 100.6, 56.0, 55.3, 52.0.

(6-Methoxy-2-(4-methoxyphenyl)benzofuran-4-yl)methanol (68)

To the solution of compound **64** (0.38 mmol, 1 eq.) in dry THF, under nitrogen atmosphere, at 0 °C was added $LiAlH_4$ 1M in THF (1.06 mmol, 3 eq.) dropwise. The mixture was stirred for 10 minutes at 0 °C. Then, the reaction mixture was quenched with HCl 1M at 0 °C. The aqueous phase was extracted with EtOAc three times. The organic phases were combined, dried over anhydrous Na_2SO_4, filtered and concentrated under reduced pressure. Purification by FC with CHX/EtOAc (7:3) as eluent gave compound **68** as a yellow solid. Yield: 89%.

M.p.: 98-99 °C.

R_f: 0.26 (CHX/AcOEt 8:2)

^{1}H NMR (300 MHz, C*D*Cl$_3$) δ (ppm): 7.74 (d, *J* = 9.0 Hz, 2H), 6.99 – 6.93 (m, 4H), 6.86 (d, *J* = 0.9 Hz, 1H), 4.88 (s, 2H), 3.86 (s, 3H), 3.85 (s, 3H).

^{13}C NMR (75 MHz, C*D*Cl$_3$) δ (ppm): 159.7, 157.7, 155.8, 155.7, 133.5, 126.0 (x2C), 123.6, 121.3, 114.3 (x2C), 110.0, 98.1, 95.3, 63.6, 55.9, 55.4.

6-Methoxy-2-(4-methoxyphenyl)benzofuran-4-carbaldehyde (65)

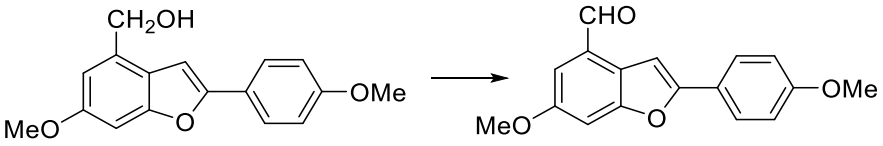

68 **65**

To the solution of compound **68** (0.27 mmol, 1 eq.) in dry DCM, DMP (0.35 mmol, 1.3 eq.) was added at 0 °C. The mixture was stirred at room temperature for 75 min. Then, the solvent was evaporated under reduced pressure. The residue was purified by FC with CHX/EtOAc as eluent (9:1 to 7:3). Yield: 97%, yellow solid.

M.p.: 121 °C.

R$_f$: 0.45 (CHX/AcOEt 8:2)

^{1}H NMR (300 MHz, C*D*Cl$_3$) δ (ppm): 10.14 (s, 1H), 7.80 (d, *J* = 9.0 Hz, 2H), 7.52 (d, *J* = 0.9 Hz, 1H), 7.30 – 7.28 (m, 2H), 6.98 (d, *J* = 9.0 Hz, 1H), 3.92 (s, 3H), 3.86 (s, 3H).

^{13}C NMR (75 MHz, C*D*Cl$_3$) δ (ppm): 191.6, 160.2, 158.3, 157.1, 156.1, 128.2, 126.4 (x2C), 122.7, 122.5, 115.3, 114.3 (x2C), 102.2, 99.3, 56.0, 55.4.

(*E*)-6-methoxy-2-(4-methoxyphenyl)-4-(4-methoxystyryl)benzofuran (66)

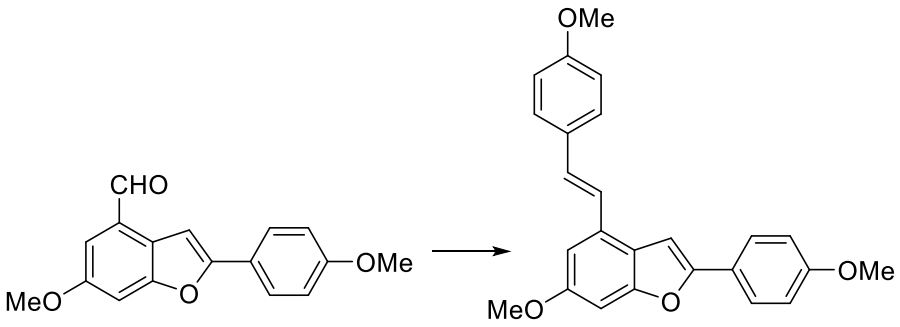

In a MW vial, compound **65** (0.23 mmol, 1 eq.) and diethyl (4-methoxybenzyl)phosphonate (0.46 mmol, 2 eq.) were solubilized in dry THF, under nitrogen atmosphere. Then, 60% NaH in mineral oil (0.69 mmol, 3 eq.) was added to the solution and the mixture was heated under microwave irradiation at 120 °C for 30 min. After cooling, the mixture was quenched by aq saturated solution of NH_4Cl and the aqueous phase was extracted with EtOAc three times. The organic phases were washed with brine, dried over anhydrous Na_2SO_4 and concentrated under reduced pressure. Purification of the crude by FC with CHX/EtOAc (8:2) as eluent gave the title compound. Yield: 54%, light yellow oil.

R_f: 0.33 (CHX/AcOEt 9:1)

^{1}H NMR (300 MHz, C*D*Cl$_3$) δ (ppm): 7.78 (d, *J* = 9.0 Hz, 2H), 7.52 (d, *J* = 9.0 Hz, 2H), 7.20 (d, *J* = 2.3 Hz, 2H), 7.08 (d, *J* = 0.9, 1H), 7.04 (d, *J* = 2.3 Hz, 1H), 6.99 – 6.92 (m, 5H), 3.90 (s, 3H), 3.86 (s, 3H), 3.85 (s, 3H).
^{13}C NMR (75 MHz, C*D*Cl$_3$) δ (ppm): 159.7, 159.6, 157.7, 156.0, 155.3, 130.6, 130.2, 129.9, 127.8, 126.0 (x2C), 124.0, 123.5, 121.6, 114.3 (x2C), 114.2, 113.7, 110.0, 107.9, 98.4, 95.2, 55.8, 55.3 (x2C).

(*E*)-2-(4-hydroxyphenyl)-4-(4-hydroxystyryl)benzofuran-6-ol (34)

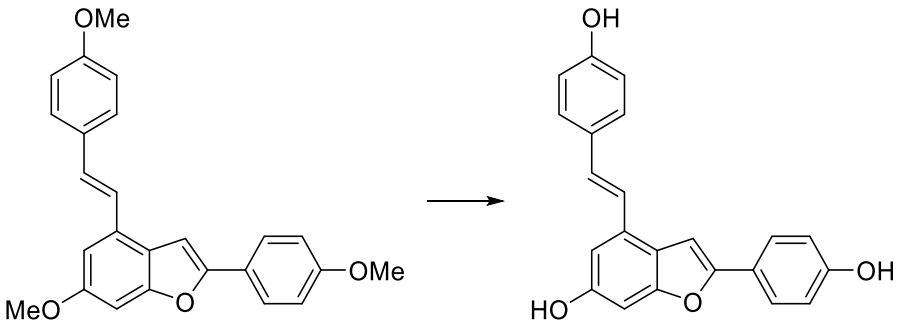

66 **64**

To a solution of compound **66** (0.07 mmol, 1 eq.) BBr_3 1M in DCM (0.65 mmol, 9 eq.) was added dropwise at 0°C. The mixture was stirred at room temperature for 6 h. The reaction was quenched with H_2O at 0 °C. The aqueous phase was extracted with EtOAc three times. The combined organic phases were dried over anhydrous Na_2SO_4, and concentrated under reduced pressure. The residue was purified by FC (DCM/MeOH 95:5) to give the desired product. Yield: 24%, brown sticky solid.

R_f: 0.31 (DCM/MeOH 95:5)

^{1}H NMR (300 MHz, CD_3OD) δ (ppm): 7.70 (d, *J* = 9.0 Hz, 2H), 7.47 (d, *J* = 9.0 Hz, 2H), 7.26 – 7.12 (m, 3H), 6.93 (d, *J* = 2.3 Hz, 1H), 6.87 – 6.79 (m, 5H).
^{13}C NMR (150 MHz, CD_3OD) δ (ppm): 158.9, 158.6, 157.4, 156.5, 156.3, 132.1, 130.9, 130.5, 129.0 (x2C), 127.0 (x2C), 124.0, 123.8, 122.2, 116.6 (x2C), 116.5 (x2C), 108.2, 98.8, 97.5.

3.2.5. Bibliography

Chand K, Rajeshwari, Hiremathad A, Singh M, Santos A, Keri RS (2017) A review on antioxidant potential of bioactive heterocycle benzofuran: Natural and synthetic derivatives. Pharmacol Reports 69:281–295. https://doi.org/10.1016/j.pharep.2016.11.007

Chibane BL, Degraeve P, Ferhout H, Bouajila J, Oulahal N (2019) Plant antimicrobial polyphenols as potential natural food preservatives. J Sci Food Agric 99:1457–1474. https://doi.org/10.1002/jsfa.9357

Elbert SM, Wagner P, Kanagasundaram T, Rominger F, Mastarlerz M (2017) Boroquinol Complexes with Fused Extended Aromatic Backbones: Synthesis and Optical Properties. Chem - A Eur J 23:935–945. https://doi.org/10.1002/chem.201604421

Elsherif MA, Hassan AS, Moustafa GO, Awad HM, Morsy NM (2020) Antimicrobial evaluation and molecular properties prediction of pyrazolines incorporating benzofuran and pyrazole moieties. J Appl Pharm Sci 10:37–43. https://doi.org/10.7324/JAPS.2020.102006

Ferreira S, Domingues F (2016) The antimicrobial action of resveratrol against Listeria monocytogenes in food-based models and its antibiofilm properties. J Sci Food Agric 96:4531–4535. https://doi.org/10.1002/jsfa.7669

Hiremathad A, Patil MR, Chethana KR, Chand K, Santos MA, Keri R (2015) Benzofuran: an emerging scaffold for antimicrobial agents. RSC Adv 5:96809–96828. https://doi.org/10.1039/c5ra20658h

Hoffmann N, Pete J-P (2001) Intramolecular [2 + 2] Photocycloaddition of Bichromophoric Derivatives of. Synthesis (Stuttg) 8:1236–1242. https://doi.org/10.1055/s-2001-15076

Iino T, Tsukahara D, Kamata K, Sasaki K, Ohyama S, Hosaka H, Hasegawa T, Chiba M, Nagata Y, Eiki J, NIshimura T (2009) Discovery of potent and orally active 3-alkoxy-5-phenoxy-N-thiazolyl benzamides as novel allosteric glucokinase activators. Bioorganic Med Chem 17:2733–2743. https://doi.org/10.1016/j.bmc.2009.02.038

Jaseer EA, Prasad DJC, Sekar G (2010) Domino synthesis of 2-arylbenzo[b]furans by copper(II)-catalyzed coupling of o-iodophenols and aryl acetylenes. Tetrahedron 66:2077–2082. https://doi.org/10.1016/j.tet.2010.01.026

Khanam H, Shamsuzzaman (2015) Bioactive Benzofuran derivatives: A review. Eur J Med Chem 97:483–504. https://doi.org/10.1016/j.ejmech.2014.11.039

Kim I, Choi J (2009) A versatile approach to oligostilbenoid natural products -

Synthesis of permethylated analogues of viniferifuran, malibatol A, and shoreaphenol. Org Biomol Chem 7:2788–2795. https://doi.org/10.1039/b901911a

King LC, Ostrum GK (1964) Selective Bromination with Copper(II) Bromide. J Org Chem 29:3459–3461. https://doi.org/10.1021/jo01035a003

Kraus GA, Gupta V (2009) A new synthetic strategy for the synthesis of bioactive stilbene dimers. A direct synthesis of amurensin H. Tetrahedron Lett. 50:7180–7183

Li XC, Ferreira D (2003) Stereoselective cyclization of stilbene derived carbocations. Tetrahedron 59:1501–1507. https://doi.org/10.1016/S0040-4020(03)00050-4

Lindgren AEG, Öberg CT, Hillgren JM, Elofsson M (2016) Total synthesis of the resveratrol oligomers (±)-Ampelopsin B and (±)-ε-Viniferin. European J Org Chem 2016:426–429. https://doi.org/10.1002/ejoc.201501486

Liu JT, Do TJ, Simmons CJ, Lynch JC, Gu W, Ma ZX, Tang W (2016) Total synthesis of diptoindonesin G and its analogues as selective modulators of estrogen receptors. Org Biomol Chem 14:8927–8930. https://doi.org/10.1039/c6ob01657j

Markina NA, Chen Y, Larock RC (2013) Efficient microwave-assisted one-pot three-component synthesis of 2,3-disubstituted benzofurans under Sonogashira conditions. Tetrahedron 69:2701–2713. https://doi.org/10.1016/j.tet.2013.02.003

Miao YH, Hu YH, Yang J, Liu T, Sun J, Wang X (2019) Natural source, bioactivity and synthesis of benzofuran derivatives. RSC Adv 9:27510–27540. https://doi.org/10.1039/c9ra04917g

Miliovsky M, Svinyarov I, Mitrev Y, Evstatieva Y, Nikolova D, Chochkova M, Bogdanov MG (2013) A novel one-pot synthesis and preliminary biological activity evaluation of cis-restricted polyhydroxy stilbenes incorporating protocatechuic acid and cinnamic acid fragments. Eur J Med Chem 66:185–192. https://doi.org/10.1016/j.ejmech.2013.05.040

Naik R, Harmalkar DS, Xu X, Jang K, Lee K (2015) Bioactive benzofuran derivatives: Moracins A-Z in medicinal chemistry. Eur J Med Chem 90:379–393. https://doi.org/10.1016/j.ejmech.2014.11.047

Saitoh M, Kunitomo J, Kimura E, Iwashita H, Uno Y, Onishi T, Uchiyama N, Kawamoto T, Tanaka T, Mol CD, Dougan DR, Textor GP, Snell GP, Takizawa M, Itoh F, Kori M (2009) 2-{3-[4-(Alkylsulfinyl)phenyl]-1-benzofuran-5-yl}-5-methyl-1,3,4-oxadiazole derivatives as novel inhibitors of glycogen synthase kinase-3β with good brain permeability. J Med Chem 52:6270–6286. https://doi.org/10.1021/jm900647e

Singh D, Mendonsa R, Koli M, Subramanian M, Nayak SK (2019) Antibacterial activity of resveratrol structural analogues: A mechanistic evaluation of the structure-activity relationship. Toxicol Appl Pharmacol 367:23–32. https://doi.org/10.1016/j.taap.2019.01.025

Várela-Fernández A, González-Rodríguez C, Varela JA, Castedo L, Saà C (2009) Cycloisomerization of aromatic homo and bis-homopropargylic alcohols via catalytic ru vinylidenes: Formation of benzofurans and isochromenes. Org Lett 11:5350–5353. https://doi.org/10.1021/ol902212h

Velu S, Thomas N, Weber JF (2012) Strategies and methods for the syntheses of natural oligomeric stilbenoids and analogues. Curr Org Chem 605–662

Vo DD, Elofsson M (2016) Total Synthesis of Viniferifuran, Resveratrol-Piceatannol Hybrid, Anigopreissin A and Analogues – Investigation of Demethylation Strategies. Adv Synth Catal 358:4085–4092. https://doi.org/10.1002/adsc.201601089

Wang M, Liu X, Zhou L, Zhu J, Sun X (2015) Fluorination of 2-substituted benzo[b]furans with Selectfluor™. Org Biomol Chem 13:3190–3193. https://doi.org/10.1039/c4ob02691h

Wu Y, Bai J, Zhong K, Huang Y, Qi H, Jiang Y, Gao H (2016) Antibacterial activity and membrane-disruptive mechanism of 3-*p*-*trans*-coumaroyl-2-hydroxyquinic acid, a novel phenolic compound from pine needles of Cedrus deodara, against Staphylococcus aureus. Molecules 21:1084. https://doi.org/10.3390/molecules21081084

Yao T, Yue D, Larock RC (2014) Synthesis of 2,3-Disubstituted Benzofurans by the Palladium-Catalyzed Coupling of 2-Iodoanisoles and Terminal Alkynes, Followed by Electrophilic Cyclization: 3-Iodo-2-phenylbenzofuran. Org Synth 91:283–292. https://doi.org/10.15227/orgsyn.091.0283

3.3. DEVELOPMENT OF SYNTHETIC STRATEGIES TO ADDRESS GRAM-NEGATIVE BACTERIA

ABSTRACT: Gram-negative bacteria infections, responsible for the most part of the hospital-acquired infections and often escaping the action of traditional antibiotics, represent a serious threat to human health. In order to broaden the spectrum of antimicrobial activity of natural stilbenoids also on Gram-negative bacteria, we developed a series of synthetic strategies to modify the stilbenoid scaffold of both monomer and dimer resveratrol-derived compounds. Synthetic approaches were developed to enable modifications of dehydro-δ-viniferin (**15**), the most promising compound as antimicrobial agent among the resveratrol-derivatives studied in our previous work. Besides further SAR studies, the synthetic routes developed would allow the construction of hybrid antibiotics, containing for example siderophore portions, in order to fight Gram-negative bacterial infections. In addition, we synthesized a series of analogues bearing a nitrogen moiety attempting to improve the interaction with the negatively charged portion of the lipopolysaccharide, constituting the outer membrane of Gram-negative bacteria.

3.3.1. Introduction

Gram-negative bacteria infections are responsible for the most part of the hospital-acquired infections, frequently “escaping” the action of traditional antibiotics. Indeed, the collectively known ESKAPE pathogens include four Gram-negative species (*Klebsiella pneumoniae*/*Escherichia coli*, *Acinetobacter baumannii*, *Pseudomonas aeruginosa*, and *Enterobacter* species), besides the two Gram-positive strains *Enterococcus faecium* and *S. aureus* (Domalaon et al. 2018; Richter and Hergenrother 2019). In 2017, the World Health Organization ((WHO) 2017) included nine Gram-negative bacteria in the list of the twelve “Priority pathogens”, for which new antibiotics are urgently needed. Indeed, the last class of antibiotics (fluoroquinolones) effective against Gram-negative bacteria was introduced in 1968 (Richter and

Hergenrother 2019). It is evident that the discovery of new molecules active against Gram-negative pathogens is of utmost importance. The scarcity of compounds endowed with Gram-negative antibacterial activity is due to the impermeable structure of the two cellular membranes of Gram-negative bacteria. Gram-positive bacteria have a cell wall made up of peptidoglycan chains and teichoic acid, surrounding the cytoplasmic membrane. On the other hand, Gram-negative bacteria present a double membrane: their cytoplasmic membrane is surrounded by a thin layer of peptidoglycan chains (inner membrane, IM), further covered by an outer membrane (OM) (Figure 3.17) (Richter and Hergenrother 2019).

The OM is an asymmetric bilayer with an inner leaflet consisting of phospholipids and an outer leaflet of chains of lipopolysaccharides (LPS). LPS is made up of the hydrophobic lipid A linked to an hydrophilic negatively charged core of oligosaccharides binding the hydrophilic O antigen. Divalent cations (Ca^{2+} or Mg^{2+}) stabilize adjacent negative charges of the oligosaccharides, resulting in a very tight stacking of LPS molecules, which limits membrane permeation. Moreover, a hydration sphere created by the hydrophilic portion of LPS further hinders the passage of hydrophobic molecules across the membrane (Figure 3.17A). Conversely, charged or noncharged small hydrophilic molecules (≤ 600 g/mol) are able to exploit OM protein channels, called porins, to enter the periplasmic space. In addition, antibiotics able to displace the divalent cations (Ca^{2+} or Mg^{2+}) between the LPS oligosaccharidic portions, such as aminoglycosides and polymixins, can pass through the OM, regardless of their molecular weight. However, hydrophilic molecules can pass the lipophilic IM, exclusively by exploiting solute-specific energy-dependent transporter proteins or the proton motive force (PMF), regulated by the proton gradient, ΔpH, and the membrane potential, $\Delta\Psi$. An additional hurdle is constituted by the high abundance of efflux pumps, membrane proteins able to expel drugs, after their passage through the OM and IM (Domalaon et al. 2018; Richter and Hergenrother 2019).

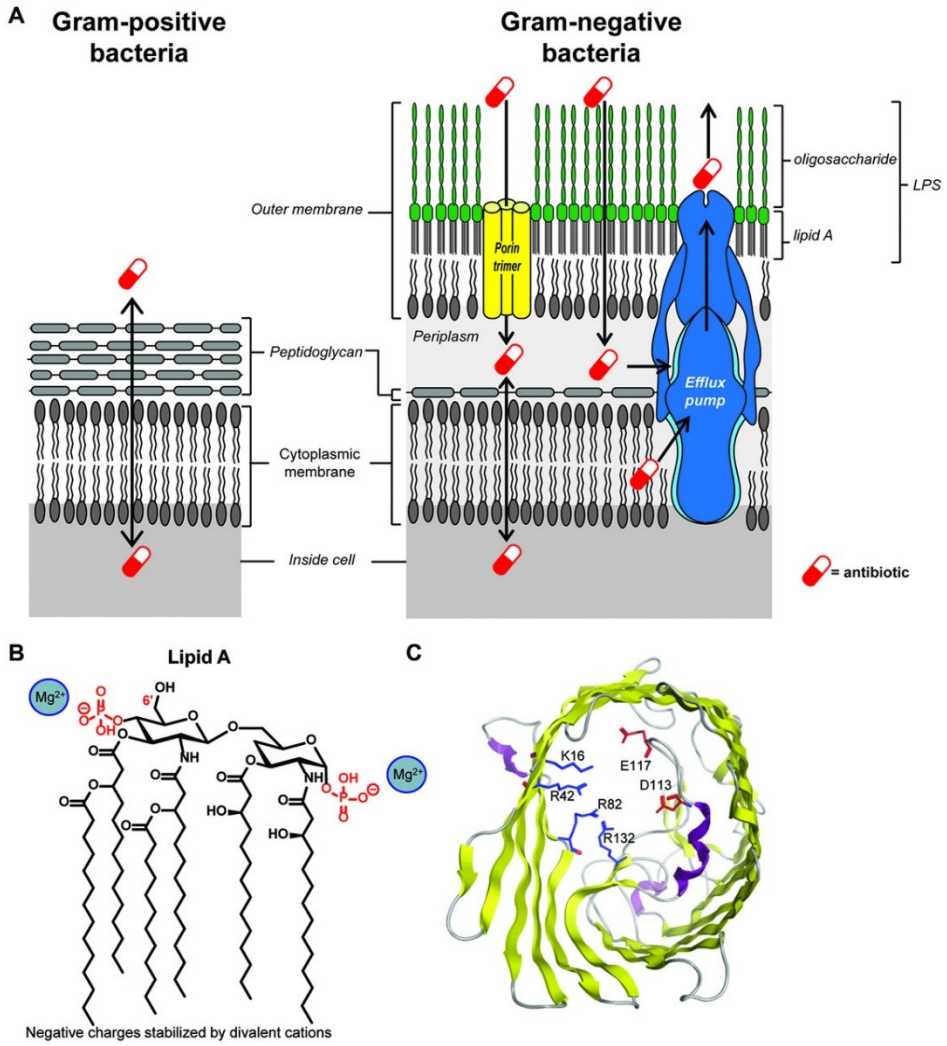

Figure 3.17. *(A) Gram-negative cellular envelope (right) consisting of two lipid membranes, whereas Gram-positive bacteria (left) present only one lipid membrane. (B) The structure of lipid A, the hydrophilic portion of LPS. The core oligosaccharide is linked to the 6' carbon. (C) Top view of OmpF, the prototypical porin from* (Richter and Hergenrother 2019)

Because of the orthogonal properties that molecules need to pass both the OM and IM, it has been difficult to rationally design antimicrobials active on Gram-negative bacteria.

3.3.1.1. Strategies against gram-negative pathogens

"eNTRy Rules"

In a recent review, Richter and Hergenrother (Richter and Hergenrother 2019) analysed the chemical characteristics that can convert compounds active against Gram-positive bacteria into compounds active against Gram-negative bacteria. To predict compounds accumulation in the Gram-negative *E. coli*, Richter and Hergenrother developed the so-called "eNTRy Rules": compounds are most likely to accumulate if they bear a nonsterically encumbered ionisable Nitrogen (primary amines resulted to be the best, but more substituted amines can accumulate as well), with low Three-dimensionality (globularity ≤ 0.25), low Rigidity (rotatable bonds ≤ 5), and preferably bearing some nonpolar functional groups. Globularity values range from 0 (indicating two- or one-dimensional object, i.e. benzene) to 1 (referring to a perfect sphere, i.e. adamantane). Rotatable bonds refer to single bonds with a nonterminal heavy atom, excluding those ones in a ring and C-N bonds that need high energy to rotate. Lastly, the nonpolar function in the molecule serves to generate an amphiphilic moment, a measure of a vector pointing from the hydrophobic core to the hydrophilic portion (amine). Molecules without a hydrophobic domain and thus lacking the amphiphilic moment are unlikely to accumulate.

Antivirulence therapy

Virulence is the ability of bacteria to harm host cells, through an array of virulence factors. These factors comprehend adhesins, facilitating bacteria colonization; toxins that alterate signal transduction in eukaryotic cells and are responsible for the development of diseases; and specialized secretion systems to inject toxins (effectors) into host cells (Rasko and Sperandio 2010).The development of agents targeting bacterial virulence mechanisms is a viable strategy, since antivirulence compounds are not bactericidal, but block bacterial communication, exerting reduced evolutionary pressure. (Domalaon et al. 2018). Noteworthy, in a recent work (Sundin et al. 2020), a

series of resveratrol-dimers bearing a benzofuran core (i.e. dehydro-δ-viniferin) were found to block an important virulence system in Gram-negative bacteria, the type III secretion system (T3SS) in *Yersinia pseudotuperculosis* and *P. aeruginosa*.

Combination therapy

Combination therapy comprehends different approaches, such as antibiotic-adjuvant combination therapy and antibiotic-antibiotic combination therapy. The first one involves the use of bioactive molecules, such as efflux pump inhibitors, membrane permeabilizers or enzyme inhibitors, in combination with an antibiotic. The second approach exploit the use of two antibiotics with two different targets in order to obtain synergism between the two drugs and to act on multiple targets in the pathogen to avoid antibiotic resistance development and to eradicate bacterial strains with intermediate susceptibility or resistance to one of two antibiotics (Domalaon et al. 2018).

Antibiotic hybrids

Molecular hybrids are heteromeric entities consisting of different bioactive agents fused to obtain the biological actions of the constituent fragments. A hybrid antibiotic may contain two or more pharmacophores, which can be different antibiotics, but also an antibiotic and adjuvants, such as siderophores, efflux pump inhibitors, resistance enzyme inhibitors. (Domalaon et al. 2018). In particular, an antibiotic conjugate containing a siderophore portion would be an interesting approach to overcome the Gram-negative bacterial barriers (Kong et al. 2019). Bacteria use iron as key cofactor in several enzymes involved in bacterial proliferation and infection process. In human serum, at physiological pH (7.35-7.40), the concentration of Fe^{3+} is about 10^{-24}M, whereas a concentration of 10^{5}-10^{6}M of Fe^{3+} is needed in bacteria for cell division to maintain the required 10^{-6}M concentration intracellularly. Due to the low solubility of Fe^{3+}, bacteria need to synthesize and secrete molecules (with a MW ranging from 200 to 2000 Da), known as

siderophores, to bind Fe^{3+} extracellularly and taking it intracellularly through siderophores binding proteins in the membrane (Hider and Kong 2010). To date, more than 500 siderophores have been identified, and, according to their iron-chelating functional groups, they can be classified into five main families: catecholates, hydroxamates, phenolates, carboxylates, and “mixed types” (Kong et al. 2019). Several sideromycins, antibiotics covalently linked to siderophores, have been shown to exploit specific iron transport systems to enter bacteria, and to be converted into antibiotics able to inactivate a bacterial target (Hider and Kong 2010). This smart natural mechanism inspired the employment of a “Trojan horse” strategy to mimic natural sideromycins.

3.3.2. Material and Methods

Procedures for the synthesis, isolation, and characterization data for the various compounds obtained are detailed in the experimental section 3.3.5.

3.3.3. Results and discussions – Development of synthetic strategies to modify dehydro-δ-viniferin

In the SAR studies performed on the simplified analogues of dehydro-δ-viniferin (Section 3.2), none of the compounds obtained resulted to be more active than the precursor. Therefore, we supposed that all the aromatic rings of dehydro-δ-viniferin were important to the antibacterial activity on *L. monocytogenes*. However, we observed that the derivative **30** showed a drastic drop of the antibacterial activity (MIC value of 743 μM against 4.42 μM of dehydro-δ-viniferin), suggesting the fundamental role of the aryl ring in position 3 of the benzofuran core in the antimicrobial activity. Conversely, compounds **29** and **31** almost retained the antibacterial activity of dehydro-δ-viniferin (MIC values of 50.3 – 44.5 μM of **29** and **31**, respectively, against 4.42 μM of **15**) (Figure 3.18).

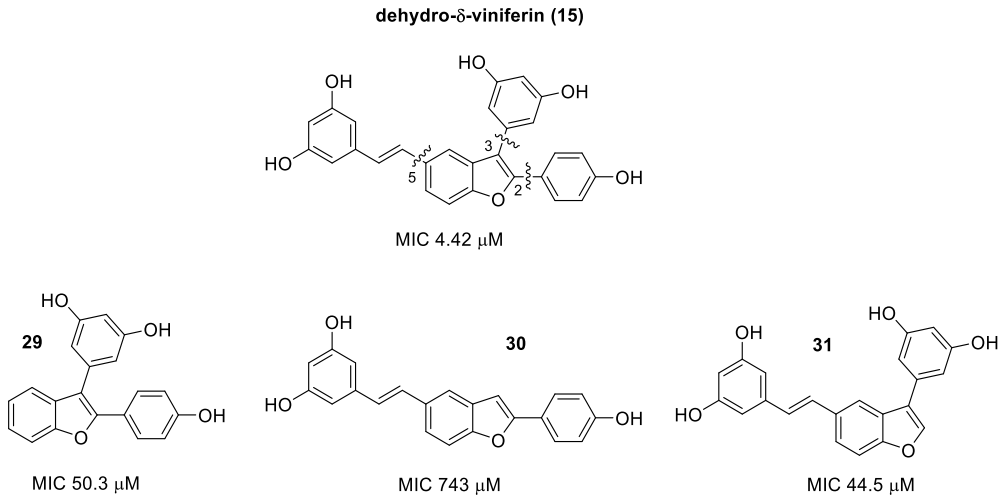

Figure 3.18. *Simplified benzofurans of dehydro-δ-viniferin and their MIC values on L. monocytogenes.*

Therefore, we were interested in investigating how the antibacterial activity could be affected by modifications on the stilbene moiety. In particular, we planned to develop synthetic strategies to replace the double bond of the stilbene moiety with bioisosteric substitutions to evaluate the importance of the geometry in the antimicrobial activity. Indeed, molecule flexibility and globularity are important factors underlined in the "eNTRy rules" described above. Then, we developed a synthetic strategy to replace the resorcinol ring on the stilbene with different aromatic rings, also containing siderophore portions, such as catechol, carboxylate and hydroxamate, on the styrene moiety. These synthetic efforts would allow SAR studies on the most active stilbenod **15** we identified in the previous studies. Moreover, the new analogues of **15** could be studied as antivirulence agents, since in a recent work dehydro-δ-viniferin (**15**) was found to block an important virulence system in Gram-negative bacteria (Sundin et al. 2020). Nonetheless, the development of synthetic strategies to exploit the 2,3-diaryl benzofuran scaffold of compound **15** could be used for the construction of hybrid antibiotics.

3.3.3.1. Dehydro-δ-viniferin bioisosteres

A series of bioisosteres of dehydro-δ-viniferin (Figure 3.19) was designed and synthesized to evaluate the importance of the geometry of the precursor in the antimicrobial activity. Moreover, different new scaffolds of the 2,3-diarylbenzofuran portion of dehydro-δ-viniferin were synthesized and synthetic protocols were studied to exploit them for the construction of hybrid antibiotics.

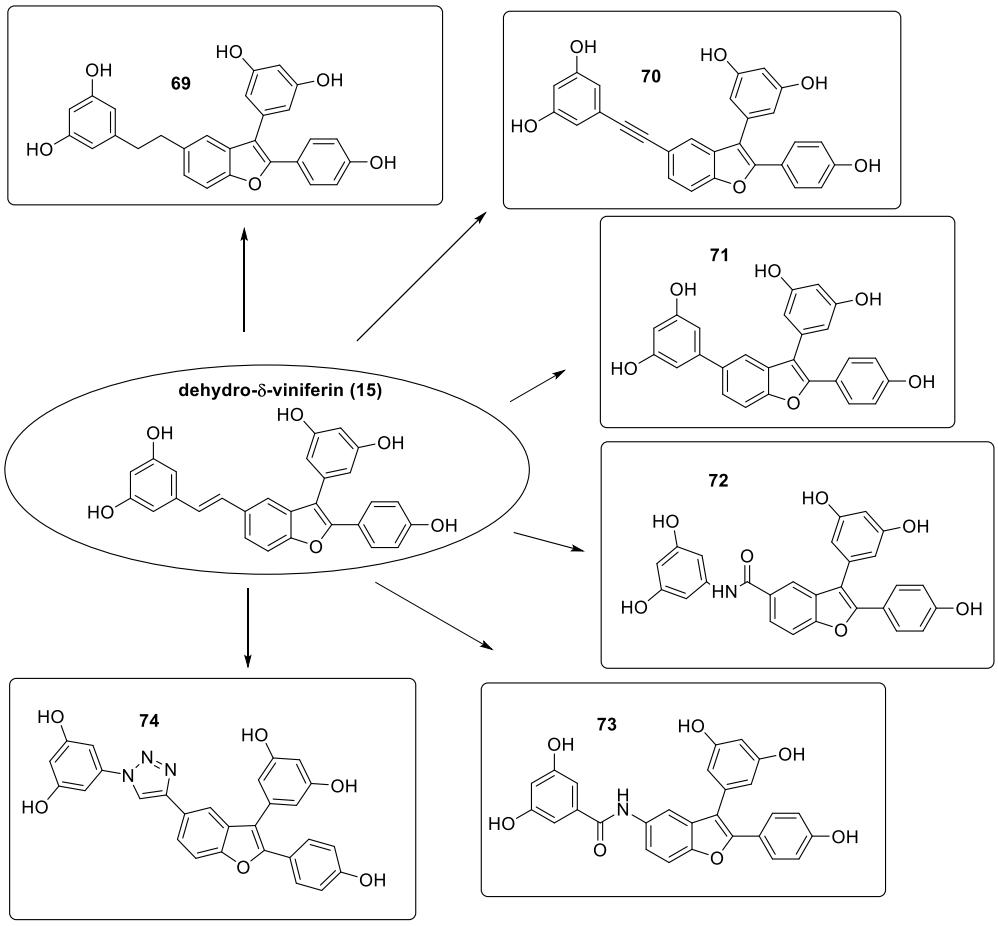

Figure 3.19. *Dehydro-δ-viniferin bioisoteres*

The hydrogenated derivative of dehydro-δ-viniferin (**69**) was obtained by hydrogenation of dehydro-δ-viniferin (**15**) with Pd/C in ethanol at room

temperature for 4h, in quantitiative yield. Interestingly, when we tried to obtain compound **75** through hydrogenation of the double bond of δ-viniferin (**10**), applying the same protocol, we obtained compound **76**, due to a benzylic hydrogenation of position 2 of the dihydrobenzofuran (Scheme 3.14). Looking at the literature, we found out that hydrogenation on Pd/C, even in mild conditions, can be used to cleave dihydrobenzofuran derivatives (Yue et al. 2017). Therefore, we tried to hydrogenate the benzofuran **69** by Kishi reduction, as described by Romero *et al.* (Romero et al. 2020) to obtain 2,3-diaryldihydrobenzofurans from 2,3-diarylbenzofuran derivatives, using TFA in presence of triethylsilane (TES). However, also this approach led to the benzofuran ring cleavage to yield derivative **76** (Scheme 3.14).

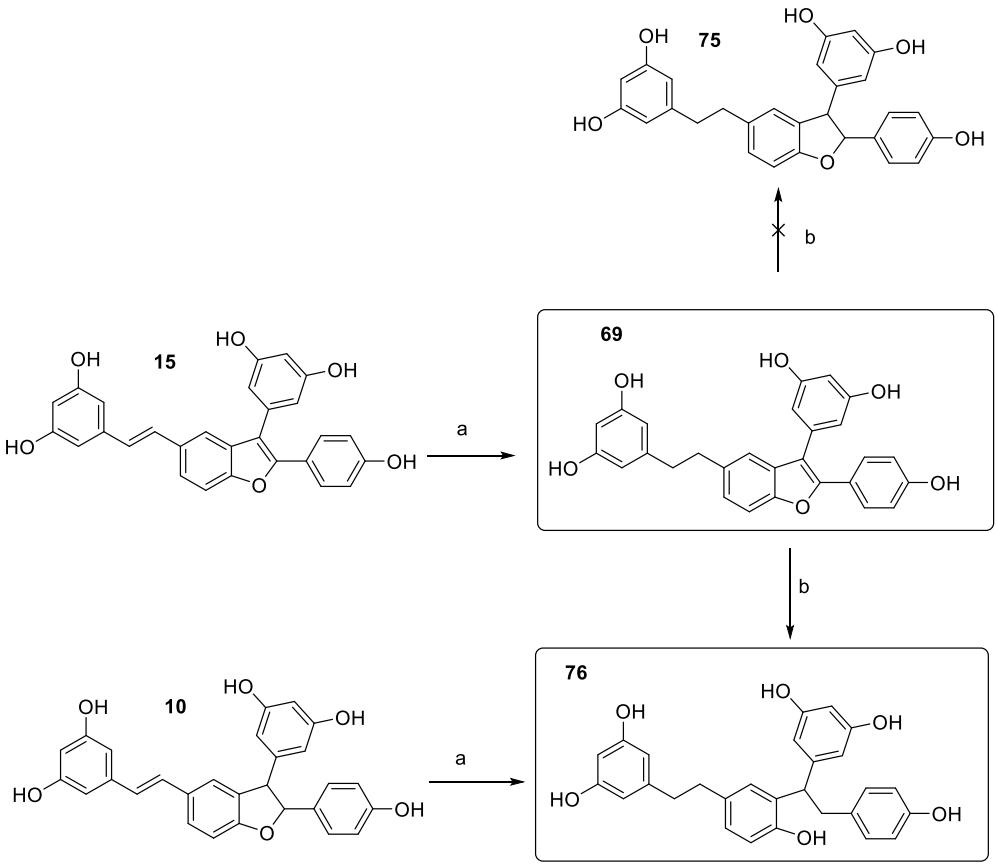

Scheme 3.14. Reagents and conditions: a) H_2, Pd/C 10% wt, EtOH, rt, 4h, quant yield; b) TFA, TES, DCM, rt, 65%.

For the synthesis of the other dehydro-δ-viniferin derivatives, we planned to construct the 2,3-diaryl benzofuran ring bearing a proper functional group (X) for the insertion of the desired fragment (Figure 3.20).

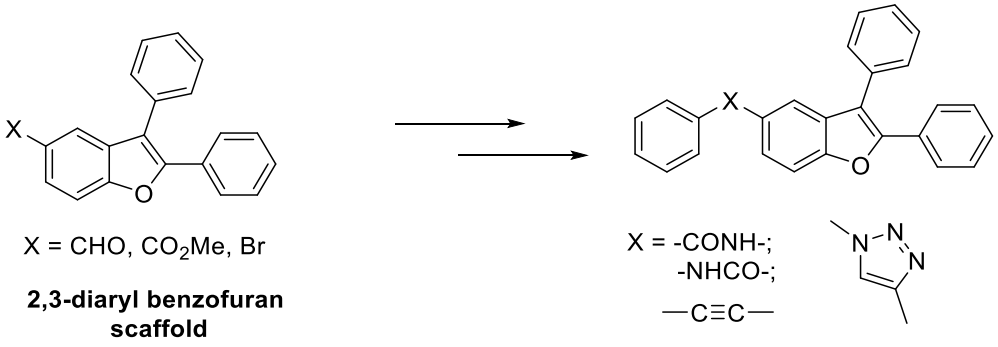

Figure 3.20. *Synthetic approach to obtain dehydro-δ-viniferin bioisosteres*

To directly obtain the desired 2,3-diaryl substituted benzofuran scaffold, we were pleased to find very effective a three-component Sonogashira/Cacchi type cyclization, developed by Markina *et al.* (Markina et al. 2013). The one-pot reaction involves a Sonogashira coupling between an *ortho*-iodophenol and an aryl-substituted terminal alkyne to generate at room temperature the corresponding internal alkyne. The alkynilphenol obtained as intermediate undergoes simultaneous cyclization with the adjacent phenol group and oxidative addition with the aryl-iodide-palladium complex, in acetonitrile at 100°C, under microwave irradiation (Scheme 3.15).

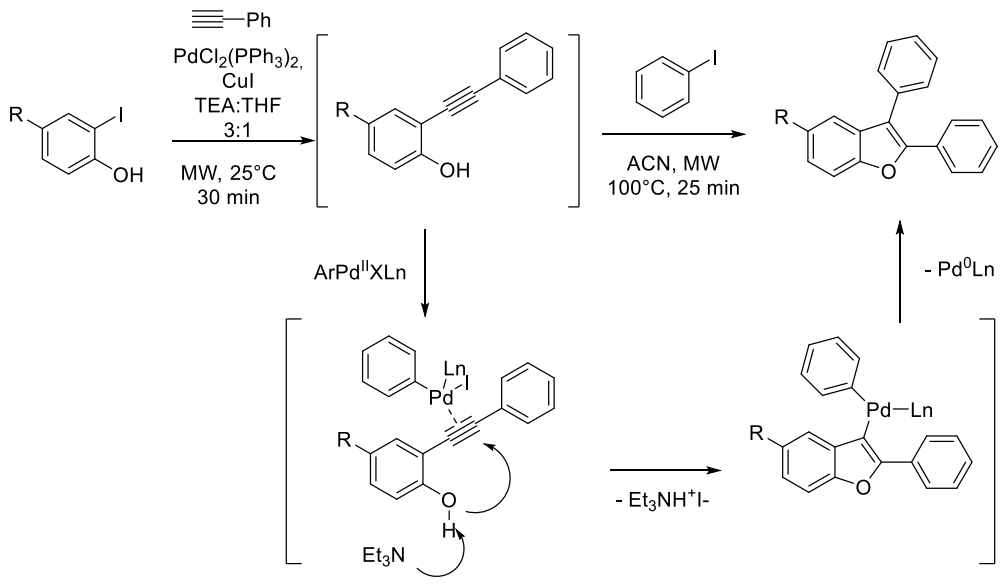

Scheme 3.15. Sonogashira-Cacchi type-tandem cyclization for the construction of 2,3-diaryl benzofuran scaffold, modified from (Hu et al. 2004)

Using this approach, 4-bromo-1-iodophenol (**77**), 4-ethynilansole (**39**) and 3,5-dimethoxy-1-iodobenzene (**78**) afforded compound **79** in 72% yield. Intermediate **79** underwent a Suzuki-coupling with (3,5-dimethoxyphenyl)boronic acid with $Pd(PPh_3)_4$ and aq 1M Cs_2CO_3 in a mixture DMF/EtOH (1:1), under microwave irradiation, for 20 min at 120°C, applying a protocol described by Markina *et al.* (Markina et al. 2013) to afford compound **80** in 91% yield. Final demethylation with BBr_3 provided compound **71** in 96% yield (Scheme 3.16).

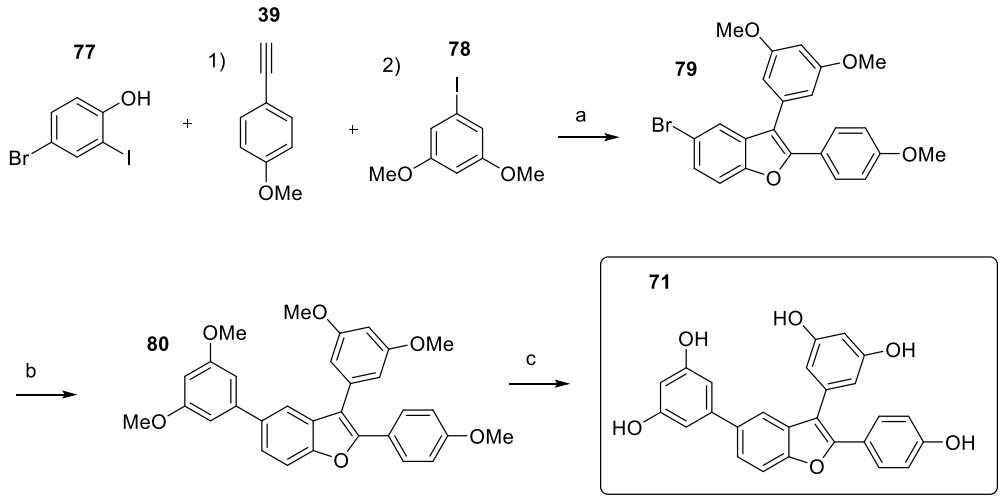

Scheme 3.16. Reagents and conditions: a) i) $PdCl_2(PPh_3)_2$·DCM, CuI, THF/TEA 1:3, rt, MW, 30 min, ii) 3,5-dimethoxy-1-iodobenzene **78**, ACN, 100°C, MW, 25 mn, 72%; b) (3,5-dimethoxyphenyl)boronic acid, $Pd(PPh_3)_4$, DMF/EtOH 1:1, aq 1M Cs_sCO_3, 120°C, 20 min, MW, 91%; c) BBr_3 1M DCM, DCM, - 78°C to rt, overnight, 96%.

The intermediate **79** was used also for the construction of the alkyne derivative **70** (Figure 3.19). In this case, in order to avoid the use of BBr_3 in the last step for the deprotection of the phenolic moieties in presence of a likely sensitive triple bond, we planned to deprotect the brominated intermediate **79**, followed by protection of the hydroxy groups as *tert*-butildimethylsilyl ethers, to avoid side reactions in the subsequent Sonogashira coupling. The demethylation of compound **79** provided intermediate **81** in 87% yield, and the protection with tert-butyldimethylsilyl chloride, in presence of imidazole in DMF, gave compound **82** in 81% yield (Scheme 3.17).

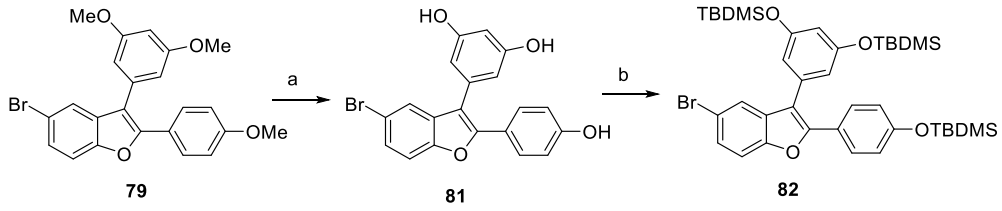

Scheme 3.17. Reagents and conditionds: a) BBr_3 1M DCM, dry DCM, - 78°C to rt, overnight, 87%; b) TBDMSCl, imidazole, DMF, 0°C to rt, overnight, 81%.

The desired terminal alkyne **83** was obtained starting from 3,5-dihydrxoybenzaldehyde **84**, which was properly protected and then subjected to Corey-Fuchs conditions (Gibtner et al. 2002). Therefore, reaction of compound **85** with CBr_4 and PPh_3 gave the terminal dibromoalkene **86** that underwent lithium-halogen exchange and α-elimination with LDA to afford **83** in excellent yield (Scheme 3.18).

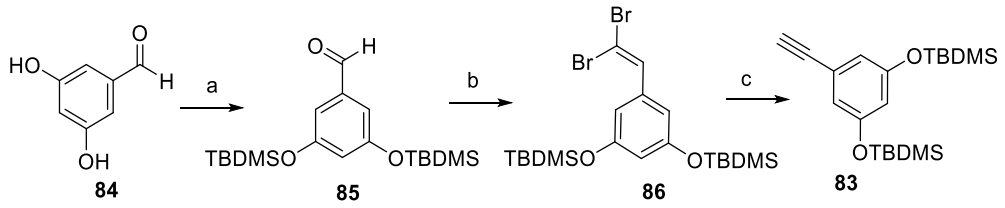

Scheme 3.18. Reagents and conditions: a) TBDMSiCl, imidazole, DMF, 0°C to rt, overnight, 65%; b) CBr_4, PPh_3, DCM, 0°C to rt, 1h, 83%, c) LDA, THF, -78°C, 1h, 91%.

Compound **83** (Scheme 3.18) was used in the final Sonogashira coupling with compound **82** (Scheme 3.17), in presence of $Pd(PPh_3)_4$ and CuI in triethylamine at reflux for 8h (Scheme 3.19). The crude obtained was directly deprotected with KF to give the desired alkyne **70** in 38% yield over two steps.

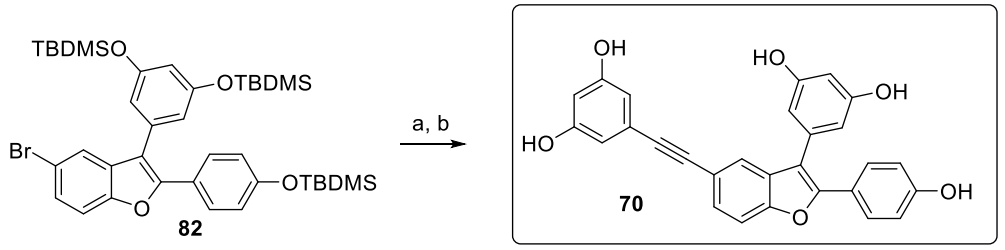

Scheme 3.19. Reagents and conditions: a) **83**, $Pd(PPh_3)_4$, CuI, TEA, 90°C, 8h; b) KF, MeOH/THF, rt, overnight, 38% over 2 steps.

Then, we focused on the synthesis of the isosteres bearing an amide in place of the double bond. The amide linkage should allow to maintain the transoid architecture of the *trans*-stilbene, conferring improved solubility and increased

polarity (Stockdale et al. 2017b, a). Moreover, amide isosteres of resveratrol have been shown similar activity to that of resveratrol (St. John et al. 2013). Therefore, the analogue **72** and its reverse-amide counterpart **73** were designed (Figure 3.21). The placement of the carbonyl and nitrogen portions of the amide linkage on different rings of the viniferin system could result in differences in electronic perturbations (Stockdale et al. 2017b, a).

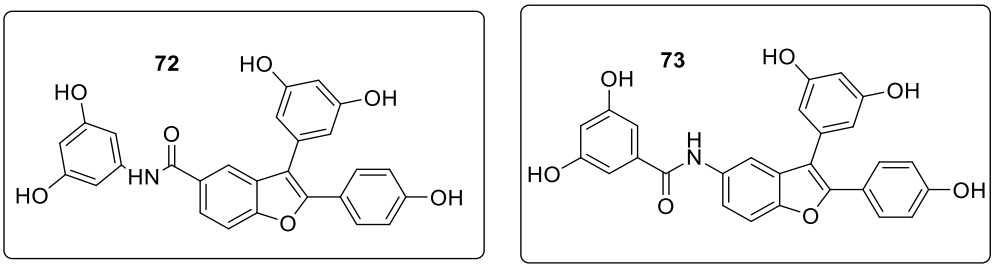

Figure 3.21. *Benzanilides of dehydro-δ-viniferin*

To synthesize the two benzanilides of dehydro-δ-viniferin, we performed the Sonogashira/Cacchi type cyclization conditions on methyl 4-hydroxy-3-iodobenzoate **43**, with 4-ethynilanisole (**39**) and 3,5-dimethoxy-1-iodobenzene (**78**), and we obtained the desired benzofuran **87** in 66% yield. Hydrolysis of the ester **87** was performed with $LiOH{\cdot}H_2O$ in a mixture of THF/water 1:1 for 24 hours. The resulting carboxylic acid **88** underwent an amide coupling with 3,5-dimethoxyaniline, in presence of EDC·HCl and HOBt, to give the desired amide **89** in 70% yield, which was smoothly demethylated with BBr_3 to afford compound **72** in 73% yield (Scheme 3.20).

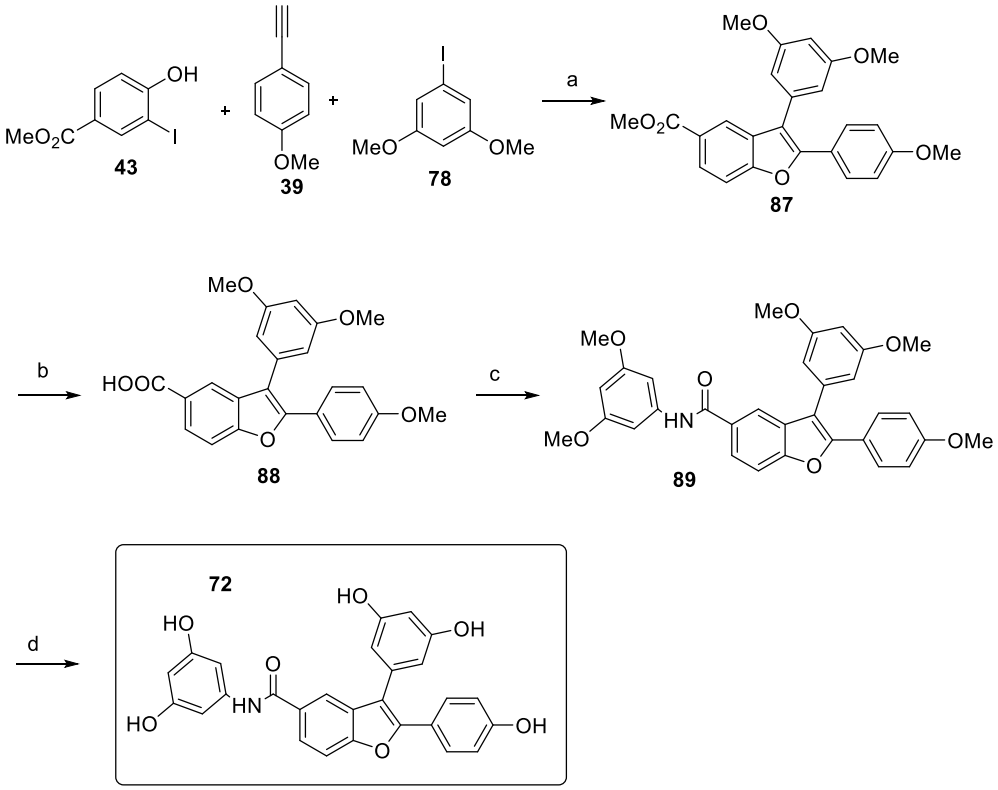

Scheme 3.20. Reagents and conditions: a) i) $PdCl_2(PPh_3)_2$·DCM, CuI, THF/TEA 1:3, rt, MW, 30 min, ii) 3,5-dimethoxy-1-iodobenzene **78**, ACN, 100°C, MW, 25 mn, 66%; b) LiOH·H_2O, THF/H_2O 1:1, rt, 24h, quant yield; c) i) EDC·HCl, HoBt, DMF; 0°C to rt, 90 min, ii) 3,5-dimethoxyaniline, DIPEA, DMF, 0°C to rt, overnight, 70%; d) BBr_3 1M DCM, DCM, - 78°C to rt, overnight, 73%.

In the case of the reverse amide **73**, the carboxylic acid **88** was converted into the corresponding aniline **90** through Curtius rearrangement with diphenylphosphorylazide (DPPA) in toluene and followed by treatment with LiOH·H_2O in water. Probably, some side reactions occurred but we were able to isolate the pure product in 34% yield. The aniline **90** was then coupled with 3,5-dimethoxybenzoic acid **91** to obtain the desired amide **92**. In this case, the final deprotection gave the final product **73** only in 3% yield (Scheme 3.21). Further investigations are needed to improve the deprotection step.

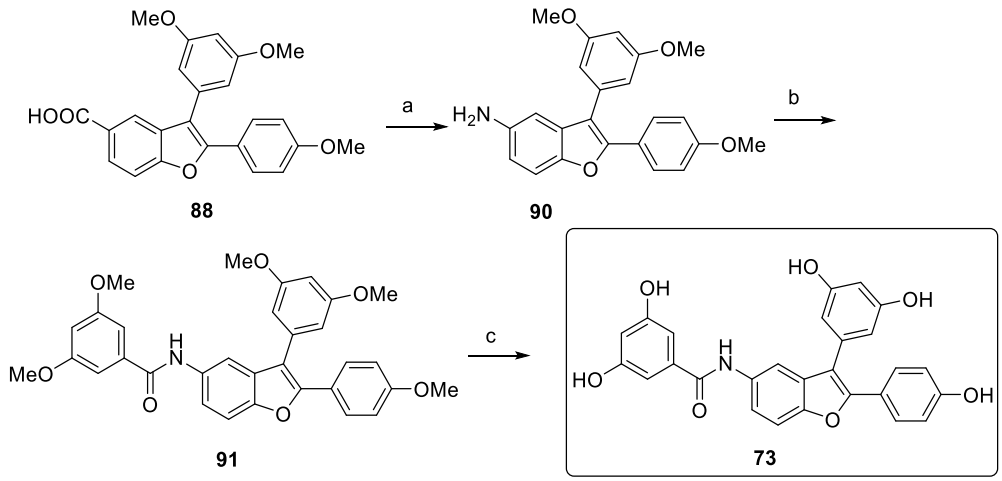

Scheme 3.21. Reagents and conditions: a) i) DPPA, toluene, 80°C, overnight; ii) $LiOH \cdot H_2O$, THF/water, rt, 5h, 34%; b) i) 3,5-dimethoxybenzoic acid **91**, EDC·HCl, HoBt, DMF; 0°C to rt, 90 min, ii) **92**, DIPEA, DMF, 0°C to rt, overnight, 70%, c) BBr_3 1M DCM, DCM, - 78°C to rt, overnight, 3%.

Looking at isosteric substitutions of the double bond of stilbenes in literature, we found that triazole-linkage was used to replace the olefinic bridge to build new analogues of resveratrol (Pagliai et al. 2006). Triazoles are fundamental building blocks in several bioactive compounds and among the most widespread bioisosteres, due to their versatile chemical characteristics. Thanks to their polarity and rigidity, triazoles can be used as bioisosteric substitutions for different functional groups, including amide, esters, carboxylic acids, heterocycles, and olefins. 1,2,3-Triazoles, stable to hydrolytic, oxidative, and reductive conditions, can mimic the rigid conformation of the double bond, avoiding undesired olefin isomerization or degradation (Bonandi et al. 2017). The triazole moiety can maintain the transoid characteristics of the stilbene double bond, besides the electronic communication between the aromatic rings. However, the architecture deriving from the triazole is not exactly the same, since the distance between the aromatic rings is increased compared to that of a *trans*-stilbene, allowing to investigate the contribute of the geometry in the interaction of the new derivatives. Moreover, the substitution of the double bond with a triazole-ring

would allow the use of combinatorial chemistry to build a library of new analogues. Indeed, using click chemistry, we planned to insert a terminal alkyne on the 2,3-diarylsubstituted benzofuranic scaffold of dehydro-δ-viniferin, followed by Huisgen [3 + 2] cycloaddition with an azide, in presence of copper salts (Kolb et al. 2001; Rostovtsev et al. 2002).

For the synthesis of the triazole derivative **74** (Figure 3.19, Scheme 3.22), we used the same precursor obtained for the synthesis of the benzanilides derivatives. Therefore, compound **87** underwent reduction with $LiAlH_4$ and subsequent oxidation with DMP to provide the corresponding aldehyde **93**. Through Corey-Fuchs reaction we obtained the alkyne **95**, which was coupled with 1-azido-3,5-dimethoxybenzene **96** by click chemistry to give the triazole derivative **97**, in 21% yield. Final deprotection with BBr_3 afforded compound **74** in 24 % yield (Scheme 3.22). Further investigations are needed to optimize the reaction conditions for the click chemistry reaction and for the final demethylation.

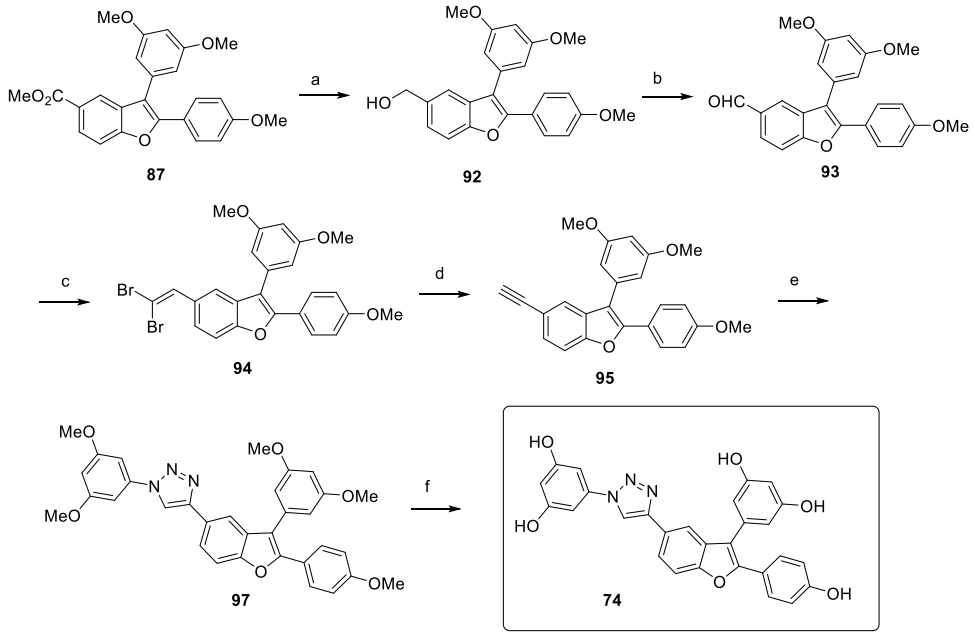

Scheme 3.22. Reagents and conditions: a) $LiAlH_4$, THF, 0°C, 20 min, quant yield; b) DMP, DCM, 0°C 15 min, 1h rt, 92%; c) PPh_3, CBr_4, DCM, 0°C 10 min, rt 10 min, 83%; d) LDA, THF, - 78°C, 1h, 85%; e) 1-azido-3,5-dimethoxybenzene **96**, $CuSO_4 \cdot 5H_2O$, Na·ascorbate, *t*-BuOH/H_2O/DMSO 1:1:1, rt, 72h, 21%, f) BBr_3 1M DCM, DCM, - 78°C to rt, overnight, 24%.

3.3.3.2. Synthetic approaches toward the synthesis of siderephores-containing analogues of dehydro-δ-viniferin

This part describes the chemical efforts to develop a versatile and effective synthetic strategy to replace the resorcinol ring on the stilbene moiety of dehydro-d-viniferin (**15**) with different aromatic rings (i.e. siderophore portions, such as catechol, carboxylate and hydroxamate) (Figure 3.22).

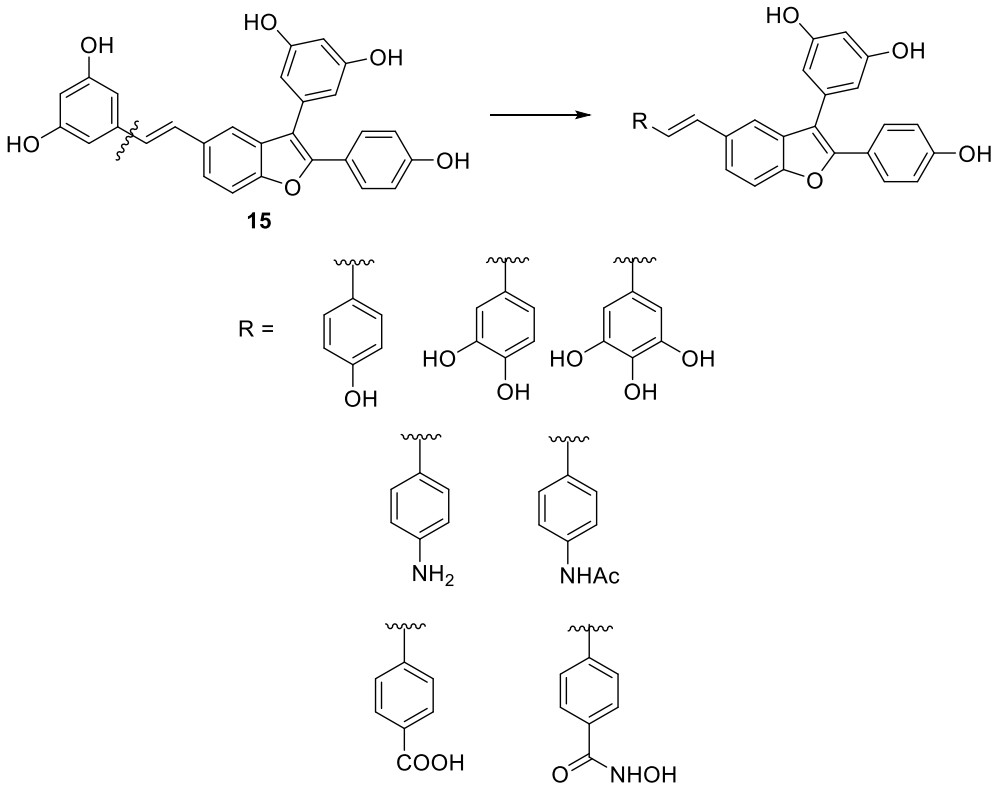

Figure 3.22. *Differently substituted dehydro-δ-viniferin (**15**) analogues.*

In particular, we aimed at developing an efficient synthetic route to obtain a properly protected benzofuran core, which could be easily functionalized with different styryl moieties. Finding an efficient synthetic route was very challenging. Different strategies were envisioned.

Firstly, we decided to exploit the intermediate **87** to obtain a phosphonate, which could undergo Horner-Wadsworth-Emmons (HWE) reaction with

different aldehydes. Therefore, compound **87** was efficiently reduced with $LiAlH_4$, as previously described, to give the alcohol **92**, which was converted into the corresponding bromide derivative **98** with PBr_3 in 87% yield. Compound **98** was reacted with triethylphosphite at 130°C overnight to afford phosphonate **99** in 92% yield. The HWE reaction with 4-methoxybenzaldehyde provided the desired methoxylated stilbene **100**, only as *trans* isomer, in excellent yield. Unfortunately, when we performed the deprotection of the methyl groups with BBr_3 at - 78°C in dry DCM, following the usual procedure, we found just degradation products (Scheme 3.23).

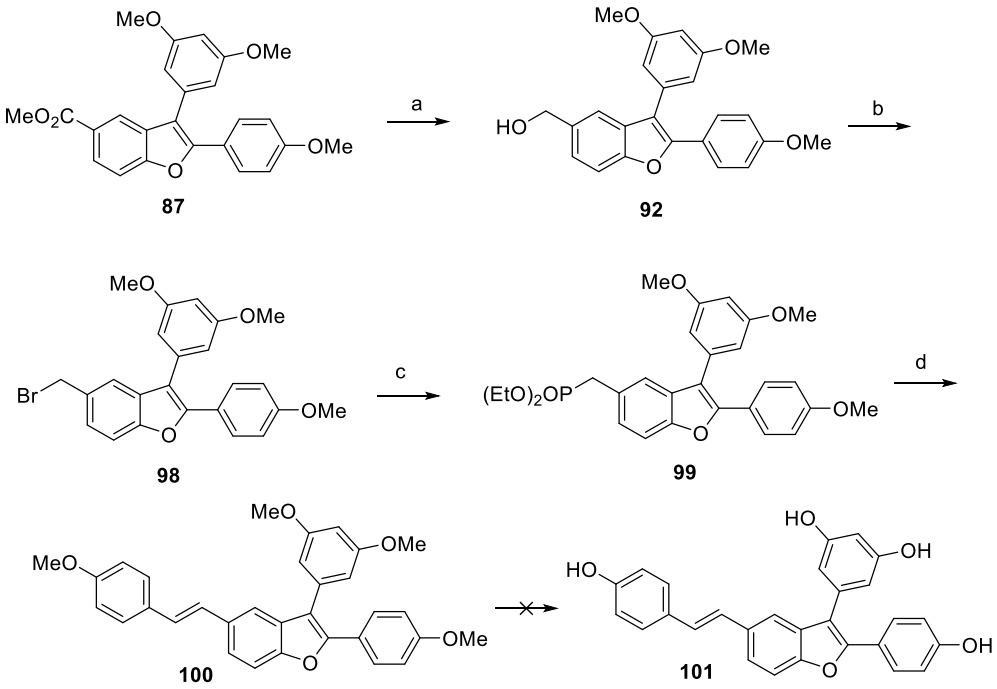

Scheme 3.23. Reagents and conditions: a) $LiAlH_4$, THF, 0°C, 20 min, quant yield; b) PBr_3, cat pyridine, Et_2O, rt to reflux, 2h, 87%; c) $P(OEt)_3$, 130°C, overnight, 92%; d) 4-methoxybenzaldehyde, NaH, 120°C, 30 min, MW, 86%.

In our previous synthetic works, we used methyl groups for protection of hydroxy groups because of the availability of the starting materials and their high stability in various reaction conditions. However, as not negligible drawback, the high stability of methyl groups required harsh conditions for the

deprotection step, which often resulted in decomposition, side products difficult to separate, and low yields. In particular, we observed that the demethylation step resulted in poor yields or degradation products when we performed it on derivatives containing the double bond of the stilbene. Therefore, our main aim consisted in finding a 2,3-diarylbenzofuran scaffold, bearing a substituent in position 5, both amenable to the insertion of the styryl moiety and stable in the demethylating conditions, that we planned to apply before the insertion of the sensitive double bond (Scheme 3.24).

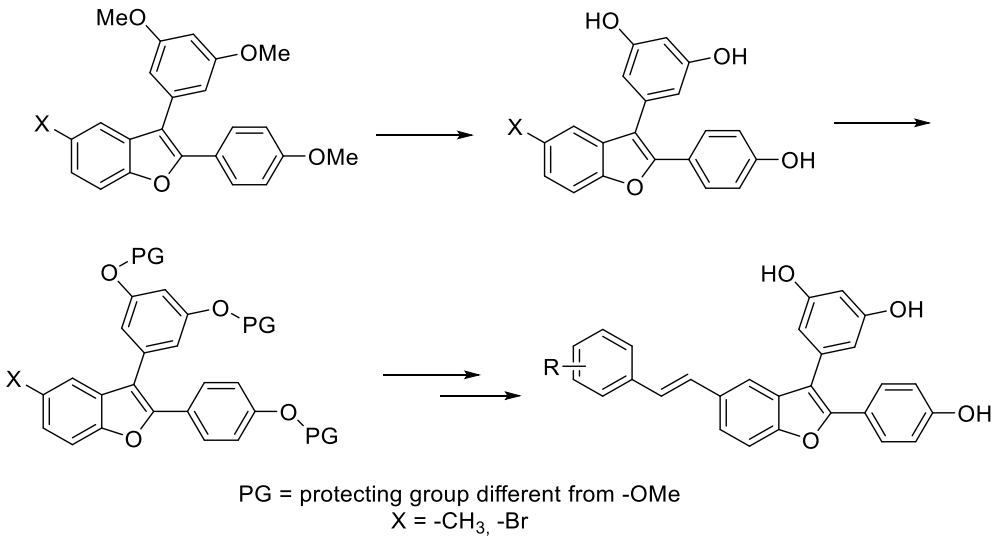

Scheme 3.24. Synthetic approach toward the synthesis of dehydro-δ-viniferin analogues

Consequently, in a second approach we decided to exploit the previously obtained 2,3-diarylbenzofuran **81** (see scheme 3.16 and 3.17 for the synthesis). We tried the direct insertion of the styryl moiety by Heck reaction with 4-hydroxystyrene (Scheme 3.25). Unfortunately, we obtained a mixture of isomers **101a** and **101b**, coeluted in column chromatography. Since our aim was to find an efficient strategy to obtain different derivatives, we did not attempt to separate the isomers by different chromatographic techniques, and we moved to another strategy.

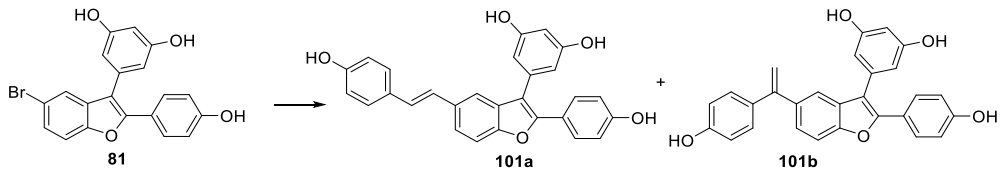

Scheme 3.25. Reagents and conditions: a) 4-hydroxystyrene, TEA, dppp, $Pd(OAc)_2$, dry DMF, 120°C, 48h.

In another synthetic route, we planned to use as starting material 2-iodo-4-methylphenol **103**, prepared in excellent yields from *para*-cresol (**102**) with *N*-iodosuccinimide and *para*-toluensulfonic acid in acetonitrile (Schmidt et al. 2013). In the one-pot-Sonogashira-Cacchi reaction conditions, the obtained intermediate gave the desired benzofuran derivative **104** in 48% yield. Intermediate **104** was smoothly demethylated to afford compound **105** in 90% yield. This time, the protection of hydroxy groups with *tert*-butyldimethylsylilchloride and imidazole in DMF at room temperature did not work well. Therefore, we performed the reaction in 1,2-dichloroethane at 60°C, following a protocol described by Romero *et al.* (Romero et al. 2020), and we obtained compound **106** in good yield (86%). Then, through a radical bromination of the methyl group with NBS and AIBN as radical initiator at reflux in CCl_4, the brominated compound **107** was obtained and converted into the corresponding phosphonium salt **108** with PPh_3 in toluene at reflux. The Wittig reaction with 3,4-bis((tert-butyldimethylsilyl)oxy)benzaldehyde **109** gave a crude with different products. Since we thought they could derive from partial desilylation of the desired product, we tried to deprotect the crude with KF. Unluckily, the product isolated by column chromatography resulted to be a mixture of compounds, maybe containing *cis* and *trans* isomers (Scheme 3.26).

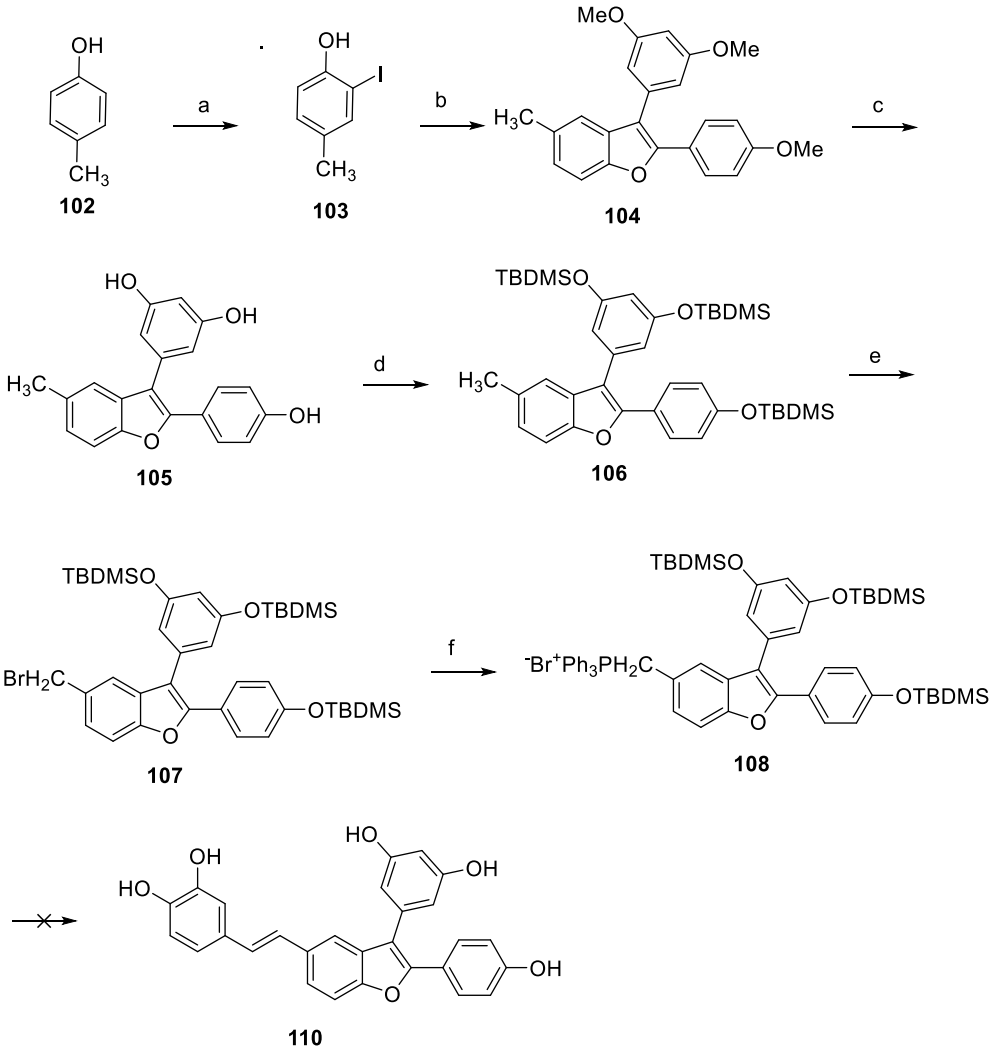

Scheme 3.26. Reagents and conditions: a) i) *p*-TsOH·H_2O, ACN, rt, 10 min; ii) NIS, rt, overnight; b) i) 4-ethynianisole **39**, $PdCl_2(PPh_3)_2$·DCM, CuI, THF/TEA 1:3, rt, MW, 30 min, ii) 3,5-dimethoxy-1-iodobenzene **78**, ACN, 100°C, MW, 25 mn, 48%; c) BBr_3 1M DCM, DCM, - 78°C to rt, overnight, 90%; d) TBDMSiCl, imidazole, DCE, 60°C, 8h, 86%; e) NBS, AIBN, CCl_4, reflux, 8h, 37%, f) PPh_3, toluene, reflux, overnight, 77%.

Therefore, we decided to use the Horner-Wadswroth-Emmons reaction, which should provide more selectively the *trans* isomer. The brominated derivative **107** was converted into the corresponding phosphonate **111** with triethylphosphite at 130°C in 84% yield. The intermediate **111** was reacted with the properly protected aldehyde **109** in presence of LDA in THF, but we

obtained the product **112** only in 16 % yield, along with impurities. Therefore, we repeated the reaction using NaH as base and this time compoun **112** was afforded in 52% yield as pure. Eventually, the final deprotection of silyl groups with tetrabutylammonium fluoride (TBAF) at 0°C in THF afforded compound **110** bearing a catechol on the styryl moiety (60% yield) (Scheme 3.27).

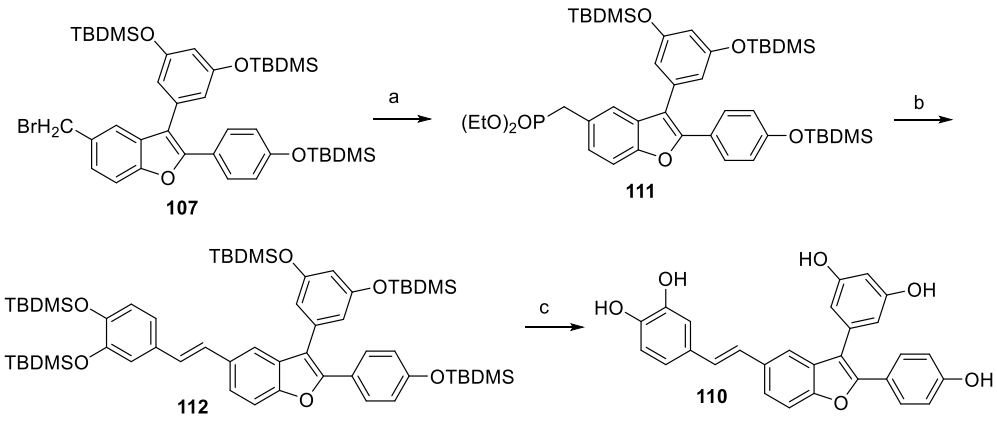

Scheme 3.27. Reagents and conditions: a) $P(OEt)_3$, 130°C, overnight, 84%; b) 4-bis((*tert*-butyldimethylsilyl)oxy)benzaldehyde **109**, NaH 60%, THF, 0°C to rt, 24 h, 52%; c) TBAF, THF, 0°C to rt, 2h, 60%.

Though further optimization experiments are needed, this novel synthetic route provided the phosphonate derivative as versatile intermediate that can be coupled with differently substituted aldehydes, through Horner-Wadsworth-Emmons reaction, to build a series of analogues containing siderophore portions or linking other antimicrobial molecules for the construction of hybrid antibiotics.

3.3.4. Results and discussion - Nitrogen containing-stilbenoid derivatives

Following the “eNTRY rules” described in the introduction section (3.3.1) to broaden the spectrum of activity of stilbenoids to Gram-negative species, we designed a series of resveratrol and pterostilbene derivatives containing a

nitrogen function. The basic group was supposed to increase the interaction of the flat structures of stilbenoids with the negatively charged portion of the LPS of the outer membrane of Gram-negative bacteria.

3.3.4.1. Acetanilides, anilines and guanidino-containing stilbenoids

Firstly, we decided to replace one hydroxy group of resveratrol and pterostilbene with an acetanilide function, as biososteric substitution, or a basic amino- (Figure 3.23) and guanidino-portions. In particular, the basic amino- and guanidino-functions, protonated at physiological pH, were supposed to mediate the interaction of the modified stilbenoids with the negatively charged outer membrane of Gram-negative bacteria.

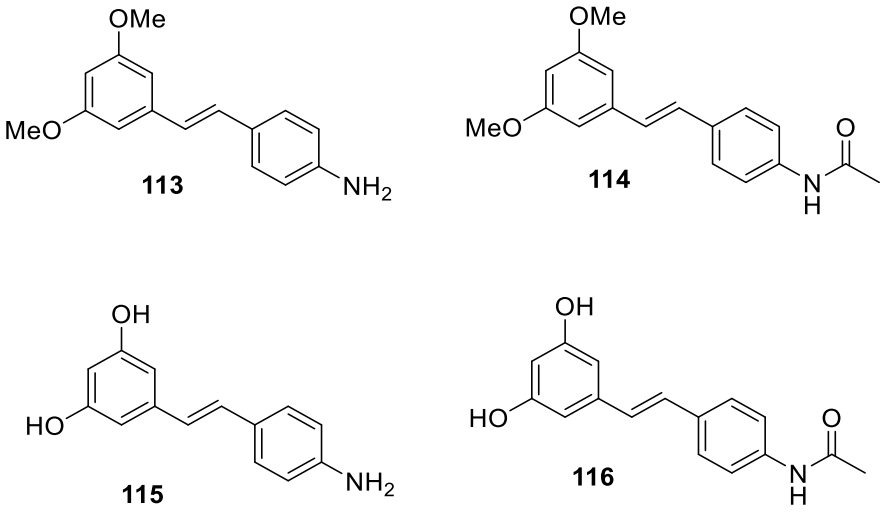

Figure 3.23 *Anilines (**113**, **115**) and acetanilides (**114**, **116**) derivatives of resveratrol and pterostilbene*

To obtain the aniline derivatives (**113** and **115**), we planned to exploit the Smiles rearrangement of aryloxyamides and subsequent hydrolysis (Coutts and Southcott 1990). In particular, we successfully applied the conditions described by Yu *et al.* (Yu et al. 2013) to perform this three-step procedure (phenol alkylation, rearrengment and hydrolysis (Mizuno and Yamano 2005)) in a one-pot reaction. Pterostilbene (**2**) reacted with 2-bromopropionamide at 60°C in a DMSO solution to give the corresponding aniline derivative **113**,

after hydrolysis with KOH at 140°C, under microwave irradiation, in 40% yield. The acetylation with acetyl chloride in standard conditions proceeded smoothly to give acetanilide **114**. Demethylation of **113** and **114** provided compounds **115** and **116**, the aniline and acetanilide analogues of resveratrol, respectively (Scheme 3.28).

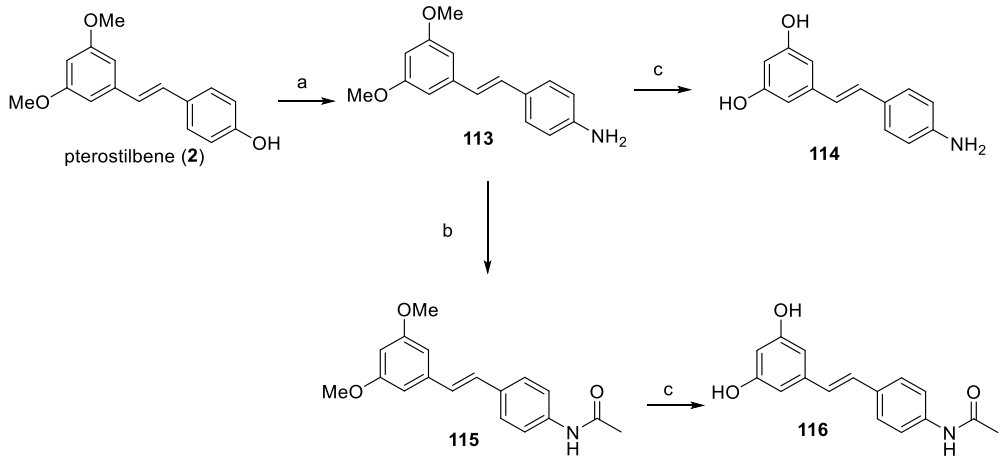

Scheme 3.28. Reagents and conditions: a) i) 2-bromopropionamide, KOH, DMSO, 60°C, 3h, MW, ii) KOH, 140°C, 3h, 40%; b) acetylchloride, TEA, DCM, 0°C to rt, 2h, 86%; c) BBr_3 1M DCM, dry DCM, 0°C to rt, 8-18h, 45-54%.

Then, we focused on the introduction of the guanidine moiety, a modification further supported by several studies reporting guanidine as a chemical function present in several molecules endowed with antimicrobial activity against both Gram-negative and Gram-positive bacteria (Ghamrawi et al. 2017; Hagras et al. 2017; Heydarifard et al. 2017; Kuppusamy et al. 2018; Song et al. 2019). Therefore, the aniline-containing derivatives obtained were used as intermediates to build the guanidino-containing stilbenoids (Figure 3.24).

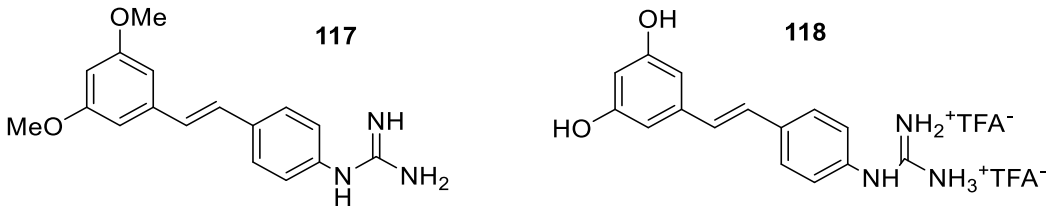

Figure 3.24. *Guanidino-containing derivatives of pterostilbene (**117**) and resveratrol (**118**)*

In literature, many methods for the synthesis of guanidines from amines have been reported, such as the use of cyanamide, carbodiimides, thioureas, isothioureas, or *S*-methylisothioureas. However, these reagents usually required the use of toxic metals as catalysts for their activation. Therefore, pyrazole and benzotriazole activated carboxamidines were developed and their efficacy in the guanidinylation process was demonstrated in mild conditions. Noteworthy, they were effective also on anilines that generally are less reactive toward guanidinylation than aliphatic amines (Katritzky and Rogovoy 2005). Following a procedure of Dud *et al* (Đud et al. 2019) for the synthesis of the guanidine analogues, we employed the guanidinylation reagent *N*,*N*'-Di-*Boc*-1H-pyrazole-1-carboxamidine to obtain compound **119** in excellent yield (93%) from **113**. The intermediate obtained was easily deprotected with TFA to give compound **117**. However, by the demethylation of compound **117** we were not able to isolate in a pure form the corresponding guanidino-analogue of resveratrol (**118**) (Scheme 3.29).

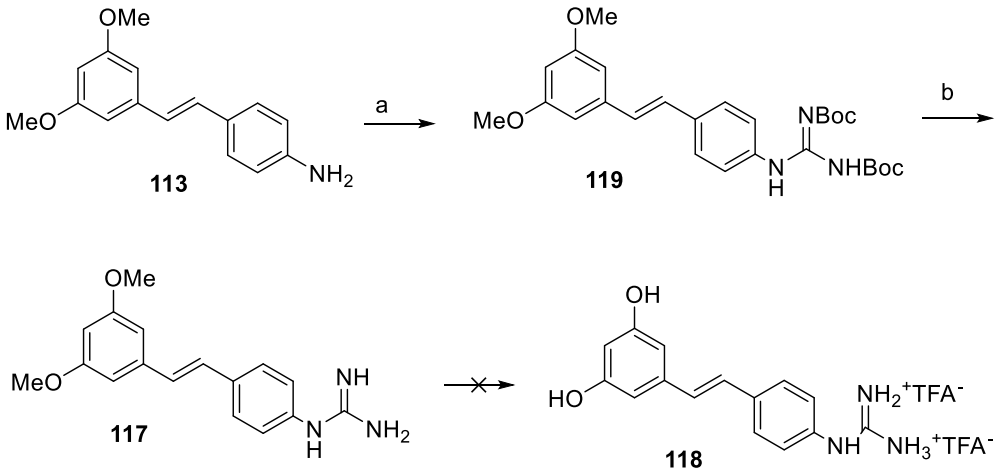

Scheme 3.29. Reagents and conditions: a) *N,N'*-Di-*Boc*-1H-pyrazole-1-carboxamidine, $CHCl_3$, rt, overnight, 93%; b) TFA, DCM, 0°C to rt, 20h, 95%.

Therefore, we decided to perform the guanidilnyation of **115**, and we obtained compound **120**, in 42% yield. Then, we attempted the deprotection step with TFA in DCM. Again, we could not obtain the desired product as a pure compound, so we guessed that the derivative was not stable in strong acidic conditions. Eventually, we found that performing the reaction with TFA, in presence of triethylsilane (TES), as described in a protocol by Salvio *et al.* (Salvio et al. 2016), we were able to isolate the desired product **118** as trifluoroacetic salt of guanidium (Scheme 3.30).

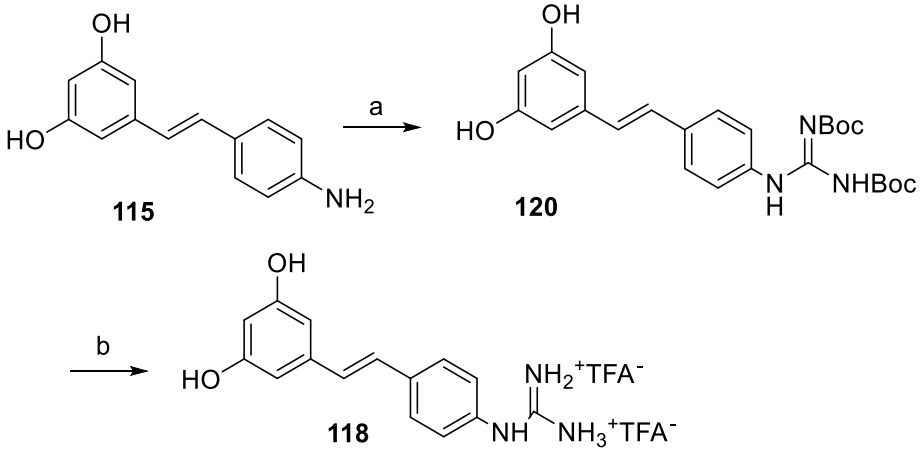

Scheme 3.30. Reagents and conditions: a) *N,N'*-Di-*Boc*-1H-pyrazole-1-carboxamidine, $CHCl_3$, rt, 48h, 42%; b) TFA, TES, DCM, rt, overnight, 82%.

Then, we decided to apply the same approaches also to the most active benzofuran-simplified derivative **34**, obtained from the SAR studies described in section 3.2. Therefore, we designed the corresponding aniline (**121**), acetanilide (**122**) and guanidinium (**123**) derivatives of compound **34** (Figure 3.25).

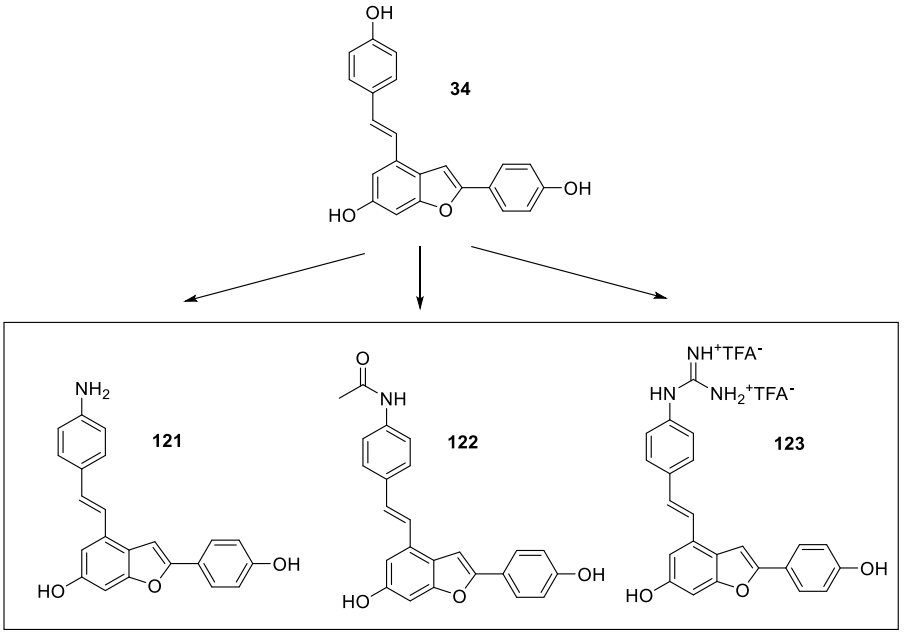

Figure 3.25. *Aniline (**121**), acetanilide (**122**) and guanidine (**123**) derivatives of compound **34**.*

In this case, aldehyde **65** (synthesis described in section 3.2) underwent a Horner-Emmons reaction with (4-aminobenzyl)phosphonate under microwave irradiation, to give **124** in 23% yield. Compound **124** was smoothly acetylated with acetylchloride in standard conditions to give the corresponding acetanilide **125**. Demethylation of **124** and **125** with BBr_3 afforded compounds **121** and **122**, in 57% and 54% yield, respectively (Scheme 3.31).

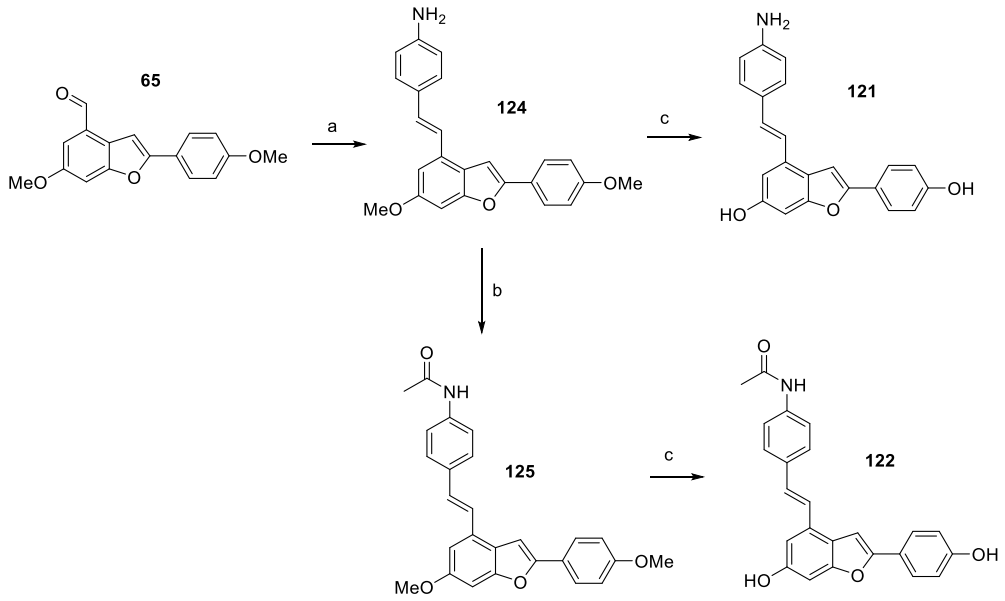

Scheme 3.31. Reagents and conditions: a) (4-aminobenzyl)phosphonate, NaH, THF, 120°C, 30 min, MW; b) acetylchloride, TEA, DCM, 0°C to rt, 2h, 96%; c) BBr_3 1M DCM, DCM, -78°C to rt, 54-57%.

In this case too, we successfully performed the guanidylation of the methoxylated derivative **124**, but we were not able to simultaneously cleave the methoxy and the carbamate groups to obtain the pure derivative **123** (Scheme 3.32a).

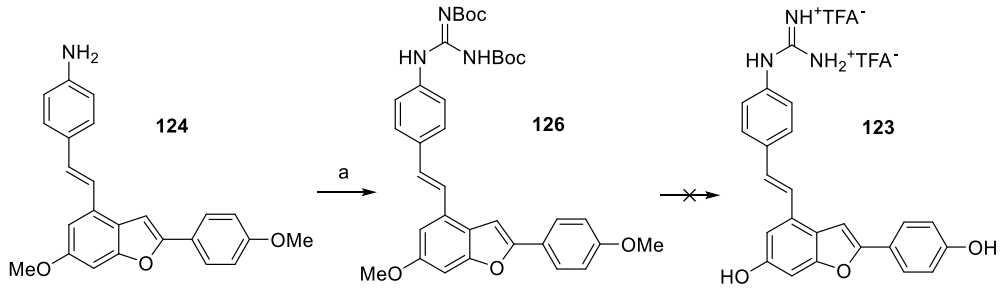

Scheme 3.32a. Reagents and conditions: a) *N,N'*-Di-*Boc*-1H-pyrazole-1-carboxamidine, $CHCl_3$, rt, 7h, 60%

Therefore, following the previous approach that allowed the isolation of the guanydinylated stilbenoid monomers, we applied the guanydinylation of the aniline **121** to give compound **127** in 60% yield. Unfortunately, we tried the deprotection of **127**, following standard procedures, consisting in the addition of TFA at 0°C to a solution of the compound in anhydrous DCM, but again we could not isolate the pure product, even after multiple purification steps with different chromatographic systems. Therefore, we applied the conditions that provided compound **118** (Scheme 3.30), adding TFA to the DCM solution of the compound, in presence of TES (Scheme 3.32b). However, also in this case we were not able to isolate the pure product. A partial deprotection was observed, followed by the formation of degradation products.

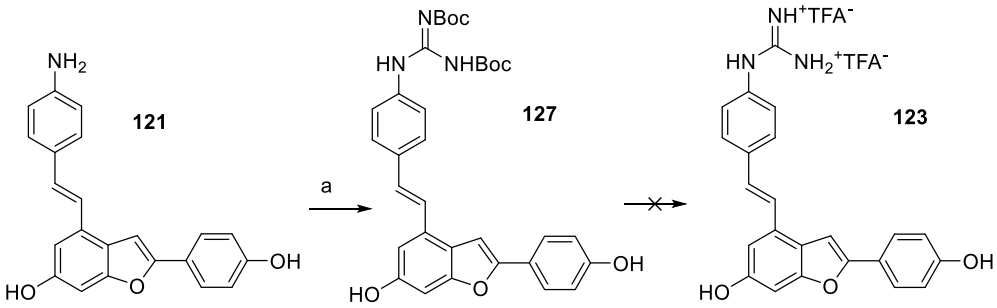

Scheme 3.32b. Reagents and conditions: a) *N,N'*-Di-*Boc*-1H-pyrazole-1-carboxamidine, $CHCl_3$, rt, 7h, 60%

3.3.4.2. Stilbenoids bearing an alkyl chain with a terminal amine

Some literature studies reported the improvement of the antimicrobial activity of stilbene derivatives by the addiction of an ammonium quaternary moiety (Chanawanno et al. 2010; Garner et al. 2010; Wan et al. 2017; Zhou et al. 2018). Therefore, we designed and synthesized another series of analogues of pterostilbene (**128-131**) and resveratrol (**132-134**) bearing an alkyl chain with a terminal amine (Figure 3.26) in order to study the effect of amines in the antimicrobial activity and in the interaction with the negatively charged Gram-negative outer membrane.

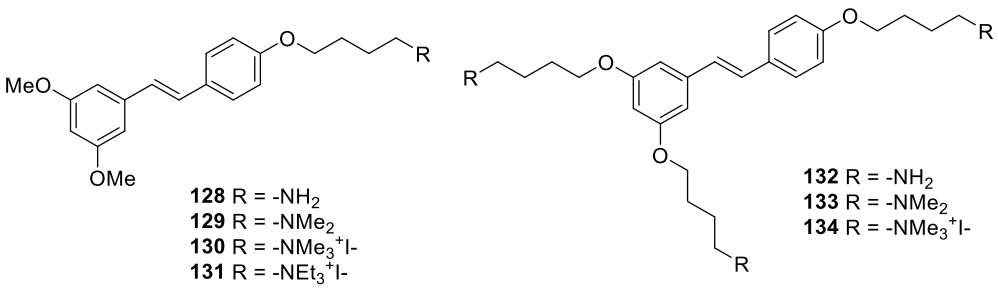

Figure 3.26. *Analogues of pterostilbene (**128-131**) and of resveratrol (**132-134**) bearing an alkyl chain with a terminal amine*

Firstly, following different procedures, we tried to directly attach a terminal halogenated alkyl amine to the hydroxy group of our derivatives, but no reaction occurred (Figure 3.27). Therefore, we planned to perform the alkylation of the phenolic moieties with a di-halogenated alkyl chain, followed by the substitution of the halogen with the desired nitrogen function.

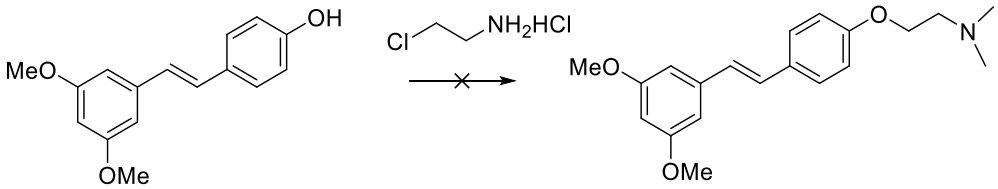

Figure 3.27. Alkylation of pterostilbene with 2-chloroethan-1-amine hydrochloride

In the case of pterostilbene (**2**), we applied a procedure described by Bavo *et al*. (Bavo et al. 2018), consisting in the alkylation of the hydroxy group with 1,4-dibromobutane, using NaOH as base, in DMSO at room temperature. We obtained compound **135** in 70% yield. The reaction with sodium azide in dry DMF at 50°C overnight afforded compound **136**, which was used without purification in the Staudinger conditions (Tian and Wang 2004) to give the compound **128** in good yield (84%). Then, by Finkelstein reaction, intermediate **135** was converted into the corresponding terminal iodoalkane **137**, which was used for the formation of the tertiary amine **129** and the ammonium salts **130** and **131** (Scheme 3.33).

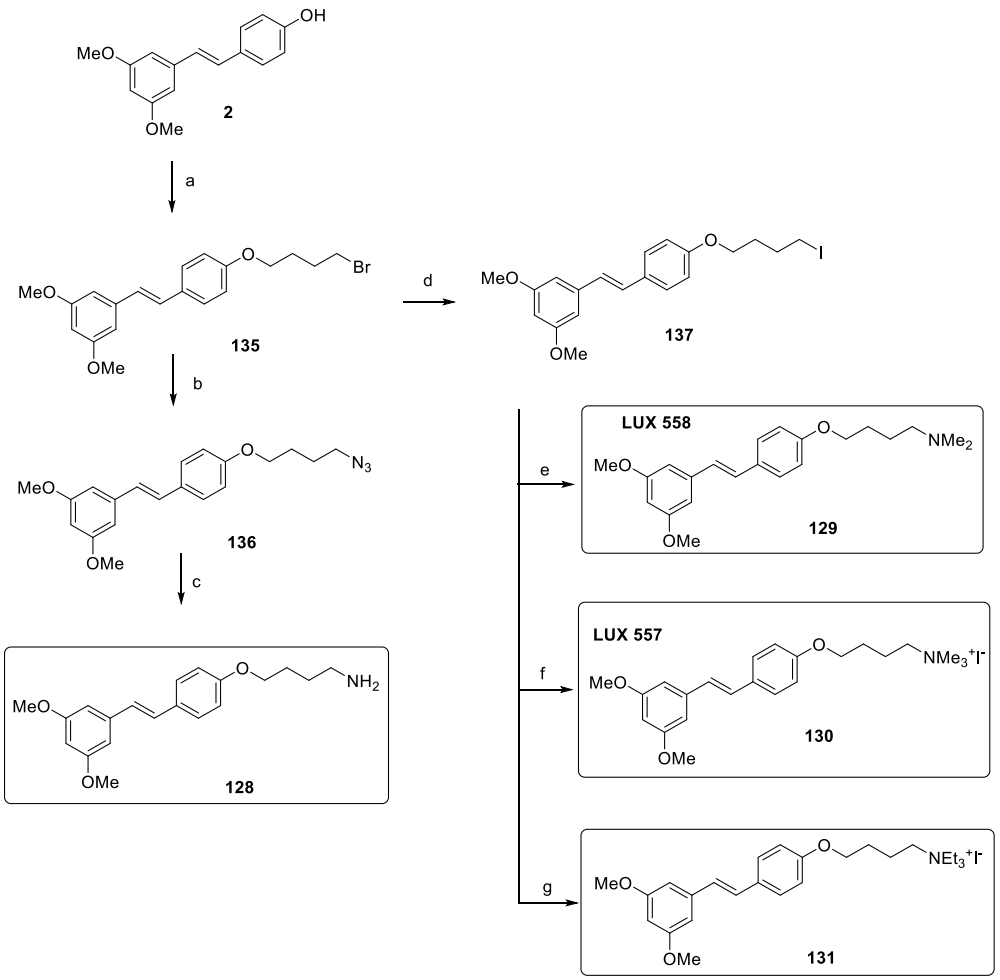

Scheme 3.33. Reagents and conditions: a) i) NaOH, DMSO, 30 min, rt, ii) 1,4-dibromobutane, rt, 4h, 70%; b) NaN_3, dry DMF, 50°C, overnight, 93%; c) PPh_3, H_2O, THF, 0°C to rt, overnight, 85%; d) NaI, dry acetone, reflux, overnight, quant yield; e) $HNMe_2$ 40% wt, THF, 60°C, 20h, quant yield; f) NMe_3, THF, 55°C, 16 h, quant yield; g) TEA, toluene, 24h, reflux, 62%.

In the case of resveratrol derivatives, firstly we tried to obtain the monoalkylated compounds **138a** and **138b**, following a procedure described by *Biasutto et al* (Biasutto et al. 2008). By column chromatography, we were able to separate and to obtain the two regioisomers in yields similar to the ones reported in literature (Scheme 3.34). These compounds could be used to link resveratrol to different other compounds, such as antibiotics or siderophore molecules for the development of hybrid antibiotics.

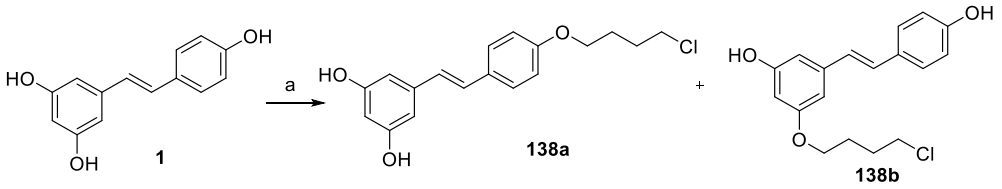

Scheme 3.34. Reagents and conditions: a) K_2CO_3, 1-bromo-4-chlorobutane, dry DMF, rt, overnight, **94a** (25%) and **94b** (16%).

Then, we focused on the synthesis of the totally alkylated resveratrol analogues (compounds **132-134**, Figure 3.26). In this case, for the alkylation reaction we used 1-bromo-4-chlorobutane, in place of 1,4-dibromobutane, in order to avoid or minimize side reactions between partially alkylated derivatives and the free hydroxy groups of resveratrol, likely resulting in undesired polymerization processes. We obtained **139**, which was further activated by Finkelstein reaction into the corresponding iodoalkane **140**. This intermediate was used to obtain compound **133** and **134**, by reaction with dimethylamine and trimethylamine, respectively. Moreover, intermediate **140** underwent reaction with sodium azide to yield derivative **141** that in Staudinger reaction conditions afforded compound **132** in 60% yield (Scheme 3.35).

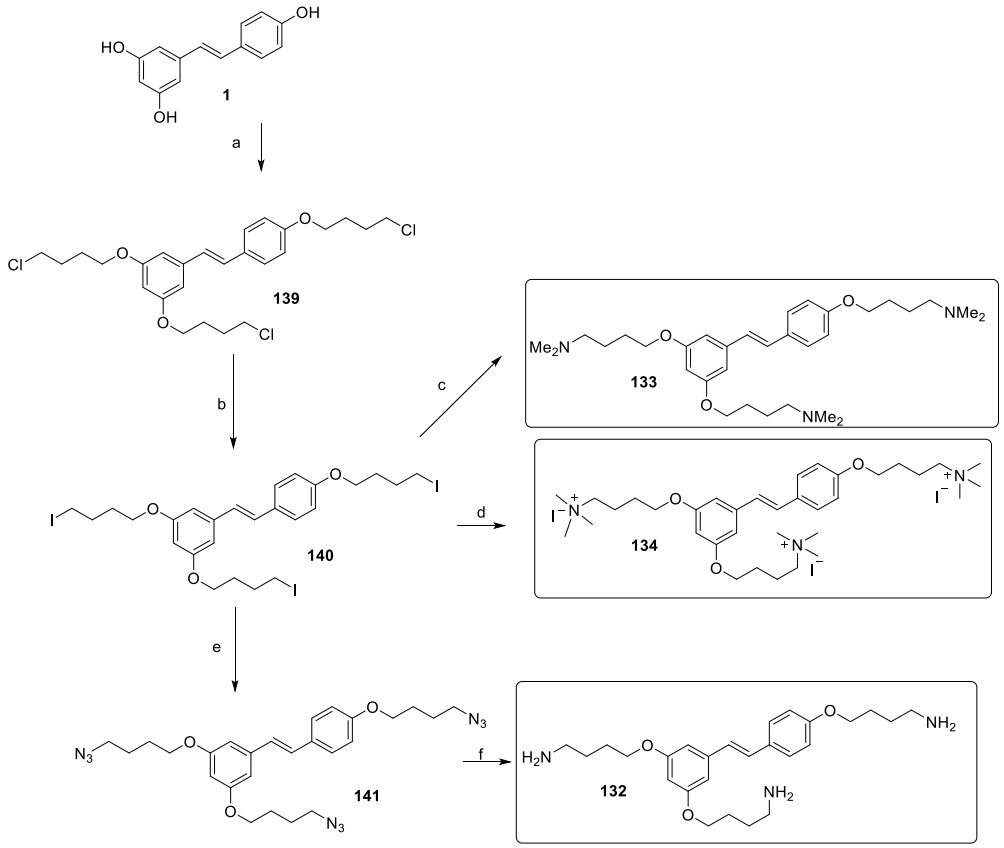

Scheme 3.35. Reagents and conditions: a) i) K_2CO_3, DMF, 15 min, rt, ii) 4-bromo-1-chlorobutane, 60°C, overnight, 73%; b) NaI, acetone, reflux, 24h, 88%; c) $HNMe_2$ 40% wt, THF, 60°C, 20h, 91%; d) NMe_3, THF, 55°C, 24 h, quant yield; e) NaN_3, DMF, 60°C, quant yield; f) PPh_3, H_2O, THF; 0°C to rt, 24h, 60%.

Biological evaluation of compounds obtained is underway.

3.3.5. Experimental section

3.3.5.1. General information

See chapter 3.1.4.1 for General information.

3.3.5.1. Experimental procedures

5-(5-(3,5-dihydroxyphenethyl)-2-(4-hydroxyphenyl)benzofuran-3-yl)benzene-1,3-diol (69)

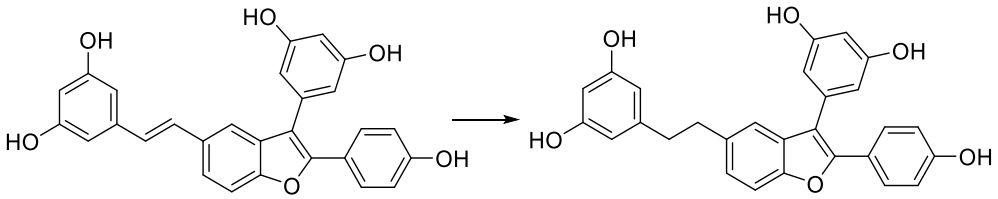

To a solution of **15** (40 mg, 0.0884 mmol, 1 eq) in EtOH (2 mL), Pd/C 10% wt (4 mg) was added and the reaction mixture was stirred under H_2 atmosphere for 4 h at room temperature. The mixture was filtered on a celite pad, washing repeatedly the filter with methanol. The filtrate was evaporated to yield the product as an amorphous reddish solid in quantitative yield.

R_f: 0.33 (DCM/MeOH 9:1)

^{1}H NMR (600 MHz, CD_3OD) δ (ppm): 7.50 – 7.46 (m, 2H), 7.34 (d, *J* = 8.4 Hz, 1H), 7.25 (d, *J* = 1.5 Hz, 1H), 7.06 (dd, J_1 = 1.5 Hz, J_2 = 8.4 Hz), 6.71 – 6.67 (m, 2H), 6.36 (d, *J* = 2.0 Hz, 1H), 6.28 (t, *J* = 2.0 Hz, 1H), 6.13 (d, *J* = 1.9 Hz, 2H), 6.08 (t, *J* = 2.0 Hz, 1H), 2.91 (t, *J* = 7.9 Hz, 2H), 2.75 (t, *J* = 7.9 Hz, 2H).
^{13}C NMR (150 MHz, CD_3OD) δ (ppm): 160.9, 160.3 (x2C), 159.2 (x2C), 153.3, 152.2, 145.0, 137.3, 135.9, 131.4, 129.2 (x2C), 125.2, 121.8, 119.6, 116.6 (x2C), 116.0, 110.6, 108.8 (x2C), 107.7 (x2C), 102.8, 101.1, 39.5, 38.6.

5-(1-(5-(3,5-dihydroxyphenethyl)-2-hydroxyphenyl)-2-(4-hydroxyphenyl)ethyl)benzene-1,3-diol (76)

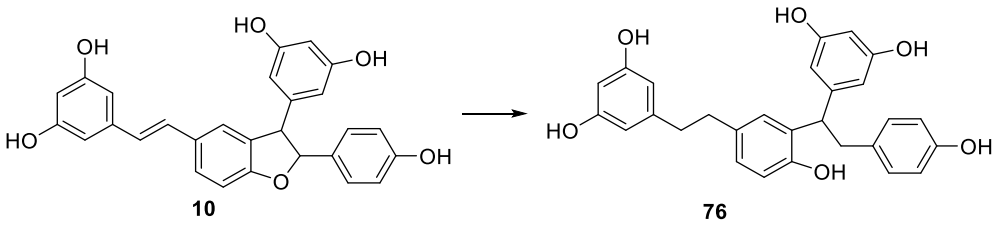

10 **76**

Procedure A: To a solution of **10** (40 mg, 0.088 mmol, 1 eq) in EtOH (2 mL), Pd/C 10% wt (4 mg) was added and the reaction mixture was stirred under H_2 atmosphere for 4 h at room temperature. The mixture was filtered on a celite pad, washing repeatedly the filter with methanol. The filtrate was evaporated to yield the product as a reddish solid in quantitative yield.

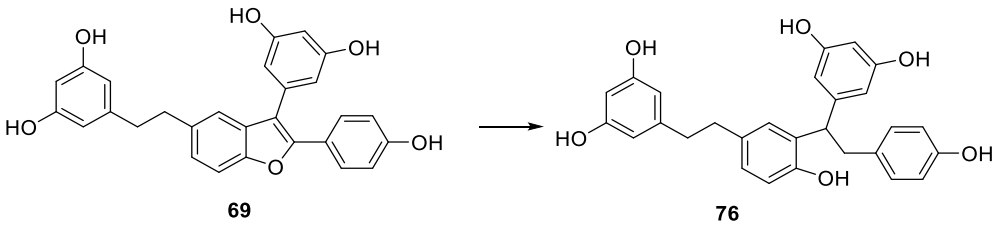

69 **76**

Procedure B: Compound **69** (20 mg, 0.044 mmol, 1 eq) was dissolved in trifluoroacetic acid (0.35 mL) and triethylsylane (10 µL, 0.066 mmol, 1.5 eq), and the mixture was stirred at room temperature overnight. The solvent was evaporated. The crude was purified on silica gel using as eluent DCM/MeOH 9:1 to give the product in 65% yield.

M.p.: 70°C dec

R_f: 0.27 (DCM/MeOH 9:1)

^{1}H NMR (600 MHz, CD_3OD) δ (ppm): 7.01 (d, *J* = 2.2 Hz, 1H), 6.92-6.85 (m, 2H), 6.77 (dd, J_1= 8.1 Hz, J_2 = 2.2 Hz, 1H), 6.62-6.53 (m, 3H), 6.22 (d, *J* = 2.2

Hz, 2H), 6.14 (d, *J* = 2.2 Hz, 2H), 6.09 (t, *J* = 2.2 Hz, 1H), 6.03 (t, *J* = 2.2 Hz, 1H), 4.44 (t, *J* = 8.7 Hz, 1H), 3.16-3.02 (m, 2H), 2.77-2-60 (m, 4H).

^{13}C NMR (150 MHz, C*D*$_3$O*D*) δ (ppm): 158.8 (x2C), 158.4 (x2C), 155.6, 153.4, 148.2, 145.4, 133.3, 132.9, 131.8, 130.6 (x2), 129.0, 127.2, 115.5, 115.2 (x2C), 107.9 (x2C), 107.8 (x2C), 100.8, 100.7, 40.9, 39.2, 39.1, 37.8.

4-bromo-2-iodophenol (77)

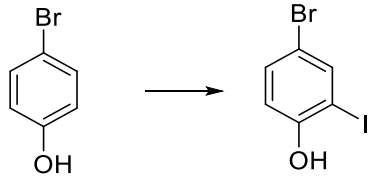

4-bromophenol **77**

4-bromophenol (500 mg, 2.89 mmol, 1 eq) was dissolved in aq 25% NH_3 (11.6 mL). A solution of KI (2.3 g, 13.872 mmol, 4.8 eq) and I_2 (734 mg, 2.89 mmol, 1 eq) in water (2.9 mL) was added and the mixture was stirred for 90 min. The reaction mixture was cooled to 0°C, diluted with water and quenched with aq 2M HCl (40 mL) (pH 2-3). The aqueous phase was extracted with EtOAc (4 x 40 mL). The combined organic phases were washed with aq saturated $NaHCO_3$ (100 mL), aq saturated $Na_2S_2O_3$ (100 mL), brine (100 mL), dried over anhydrous Na_2SO_4, filtered and evaporated. The crude was purified on silica gel by column chromatography using as eluent Hex/DCM (from 7:3 to 4:6). The product was obtained as white solid in 68% yield. Analytical data confirmed the ones reported in literature (Csékei et al. 2008).

M.p.: 71°C

R_f: 0.27 Hex/DCM 7:3

^{1}H NMR (C*D*Cl$_3$ 300 MHz) *δ* (ppm): 7.76 (d, 1H, *J*=2.2 Hz), 7.34 (dd, 1H, J_1 = 8.7, J_2 = 2.4 Hz), 6.87 (d, 1H, *J* = 8.7 Hz), 5.20 (br s, 1H).

^{13}C NMR (C*D*Cl$_3$, 75 MHz) *δ* (ppm): 154.2, 139.7, 133.0, 116.2, 113.0, 86.1.

1-iodo-3,5-dimethoxybenzene

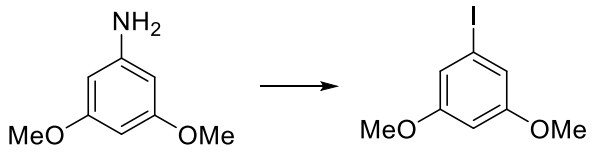

3,5-dimethoxyaniline **78**

To a suspension of 3,5-dimethoxyanline (500 mg, 3.264 mmol, 1 eq) in water (5.92 mL) at 0°C, aq 12M HCl (2.03 mL, 24.3 mmol, 7.46 eq) was added, followed by the portionwise addition of $NaNO_2$ (271 mg, 3.93 mmol, 1.2 eq). Then, KI (5.422 mmol, 32.64 mmol, 10 eq) was slowly added at 0°C and the mixture was stirred for 1 h at the same temperature and then allowed to warm to room temperature and stirred overnight. The reaction mixture was quenched with aq 20% Na_2SO_3 (100 mL) and the aqueous phase was extracted with EtOAc (4 x 80 mL). The combined organic layers were washed with water, brine, dried over anhydrous Na_2SO_4, filtered and evaporated. The crude was purified on silica gel using as eluent CHX/AcOEt (from 100% to 95%) to give the product as a white solid in 57% yield. The analytical data agreed with the ones previously reported (Krzyzanowski et al. 2018)

M.p.: 74-75°C

R_f: 0.61 CHX: AcOEt 95:5

^{1}H NMR (300 MHz, C*D*Cl$_3$) δ ppm: 6.86 (d, *J* = 2.2 Hz, 2H), 6.40 (t, *J* = 2.2 Hz, 1H), 3.76 (s, 6H).
^{13}C NMR (75 MHz, C*D*Cl$_3$) δ ppm: 161.22 (x2C), 115.95, 100.82, 94.21, 55.64 (x2C).

5-bromo-3-(3,5-dimethoxyphenyl)-2-(4-methoxyphenyl)benzofuran (79)

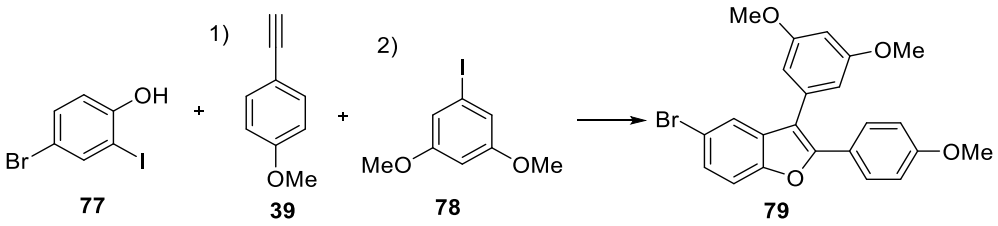

77 39 78 79

4-Bromo-2-iodophenol **77** (1g, 3.411 mmol, 1 eq) and $PdCl_2(PPh_3)_2$ (72 mg, 0.1023 mmol, 0.03 eq) were dissolved in dry THF (3.4 mL) in a microwave vial under N_2 atmosphere. Dry TEA (10.2 mL) and CuI (13 mg, 0.0682 mmol, 0.02 eq) were added and the reaction mixture was stirred for 10 min. Then, **39** (530 µL, 4.09 mmol, 1.2 eq) was added and the mixture was stirred in microwave reactor for 30 min at room temperature. After that, 1-iodo-3,5-dimethoxybenzene **78** (900 mg, 3.411 mmol, 1 eq) and dry acetonitrile (13.6 mL) were added and the mixture was stirred at 100°C for 25 min, under microwave irradiation. The reaction mixture was allowed to cool to room temperature and the solvent was evaporated. The crude was purified on silica gel using as eluent CHX/DCM (from 65:35 to 6:4) to give the desired compound as yellowish solid (72% yield).

M.p.: 125-126°C

R_f: 0.5 (CHX/DCM 6:4)

^{1}H NMR (300 MHz, CD_3OD) δ (ppm): 7.65 – 7.58 (m, 3H), 7.44 – 7.39 (m, 2H), 6.90 – 6.84 (m, 2H), 6.60 (d, *J* = 1.9 Hz, 2H), 6.52 (t, *J* = 1.9 Hz, 1H), 3.83 (s, 3H), 3.79 (s, 3H)

^{13}C NMR (150 MHz, CD_3OD) δ (ppm): 161.3 (x2C), 160.0, 152.4, 152.0, 134.2, 132.4, 128.6 (x2C), 127.0, 122.6, 122.4, 116.0, 115.4, 113.9 (x2C), 112.4, 107.6 (x2C), 100.0, 55.4, 55.3 (x2C).

3,5-Bis(3,5-dimethoxyphenyl)-2-(4-methoxyphenyl)benzofuran (80)

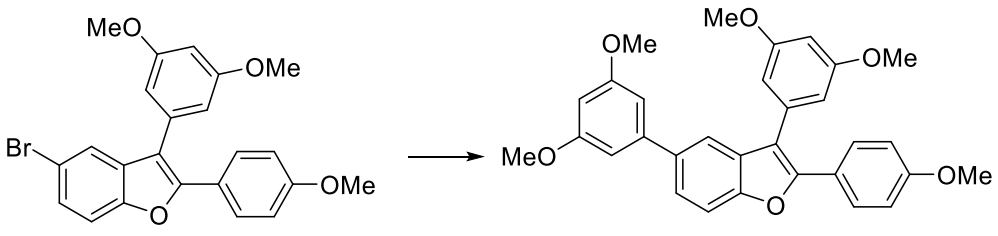

79 **80**

In a microwave vial, compound **79** (40 mg, 0.0911 mmol, 1 eq) and 3,5-dimethoxyphenylboronic acid (0.109 mmol, 20 mg, 1.2 eq) were dissolved in a mixture DMF/EtOH 1:1 (1.5 mL), previously degassed, under N_2 atmosphere. Then, $Pd(PPh_3)_4$ (5.3 mg, 0.0045 mmol, 0.05 eq) and aq 1M Cs_2CO_3 (0.23 mL, 0.23 mmol, 2.5 eq) were added and the resulting mixture was stirred in at 120°C for 20 min under microwave irradiation. The mixture was cooled, diluted with EtOAc, and washed with a mixture water/brine 1:1 three times. The organic layer was dried over anhydrous Na_2SO_4, filtered, and evaporated. The crude was purified on silica gel by column chromatography using CHX/AcoEt 9:1 as eluent. The product was obtained as a white solid (91%) (Markina et al. 2013).

M.p.: 105 – 107 °C

R_f: 0.24 CHX/AcOEt 9: 1

^{1}H NMR (600 MHz, C*D*Cl$_3$) δ (ppm): 7.71 – 7.67 (m, 3H), 7.60 (d, *J* = 8.4 Hz, 1H), 7.55 (dd, J_1 = 1.5 Hz, J_2 = 8.4 Hz), 6.94 – 6.89 (m, 2H), 6.77 (d, *J* = 2.0 Hz, 2H), 6.70 (d, *J* = 2.2 Hz, 2H), 6.57 (t, *J* = 2.2 Hz, 1H), 6.49 (t, *J* = 2.0 Hz, 1H), 3.88 (s, 6H), 3.86 (s, 3H), 3.82 (s, 6H).

^{13}C NMR (150 MHz, C*D*Cl$_3$) δ (ppm): 161.3 (x2C), 161.0 (x2C), 159.8, 153.1, 151.4, 144.0, 136.6. 134.8, 130.8, 128.5 (x2C), 124.0, 123.1, 118.3, 116.1, 113.9 (x2C), 111.0, 107.7 (x2C), 105.9 (x2C), 100.0, 98.8, 55.4 (x4C), 55.3.

5,5'-(2-(4-Hydroxyphenyl)benzofuran-3,5-diyl)bis(benzene-1,3-diol) (71)

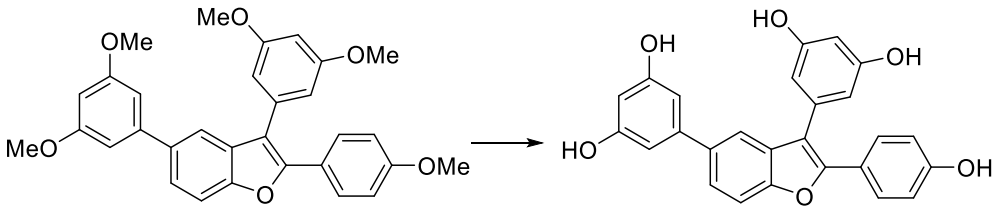

80 **71**

To a solution of compound **80** (60 mg, 0.1213 mmol, 1 eq) in dry DCM (1.2 mL) at -78°C, 1M BBr_3 in DCM (0.67 mL, 0.67 mmol, 5 eq) was added dropwise and the resulting mixture was allowed to warm to room temperature and stirred overnight. The mixture was quenched with aq 5% $NaHCO_3$ at 0°C (pH 7). The aqueous layer was extracted with EtOAc (3 x 10 mL). The combined organic layers were dried over anhydrous Na_2SO_4, filtered, and evaporated. The crude was purified on silica gel by column chromatography using as eluent DCM/MeOH 9:1. The product was obtained as yellowish solid.

M.p.: 161 – 163 °C

R_f: 0.25 DCM/MeOH 9:1

^{1}H NMR (600 MHz, CD_3OD) δ (ppm): 7.66 – 7.48 (m, 5H), 6.84 – 6.76 (m, 2H), 6.58 (d, *J* = 2.0 Hz, 2H), 6.47 (d, *J* = 2.1 Hz, 2H), 6.35 (t, *J* = 2.0 Hz, 1H), 6.26 (t, *J* = 2.1 Hz, 1H).

^{13}C NMR (150 MHz, CD_3OD) δ (ppm): 160.2 (x2C), 159.8 (x2C), 159.2, 154.7, 152.9, 145.0, 137.8, 136.0, 131.9, 129.7 (x2C), 124.5, 123.2, 118.7, 116.9, 116.3 (x2C), 111.7, 109.1 (x2C), 106.8 (x2C), 102.9, 102.2.

5-(5-Bromo-2-(4-hydroxyphenyl)benzofuran-3-yl)benzene-1,3-diol (81)

79 **81**

To a solution of compound **79** (700 mg, 1.593 mmol, 1 eq) in dry DCM (15.9 mL), under nitrogen atmosphere, at -78°C, BBr_3 1M in DCM (5.3 mL, 5.3 mmol, 3.3 eq) was added dropwise, and the resulting mixture was slowly allowed to warm to room temperature and stirred overnight. The reaction mixture was quenched at 0°C with aq 5% $NaHCO_3$ (pH 7). The aqueous layer was extracted with EtOAc three times. The combined organic layers were dired over anhydrous Na_2SO_4, filtered, and evaporated. The crude was purified on silica gel by column chromatography, using DCM/MeOH (95:5) as eluent to afford the product as a brownish amorphous solid in 87% yield.

R_f: 0.27 (DCM/MeOH 95:5)

^{1}H NMR (600 MHz, C*D*$_3$O*D*) δ (ppm): 7.55 – 7.52 (3H, m), 7.44 (d, J = 8.6 Hz, 1H), 7.39 (dd, J_1 = 1.9 Hz, J_2 = 8.6 Hz), 6.80 – 6.76 (2H, m), 6.39 (d, J = 2.2 Hz, 2H), 6.34 (t, J = 2.2 Hz, 1H).

^{13}C NMR (600 MHz, C*D*$_3$O*D*) δ (ppm): 160.3 (x2C), 159.6, 153.8, 153.7, 135.3, 133.7, 129.8 (x2C), 127.9, 123.1, 122.6, 116.9, 116.4 (x2C), 116.2, 113.4, 108.9 (x2C), 103.2.

((5-(5-Bromo-2-(4-((tert-butyldimethylsilyl)oxy)phenyl)benzofuran-3-yl)-1,3-phenylene)bis(oxy))bis(tert-butyldimethylsilane) (82)

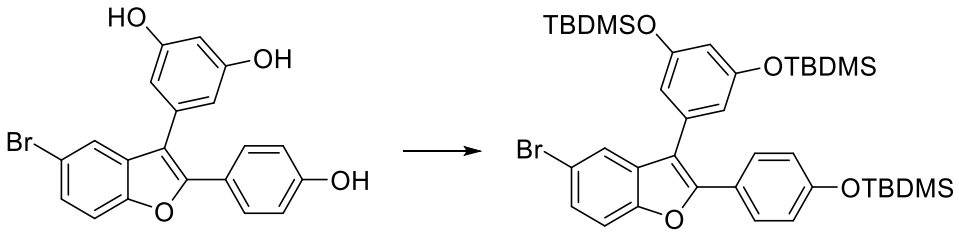

81 **82**

Following a procedure by Romero *et al* (Romero et al. 2020), imidazole (131 mg, 1.926 mmol, 4.5 eq) and TBDMSCl (252 mg, 1.669 mmol, 3.9 eq) were added to a suspension of compound **81** (170 mg, 0.428 mmol, 1 eq) in 1,2-dichloroethane (4.3 mL), and the resulting mixture was stirred at 60°C for 8h, under N_2 atmosphere. The mixture was allowed to cool to room temperature and quenched with brine. The aqueous phase was extracted three times with EtOAc. The combined organic layers were dried over anhydrous Na_2SO_4, filtered, and evaporated. The crude was purified on silica gel by column chromatography, using as eluent CHX/DCM 95:5 to afford the desired product as foamy white solid in 81% yield.

R_f: 0.36 CHX/DCM 95:5

^{1}H NMR (600 MHz, C*D*Cl$_3$) δ (ppm): 7.58 – 7.53 (m, 3H), 7.39 – 7.37 (m, 2H), 6.81 – 6.76 (m, 2H), 6.54 (d, *J* = 2.4 Hz, 2H), 6.41 (t, *J* = 2.4 Hz, 1H), 0.98 (s, 27H), 0.19 (s, 18H).

^{13}C NMR (150 MHz, C*D*Cl$_3$) *δ* (ppm): 158.6 (x2C), 157.7, 153.8, 153.2, 135.3, 133.9, 129.8 (x2C), 128.3, 124.6, 123.8, 121.6 (x2C), 117.3, 116.7, 116.1 (x2C), 113.7, 113.4, 27.0 (x9C), 19.6 (x3C), -2.9 (x6C).

3,5-Bis(*tert*-butyldimethylsilyloxy)benzaldehyde (85)

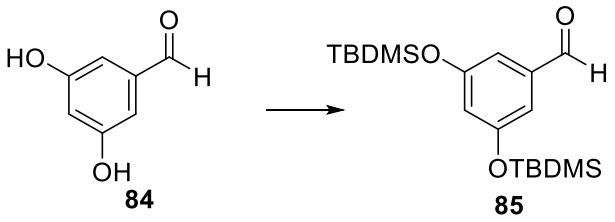

To a solution of 3,5-dihydroxybenzaldehyde **84** (300 mg, 2.172 mmol, 1 eq) in dry DMF (8 mL) at 0°C, under N_2 atmosphere, imidazole (739 mg, 10.86 mmol, 5 eq) and *tert*-butyldimethylsilylchloride (786 mg, 5.212 mmol, 2.4 eq) were added, and the resulting mixture was stirred at 0°C for 15 min and then at room temperature overnight. The reaction mixture was diluted with EtOAc (30 mL) and washed with a mixture of 0.1M HCl/brine 1:1 (5 x 20 mL).The organic phase was dried over anhydrous Na_2SO_4, filtered, and evaporated. The crude was purified on silica gel by column chromatography using as eluent CHX/AcOEt (from 100% to 98%). The product was obtained as a transparent oil in 74% yield. The analytical data were in agreement with previous data reported in literature (Hoshino et al. 2010).

R_f: 0.63 CHX/AcOEt 98:2

^{1}H NMR (300MHz, C*D*Cl3) δ (ppm): 9.86 (s, 1 H), 6.95 (d, J= 2.1 Hz, 1 H), 6.58 (t, J = 2.1 Hz, 1 H), 0.98 (s, 18 H), 0.21 (s, 12 H).
^{13}C NMR (75 MHz, C*D*Cl3) δ (ppm): 191.6, 157.6 (x2C), 138.8, 118.6, 114.6 (x2C), 25.9 (x2C), 18.5 (x6C), -4.1 (x4C).

((5-(2,2-Dibromovinyl)-1,3-phenylene)bis(oxy))bis(*tert*-butyldimethylsilane) (86)

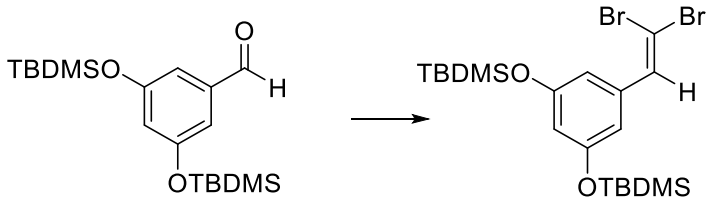

85 **86**

To a solution of CBr_4 (1.067 g, 3.2183 mmol, 2 eq) in dry DCM (5.7 mL) at 0°C, PPh_3 (1.688 g, 6.4367 mmol, 4 eq) was added and the orange mixture was stirred for 10 min at 0°C. Then, a solution of compound **85** (590 mg, 1.609 mmol, 1 eq) in dry DCM (16 mL) was slowly added at 0°C, and the resulting mixture was stirred for 10 min at the same temperature and 10 min at room temperature. The reaction was quenched with water (30 mL) and the aqueous phase was extracted with DCM (3 x 30 mL). The combined organic layers were dried over anhydrous Na_2SO_4, filtered, and evaporated. The crude was purified on silica gel by flash column chromatography, using as eluent CHX/DCM (from 95% to 90%). The product was obtained as a transparent oil in 90% yield. The analytical data were in agreement with previous data reported in literature (Gibtner et al. 2002).

R_f: 0.75 CHX: DCM 9:1

^{1}H NMR (300 MHz, C*D*Cl$_3$) δ (ppm): 7.33 (s, 1 H), 6.63 (d, J = 2.2 Hz, 2 H), 6.31 (t, J = 2.2 Hz, 1 H), 0.95 (s, 18 H), 0.18 (s, 12 H).

^{13}C NMR (75 MHz, C*D*Cl$_3$) δ (ppm): 156.47 (x2C), 136.71, 136.60, 113.43 (x2C), 112.66, 89.44, 25.66 (x6 C), 18.21 (x2C), −4.39 (x4C).

((5-Ethynyl-1,3-phenylene)bis(oxy))bis(tert-butyldimethylsilane) (83)

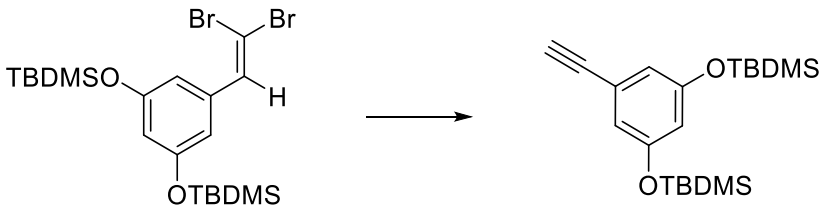

86 **83**

To a solution of compound **86** (340 mg, 0.651 mmol, 1 eq) in dry THF (7.5 mL) at -78°C, under N_2 atmosphere, LDA 1M in THF (1.95 mL, 1.95 mmol, 3 eq) was added dropwise and the solution was stirred at - 78°C for 1h. The reaction was cautiously quenched with water and the aqueous phase was extracted with EtOAc three times. The combined organic layers were dried over anhydrous Na_2SO_4, filtered, and evaporated. The crude was purified on silica gel by column chromatography, using as eluent CHX/DCM (from 100% to 95%) to afford the desired product as transparent oil (91%). The analytical data were in agreement with previous data reported in literature (Gibtner et al. 2002)

R_f: 0.47 CHX/DCM 95:5

^{1}H NMR (300 MHz, C*D*Cl$_3$) δ (ppm): 6.59 (d, J = 2.2 Hz, 2 H), 6.34 (t, J = 2.2 Hz, 1 H), 2.99 (s, 1 H), 0.96 (s, 18 H), 0.18 (s, 12 H).

^{13}C NMR (75 MHz, C*D*Cl$_3$) δ (ppm): 156.39 (x2C), 123.07, 117.22 (x2C), 113.72, 83.53, 76.51, 25.62 (x6C), 18.17 (x2C), −4.45 (x4C).

5-((3-(3,5-Dihydroxyphenyl)-2-(4-hydroxyphenyl)benzofuran-5-yl)ethynyl)benzene-1,3-diol (70)

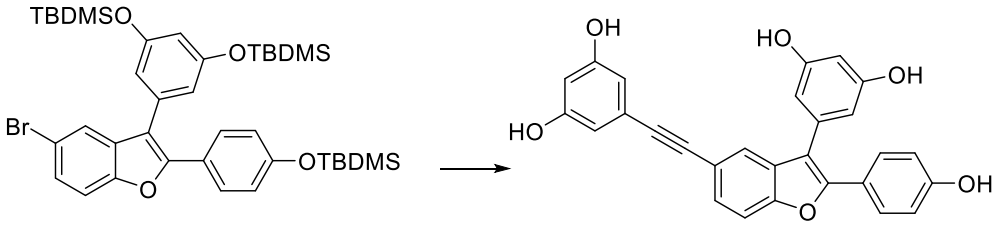

82 **70**

Compound **82** (240 mg, 0.324 mmol, 1 eq) and compound **83** (130 mg, 0.3564 mmol, 1.1 eq) were dissolved in previously degassed dry TEA (5 mL). $Pd(PPh_3)_4$ (11.2 mg, 0.0097 mmol, 0.03 eq) was added and the mixture was stirred for 10 min. Then, CuI (1.23 mg, 0.0065 mmol, 0.02 eq) was added and the mixture was refluxed for 8h, under N_2 atmosphere. The solvent was evaporated, and the resulting black residue was suspended in MeOH (6 mL). A solution of KF (280 mg, 4.86 mmol, 15 eq) in a mixture of MeOH/THF 1:1 (12 mL) was added dropwise. The reaction mixture was stirred overnight at room temperature. The solvents were evaporated and the residue was dissolved with some drops of MeOH and diluted with AcOEt. The organic phase was washed with a mixture of water/brine 1:1 (3 x 20 mL) and brine (3 x 20 mL). The organic layer was dried over anhydrous Na_2SO_4, filtered, and evaporated. The crude was purified on silica gel by column chromatography, using as eluent DCM/MeOH 9:1. A fraction containing some impurities was further purified on silica gel by column chromatography using as eluent CHX/Acetone 1:1. The product was obtained as yellow foamy solid in 38% yield over two steps.

M.p.: 164 – 165°C

R_f: 0.23 DCM/MeOH 9:1 or 0.38 CHX/Acetone 1:1

^{1}H NMR (300 MHz, CD_3OD) δ (ppm): 7.62 – 7.47 (m, 4H), 7.41 (dd, J_1 = 1.6 Hz, J_2 = 8.5 Hz, 1H), 6.77 (d, J = 8.8 Hz, 2H), 6.43 (d, J = 2.2 Hz, 2H), 6.41 (d, J = 2.2 Hz, 2H), 6.33 (t, J = 2.2 Hz, 1H), 6.26 (t, J = 2.3 Hz, 1H).

^{13}C NMR (600 MHz, CD_3OD) δ (ppm): 160.3 (x2C), 159.7 (x3C), 154.8, 153.5, 135.6, 133.0, 129.9 (x2C), 128.8, 125.9, 124.0, 122.9, 119.5, 116.4 (x2C), 112.1, 111.7, 110.9 (x2), 109.1 (x2C), 104.4, 103.2, 89.5, 89.2.

Methyl 3-(3,5-dimethoxyphenyl)-2-(4-methoxyphenyl)benzofuran-5-carboxylate (87)

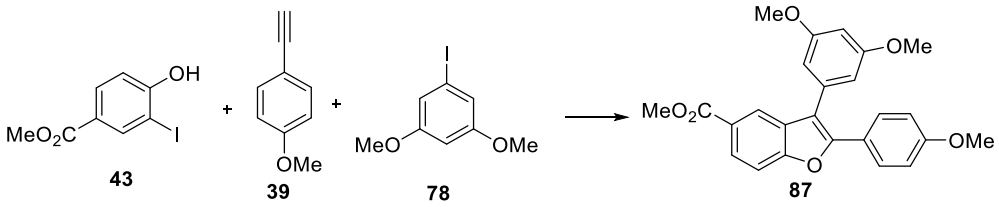

43 39 78 87

Methyl 4-hydroxy-3-iodobenzoate **43** (100 mg, 0.35965 mmol, 1 eq) and $PdCl_2(PPh_3)_2$ (7.57 mg, 0.01079 mmol, 0.03 eq) were dissolved in dry THF (0.35 mL) in a microwave vial under N_2 atmosphere. Dry TEA (1.1 mL) and CuI (1.4 mg, 0.007 mmol, 0.02 eq) were added and the reaction mixture was stirred for 10 min. Then, 4-ethynilanisole **39** (56 µL, 0.432 mmol, 1.2 eq) was added and the mixture was stirred in a microwave reactor for 30 min at room temperature. After that, 1-iodo-3,5-dimethoxybenzene **78** (95 mg, 0.35965, 1 eq) and dry acetonitrile (1.43 mL) were added and the mixture was stirred at 100°C for 25 min, under microwave irradiation. The reaction mixture was allowed to cool to room temperature and the solvent was evaporated. The crude was purified on silica gel using as eluent CHX/DCM (from 1:1 to 3:7) to give the desired compound as a yellow solid (66% yield).

M.p.: 175 – 177 °C

R_f: 0.26 (CHX/DCM 1:1)

^{1}H NMR (300 MHz, C*D*Cl$_3$) δ (ppm): 8.19 (dd, J_1= 0.6 Hz, J_2 = 1.8 Hz, 1H), 8.03 (dd, J_1= 1.8 Hz, J_2 = 8.6 Hz, 1H), 7.67 -7.60 (m, 2H), 7.54 (dd, J_1= 0.6 Hz, J_2 = 8.6 Hz, 1H), 6.91-6.83 (m, 2H), 6.63 (d, J = 2.3 Hz, 2H), 6.54 (t, J = 2.3 Hz, 1H), 3.91 (s, 3H), 3.83 (s, 3H), 3.79 (6H, s).

^{13}C NMR (150 MHz, C*D*Cl$_3$) δ (ppm): 167.3, 161.3 (x2C), 160.0, 156.3, 152.0, 134.2, 130.5, 128.5 (x2C), 126.1, 125.3, 122.6, 122.2, 116.2, 114.0 (x2C), 110.8, 107.7 (x2C), 100.1, 55.4 (x2C), 55.3, 52.0.

3-(3,5-dimethoxyphenyl)-2-(4-methoxyphenyl)benzofuran-5-carboxylic acid (88)

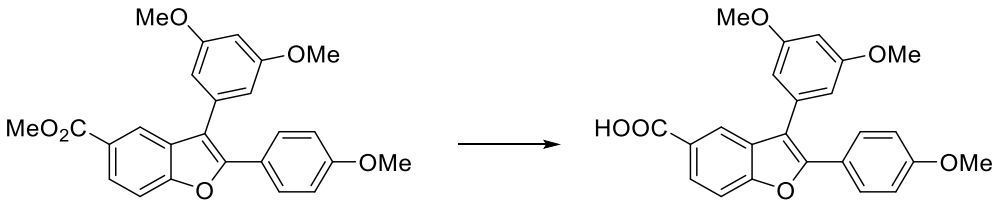

87 **88**

Compound **87** (90 mg, 0.215 mmol, 1 eq) was dissolved in THF (2.8 mL). Then a solution of LiOH·H$_2$O (45 mg, 1.075 mmol, 5 eq) in water (2.8 mL) was added and the resulting suspension was stirred for 24h. When the reaction was completed, we observed that the suspension had become a clear solution. The organic solvent was evaporated and the aqueous phase was quenched at 0°C with aq 1M HCl (pH 2-3). The aqueous phase was extracted with EtOAc three times. The combined organic phases were washed with brine, dried over anhydrous Na_2SO_4, filtered and evaporated. The product was obtained as a yellowish solid in quantitative yield.

M.p.: 262 – 264°C

R_f: 0.33 (CHX/AcOEt 3:2)

^{1}H NMR (600 MHz, DMSO-*d*$_6$) δ (ppm): 12.91 (brs, 1H), 7.98 (d, *J* = 1.6 Hz, 1H), 7.94 (dd, J_1 = 1.6 Hz, J_2 = 8.6 Hz, 1H), 7.60 – 7.56 (m, 2H), 7.03 – 6.98 (m, 2H), 6.62 (t, *J* = 2.0 Hz, 1H), 6.60 (d, *J* = 2.0 Hz, 2H), 3.77 (s, 3H), 3.74 (s, 6H).

^{13}C NMR (150 MHz, DMSO-*d*$_6$) δ (ppm): 167.3, 161.1 (x2C), 160.0, 155.4, 151.5, 133.4, 129.8, 128.3 (x2C), 126.3, 126.1, 121.6, 121.2, 115.6, 114.3 (x2C), 111.2, 107.4 (x2C), 99.8, 55.3 (x3C).

N,3-bis(3,5-dimethoxyphenyl)-2-(4-methoxyphenyl)benzofuran-5-carboxamide (89)

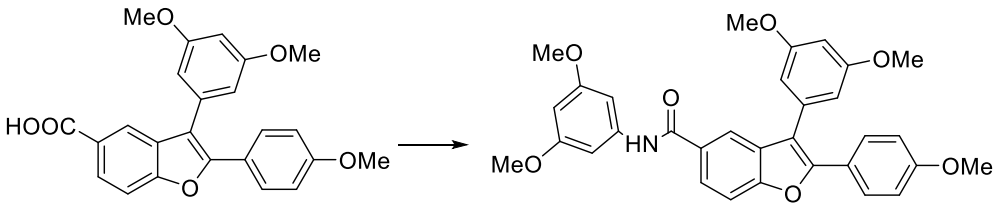

88 **89**

To the solution of compound **88** (48 mg, 0.119 mmol, 1 eq) in dry DMF (1 mL) at 0°C, under N_2 atmosphere, EDC·HCl (34.4 mg, 0.179 mmol, 1.5 eq) and HOBt (24 mg, 0.179 mmol, 1.5 eq) were added. The ice-bath was removed and the mixture was stirred at room temperature for 1h. Then, the reaction was cooled again to 0°C, and DIPEA (41 µL, 0.239 mmol, 2 eq) and 3,5-dimethoxyaniline (22 mg, 0.143 mmol, 1.2 eq) were added and the mixture was warmed to room temperature and stirred overnight. The reaction was quenched with aq 1M HCl (10 mL) and extracted with EtOAc (3 x 10 mL). The combined organic phases were washed wit aq saturated $NaHCO_3$ (20 mL), brine (2 x 20 mL), dried over anhydrous Na_2SO_4, filtered, and evaporated. The crude was purified on silica gel by column chromatography using as eluent CHX: AcOEt 7:3. The product was obtained as brownish solid.

M.p.: 166 – 167 °C

R_f: 0.36 (CHX/AcOEt 7:3)

^{1}H NMR (600 MHz, C*D*Cl$_3$) δ (ppm): 7.94 (d, *J* = 1.8 Hz, 1H), 7.83 (dd, J_1 = 8.6 Hz, J_2 = 2.0 Hz, 1H), 7.81 (brs, 1H), 7.69 – 7.62 (m, 2H), 7.59 (d, *J* = 8.6 Hz, 1H), 6.91 (d, *J* = 2.2 Hz, 2H), 6.90 – 6.82 (m, 2H), 6.63 (d, *J* = 2.3 Hz, 2H), 6.54 (t, *J* = 2.3 Hz, 1H), 6.27 (t, *J* = 2.2 Hz, 1H), 3.83 (s, 3H), 3.79 (s, 6H).
^{13}C NMR (150 MHz, C*D*Cl$_3$) δ (ppm): 166.1, 161.4 (x2C), 160.1 (x2C), 160.1, 155.5, 152.3, 139.9, 134.2, 130.7, 130.2, 128.5 (x2C), 123.7, 122.5, 118.9, 116.0, 114.0 (x2C), 111.2, 107.7 (x2C), 100.0, 98.3 (x2C), 97.0, 55.4 (x4C), 55.3.

N,3-bis(3,5-dihydroxyphenyl)-2-(4-hydroxyphenyl)benzofuran-5-carboxamide (72)

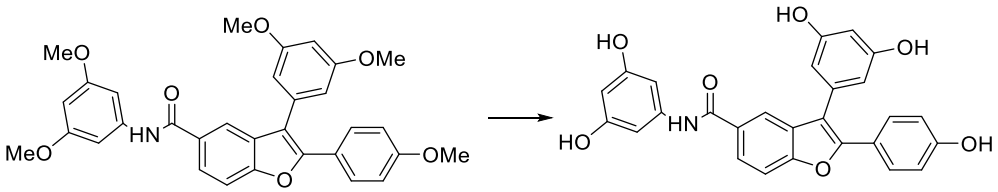

To a solution of compound **89** (35 mg, 0.0645 mmol, 1 eq) in dry DCM (1.2 mL) at - 78°C, 1M BBr_3 in DCM (0.43 mL, 0.43 mmol, 6.6 eq) was added dropwise and the resulting mixture was allowed to warm to room temperature and stirred overnight. The mixture was quenched with aq 5% $NaHCO_3$ at 0°C (pH 7). The aqueous layer was extracted with EtOAc (3 x 10 mL). The combined organic layers were dried over anhydrous Na_2SO_4, filtered, and evaporated. The crude was purified on silica gel by column chromatography using as eluent DCM/MeOH 85:15. The product was obtained as brownish sticky solid (73% yield).
M.p.: 199 – 201 °C

R_f: 0.36 DCM/MeOH 85:15

^{1}H NMR (600 MHz, CD_3O*D*) δ (ppm): 8.06 (d, *J* = 1.6 Hz, 1H), 7.88 (dd, J_1 = 8.8 Hz, J_2 = 1.6 Hz), 7.63 (d, *J* = 8.8 Hz, 1H), 7.61 – 7.55 (m, 2H), 6.85 – 6.78

(m, 2H), 6.74 (d, *J* = 1.8 Hz, 2H), 6.46 (d, *J* = 2.0 Hz, 2H), 6.36 (t, *J* = 2.0 Hz, 1H), 6.10 (t, *J* = 1.8 Hz, 1H).

^{13}C NMR (150 MHz, C*D$_3$OD*) δ (ppm): 169.2, 160.3 (x2C), 159.6 (x2C), 159.5, 156.9, 153.8, 141.4, 135.5, 131.7, 131.5, 129.8 (x2C), 125.1, 122.7, 120.8, 117.0, 116.4 (x2C), 111.7, 109.2 (x2C), 103.2, 101.2 (x2C), 100.1.

3-(3,5-dimethoxyphenyl)-2-(4-methoxyphenyl)benzofuran-5-amine (90)

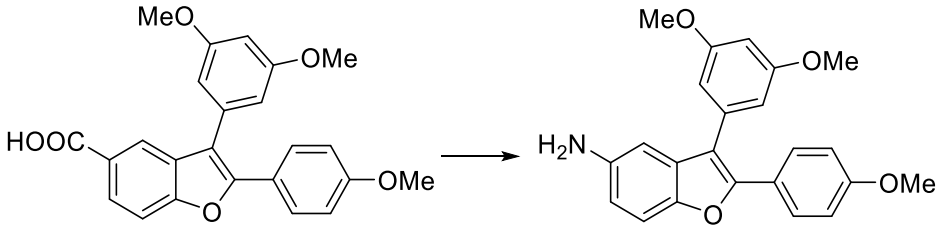

88 **90**

To a solution of compound **88** (50 mg, 0.1236 mmol, 1 eq) in dry toluene (2 mL) at room temperature, under N_2 atmosphere, dry TEA (172 µL, 1.236 mmol, 10 eq) was added, followed by the dropwise addition of diphenylphosphoryl azide (266 µL, 1.236 mmol, 10 eq). The mixture was stirred at room temperature for 15 min, and then heated to 80°C and stirred overnight. The reaction mixture was cooled down, toluene was removed, and the resulting residue was dissolved in THF (2 mL). Aq 4 M LiOH·H_2O (22 eq) was added and the mixture was stirred vigorously for 5h. Then, the mixture was diluted with water and extracted with EtOAc (3 x 20 mL). The combined organic layers were washed with brine, dried over anhydrous Na_2SO_4, filtered, and evaporated. The crude was purified on silica gel, using as eluent DCM/AcOEt 95:5 to afford the product as brownish sticky solid (34%).

R_f: 0.34 (DCM/AcOEt 95:5)

^{1}H NMR (600 MHz, C*D*Cl$_3$) δ (ppm): 7.63 – 7.58 (m, 2H), 7.32 (d, *J* = 8.3 Hz, 1H), 6.87 – 6.82 (m, 3H), 6.74 (dd, J_1 = 8.3 Hz, J_2 = 2.0 Hz), 6.61 (d, *J* = 2.1Hz, 2H), 6.49 (t, *J* = 2.1 Hz, 1H), 3.81 (s, 3H), 3.77 (s, 6H).

^{13}C NMR (150 MHz, C*D*Cl$_3$) δ (ppm): 161.1, 159.6 (x2C), 151.3, 148.5, 141.5, 135.2, 131.1, 128.4 (x2C), 123.4, 115.6, 113.8 (x2C), 113.6, 111.2, 107.6 (x2C), 105.1, 99.8, 55.4 (x2C), 55.3.

3,5-dimethoxybenzoic acid

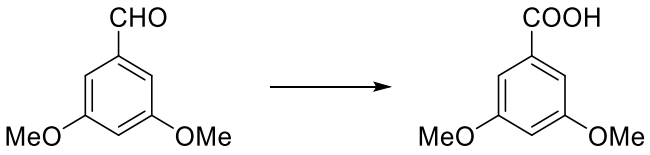

To a solution of 3,5-dimethoxybenzaldehyde (100 mg, 0.602 mmol, 1 eq) in *t*-BuOH (6 mL) and water (3 mL), 2-methyl-2-butene (701 µL, 6.62 mmol, 11 eq) was added, followed by the addition of aq 2M NaH_2PO_4 (415 mg, 3.01 mmol, 5 eq) and aq 1.2 M $NaClO_2$ (204 mg, 1.805 mmol, 3 eq). The mixture was stirred at room temperature for 30 min. The mixture was quenched with brine and the aqueous layer was extracted three times with EtOAc. The combined organic layers were concentrated and the residue was treated with aq 1N NaOH. The aqueous layer was extracted with EtOAc four times to remove 2-methyl-2-butene and other impurities. Then, the aqueous layer was treated with aq 2M HCl (pH 2) and extracted with EtOAc three times. The combined organic layers were dried over anhydrous Na_2SO_4, filtered and evaporated to afford the pure product as a white solid (64%). Analytical data were in agreement with data reported in literature (Song et al. 2012).

M.p.: 182-184°C

R_f: 0.5 (DCM/MeOH 95:5)

^{1}H NMR (300 MHz, C*D*$_3$O*D*) δ (ppm): 7.12 (d, 2 H, *J* = 2.4 Hz), 6.66 (t, 1 H, *J* = 2.4 Hz), 3.78 (s, 6 H).
^{13}C NMR (75 MHz, C*D*$_3$O*D*) δ (ppm): 168.2, 161.0 (x2C), 132.6, 107.1 (x2C), 105.0, 54.8 (x2C).

***N*-(3-(3,5-dimethoxyphenyl)-2-(4-methoxyphenyl)benzofuran-5-yl)-3,5-dimethoxybenzamide (91)**

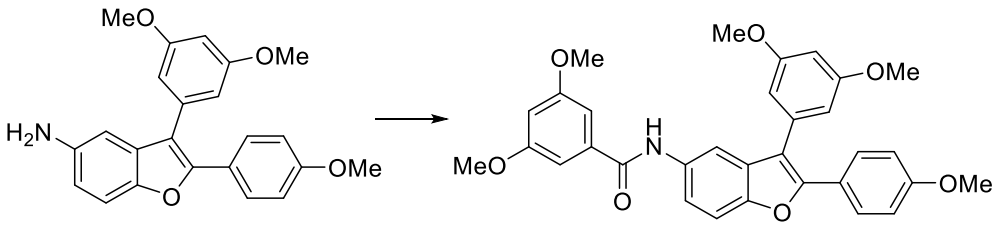

To a solution of 3,5-dimethoxybenzoic acid (21 mg, 0.115 mmol, 1.2 eq) in dry DMF (1 mL) at 0°C, under N_2 atmosphere, EDC·HCl (33 mg, 0.173 mmol, 1.8 eq) and HoBt (23 mg, 0.173 mmol, 1.8 eq) were added. The ice-bath was removed and the mixture was stirred at room temperature for 1h. Then, the reaction was cooled again to 0°C, and DIPEA (38 µL, 0.22 mmol, 2.3 eq) and a solution of compound **90** (36 mg, 0.0959 mmol, 1 eq) in dry DMF (1 mL) were added. The mixture was warmed to room temperature and stirred overnight. The reaction was quenched with aq 1M HCl (20 mL) and extracted with EtOAc (3 x 20 mL). The combined organic phases were washed wit aq saturated $NaHCO_3$ solution (30 mL), brine (2 x 30 mL), dried over anhydrous Na_2SO_4, filtered, and evaporated. The crude was purified on silica gel by column chromatography using as eluent CHX/AcOEt 7:3. The product was obtained as an amorphous solid in 70% yield.

R_f: 0.37 (CHX/AcOEt 7:3)

^{1}H NMR (600 MHz, C*D*Cl$_3$) δ (ppm): 7.83 (brs, 1H), 7.74 (d, *J* = 1.6 Hz, 1H), 7.68 – 7.64 (m, 2H), 7.57 (dd, J_1= 8.5 Hz, J_2 = 1.6 Hz, 1H), 7.50 (d, *J* = 8.5 Hz, 1H), 7.00 (d, *J* = 2.2 Hz, 1H), 6.91 – 6.86 (m, 2H), 6.65 (d, *J* = 2.3 Hz, 2H), 6.62 (t, *J* = 2.2 Hz, 1H), 6.52 (t, *J* = 2.3 Hz, 1H), 3.85 (s, 6H), 3.84 (s, 3H), 3.80 (s, 6H).

^{13}C NMR (150 MHz, C*D*Cl$_3$) δ (ppm): 165.2, 161.2 (x2C), 161.0 (x2C), 159.8, 151.7, 150.9, 137.3, 134.6, 133.3, 130.8, 128.5 (x2C), 123.0, 117.9, 116.0,

113.9 (x2C), 111.8, 111.1, 107.6 (x2C), 104.9 (x2C), 103.8, 100.0, 55.6 (x2C), 55.4 (x2C), 55.3.

N-(3-(3,5-dihydroxyphenyl)-2-(4-hydroxyphenyl)benzofuran-5-yl)-3,5-dihydroxybenzamide (73)

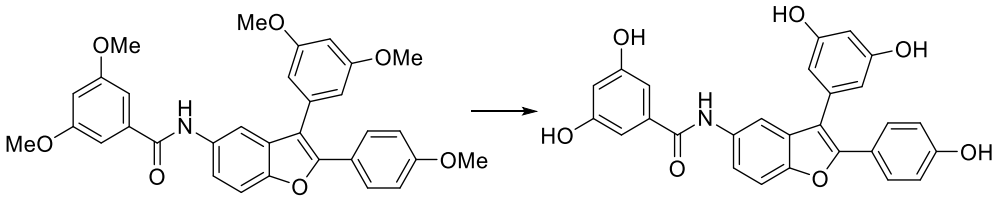

To a solution of compound **91** (36 mg, 0.0667 mmol, 1 eq) in dry DCM at -78°C, under nitrogen atmosphere, BBr_3 1M in DCM (0.44 ml, 0.44 mmol, 6.6 eq) was added dropwise, and the resulting mixture was allowed to warm to room temperature and stirred overnight. The reaction was cooled to 0°C and quenched with aq 5% $NaHCO_3$. The aqueous layer was extracted with EtOAc three times, and the combined organic layers were dried over anhydrous Na_2SO_4, filtered and evaporated. The crude was purified on silica gel by column chromatography, using as eluent DCM/MeOH (from 9:1 to 8:2) to afford the desired product in 3% yield, as a white sticky solid.

R_f: 0.52 (DCM/MeOH 85:15)

^{1}H NMR (600 MHz, C*D*$_3$O*D*) δ (ppm): 7.86 (s, 1H), 7.58 – 7.53 (m, 2H), 7.52 – 7.42 (m, 2H), 6.83 (d, *J* = 2.1 Hz, 2H), 6.80 – 6.76 (m, 2H), 6.46 (t, *J* = 2.1 Hz, 1H), 6.44 (d, *J* = 2.2 Hz, 2H), 6.33 (t, *J* = 2.2 Hz, 1H), 7.12 (d, 2 H, *J* = 2.4 Hz), 6.66 (t, 1 H, *J* = 2.4 Hz), 3.78 (s, 6 H).

^{13}C NMR (75 MHz, C*D*$_3$O*D*) δ (ppm): 169.2, 160.2 (x3C), 159.9 (x2C), 153.2, 152.3, 139.3, 138.4, 135.9, 134.9, 129.6 (x2C), 123.1, 119.7, 117.0, 116.3 (x2C), 113.8, 111.5, 109.1 (x2C), 107.0 (x2C), 106.8, 103.0.

(3-(3,5-dimethoxyphenyl)-2-(4-methoxyphenyl)benzofuran-5-yl)methanol (92)

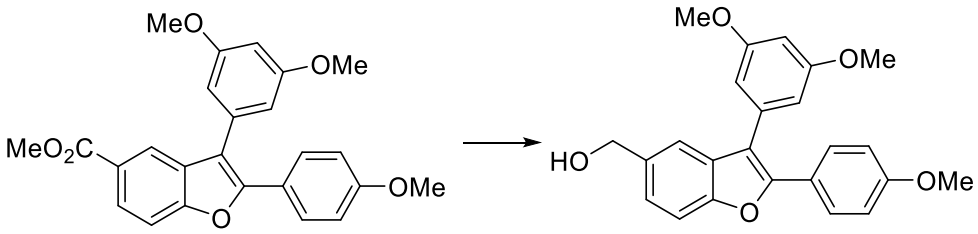

87 **92**

To a solution of compound **87** (220 mg, 0.5257 mmol, 1 eq) in dry THF (5.3 mL) at 0°C, under N_2 atmosphere, $LiAlH_4$ 1M in THF (1.58 mL, 158 mmol, 3 eq) was added dropwise and the yellow solution was stirred for 20 min at 0°C. Then, the reaction mixture was quenched with aq 1M HCl at 0°C and the aqueous layer was extracted with EtOAc three times. The combined organic layers were dried over anhydrous Na_2SO_4, filtered, and evaporated. The crude was purified on silica gel by column chromatography using as eluent CHX/AcOEt 6:4 to afford the product as a yellow foamy solid in quantitative yield. Analytical data were in agreement with data reported in literature (Teng et al. 2020)

R_f: 0.44 (CHX/AcOEt 6:4)

^{1}H NMR (600 MHz, C*D*Cl$_3$) δ (ppm): 7.64 (d, *J* = 8.9 Hz, 2H), 7.51 (d, *J* = 8.3 Hz, 1H), 7.49 (d, *J* = 1.6 Hz, 1H), 7.32 (dd, J_1 = 8.3, J_2 = 1.8 Hz, 1H), 6.87 (d, *J* = 8.9 Hz, 2H), 6.63 (d, *J* = 2.3 Hz, 2H), 6.52 (t, *J* = 2.3 Hz, 1H), 4.75 (s, 2H), 3.82 (s, 3H), 3.78 (s, 6H).

^{13}C NMR (150 MHz, C*D*Cl$_3$) δ (ppm): 161.4 (x2C), 160.0, 153.5, 151.5, 135.9, 135.0, 130.7 (x2C), 128.6, 124.0, 123.2, 118.7, 116.1, 114.1 (x2C), 111.2, 107.9 (x2C), 100.0, 65.9, 55.6 (x3C).

3-(3,5-dimethoxyphenyl)-2-(4-methoxyphenyl)benzofuran-5-carbaldehyde (93)

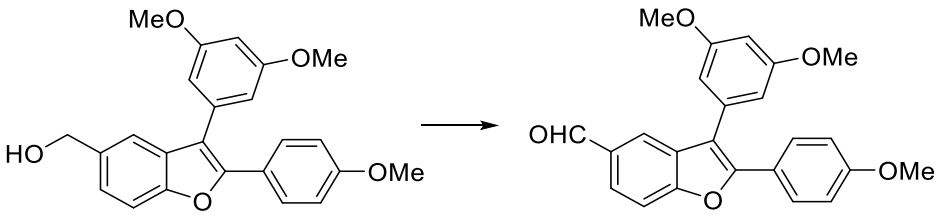

DMP was added to a solution of compound **92** (92 mg, 0.2356 mmol, 1 eq) in dry DCM (1.8 mL), under N_2 atmosphere, at 0°C. After 15 min, the ice-bath was removed and the reaction mixture was stirred at room temperature for 1h. The solvent was removed by rotary evaporation, and the crude was purified on silica gel, using as eluent CHX/AcOEt 8:2 to afford the product as a yellowish oil (92% yield). Analytical were in agreement with data reported in literature (Teng et al. 2020)

R_f: 0.42 (CHX: AcOEt 8:2)

^{1}H NMR (600 MHz, C*D*Cl$_3$) δ (ppm): 10.03 (s, 1H), 8.02 (d, *J* = 1.7 Hz, 1H), 7.87 (dd, J_1 = 8.4, J_2 = 1.7 Hz, 1H), 7.65 (d, *J* = 8.9 Hz, 2H), 7.63 (d, *J* = 8.4 Hz, 1H), 6.88 (d, *J* = 8.9 Hz, 2H), 6.63 (d, *J* = 2.3 Hz, 2H), 6.55 (t, *J* = 2.3 Hz, 1H), 3.83 (s, 3H), 3.80 (s, 6H).

^{13}C NMR (150 MHz, C*D*Cl$_3$) δ (ppm): 191.9, 161.5 (x2C), 160.4, 157.3, 152.7, 134.1, 132.5, 131.3, 128.8 (x2C), 126.0, 123.3, 122.5, 116.3, 114.2 (x2C), 111.8, 107.8 (x2C), 100.2, 55.6 (3xC).

5-(2,2-dibromovinyl)-3-(3,5-dimethoxyphenyl)-2-(4-methoxyphenyl)benzofuran (94)

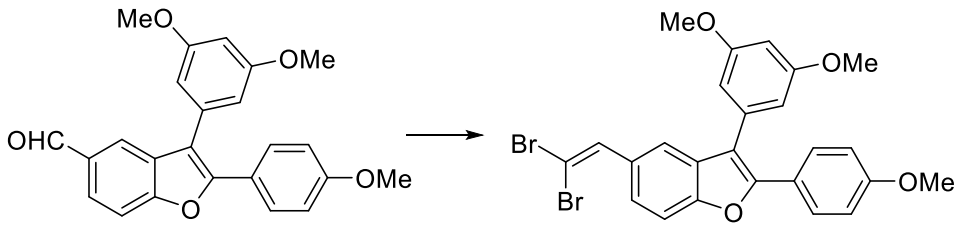

93 **94**

To a solution of CBr_4 (128 mg, 0.386 mmol, 2 eq) in dry DCM (0.7 mL) at 0°C, PPh_3 (203 mg, 0.772 mmol, 4 eq) was added and the orange mixture was stirred for 10 min at 0°C. Then, a solution of compound **93** (75 mg, 0.1931 mmol, 1 eq) in dry DCM (2 mL) was slowly added at 0°C, and the resulting mixture was stirred for 10 min at the same temperature and 10 min at room temperature. The reaction was quenched with water (10 mL) and the aqueous phase was extracted with DCM (3 x 10 mL). The combined organic layers were dried over anhydrous Na_2SO_4, filtered, and evaporated. The crude was purified on silica gel by column chromatography, using as eluent CHX/AcOEt 95:5. The product was obtained as white solid in 83% yield.

M.p.: 161 – 162 °C

R_f: 0.25 CHX/AcOEt 95:5

^{1}H NMR (600 MHz, C*D*Cl$_3$) δ (ppm): 7.61 (d, *J* = 1.5 Hz, 1H), 7.65 – 7.61 (m, 2H), 7.55 (s, 1H), 7.50 (d, *J* = 8.4 Hz, 1H), 7.47 (dd, J_1 = 8.4 Hz, J_2 = 1.5 Hz), 6.90 – 6.85 (m, 2H), 6.63 (d, *J* = 2.2 Hz, 2H), 6.51 (t, *J* = 2.2 Hz, 1H), 3.82 (s, 3H), 3.78 (s, 6H).

3-(3,5-dimethoxyphenyl)-5-ethynyl-2-(4-methoxyphenyl)benzofuran (95)

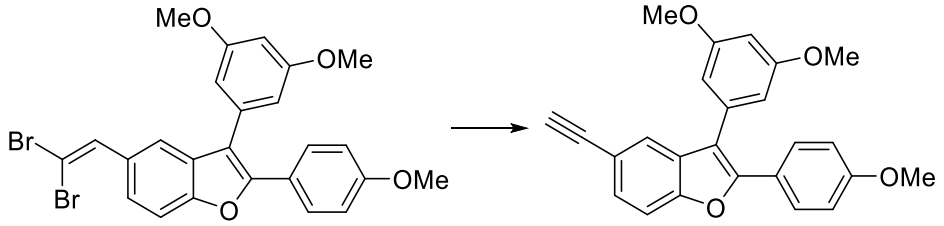

94 **95**

To a solution of compound **94** (80 mg, 0.147 mmol, 1 eq) in dry THF (7.5 mL) at - 78°C, under N_2 atmosphere, LDA 1M in THF (0.44 mL, 0.44 mmol, 3 eq) was added dropwise and the solution was stirred at the same temperature for 1h. The reaction was cautiously quenched with water and the aqueous phase was extracted with EtOAc three times. The combined organic layers were dried over anhydrous Na_2SO_4, filtered, and evaporated. The crude was purified on silica gel by column chromatography, using as eluent CHX/AcOEt (from 95:5 to 9:1). The product was afforded as a white solid in 85% yield.

M.p.: 147 – 148 °C

R_f: 0.24 CHX/AcOEt 95:5

^{1}H NMR (600 MHz, C*D*Cl$_3$) δ (ppm): 7.65 (d, *J* = 1.6 Hz, 1H), 7.64 – 7.61 (m, 2H), 7.45 (d, *J* = 8.5 Hz, 1H), 7.43 (dd, J_1 = 8.5 Hz, J_2 = 1.6 Hz), 6.88 – 6.85 (m, 2H), 6.61 (d, *J* = 2.3 Hz, 2H), 6.51 (t, *J* = 2.3 Hz, 1H), 3.82 (s, 3H), 3.78 (s, 6H), 3.00 (s, 1H).

^{13}C NMR (150 MHz, C*D*Cl$_3$) δ (ppm): 161.3 (x2C), 160.0, 153.6, 151.7, 134.3, 130.5, 128.5 (x2C), 128.4, 124.0, 122.7, 116.6, 115.6, 113.9 (x2C), 111.0, 107.6 (x2C), 100.0, 84.1, 75.7, 55.4 (x2C), 55.3.

1-azido-3,5-dimethoxybenzene (96)

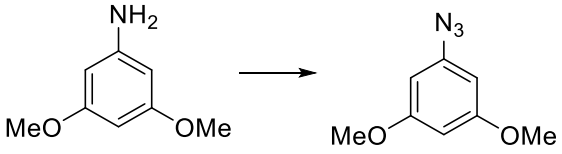

3,5-dimethoxyaniline **96**

To a suspension of 3,5-dimethoxyaniline (200 mg, 1.3056 mmol, 1 eq) in water (3.3 mL) at -5°C, conc HCl was added, followed by the dropwise addition of $NaNO_2$ (108 mg, 1.57 mmol, 1.2 eq) in water (0.5 mL). The red mixture was stirred at - 3°C for 20 min. Then, a solution of NaN_3 (102 mg, 1.57 mmol, 1.2 eq) in water (0.5 mL) was added and the mixture was slowly allowed to warm to room temperature and stirred for 2h. The reaction was diluted with water and extracted with EtOAc (3x15 mL). The combined organic layers were washed with aq 0.1M HCl (30 mL), water (30 mL), brine (30 mL), dried over anhydrous Na_2SO_4, filtered and concentrated. The crude was purified on silica gel using as eluent CHX/AcOEt 95:5 to afford the product as a white solid (30% yield). Analytical data were in agreement with data reported in literature (Yamamoto et al. 2016).

M.p.: 41-42

R_f: 0.49 CHX/AcOEt 95:5

^{1}H NMR (300 MHz, C*D*Cl$_3$) δ (ppm): 6.25 (t, *J* = 2.2 Hz, 1H), 6.19 (d, *J* = 2.2 Hz, 2H), 3.78 (s, 6H).
^{13}C NMR (75 MHz, C*D*Cl$_3$) δ (ppm): 161.8 (x2C), 142.1, 97.6, 97.4, 55.6 (x2C).

1-(3,5-dimethoxyphenyl)-4-(3-(3,5-dimethoxyphenyl)-2-(4-methoxyphenyl)benzofuran-5-yl)-1H-1,2,3-triazole (97)

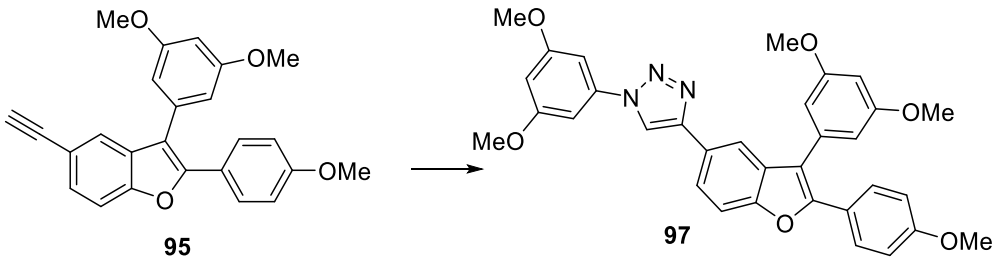

To a suspension of alkyne **95** (40 mg, 0.104 mmol, 1 eq) and compound **96** (19 mg, 0.104 mmol, 1eq) in a mixture of *t*-BuOH (0.5 mL), H_2O (0.5 mL) and THF (0.2 mL), a suspension of $CuSO_4 \cdot H_2O$ (1.3 mg, 0.005 mmol, 0.05 eq) and sodium ascorbate (4 mg, 0.0208 mmol, 0.2 eq) in water (0.2 mL) was added. The mixture was stirred for 3 days at room temperature. The reaction mixture was diluted with water and extracted with EtOAc three times. The combined organic layers were dried over anhydrous Na_2SO_4, filtered, and evaporated. The crude was purified on silica gel using as eluent CHX/AcOEt (from 75:25 to 7:3) to afford the product as a yellowish sticky solid in 21% yield.

R_f: 0.22 CHX/AcOEt 75:25

^{1}H NMR (600 MHz, C*D*Cl$_3$) δ (ppm): 8.14 (s, 1H), 7.94 (d, *J* = 1.3 Hz, 1H), 7.90 (dd, J_1 = 8.5 Hz, J_2 = 1.3 Hz, 1H), 7.69 – 7.63 (m, 2H), 7.60 (d, *J* = 8.5 Hz, 1H), 6.96 (d, *J* = 2.2 Hz, 2H), 6.90 – 6.86 (m, 2H), 6.67 (d, *J* = 2.3 Hz, 2H), 6.54 (t, *J* =. 2.3 Hz, 1H), 6.52 (t, *J* = 2.2 Hz, 1H), 3.87 (s, 6H), 3.83 (s, 3H), 3.80 (s, 6H).

^{13}C NMR (150 MHz, C*D*Cl$_3$) δ (ppm): 162.9 (x2C), 162.7 (x2C), 161.3, 155.2. 152.9, 150.0, 140.0, 136.1, 132.4, 129.9 (x2C), 126.8, 124.3, 124.0, 118.8, 118.5, 117.4, 115.3 (x2C), 112.8, 109.2 (x2C), 102.0, 101.4, 100.3 (x2C), 57.1 (x2C), 56.9 (x2C), 56.7.

5-(5-(1-(3,5-dihydroxyphenyl)-1H-1,2,3-triazol-4-yl)-2-(4-hydroxyphenyl)benzofuran-3-yl)benzene-1,3-diol (74)

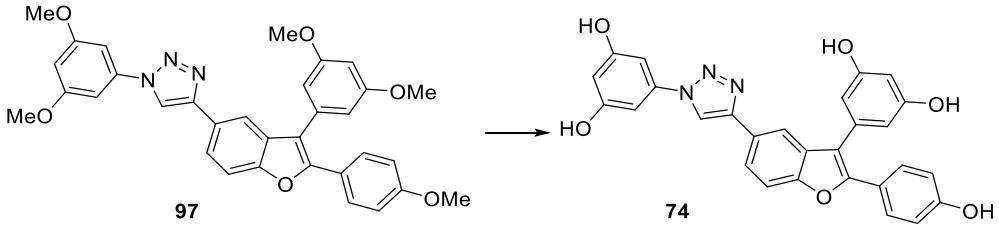

To a solution of compound **97** (12 mg, 0.0213 mmol, 1 eq) in dry DCM (1 mL) at – 78°C, under nitrogen atmosphere, BBr_3 1M in DCM (0.140 ml, 0.140 mmol, 6.6 eq) was added dropwise and the resulting mixture was slowly allowed to warm to room temperature and stirred overnight. The reaction mixture was quenched with aq 5% $NaHCO_3$ at 0°C (pH 7). The aqueous layer was extracted with EtOAc three times. The combined organic layers were dried over anhydrous Na_2SO_4, filtered, and evaporated. The crude was purified on silica gel by column chromatography using as eluent DCM/MeOH 9:1, followed by a second column chromatography using as eluent CHX/Acetone 1:1 to afford the product as an amorphous white solid in 24% yield.

R_f: 0.36 (DCM/MeOH 9:1)

^{1}H NMR (600 MHz, CD_3OD) δ (ppm): 8.73 (s, 1H), 8.00 (d, *J* = 1.4 Hz, 1H), 7.86 (dd, J_1 = 8.5 Hz, J_2 = 1.4 Hz, 1H), 7.61 (d, *J* = 8.5 Hz, 1H), 7.58 – 7.54 (m, 2H), 6.81 (d, *J* = 2.0 Hz, 2H), 6.79 – 6.76 (m, 2H), 6.45 (d, *J* = 2.0 Hz, 2H), 6.36 (t, *J* = 2.0 Hz, 1H), 6.35 (t, *J* = 2.0 Hz, 1H).

5-(Bromomethyl)-3-(3,5-dimethoxyphenyl)-2-(4-methoxyphenyl)benzofuran (98)

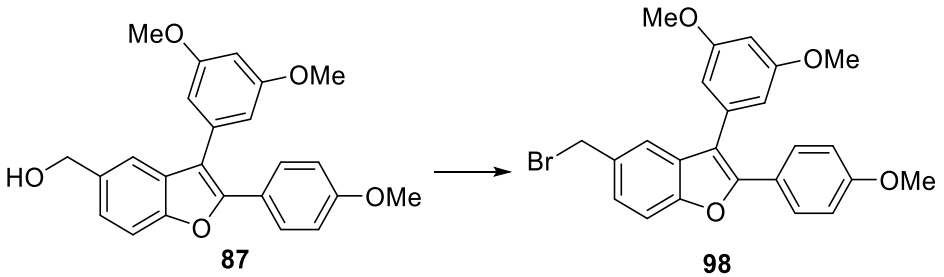

To a suspension of compound **92** (200 mg, 0.5122 mmol, 1 eq) in dry Et_2O (2.6 mL) at room temperature, under N_2 atmosphere, catalytic pyridine (2 µL, 0.026 mmol, 0.05 eq) was added, followed by the dropwise addition of PBr_3 (40 µL, 0.5122 mmol, 1 eq), and the mixture was stirred at reflux (40°C) for 90 min. The reaction was cooled to room temperature and quenched with ice and water. The aqueous phase was extracted with EtOAc three times. The combined organic layers were washed with brine twice, dried over anhydrous Na_2SO_4, filtered and evaporated, to afford the product as yellow oil. The product was used immediately for the next step without any further purification.

R_f: 0.41 CHX: AcOEt 9:1

Diethyl ((3-(3,5-dimethoxyphenyl)-2-(4-methoxyphenyl)benzofuran-5-yl)methyl)phosphonate (99)

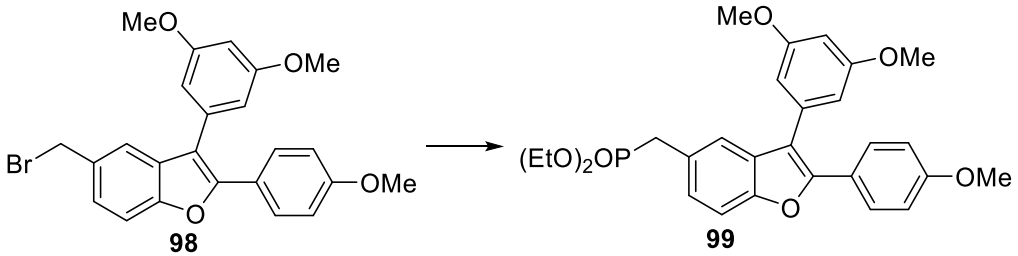

Compound **98** (182 mg, 0.4015 mmol, 1 eq) was dissolved with triethylphosphite (200 µL, 1.166 mmol, 2.9 eq) and heated at 130°C overnight. Triethylphosphite in excess was evaporated and the crude was purified on silica gel by flash column chromatography, using as eluent CHX/AcOEt 3:7. The product was obtained as a yellow oil in 80% yield over two steps.

R_f: 0.19 CHX/AcOEt 3: 7

^{1}H NMR (300 MHz, C*D*Cl$_3$) δ (ppm): 7.65 – 7.60 (m, 2H), 7.56 (s, 1H), 7.45 (d, *J* = 8.3 Hz, 1H), 7.38 (d, *J* = 2.1 Hz, 1H), 7.25 (dd, J_1 = 8.3 Hz, J_2 = 2.1 Hz), 6.88 – 6.83 (m, 2H), 6.61 (d, *J* = 2.2 Hz, 2H), 6.50 (t, *J* = 2.2 Hz, 1H), 4.05 – 3.95 (m, 4H), 3.82 (s, 3H), 3.78 (s, 6H), 3.21 (d, *J* = 21.0 Hz, 2H), 1.25 – 1.20 (m, 6H).

(E)-3-(3,5-dimethoxyphenyl)-2-(4-methoxyphenyl)-5-(4-methoxystyryl)benzofuran (100)

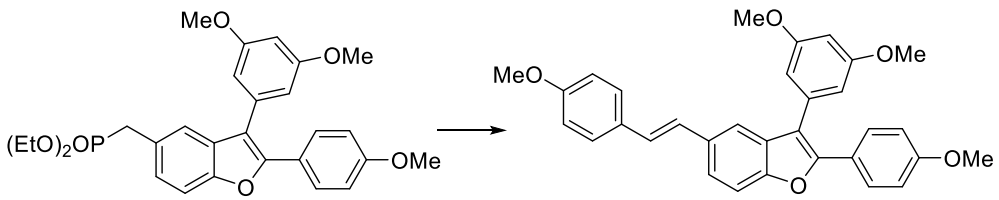

99 **100**

In a MW vial, a suspension of compound **99** (70 mg, 0.135 mmol, 1.5 eq) with *p*-anisaldehyde (11 µL, 0.0914 mmol, 1 eq) and 60% NaH (11 mg, 0.274 mmol, 3 eq) in dry THF (1.6 mL) was stirred at 120°C for 30 min under microwave irradiation. The reaction mixture was cooled to room temperature, and quenched with aq saturated NH_4Cl. The aqueous phase was extracted with EtOAc three times. The combined organic layers were washed with water, brine, dried over anhydrous Na_2SO_4, filtered, and evaporated. The crude was purified on silica gel by column chromatography, using as eluent

CHX/AcOEt (from 9:1 to 85:15) to yield the product as a golden foamy solid (86%).

R_f: 0.32 (CHX/AcOEt 85:15)

^{1}H NMR (600 MHz, C*D*Cl$_3$) δ (ppm): 7.65 – 7.61 (m, 2H), 7.56 (s, 1H), 7.51 – 7.46 (m, 2H), 7.45 – 7.42 (m, 2H), 7.06 (d, *J* = 16.1 Hz, 1H), 7.01 (d, *J* = 16.1 Hz, 1H), 6.91 – 6.88 (m, 2H), 6.88 – 6.84 (m, 2H), 6.66 (d, *J* = 1.6 Hz, 2H), 6.54 (t, *J* = 1.6 Hz, 1H), 3.83 (s, 6H), 3.80 (s, 6H).
^{13}C NMR (150 MHz, C*D*Cl$_3$) δ (ppm): 161.2 (x2C), 159.7, 159.1, 153.3, 151.3, 134.9, 132.9, 130.8, 130.4, 128.4 (x2C), 127.5 (x2C), 127.1, 126.9, 123.1, 122.9, 117.3, 116.0, 114.1 (x2C), 113.9 (x2C), 111.0, 107.7 (x2C), 99.9, 55.4 (x2C), 55.3 (x2C).

2-iodo-4-methylphenol (103)

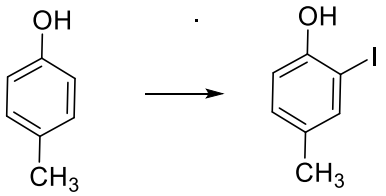

102 **103**

To a solution of *para*-cresol **102** (500 mg, 4.6236 mmol, 1 eq) in dry ACN (4.62 mL) at room temperature, under N_2 atmosphere, *para*-toluensulfonic acid monohydrate (880 mg, 4.6236 mmol, 1 eq) was added and the suspension was stirred for 10 min to give a clear solution. Then, *N*-iodosuccinimide (1.037 g, 4.6236 mmol, 1 eq) was added and the reaction mixture was stirred overnight at room temperature. The reaction was quenched with aq 20% $Na_2S_2O_5$ (100 mL) and extracted with EtOAc (3 x 70 mL). The combined organic layers were washed with brine, dried over anhydrous Na_2SO_4, filtered and evaporated. The crude was purified on silica gel using as eluent CHX/DCM (from 1:1 to 4:6) to afford the desired product as transparent oil in

97% yield. Analytical data were in agreement with data reported in literature (Schmidt et al. 2013).

R_f: 0.35 (CHX/DCM 1:1)

^{1}H NMR (600 MHz, C*D*Cl$_3$) δ (ppm): 7.48 (d, *J* = 1.3 Hz, 1H), 7.04 (dd, J_1 = 8.2 Hz, J_2 = 1.5 Hz, 1H), 6.88 (d, *J* = 8.2 Hz, 1H), 5.21 (s, 1H), 2.25 (s, 3H).
^{13}C NMR (150 MHz, C*D*Cl$_3$) δ (ppm): 152.6, 138.4, 132.1, 131.0, 114.8, 85.5, 20.1.

3-(3,5-dimethoxyphenyl)-2-(4-methoxyphenyl)-5-methylbenzofuran (104)

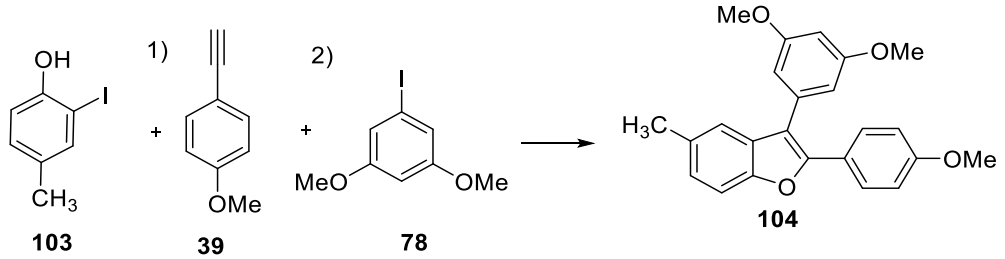

103 **39** **78** **104**

Compound **103** (100 mg, 0.4273 mmol, 1 eq) and $PdCl_2(PPh_3)_2$ (9 mg, 0.0128 mmol, 0.03 eq) were dissolved in dry THF (0.43 mL) in a microwave vial, under N_2 atmosphere. Dry TEA (1.2 mL) and CuI (1.6 mg, 0.0085 mmol, 0.02 eq) were added and the reaction mixture was stirred for 10 min. Then, 4-ethynilanisole **39** (67 µL, 0.513 mmol, 1.2 eq) was added and the mixture was stirred in a microwave reactor for 30 min at room temperature. After that, 1-iodo-3,5-dimethoxybenzene **78** (95 mg, 0.35965, 1 eq) and dry acetonitrile (1.43 mL) were added and the mixture was stirred at 100°C for 25 min, under microwave irradiation. The reaction mixture was allowed to cool to room temperature and the solvent was evaporated. The crude was purified on silica gel using as eluent CHX/DCM (from 1:1 to 4:6) to give the desired compound as a sticky yellow solid (48% yield).

R_f: 0.29 (CHX: DCM 6:4)

^{1}H NMR (300 MHz, C*D*Cl$_3$) δ (ppm): 7.65 – 7.61 (m, 2H), 7.40 (d, *J* = 8.2 Hz, 1H), 7.28 (d, *J* = 1.5 Hz, 1H), 7.11 (dd, J_1 = 8.2 Hz, J_2 = 1.5 Hz, 1H), 6.88 – 6.84 (m, 2H), 6.64 (d, *J* = 2.2 Hz, 2H), 6.51 (t, *J* = 2.2 Hz, 1H), 3.82 (s, 3H), 3.79 (s, 6H), 2.42 (s, 3H).

^{13}C NMR (150 MHz, C*D*Cl$_3$) δ (ppm): 161.2 (x2C), 160.5, 152.1, 150.8, 135.2, 132.3, 130.4, 128.4 (x2C), 125.5, 123.3, 119.6, 115.7, 113.8 (x2C), 110.4, 107.7, 99.8, 55.4 (x2C), 55.3 (x2C), 21.4.

5-(2-(4-hydroxyphenyl)-5-methylbenzofuran-3-yl)benzene-1,3-diol (105)

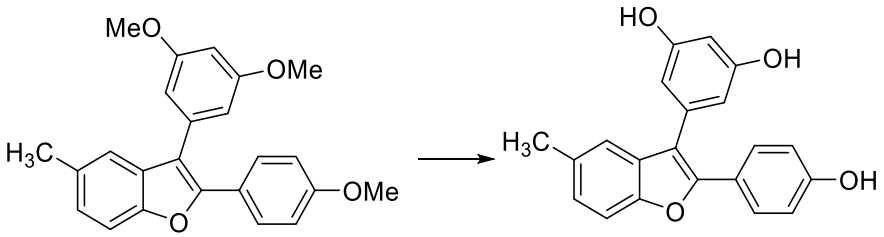

104 **105**

To the solution of compound **104** (75 mg, 0.2 mmol, 1 eq) in dry DCM (2 mL) at - 78°C, 1M BBr_3 in DCM (0.66 mL, 0.66 mmol, 3.3 eq) was added dropwise and the resulting mixture was allowed to warm to room temperature and stirred overnight. The mixture was quenched with aq 5% $NaHCO_3$ at 0°C (pH 7). The aqueous layer was extracted with EtOAc (3 x 10 mL). The combined organic layers were dried over anhydrous Na_2SO_4, filtered, and evaporated. The crude was purified on silica gel by column chromatography using as eluent DCM/ MeOH 95:5. The product was obtained as yellow solid in 90% yield.

M.p.: 58 – 60°C

R_f: 0.34 DCM/MeOH 95:5

^{1}H NMR (600 MHz, C*D*$_3$O*D*) δ (ppm): 7.54 – 7.51 (m, 2H), 7.37 (d, *J* = 8.4 Hz, 1H), 7.26 (d, *J* = 1.5 Hz, 1H), 7.11 (dd, J_1 = 8.4 Hz, J_2 = 1.5 Hz, 1H), 6.79 – 6.75 (m, 2H), 6.41 (d, *J* = 2.2 Hz, 2H), 6.33 (t, *J* = 2.2 Hz, 1H), 2.42 (s, 3H).
^{13}C NMR (150 MHz, C*D*$_3$O*D*) δ (ppm): 160.1 (x2C), 159.0, 153.5, 152.2, 136.3, 133.4, 131.6, 129.6 (x2C), 126.3, 123.5, 120.4, 116.6, 116.2 (x2C), 111.1, 109.1 (x2C), 102.8, 21.4.

((5-(2-(4-((*tert*-butyldimethylsilyl)oxy)phenyl)-5-methylbenzofuran-3-yl)-1,3-phenylene)bis(oxy))bis(*tert*-butyldimethylsilane) (106)

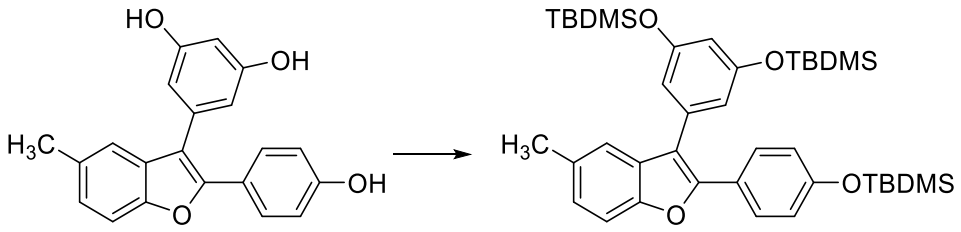

105 **106**

Imidazole (277 mg, 4.062 mmol, 4.5 eq) and TBDMSCl (531 mg, 3.52 mmol, 3.9 eq) were added to a suspension of compound **105** (300 mg, 0.9026 mmol, 1 eq) in 1,2-dichloroethane (9 mL), and the resulting mixture was stirred at 60°C overnight, under N_2 atmosphere. The mixture was allowed to cool to room temperature and quenched with brine. The aqueous phase was extracted with EtOAc three times. The combined organic layers were dried over anhydrous Na_2SO_4, filtered, and evaporated. The crude was purified on silica gel by column chromatography, using as eluent CHX/DCM (from 100% to 95%), to afford the desired product as foamy white solid in 86% yield.

R_f: 0.51 CHX: DCM 95:5

^{1}H NMR (600 MHz, C*D*Cl$_3$) δ (ppm): 7.57 – 7.53 (m, 2H), 7.39 (d, *J* = 8.2 Hz, 1H), 7.23 (d, *J* = 1.3 Hz, 1H), 7.10 (dd, J_1 = 8.2 Hz, J_2 = 1.3 Hz), 6.79 – 6.75

(m, 2H), 6.58 (d, *J* = 2.3 Hz, 2H), 6.40 (t, *J* = 2.3 Hz, 1H), 2.42 (s, 3H), 0.98 (s, 27H), 0.20 (s, 6H), 0.18 (s, 12H).

((5-(5-(bromomethyl)-2-(4-((*tert*-butyldimethylsilyl)oxy)phenyl)benzofuran-3-yl)-1,3-phenylene)bis(oxy))bis(*tert*-butyldimethylsilane) (107)

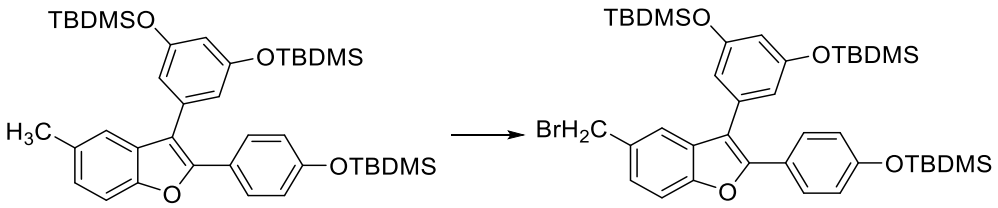

106 **107**

To a solution of compound **106** (500 mg, 0.74 mmol, 1 eq) in CCl_4 (7.4 mL), *N*-bromosuccinimide (145 mg, 0.8146 mmol, 1.1 eq) and AIBN (12 mg, 0.074 mmol, 0.1 eq) were added and the mixture was refluxed for 8h, under N_2 atmosphere. The reaction mixture was cooled to room temperature, filtered and the filtrate was evaporated. The crude was purified on silica gel using as eluent CHX/DCM (from 95% to 90%). The product was obtained as a transparent oil.

R_f: 0.2 CHX/DCM 98:2

^{1}H NMR (600 MHz, C*D*Cl$_3$) δ (ppm): 7.58 – 7.52 (m, 2H), 7.48 – 7.44 (m, 2H), 7.33 (dd, J_1 = 8.4 Hz, J_2 = 1.3 Hz), 6.79 – 6.75 (m, 2H), 6.57 (d, *J* = 1.9 Hz, 2H), 6.42 (t, *J* = 1.9 Hz, 1H), 4.60 (s, 2H), 0.98 (s, 27H), 0.20 (s, 6H), 0.19 (s, 12H).

((3-(3,5-bis((*tert*-butyldimethylsilyl)oxy)phenyl)-2-(4-((*tert*-butyldimethylsilyl)oxy)phenyl)benzofuran-5-yl)methyl)triphenylphosphonium bromide (108)

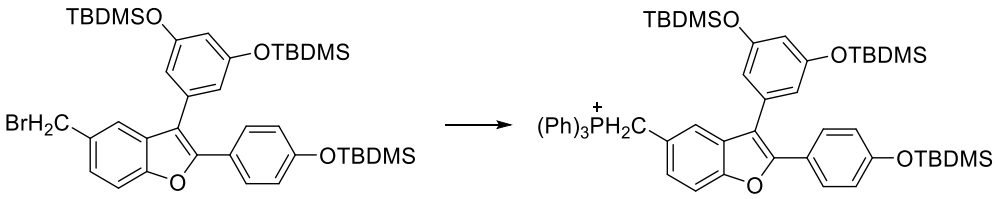

107 **108**

To a solution of compound **107** (200 mg, 0.265 mmol, 1 eq) in dry toluene (2.7 mL) at room temperature, under N_2 atmosphere, triphenylphosphine (104 mg, 0.3975 mmol, 1.5 eq) was added and the mixture was refluxed overnight. The mixture was cooled to room temperature, and toluene was evaporated. The residue was triturated with hexane, filtered and washed with other hexane. A white solid was obtained in 77% yield.

R_f: 0.56 DCM/MeOH 9:1

^{1}H-NMR (600 MHz, C*D*Cl$_3$) δ (ppm): 7.54 (d, *J* = 8.5 Hz, 1H), 7.51 – 7.45 (m, 2H), 7.35 (d, *J* = 8.5 Hz, 1H), 6.43 (s, 1H), 6.38 (t, *J* = 1.8 Hz, 1H), 6.28 (d, *J* = 1.8 Hz, 2H), 5.42 (d, *J* = 13.8 Hz, 2H), 0.96 (s, 27 H), 0.19 (s, 6H), 0.16 (s, 12H).

3,4-bis((tert-butyldimethylsilyl)oxy)benzaldehyde (109)

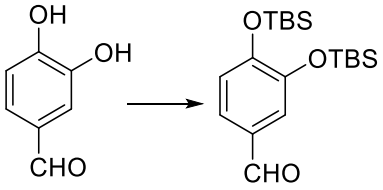

To a solution of 3,4-dihydroxybenzaldehyde (200 mg, 1.448 mmol, 1 eq) in 1,2-dichloroethane (14.5 mL), imidazole (296 mg, 4.344 mmol, 3 eq) and

TBDMSCl (567.5 mg, 3.765 mmol, 2.6 eq) were added and the resulting suspension was heated at 60°C for 6h. The reaction mixture was allowed to warm to room temperature and then quenched with brine. The aqueous layer was extracted with DCM three times. The combined organic layers were dried over anhydrous Na_2SO_4, filtered, and evaporated. The crude was purified on silica gel by column chromatography using as eluente CHX/AcOEt (95:5) to afford the product as a brown oil. Analytical data were in agreement with those reported in literature (Li et al. 2014).

R_f: 0.55 CHX/AcOEt 95:5

^{1}H NMR (600 MHz, C*D*Cl$_3$) δ (ppm): 9.80 (s, 1H), 7.35 (m, 2H), 6.91 (m, 1H), 0.97 (m, 18H), 0.21 (m, 12 H).

^{13}C NMR (150 MHz, C*D*Cl$_3$) δ (ppm): 190.8, 153.3, 135.5, 129.3, 125.2, 120.7, 120.5, 25.8 (x6C), 128.4 (x2C), -4.1 (x4C).

Diethyl ((3-(3,5-bis((tert-butyldimethylsilyl)oxy)phenyl)-2-(4-((tert-butyldimethylsilyl)oxy)phenyl)benzofuran-5-yl)methyl)phosphonate) (111)

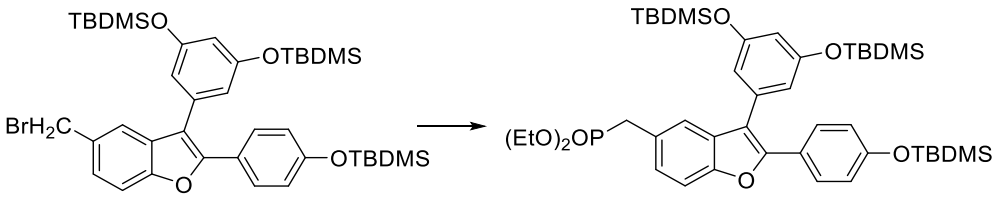

107 **111**

Compound **107** (150 mg, 0.199 mmol, 1 eq) in triethylphosphite (0.2 mL, 1.167 mmol, 5.9 eq) was heated at 130°C overnight in a sealed vial. Triethylphosphite was evaporated and the crude was purified on silica gel by

column chromatography using as eluent CHX/AcOEt (6:4) to afford the product as a transparent oil in 84% yield.

R_f: 0.33 CHX/AcOEt 6:4

^{1}H NMR (600 MHz, C*D*Cl$_3$) δ (ppm): 7.56 – 7.52 (m, 2H), 7.44 (d, *J* = 8.5 Hz, 1H), 7.30 – 7.26 (m, 2H), 6.80 – 6.75 (m, 2H), 6.56 (d, *J* = 2.2 Hz, 2H), 6.40 (t, *J* = 2.2 Hz, 1H), 4.04 – 3.94 (m, 4H), 3.21 (d, *J* = 21.0 Hz, 2H), 1.22 (t, *J* = 7.0 Hz, 6H), 1.00 – 0.95 (m, 27H), 0.20 (s, 6H), 0.17 (s, 12H).

(E)-((4-(2-(3-(3,5-bis((tert-butyldimethylsilyl)oxy)phenyl)-2-(4-((tert-butyldimethylsilyl)oxy)phenyl)benzofuran-5-yl)vinyl)-1,2-phenylene)bis(oxy))bis(tert-butyldimethylsilane) (112)

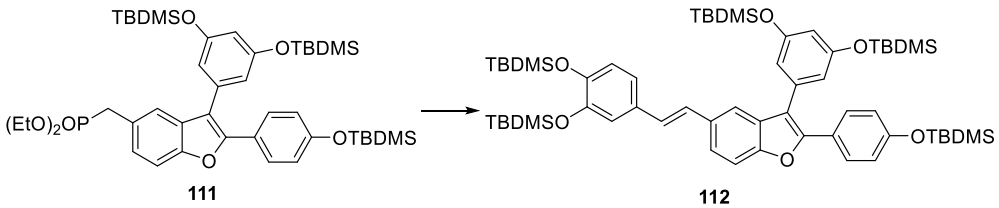

111 112

To a solution of compound **111** (80 mg, 0.099 mmol, 1 eq) in dry THF (0.86 mL) at 0°C, under nitrogen atmosphere, 60% NaH (8 eq, 0.8 mmol, 32 mg) was added and the mixture was stirred at 0°C for 45 min. Then, a solution of the aldehyde **109** (188 mg, 0.514 mmol, 5.2 eq) was added dropwise and the solution was allowed to warm to room temperature and stirred overnight. The reaction mixture was quenched with aq 5% $NaHCO_3$. The aqueous layer was extracted with EtOAc five times. The combined organic layers were dried over anhydrous Na_2SO_4, filtered, and evaporated. The crude was purified on silica gel using as eluent CHX/DCM 95:5 to afford the product as transparent sticky solid in 52% yield.

R_f: 0.65 CHX/DCM 95:5

^{1}H NMR (600 MHz, C*D*Cl$_3$) δ (ppm): 7.59 – 7.55 (m, 2H), 7.54 (s, 1H), 7.46 (d, *J* = 8.5 Hz, 1H), 7.44 (d, *J* = 8.5 Hz, 1H), 7.00 – 6.94 (m, 4H), 6.93 (d, *J* = 16.5 Hz, 1H), 6.81 (d, *J* = 7.9 Hz, 1H), 6.79 – 6.76 (m, 2H), 6.61 (d, *J* = 1.8 Hz, 2H), 6.43 (t, *J* = 1.8 Hz, 2H), 1.05 – 0.95 (m, 45H), 0.23 (s, 6H), 0.21 (s, 6H), 0.20 (s, 18H).

(*E*)-4-(2-(3-(3,5-dihydroxyphenyl)-2-(4-hydroxyphenyl)benzofuran-5-yl)vinyl)benzene-1,2-diol (110)

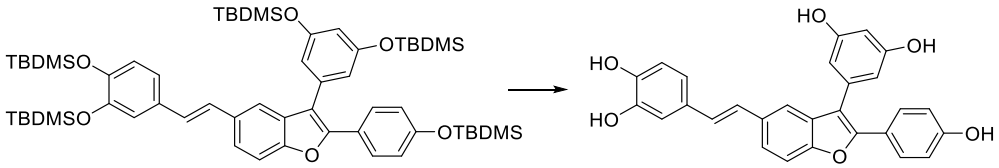

112 **110**

To the solution of compound **112** (26 mg, 0.026 mmol, 1 eq) in dry THF (0.5 mL) TBAF 1M in THF (0.169 mL, 0.169 mmol, 6.5 eq) was added at 0°C and the reaction mixture was stirred at room temperature for 90 min. The mixture was quenched with water and the aqueous layer was extracted with EtOAc three times. The combined organic layers were washed with aq 0.1 M HCl three times, dried over anhydrous Na_2SO_4, filtered, and evaporated. The crude was purified on silica gel by column chromatography to afford the desired product in 60 %yiels, as a transparent sticky solid.

R_f: 0.43 DCM/MeOH 9:1

^{1}H NMR (600 MHz, CD_3O*D*) δ (ppm): 7.56 – 7.51 (m, 3H), 7.48 (dd, J_1 = 8.6 Hz, J_2 = 1.5 Hz, 1H), 7.45 (d, *J* = 8.6 Hz, 1H), 7.01 (d, *J* = 16.1 Hz, 1H), 7.00 (d, *J* = 1.5 Hz, 1H), 6.95 (d, *J* = 16.1 Hz, 1H), 6.86 (dd, J_1 = 8.0 Hz, J_2 = 1.5 Hz), 6.79 – 6.75 (m, 2H), 6.73 (d, *J* = 8.0 Hz, 1H), 6.43 (d, *J* = 2.1 Hz, 1H), 6.34 (t, *J* = 2.1 Hz, 1H).

^{13}C NMR (150 MHz, C*D$_3$OD*) δ (ppm): 160.2 (x2C), 159.2, 154.6, 152.7, 146.5, 146.3, 136.1, 134.6, 132.0, 131.4, 129.6 (x2C), 128.8, 127.1, 123.7, 123.3, 120.1, 118.1, 116.9, 116.4, 116.3 (x2C), 113.7, 111.8, 109.2 (x2C), 103.0.

E)-4-(3,5-dimethoxystyryl)aniline (113)

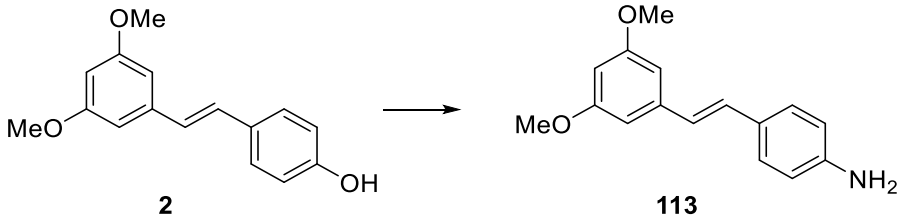

2 **113**

A mixture of pterostilbene (**2**) (3.90 mmol, 1 eq), 2-bromopropionamide (4.29 mmol, 1.1 eq) and KOH 85% (3.90 mmol, 1 eq) in DMSO (11.5 mL) was heated at 60 °C for 3h, under microwave irradiation. Then KOH 85% (4.29 mmol, 1.1 eq) was added to the solution and the mixture was heated under microwave irradiation at 140 °C for 3h. After cooling, the mixture was quenched with brine solution. The aqueous phase was extracted with DCM three times. The combined organic phases were washed again with brine twice, dried over anhydrous Na_2SO_4, filtered and concentrated under reduced pressure. The crude was purified by FC with CHX/EtOAc (from 8:2 to 7:3) as eluent. Yield: 40%, light brown solid.

M.p.: 87 – 89°C

R_f: 0.51 (CHX/AcOEt 6:4)

^{1}H NMR (300 MHz, C*D*Cl$_3$) δ (ppm): 7.33 (d, *J* = 8.5 Hz, 2H), 7.00 (d, *J* = 16.2 Hz, 1H), 6.85 (d, *J* = 16.2 Hz, 1H), 6.68 – 6.63 (m, 4H), 6.36 (t, *J* = 2.3 Hz, 1H), 3.83 (s, 6H).

^{13}C NMR (75 MHz, C*D*Cl$_3$) δ (ppm): 160.9 (×2C), 146.3, 140.0, 129.2, 127.8 (×3C), 125.1, 115.2 (×2C), 104.2 (×2C), 99.4, 55.3 (×2C).

(*E*)-*N*-(4-(3,5-dimethoxystyryl)phenyl)acetamide (114)

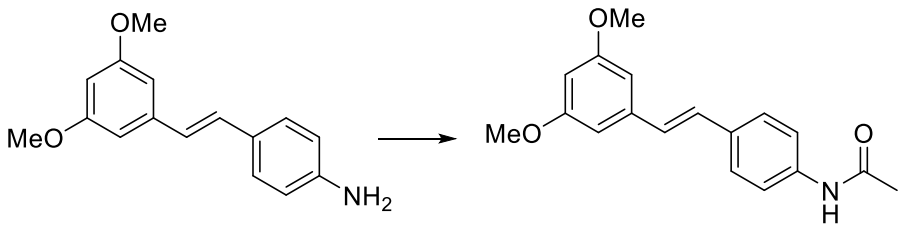

To a solution of compound **113** (0.078 mmol, 1 eq) in DCM (200 μL) was added TEA (0.156 mmol, 2 eq) and the mixture was stirred at 0 °C for 10 min. Then, acetyl chloride (0.086 mmol, 1.1 eq) was added and the reaction mixture was stirred at room temperature for 2h. The reaction was quenched with water and the solution was diluted with DCM. The organic phase was washed with aq 0.5 M HCl three times, dried over anhydrous Na_2SO_4, filtered, and evaporated. The crude was purified by FC with CHX/EtOAc as eluent (from 7:3 to 3:7) to afford the product as a white solid. Yield: 86%.

M.p.: 139 – 141°C

R_f: 0.25 (CHX/AcOEt 1:1)

^{1}H NMR (300 MHz, C*D*Cl$_3$) δ (ppm): 7.52 – 7.43 (m, 4H), 7.33 (bs, 1H (NH)), 7.03 (d, *J* = 16.3 Hz, 1H), 6.95 (d, *J* = 16.3 Hz, 1H), 6.65 (d, *J* = 2.3 Hz, 2H), 6.38 (t, *J* = 2.3 Hz, 1H), 3.82 (s, 6H), 2.18 (s, 3H).

^{13}C NMR (75 MHz, C*D*Cl$_3$) δ (ppm): 168.2, 160.9 (×2C), 139.4, 137.4, 133.3, 128.4, 127.9, 127.2 (×2C), 119.9 (×2C), 104.5 (×2C), 99.4, 55.3 (×2C), 24.6.

(*E*)-5-(4-aminostyryl)benzene-1,3-diol (115)

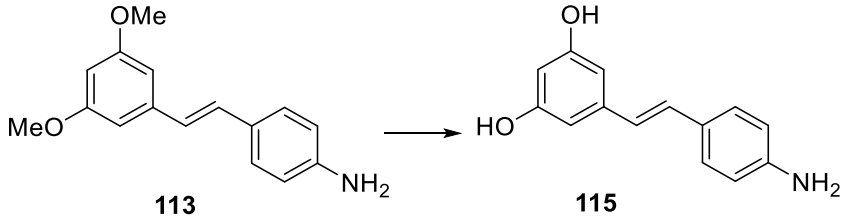

113 **115**

To a solution of **113** (200 mg, 0.783, 1 eq) in dry DCM (11.6 mL), under N_2 at 0 °C, BBr_3 1M DCM solution (3.92 mL, 3.92 mmol, 5 eq) was added dropwise. Then mixture was allowed to warm to room temperature, and stirred overnight. The reaction solution was quenched with an aqueous solution 5% $NaHCO_3$ at 0 °C (pH 8-9). The aqueous phase was extracted with EtOAc four times. The combined organic layers were dried over anhydrous Na_2SO_4, filtered, and concentrated under reduced pressure. The residue was purified by FC with CHX/EtOAc (from 1:1 to 4:6) as eluent to give the desired product as a brownish solid. Yield: 45%.

M.p.: 194 – 196 °C

R_f: 0.20 (CHX : AcOEt 6:4)

^{1}H NMR (300 MHz, CD_3OD) δ (ppm): 7.26 (d, *J* = 8.3 Hz, 2H), 6.91 (d, *J* = 16.3 Hz, 1H), 6.73 (d, *J* = 16.3 Hz, 1H), 6.68 (d, *J* = 8.5 Hz, 2H), 6.42 (d, *J* = 2.2 Hz, 2H), 6.14 (t, *J* = 2.2 Hz, 1H).
^{13}C NMR (75 MHz, CD_3OD) δ (ppm): 158.2 (×2C), 147.3, 140.2, 128.4, 127.3, 127.1 (×2C), 124.3, 115.0 (×2C), 104.2 (×2C), 101.0.

(*E*)-*N*-(4-(3,5-dihydroxystyryl)phenyl)acetamide (114)

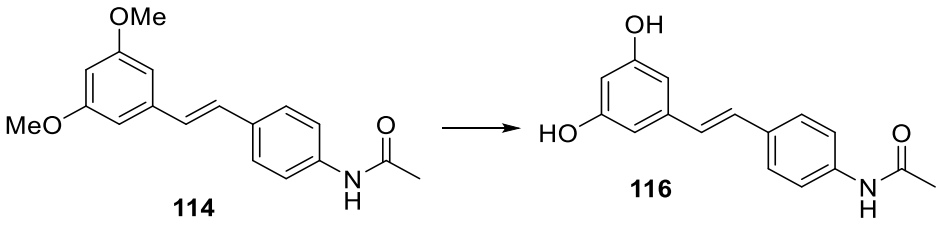

To a solution of compound **114** (0.134 mmol, 1 eq) in dry DCM (2.6 mL), BBr_3 1M DCM solution (0.807 mmol, 6 eq) was added dropwise at 0 °C. The mixture was stirred at room temerature for 9 hours. The reaction was quenched with H_2O at 0 °C. The aqueous phase was extracted with EtOAc three times. The combined organic phases were dried over anhydrous Na_2SO_4, filtered, and

concentrated under reduced pressure. The residue was purified by FC with CHX/EtOAc (from 4:6 to 2:8) as eluent to give the desired product as a pale yellow solid. Yield: 54%.

M.p.: 210°C (dec)

R_f: 0.1 (CHX/AcOEt 1:1)

^{1}H NMR (300 MHz, C*D*$_3$O*D*) δ (ppm): 7.53 (d, *J* = 8.8 Hz, 2H), 7.45 (d, *J* = 8.8 Hz, 2H), 6.99 (d, *J* = 16.3 Hz, 1H), 6.91 (d, *J* = 16.3 Hz, 1H), 6.47 (d, *J* = 2.3 Hz, 2H), 6.18 (t, *J*= 2.3 Hz, 1H), 2.12 (s, 3H).
^{13}C NMR (75 MHz, CD$_3$OD) δ (ppm): 170.1, 158.3 (×2C), 139.5, 137.8, 133.3, 127.7, 127.5, 126.5 (×2C), 119.8 (×2C), 104.6 (×2C), 101.7, 22.4.

(*E*)-1-(4-(3,5-dimethoxystyryl)phenyl) (*N*,*N*-di-*tert*-butoxycarbonyl)guanidine (119)

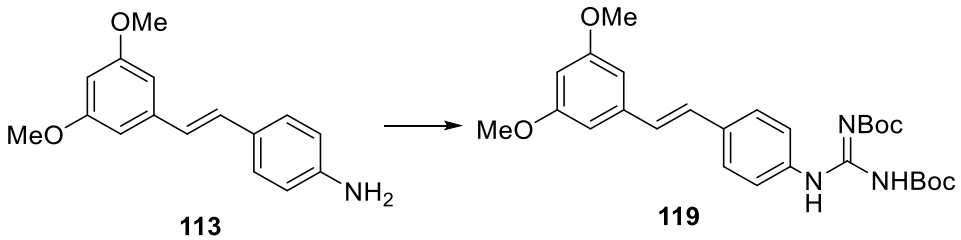

A solution of compound **113** (60 mg, 0.2349 mmol, 1 eq) and *N*,*N*'-Di-*Boc*-1H-pyrazole-1-carboxamidine (0.2525 mmol, 1.5 eq) in dry $CHCl_3$ (7 mL) was stirred at room temperature overnight. The solvent was evaporated under reduced pressure and the crude was purified by FC with eluent CHX/EtOAc (from 100% to 9:1). Yield: 93%, white solid.

M.p.: 133-135°C

R_f: 0.78 (CHX/AcOEt 7.3)

^{1}H NMR (300 MHz, C*D*Cl$_3$) δ (ppm): 11.6 (bs, 1H (NH)), 10.4 (bs, 1H (NH), 7.62 (d, *J* = 8.6 Hz, 2H), 7.46 (d, *J* = 8.6 Hz, 2H), 7.04 (d, *J* = 16.3 Hz, 1H),

6.96 (d, *J* = 16.3 Hz, 1H), 6.66 (d, *J* = 2.3 Hz, 2H), 6.39 (t, *J* = 2.3 Hz, 1H), 3.83 (s, 6H), 1.54 (s, 18H).

^{13}C NMR (75 MHz, C*D*Cl$_3$) δ (ppm): 163.5, 161.0 (×2C), 153.3 (×2C), 139.4, 136.4, 133.6, 128.6, 128.0, 127.0 (×2C), 122.1 (×2C), 104.5 (×2C), 99.9, 83.8, 79.7, 55.3 (×2C), 28.2 (×6C).

(E)-1-(4-(3,5-dimethoxystyryl)phenyl)guanidine (117)

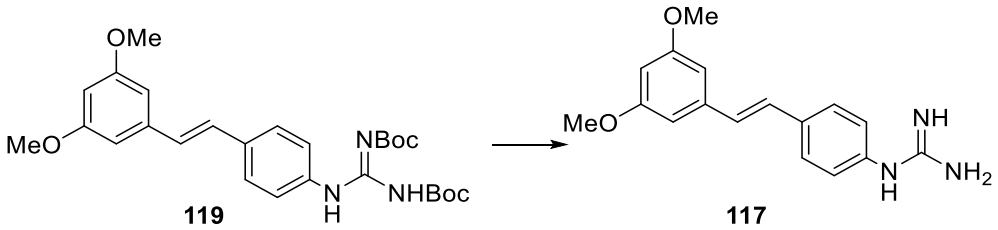

In a round-bottom flask, compound **119** (0.090, 1 eq) was solubilized in dry DCM (770 μL). To the solution TFA (1.809 mmol, 20 eq) was added dropwise at 0 °C. The mixture was stirred at room temperature for 20 h. The reaction was quenched with aq 5% $NaHCO_3$ and some drops of aq saturated KOH to reach pH≈11. The aqueous phase was extracted with EtOAc three times. The combined organic phases were dried over anhydrous Na_2SO_4, filtered and concentrated under reduced pressure to yield the pure product as a sticky solid (95% yield).

R_f: 0.2 (DCM/MeOH 9:1).

^{1}H NMR (300 MHz, C*D*Cl$_3$) δ (ppm): 7.44 (d, *J* = 8.6 Hz, 2H), 7.10 (d, *J* = 8.6 Hz, 2H), 6.98 (d, *J* = 16.7 Hz, 1H), 6.93 (d, *J* = 16.7 Hz, 1H), 6.61 (d, *J* = 2.3 Hz, 2H), 6.37 (t, *J* = 2.3 Hz, 1H), 3.79 (s, 6H).

^{13}C NMR (75 MHz, C*D*Cl$_3$) δ (ppm): 161.0 (×2C), 155.9, 138.8, 135.9, 135.5, 129.6, 128.0 (×2C), 127.6, 125.0 (×2C), 104.7 (×2C), 100.2, 55.3 (×2C).

(*E*)-1-(4-(3,5-dihydroxystyryl)phenyl)(*N*,*N*-di-*tert*-butoxycarbonyl)guanidine (120)

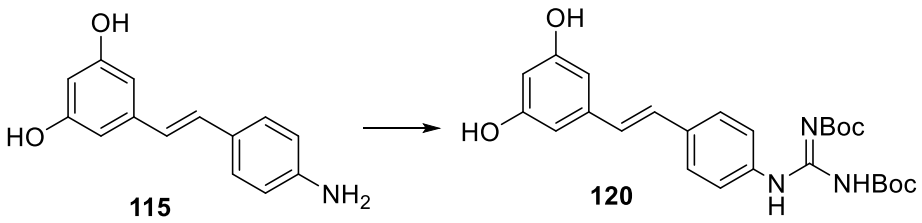

Compound **115** was dissolved (80 mg, 0.352 mmol, 1 eq) in some drops of methanol and dry $CHCl_3$ (10 mL). *N*,*N*'-Di-*Boc*-1H-pyrazole-1-carboxamidine (164 mg, 0.528 mmol, 1.5 eq), and the resulting suspension was stirred for 48 h. The solvent was evaporated and the rude was purified by FC using a gradient of a mixture of CHX/AcOEt (from 9:1 to 6:4). The compound was obtained as white solid (70 mg, 42%).

R_f: 0.44 (CHX : AcOEt 6:4)

^{1}H NMR (600 MHz, Acetone-d_6) δ (ppm): 11.73 (brs, 1H), 10.34 (brs, 1H), 8.22 (brs, 2H), 7.74 – 7.69 (m, 2H, 7.58 – 7.54 (m, 2H), 7.08 (d, *J* = 16.5 Hz, 1H), 7.05 (d, *J* = 16.5 Hz, 1H), 6.57 (d, *J* = 2.2 Hz, 2H), 6.29 (t, *J* = 2.2 Hz, 1H), 1.57 (s, 9H), 1.46 (s, 9H).

^{13}C NMR (150 MHz, Acetone-d_6) δ (ppm): 164.5, 159.7 (x2C), 154.3, 154.1, 140.5, 137.5, 134.9, 129.4, 128.5, 127.8 (x2C), 123.0 (x2C), 106.0 (x2C), 103.2, 84.6, 79.7, 28.4 (x3C), 28.2 (x3C).

(*E*)-1-(4-(3,5-dihydroxystyryl)phenyl)guanidine (118)

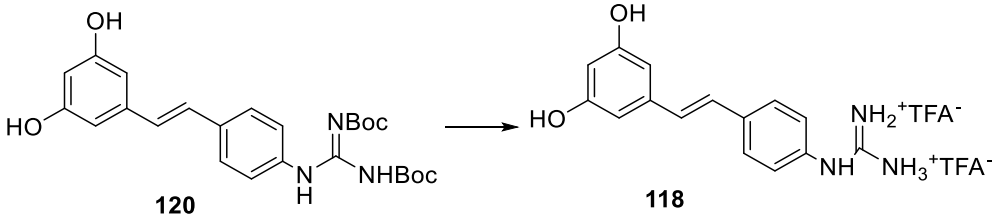

To a suspension of compound **120** (43 mg, 0.0916, 1 eq) in dry DCM (3 mL) under nitrogen atmosphere, TFA (182 µL, 2.318 mmol, 26 eq) was added dropwise, followed by the quick addition of TES (73 µL, 0.458 mmol, 5 eq). The mixture was stirred at room temperature for 24 h. A formation of a white precipitated was observed. The solvent was evaporated to give the final product as yellow brownish sticky solid in 82% yield.

R_f: 0.5 (AcOEt /MeOH 9:1)

^{1}H NMR (600 MHz, CD_3OD) δ (ppm): 7.66 – 7.58 (2H, m), 7.31 – 7.24 (2H, m), 7.07 (d, *J* = 16.7 Hz, 1H), 7.05 (d, *J* = 16.7 Hz, 1H), 6.50 (d, *J* = 1.4 Hz, 2H), 6.23 (t, *J* = 1.4 Hz, 1H).
^{13}C NMR (150 MHz, CD_3OD) δ (ppm): 159.8 (x2C), 158.1, 140.4, 138.3, 135.1, 131.2, 128.9 (x2C), 128.1, 126.6 (x2C), 106, 2 (x2C), 103.5.

(*E*)-4-(2-(6-methoxy-2-(4-methoxyphenyl)benzofuran-4-yl)vinyl)aniline (124)

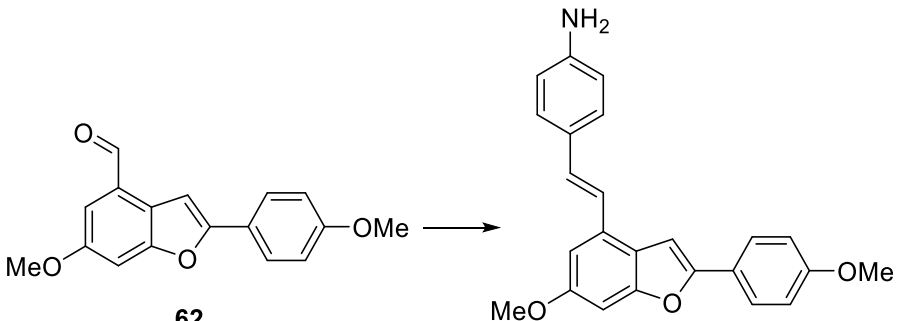

In a microwave vial, a suspension of compound **62** (200 mg, 0.7084 mmol, 1 eq) with diethyl (4-aminobenzyl)phosphonate (345 mg, 1.417 mmol, 2 eq) and 60 % NaH (85 mg, 2.125 mmol, 3 eq) in dry THF (6 mL) was stirred at 120°C for 30 min under microwave irradiation. The reaction mixture was cooled, and quenched with aq saturated NH_4Cl. The aqueous phase was extracted with EtOAc three times. The combined organic layers were washed with brine,

dried over anhydrous Na_2SO_4, filtered, and evaporated. The crude was purified by column chromatography, using CHX/AcOEt (9:1 to 7:3) as eluent to yield the product as a brown sticky solid in 23% yield.

R_f: 0.18 (CHX/AcOEt 7:3)

^{1}H NMR (300 MHz, C*D*Cl$_3$) δ (ppm): 7.82 – 7.74 (m, 2H), 7.45 – 7.36 (m, 2H), 7.19 (d, *J* = 16.4 Hz, 1H), 7.13 (d, *J* = 16.4 Hz, 1H), 7.08 (d, *J* = 0.9 Hz, 1H), 7.01 (d, *J* = 2.1 Hz, 1H), 7.00 – 6.92 (m, 3H), 6.76-6.65 (m, 2H), 3.89 (s, 3H), 3.86 (s, 3H).
^{13}C NMR (75 MHz, C*D*Cl$_3$) δ (ppm): 159.7, 157.8, 156.0, 155.2, 146.4, 131.0, 130.5, 128.0, 127.9 (×2C), 126.0 (×2C), 123.6, 122.4, 121.5, 115.2 (×2C), 114.3 (x2C), 107.7, 98.5, 94.9, 55.8, 55.4.

(E)-4-(4-aminostyryl)-2-(4-hydroxyphenyl)benzofuran-6-ol (121)

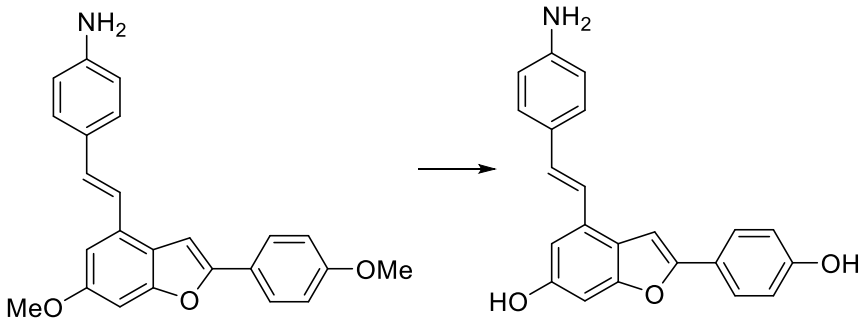

124 **121**

To a solution of compound **124** (61 mg, 0.164 mmol, 1 eq) in dry DCM (13 mL) under nitrogen atmosphere at -78°C, BBr_3 1M DCM solution was added dropwise and the resulting reaction mixture was slowly allowed to warm to room temperature and stirred for 7h. The mixture was quenched at 0°C with aq 5% $NaHCO_3$ (pH 7). The aqueous phase was extracted with EtOAc three times. The combined organic layers were dried over anhydrous Na_2SO_4, filtered, and evaporated. The crude was purified by column chromatography

using DCM/MeOH 95:5 as eluent. The product was obtained as brown solid (57%).

M.p.: 192°C (dec)

R_f: 0.30 (CHX/AcOEt 1:1)

^{1}H NMR (300 MHz, CD_3OD) δ (ppm): 7.74 – 7.66 (m, 2H), 7.43 – 7.34 (m, 2H, 7.18 (d, *J* = 16.4 Hz, 1H), 7.17 (d, *J* = 1.0 Hz, 1H), 7.11 (d, *J* = 16.4 Hz, 1H), 6.92 (d, *J* = 2.0 Hz, 1H), 6.89 – 6.82 (m, 2H), 6.78 (dd, J_1 = 2.0 Hz, J_2 = 1.0 Hz), 6.75 – 6.70 (m, 2H).
^{13}C NMR (75 MHz, CD_3OD) δ (ppm): 157.5, 156.0, 155.0, 154.9, 147.6, 131.1, 130.0, 127.4, 127.3 (x2C), 125.5 (x2C), 122.4, 121.3, 120.7, 115.2 (x2C), 115.0 (x2C), 107.2, 97.4, 95.9.

(E)-N-(4-(2-(6-methoxy-2-(4-methoxyphenyl)benzofuran-4-yl)vinyl)phenyl)acetamide (125)

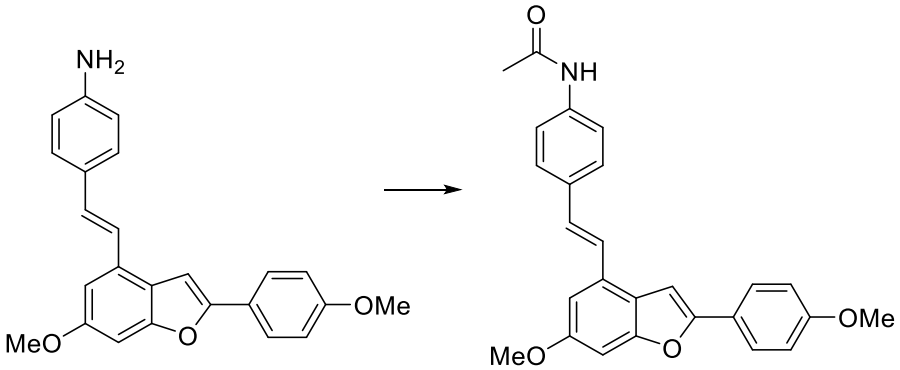

124 **125**

To a solution of compound **124** (30 mg, 0.081 mmol, 1 eq) in dry DCM (0.6 mL), TEA (22.5 µL, 0.162 mmol, 2 eq) and acetyl chloride (6.3 µL, 0.089 mmol, 1.1 eq) were added at 0°C and the mixture was stirred 10 min at the same temperature and 2h at room temperature. The reaction mixture was quenched with brine at 0°C. The aqueous layer was extracted with DCM three times, and

the combined organic layers were dried over anhydrous Na_2SO_4, filtered, and evaporated to yield the product as a brown sticky solid in 96% yield.

R_f: 0.31 (CHX/AcOEt 1:1)

^{1}H NMR (300 MHz, DMSO-*d*$_6$) δ (ppm): 10.04 (s, 1H), 7.88 – 7.75 (m, 2H), 7.70 (s, 1H), 7.68 – 7.58 (m, 4H), 7.43 (d, *J* = 16.6 Hz, 1H), 7.35 (d, *J* = 8.6 Hz, 1H), 7.16 – 7.10 (m, 2H), 7.09 – 6.98 (m, 2H), 3.84 (3H, s), 3.81 (s, 3H), 2.05 (3H, s).

^{13}C NMR (75 MHz, DMSO-*d*$_6$) δ (ppm): 168.7, 159.3, 158.1, 155.9, 155.0, 139.5, 132.4, 130.7, 130.3, 127.6 (x2C), 126.2 (x2C), 124.6, 123.2, 121.6, 119.4 (x2C), 115.0 (x2C), 108.3, 99.9, 95.9, 56.2, 55.7, 24.5.

(*E*)-*N*-(4-(2-(6-hydroxy-2-(4-hydroxyphenyl)benzofuran-4-yl)vinyl)phenyl)acetamide (122)

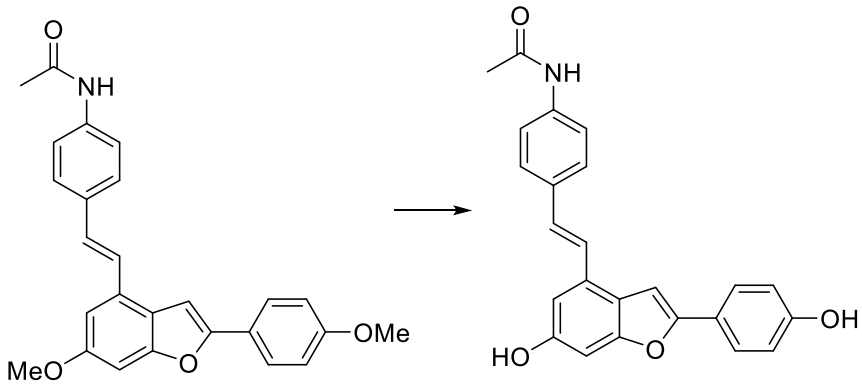

To a solution of compound **125** (25 mg, 0.06 mmol, 1 eq) in dry DCM (1.4 mL) at 0°C, BBr_3 1M in DCM (0.363 mL, 0.363 mmol, 6 eq) was added and the mixture was allowed to warm to room temperature and stirred overnigh. The reaction mixture was quenched with water at 0°C and the aqueous layer was extracted with EtOAc three times. The combined organic layers were dried over anhydrous Na_2SO_4, filtered, and evaporated. The crude was purified on

silica gel by FC using as eluent DCM/MeOH (from 9:1 to 8:2). The product was afforded as brownish solid in 54% yield.

M.p.: 205-207°C

R_f: 0.36

^{1}H NMR (300 MHz, MeOD) δ (ppm): 7.74 – 7.67 (m, 2H), 7.62 – 7.55 (m, 4H), 7.35 (d, *J* = 16.6 Hz, 1H), 7.21 (d, *J* = 0.9 Hz, 1H), 7.19 (d, *J* = 16.6 Hz, 1H), 6.97 (d, *J* = 2.0 Hz, 1H), 6.89 – 6.83 (m, 2H), 6.82 (dd, J_1 = 2.0 Hz, J_2 = 0.9 Hz, 1H), 2.13 (s, 3H).
^{13}C NMR (75 MHz, MeO*D*) δ (ppm): 170.2, 157.5, 156.0, 155.3, 154.9, 138.0, 133.4, 130.2, 128.9, 126.6 (x2C), 125.6 (x2C), 124.8, 122.4, 121.0, 119.8 (x2C), 115.2 (x2C), 107.8, 97.4, 96.6, 22.4.

(*E*)-1-(4-(2-(6-methoxy-2-(4-methoxyphenyl)benzofuran-4-yl)vinyl)phenyl)(*N*,*N*-di-*tert*-butoxycarbonyl)guanidine (126)

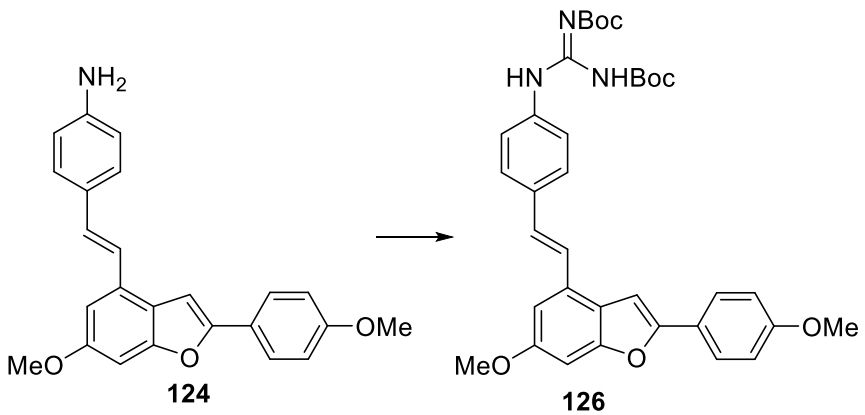

To the solution of compound **124** (73 mg, 0.1965 mmol, 1 eq) in dry $CHCl_3$ (5.8 mL), *N*,*N*'-Di-*Boc*-1H-pyrazole-1-carboxamidine was added and the mixture was stirred for 5h at room temperature. The solvent was evaporated and the crude was purified on silica gel using as eluent CHX/AcOEt (from 100% to 90%) to afford the product as brownish sticky solid in 60% yield.

R_f: 0.71 (CHX/AcOEt 7:3)

^{1}H NMR (300 MHz, C*D*Cl$_3$) δ (ppm): 11.65 (brs, 1H), 10.43 (s, 1H), 7.83 – 7.74 (m, 2H), 7.71 – 7.62 (m, 2H), 7.59 – 7.50 (m, 2H), 7.29 (d, *J* = 16.3 Hz, 1H), 7.18 (d, *J* = 16.3 Hz, 2H), 7.08 (d, *J* = 1.08 Hz, 1H), 7.05 (d, *J* = 2.1 Hz), 7.01 – 6.93 (m, 3H), 3.90 (s, 3H), 3.86 (s, 3H), 1.59 – 1.50 (s, 18 H).
^{13}C NMR (75 MHz, C*D*Cl$_3$) δ (ppm): 163.5, 159.7, 157.7 (x2C), 156.0, 155.4, 153.3, 136.4, 133.8, 130.3, 129.5, 127.1 (x2C), 126.0 (x2C), 125.4, 123.5, 122.2 (x2C), 121.7, 114.3 (x2C), 108.0, 98.4, 95.5, 83.8, 79.7, 55.8, 55.4, 28.2 (x6C).

(*E*)-1-(4-(2-(6-hydroxy-2-(4-hydroxyphenyl)benzofuran-4-yl)vinyl)phenyl))(*N*,*N*-di-*tert*-butoxycarbonyl)guanidine (127)

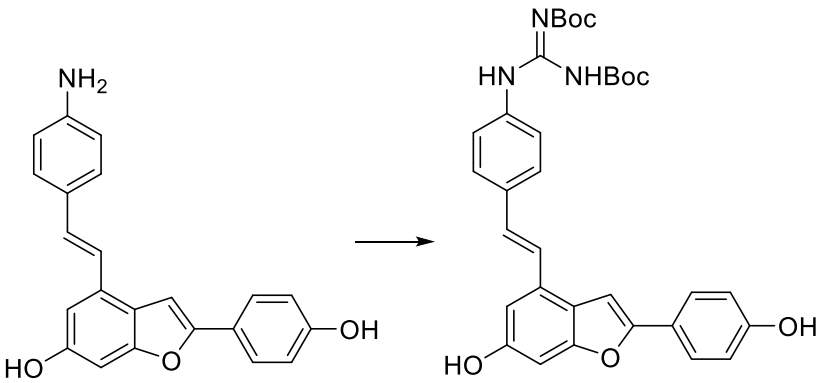

121 **127**

To the solution of compound **121** (32.4 mg, 0.094 mmol, 1 eq) in MeOH (0.1 mL) and dry $CHCl_3$ (2.4 mL), *N*,*N*'-Di-*Boc*-1H-pyrazole-1-carboxamidine was added and the mixture was stirred at room temperature for 24h. The solvent was evaporated and the crude was purified on silica gel using as eluent hexane/AcOEt 1:1, followed by a second column chromatography using DCM/MeOH (98:2) as eluent to afford the product as brown sticky solid in 39% yield.

R_f: 0.44 (DCM/MeOH 98:2)

^{1}H NMR (300 MHz, C*D*Cl$_3$) δ (ppm): 11.68 (brs, 1H), 10.26 (s, 1H), 7.65 – 7.61 (m, 2H), 7.41 – 7.36 (m, 2H), 7.28 – 7.22 (m, 2H), 6.97 (d, *J* = 16.3 Hz, 1H), 6.91 (d, *J* = 16.3 Hz, 1H), 6.88 (s, 1H), 6.85 – 6.81 (m, 2H), 6.79 – 6.75 (m, 2H), 1.55 (s, 9H), 1.51 (s, 9H).

^{13}C NMR (75 MHz, C*D*Cl$_3$) δ (ppm): 163.2, 155.9, 155.7, 155.0, 154.7, 153.9, 153.3, 135.1, 134.8, 129.9, 128.7, 126.9 (x2C), 126.0 (x2C), 125.4, 124.0, 123.5 (x2C), 121.4, 115.9 (x2C), 108.4, 98.2, 97.7, 84.0, 80.3, 28.1 (x6C).

(E)-3′,5′-Dimethoxy-4-(4-bromobutyloxy)stilbene (135)

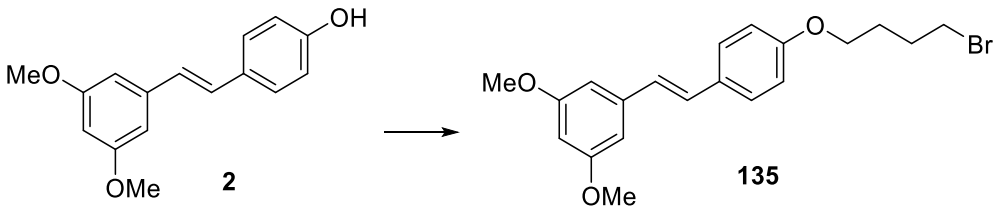

To a suspension of NaOH (65.5 mg, 1.64 mmol, 2.1 eq) in DMSO (5.6 mL) at room temperature, under N_2 atmosphere, pterostilbene (**2**) (200 mg, 0.78 mmol, 1 eq) was added and the suspension turned yellow and was stirred for 30 min. Then, 1,4-dibromobutane (186 µL, 1.56 mmol, 2 eq) was added and the reaction mixture was stirred for 4 hours, at the same temperature. We observed that the yellow color of the suspension disappeared with the reaction progress. The reaction was quenched with aq 2M HCl and cold water was added leading to the formation of a precipitate, which was filtered, washed with water and dried. The crude was purified by FC using CHX/AcOEt (from 100% to 90%) as eluent to afford the product as white solid (70% yield).

M.p.: 89-90°C

R_f: 0.41 (CHX/AcOEt 9:1)

^{1}H NMR (600 MHz, C*D*Cl$_3$) δ (ppm): 7.49 – 7.45 (m, 2H), 7.07 (d, *J* = 16.2 Hz, 1H), 6.94 (d, *J* = 16.2 Hz, 1H), 6.93 - 6.89 (m, 2H), 6.68 (d, *J* = 2.0 Hz, 2H),

6.41 (t, *J* = 2.0 Hz, 1H), 4.05 (t, *J* = 6.1 Hz, 2H), 3.87 (s, 6H), 3.53 (t, *J* = 6.7 Hz, 2H), 2.15 – 2.08 (m, 2H), 2.03 – 1.96 (m, 2H).

(*E*)-1-(4-(4-azidobutoxy)styryl)-3,5-dimethoxybenzene (136)

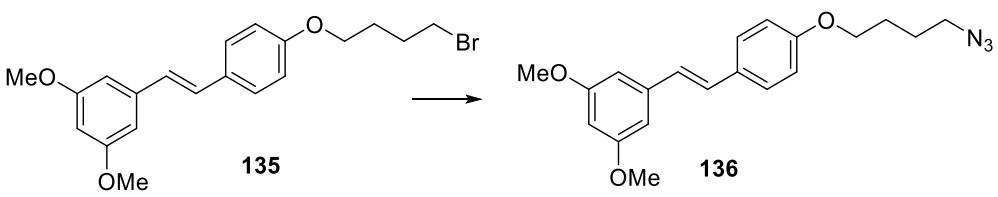

To the solution of compound **135** (70 mg, 0.179 mmol, 1 eq) in dry DMF (0.5 mL) at room temperature, under N_2 atmosphere, sodium azide (23 mg, 0.358 mmol, 2 eq) was cautiously added, and the resulting mixture was stirred at 50°C overnight. The mixture was allowed to cool to room temperature, and then diluted with water (15 mL). The aqueous phase was extracted with EtOAC (3 x 10 mL). The combined organic phases were washed with a mixture of water/brine 1:1 (3 x 20 mL), dried over anhydrous Na_2SO_4, filtered, and evaporated, to give the product enough pure to be used for the next step without any further purification.

(*E*)-4-(4-(3,5-dimethoxystyryl)phenoxy)butan-1-amine (128)

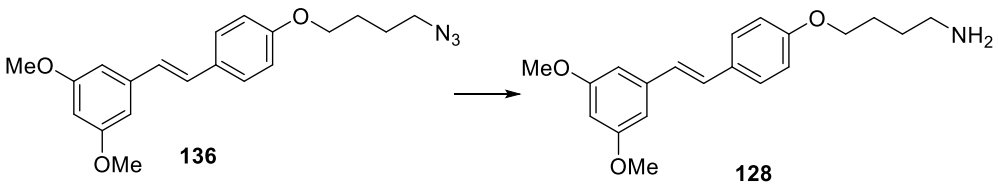

In a round-bottom flask, compound **136** (50 mg, 0.1415 mmol, 1 eq) was dissolved in THF (2.7 mL) and water (0.1 mL). Then, triphenylphospine (223 mg, 0.849 mmol, 6 eq), was added portionwise at 0°C. The reaction mixture was allowed to warm to room temperature and stirred overnight. The solvent was evaporated, and the residue was diluted with EtOAc and washed with

water. Aq 1M NaOH was added to the aqueous phase (pH 11) that was extracted with EtOAC three times. The combined organic layers were washed with brine, dried over anhydrous Na_2SO_4, filtered and evaporated to give an oil. The crude was purified on silica gel by column chromatography, using as eluent DCM/MeOH 9:1. The product was obtained as a clear oil in 67% yield over two steps.

R_f: 0.42 (DCM : MeOH 9:1)

^{1}H NMR (600 MHz, C*D*$_3$O*D*) δ (ppm): 7.47−7.42 (m, 2H), 7.07 (d, *J* = 16.5 Hz, 1H), 6.93 (d, *J* = 16.5 Hz, 1H), 6.90 − 6.87 (m, 2H), 6.67 (d, *J* = 1.7 Hz, 2H), 6.37 (t, J = 1.7 Hz, 1H), 4.02 – 3.97 (m, 2H), 3.79 (s, 6H), 2.74 – 2.71 (2H, m), 1.85 – 1.76 (m, 2H), 1.70 – 1.63 (m, 2H).

^{13}C NMR (150 MHz, C*D*$_3$O*D*) δ (ppm): 162.5 (x2C), 160.3, 141.2, 131.4, 129.7, 128.8 (x2C), 127.5, 115.7 (x2C), 105.3 (x2C), 100.5, 68.7, 55.7 (x2C), 42.1, 30.0, 27.8.

(E)-3′,5′-Dimethoxy-4-(4-iodobutyloxy)stilbene (137)

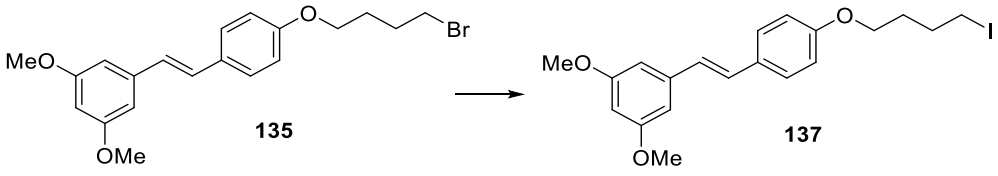

In a saturated solution of NaI (1g) in dry acetone (2 mL), compound **135** (45 mg, 0.115 mmol, 1 eq) was dissolved and refluxed overnight, under N_2 atmosphere. Acetone was evaporated and the resulting residue was diluted with EtOAc and washed twice with aq 10% $Na_2S_2O_5$. The aqueous phases were further extracted with EtOAc twice. The combined organic layers were dried over anhydrous Na_2SO_4, filtered, and evaporated to give the product as white solid in quantitative yield. Analytical data were in agreement with literature report (Bavo et al. 2018).

M.p.: 124°C

R_f: 0.5 (CHX/AcOEt 9:1)

^{1}H NMR (300 MHz, C*D*Cl$_3$) δ (ppm): 7.43 (d, J = 8.7 Hz, 2H), 7.03 (d, J = 16.3 Hz, 1H), 6.96− 6.76 (m, 3H), 6.65 (d, J = 2.2 Hz, 2H), 6.38 (t, J = 2.2 Hz, 1H), 4.01 (t, J = 6.0 Hz, 2H), 3.83 (s, 6H), 3.27 (t, J = 6.8 Hz, 2H), 2.14−1.85 (m, 4H).

(*E*)-4-(4-(3,5-dimethoxystyryl)phenoxy)-*N*,*N*-dimethylbutan-1-amine (129)

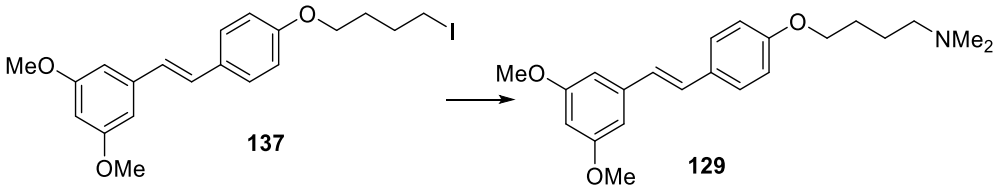

To the solution of compound **137** (40mg, 0.0908 mmol, 1 eq) in dry THF (3mL) at room temperature dimethylamine 40% wt in water (0.205 mL, 1.817 mmol, 20 eq) was added, and the resulting mixture was stirred at 60°C for 20h. The reaction mixture was cooled to room temperature, and the solvent was evaporated. The residue was diluted with EtOAc and the organic phase was washed with aq 1M NaOH (20 mL). The aqueous phase was extracted with EtOAc (3x 15 mL). The combined organic layers were dried over anhydrous Na_2SO_4, filtered, and evaporated to give the product as yellowish oil in quantitative yield.

R_f: 0.53 (DCM/MeOH 9:1)

^{1}H NMR (600 MHz, C*D*$_3$O*D*) δ (ppm): 7.50−7.44 (m, 2H), 7.08 (d, *J* = 16.1 Hz, 1H), 6.94 (d, *J* = 16.1 Hz, 1H), 6.91 − 6.88 (m, 2H), 6.78 (d, *J* = 1.8 Hz, 2H), 6.37 (t, *J* = 1.8 Hz, 1H), 4.01 (t, *J* = 6.1 Hz, 2H), 3.80 (s, 6H), 2.42 (t, *J* = 7.4 Hz, 2H), 2.28 (s, 6H), 1.82 – 1.76 (m, 2H), 1.73 – 1.66 (m, 2H).

^{13}C NMR (150 MHz, C*D*$_3$O*D*) δ (ppm): 162.5 (x2C), 160.2, 141.2, 131.3, 129.7, 128.9 (x2C), 127.5, 115.7 (x2C), 105.3 (x2C), 100.5, 68.7, 60.3, 55.7 (x2C), 45.3 (x2C), 28.3. 24.8.

(*E*)-3′,5′-Dimethoxy-4-(4-trimethylammoniumbutyloxy)stilbene Iodide (130)

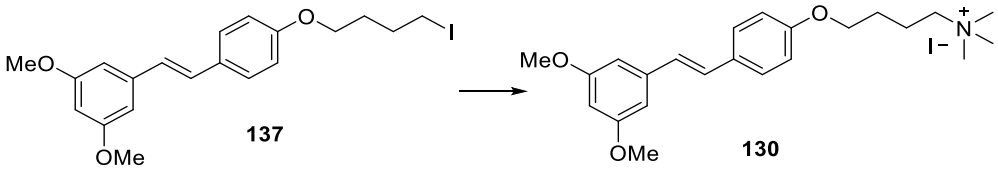

To the solution of compound **137** (50mg, 0.1136 mmol, 1 eq) in dry THF (3.4 mL) at room temperature, under N_2 atmosphere, trimethylamine 30-35% wt in EtOH (0.55 mL, 3.974 mmol, 35 eq) was added, and the resulting mixture was stirred for 16 h at 55°C. The solvent was evaporated to give the product, as a white solid, in quantitative yield.

M.p.: 184-186°C

^{1}H NMR (600 MHz, C*D*$_3$O*D*) δ (ppm): 7.52−7.45 (m, 2H), 7.09 (d, *J* = 16.2 Hz, 1H), 6.98 – 6.91 (m, 3H), 6.68 (d, *J* = 2.2 Hz, 2H), 6.38 (t, *J* = 2.2 Hz, 1H), 4.09 (t, *J* = 5.7 Hz, 2H), 3.80 (s, 6H), 3.49 – 3.42 (m, 2H), 3.16 (s, 9H), 2.07 – 1.97 (m, 2H), 1.93 – 1.83 (m, 2H).

^{13}C NMR (150 MHz, C*D*$_3$O*D*) δ (ppm): 161.5 (x2C), 159.9, 141.1, 131.7, 129.6, 128.9 (x2C), 127.3, 115.8 (x2C), 105.3 (x2C), 100.5, 68.0, 67.6, 55.8 (x3C), 53.6 (x2C), 27.1, 21.1.

(*E*)-3′,5′-Dimethoxy-4-(4-triethylammoniumbutyloxy)stilbene Iodide (131)

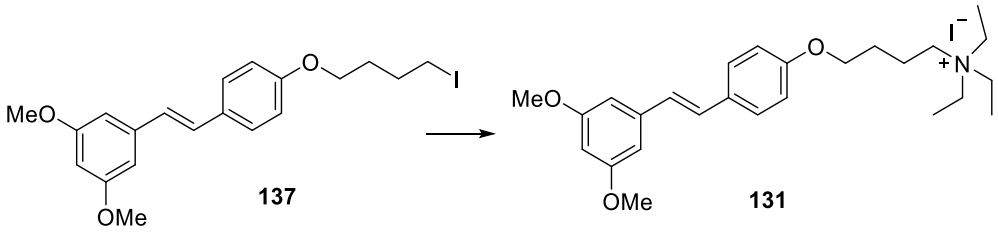

The solution of compound **137** (50 mg, 0.114 mmol, 1 eq) in TEA (342 µL, 2.45 mmol, 21.6 eq) and toluene (342 µL) was refluxed for 24 h. The solvent was evaporated and the residue was triturated with diethylether to give a precipitate, which was filtered and further washed with diethylether. A brownish solid was obtained (62%). Analytical data corresponded to literature report (Bavo et al. 2018).

M.p.: 138°C

^{1}H NMR (300 MHz, C*D*$_3$O*D*) δ (ppm): 7.54−7.43 (m, 2H), 7.10 (d, J = 16.3 Hz, 1H), 7.01−6.86 (m, 3H), 6.69 (d, J = 2.2 Hz, 2H), 6.37 (t, J = 2.2 Hz, 1H), 4.05 (t, J = 5.4 Hz, 2H), 3.79 (s, 6H), 3.37−3.25 (m, 8H), 1.85 (m, 4H), 1.26 (t, J = 7.4, 9H).

^{13}C NMR (75 MHz, C*D*$_3$O*D*) δ (ppm): 161.1 (x2C), 158.5, 139.7, 130.2, 128.2, 127.6 (x2C), 126.3, 114.4 (x2C), 103.9 (x2C), 99.1, 66.6, 56.2, 54.5 (x3C), 52.57 (x2C), 25.59, 18.30, 6.47 (x3C).

(*E*)-3-(4-chlorobutoxy)-5-(4-hydroxystyryl)phenol (138a) and (*E*)-5-(4-(4-chlorobutoxy)styryl)benzene-1,3-diol (138b)

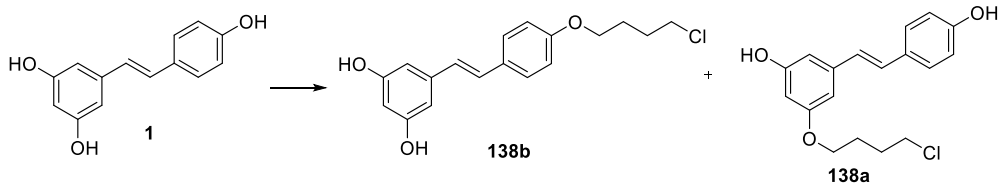

To a solution of resveratrol (**1**) (1g, 4.38 mmol, 1 eq) in dry DMF (5 mL), under N_2 atmosphere, at room temperature, K_2CO_3 (665 mg, 4.819 mmol, 1.1 eq) and 1-bromo-4-chlorobutane (757 µL, 1.126 g, 6.57 mmol, 1.5 eq) were added. The dark reaction mixture was stirred overnight at room temperature. The reaction was cautiously quenched with aq 1M HCl (20 mL), and the aqueous phase was extracted with EtOAc (3x20 mL). The combined organic layers were washed with a mixture of water/brine 1:1 (3x30 mL), dried over anhydrous Na_2SO_4, filtered, and evaporated. The crude was purified on silica gel by column chromatography, using as eluent DCM/AcOEt 9:1 to give **138b** (16% yield) and **138a** (25% yield) as brownish solids.

(*E*)-3-(4-chlorobutoxy)-5-(4-hydroxystyryl)phenol (138a)

R_f: 0.46 DCM/ AcOEt 9:1

M.p.: 129 – 131 °C

^{1}H-NMR (600 MHz, Acetone-d_6) δ (ppm): 8.34 (brs, 1H), 7.45 – 7.40 (m, 2H), 7.08 (d, *J* = 16.2 Hz, 1H), 6.92 (d, *J* = 16.2 Hz, 1H), 6.86 – 6.81 (m, 2H), 6.64 (t, *J* = 1.8 Hz, 1H), 6.62 (t, *J* = 1.8 Hz, 1H), 6.32 (t, *J* = 1.8 Hz, 1H), 4.03 (t, *J* = 6.1 Hz, 2H), 3.71 (s, 6H), 2.00 – 1.94 (m, 2H), 1.94 – 1.88 (m, 2H).

(*E*)-5-(4-(4-chlorobutoxy)styryl)benzene-1,3-diol (138b)

Analytical data corresponded to the ones reported in literature (Biasutto et al. 2008; Bavo et al. 2018)

R_f: 0.29 DCM/AcOEt 9: 1

M.p.: 148°C

^{1}H NMR (300 MHz, DMSO-d_6) δ (ppm): 9.21 (broad signal, s, 2H), 7.50 (d, 2H, J = 8.7 Hz), 7.02-6.82 (m, 4H), 6.40 (d, 2H, J = 2.0 Hz), 6.12 (t, 1H, J = 2.0 Hz), 4.02 (t, 2H, 5.9 Hz), 3.72 (t, 2H, J = 5.9 Hz), 1.98-1.76 (m, 4H).
^{13}C NMR (75 MHz, DMSO-d_6) δ (ppm): 158.5 (x2C), 158.2, 139.1, 129.6, 127.8, 127.4 (x2C), 126.6, 114.6 (x2C), 104.4 (x2C), 66.7 (x2C), 45.2, 28.9, 26.1.

(E)-1,3-bis(4-chlorobutoxy)-5-(4-(4-chlorobutoxy)styryl)benzene (139)

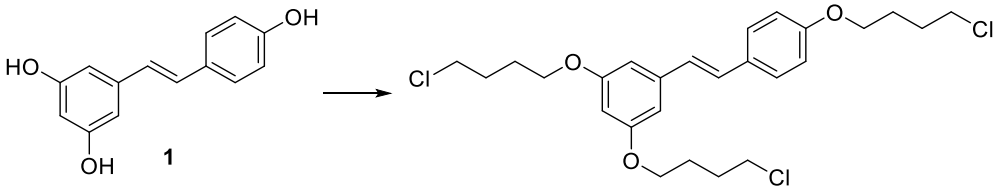

139

To a solution of resveratrol (**1**) (100 mg, 0.438 mmol, 1 eq) in dry DMF (2 mL), under N_2 atmosphere, K_2CO_3 (211 mg, 1.533 mmol, 3.5 eq) was added and the resulting mixture was stirred for 15 min at room temperature. Then, 1-bromo-4-chlorobutane (151 µL, 225 mg, 1.314 mmol, 9 eq) was added and the mixture was stirred at 60°C overnight. The reaction mixture was allowed to cool to room temperature and then quenched with aq 1M HCl. The aqueous phase was extracted with EtOAc three times. The combined organic layers were washed with brine solution, dried over anhydrous Na_2SO_4, filtered, and evaporated. The crude was purified on silica gel by column chromatography, using as eluent CHX/AcOEt (From 100% to 80%). The product was obtained as a transparent oil (73% yield).

R_f: 0.42 CHX/AcOEt 9: 1

^{1}H NMR (600 MHz, C*D*Cl$_3$) δ (ppm): 7.46 – 7.40 (m, 2H), 7.03 (d, *J* = 16.0 Hz, 1H), 6.89 (d, *J* = 16.0 Hz, 1H), 6.89 – 6.87 (m, 2H), 6.64 (d, *J* = 2.1 Hz, 2H), 6.35 (t, *J* = 2.1 Hz, 1H), 4.07 – 3.98 (m, 6H), 3.68 – 3.60 (m, 4H), 3.53 – 3.48 (m, 2H), 2.14 – 2.05 (m, 2H), 2.04 – 1.92 (m, 10H).

(*E*)-1,3-bis(4-iodobutoxy)-5-(4-(4-iodobutoxy)styryl)benzene (140)

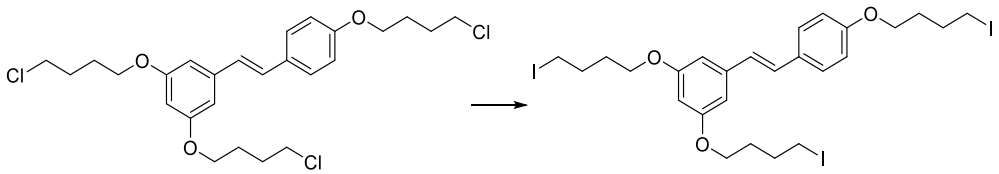

139 **140**

In a saturated solution of NaI (3g) in dry acetone (6 mL), compound **139** (150 mg, 0.3 mmol, 1 eq) was dissolved and refluxed overnight, under N_2 atmosphere. Acetone was evaporated and the residue was diluted with EtOAc and washed with aq 10% $Na_2S_2O_5$ three times. The aqueous phases were further extracted with EtOAc twice. The combined organic layers were dried over anhydrous Na_2SO_4, filtered, and evaporated to give the product as sticky white solid, in 83% yield. The compound obtained was used without any further purification for the next step.

R_f: 0.59 (CHX/AcOEt 9:1)

^{1}H NMR (300 MHz, C*D*Cl$_3$) δ (ppm): 7.44 – 7.40 (m, 2H), 7.02 (d, *J* = 16.2 Hz, 1H), 6.87 (d, *J* = 16.2 Hz, 1H), 6.88 – 6.86 (m, 2H), 6.62 (d, *J* = 2.2 Hz, 2H), 6.33 (t, *J* = 2.2 Hz, 1H), 4.02 – 3.98 (m, 6H), 3.29 – 3.24 (m, 6H), 2.07 – 2.00 (m, 6H), 1.94 – 1.88 (m, 6H).

^{13}C NMR (150 MHz, C*D*Cl$_3$) δ (ppm): 160.2 (x2C), 158.7, 139.7, 130.0, 128.7, 127.8 (x2C), 126.5, 114.7 (x2C), 105.0 (x2C), 100.5, 66.7 (x3C), 30.1 (x6C), 6.4 (x3C).

(*E*)-1,3-bis(4-azidobutoxy)-5-(4-(4-azidobutoxy)styryl)benzene (141)

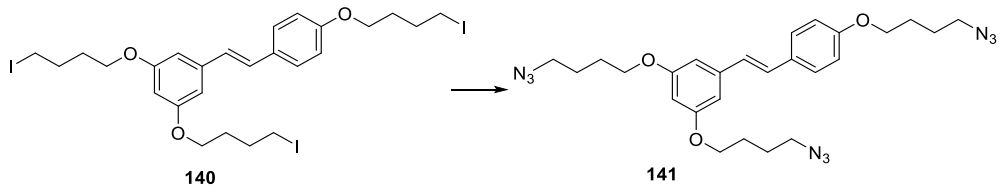

140 **141**

To a solution of compound **140** (60 mg, 0.0775 mmol, 1 eq) in dry DMF (1.8 mL) at room temperature, under N_2 atmosphere, sodium azide (23 mg, 0.358 mmol, 2 eq) was cautiously added, and the resulting mixture was stirred at 60°C for 4h. The mixture was allowed to cool to room temperature, and then diluted with water (15 mL). The aqueous phase was extracted with EtOAc (3 x 10 mL). The combined organic phases were washed with a mixture of water/brine 1:1 (3 x 20 mL), dried over anhydrous Na_2SO_4, filtered, and evaporated, to give the product enough pure to be used for the next step without any further purification. The product was obtained as a colorless oil.

R_f: 0.32 (CHX/AcOEt 9:1)

^{1}H NMR (600 MHz, C*D*Cl$_3$) δ (ppm): 7.46 – 7.39 (m, 2H), 7.02 (d, *J* = 16.3 Hz, 1H), 6.91 – 6.85 (m, 3H), 6.63 (d, *J* = 1.8 Hz, 2H), 6.35 (t, *J* = 1.8 Hz, 1H), 4.05 – 3.98 (m, 6H), 3.42 – 3.34 (m, 6H), 1.93 – 1.85 (m, 6H), 1.84 – 1.76 (m, 6H).

(*E*)-4,4'-((5-(4-(4-aminobutoxy)styryl)-1,3-phenylene)bis(oxy))bis(butan-1-amine) (132)

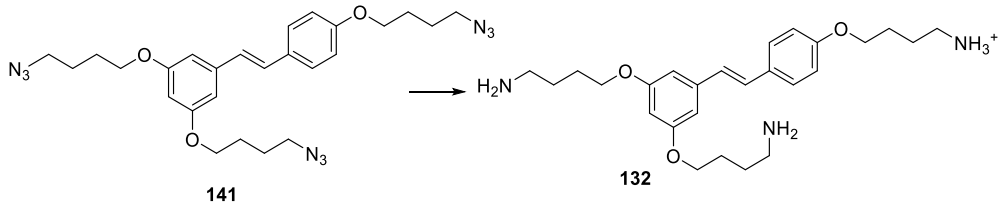

141 **132**

In a round-bottom flask, compound **141** (40 mg, 0.0775 mmol, 1 eq) was dissolved in THF (1.5 mL) and water (50 µL). Then, PPh_3 (336 mg, 1.395 mmol, 18 eq), was added portionwise at 0°C. The reaction mixture was allowed to warm to room temperature and stirred for 24h. The solvent was evaporated, and the residue was diluted with EtOAc and washed with aq 1M HCl. The aqueous phase was extracted with EtOAc four times. To the acidic aqueous phase, aq 1M NaOH was added. The resulting alkaline aqueous phase (pH 12) was extracted with EtOAc three times. The combined organic layers were dried over anhydrous Na_2SO_4, filtered and evaporated to give the product as yellowish sticky solid (60%).

R_f: 0.36 (*n*-BuOH/H_2O/AcOH 4:2:1)

^{1}H NMR (600 MHz, C*D$_3$OD*) δ (ppm): 7.51 – 7.49 (m, 2H), 7.06 (d, *J* = 16.2 Hz, 1H), 6.96 − 6.86 (m, 3H), 6.66 (d, *J* = 2.2 Hz, 2H), 6.36 (t, *J* = 2.2 Hz, 1H), 4.06 – 3.94 (m, 6H), 3.28 – 3.21 (m, 2H), 2.78 – 2.68 (m, 4H), 1.98 -1.91 (m, 2H), 1.87 – 1.74 (m, 6H), 1.73 – 1.62 (m, 6H).
^{13}C NMR (150 MHz, C*D$_3$OD*) δ (ppm): 161.6 (x2C), 160.2, 141.2, 131.4, 129.7, 128.8 (x2C), 127.6, 115.7 (x2C), 105.9 (x2C), 101.6, 68.7 (x2), 68.6, 41.9 (x2C), 40.2, 29.4 (x2C), 27.8 (x2C), 27.7, 27.1.

(*E*)-4,4'-((5-(4-(4-(dimethylamino)butoxy)styryl)-1,3-phenylene)bis(oxy))bis(*N*,*N*-dimethylbutan-1-amine) (133)

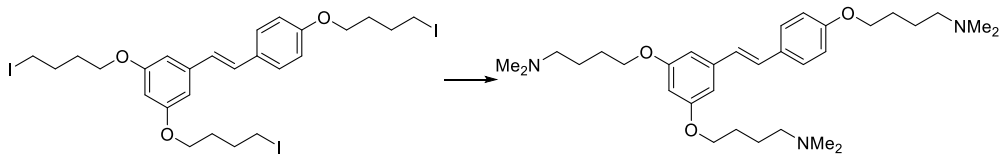

140 **133**

To a solution of compound **140** (70mg, 0.0904 mmol, 1 eq) in dry THF (3mL) at room temperature, dimethylamine 40% wt in water (0.611 mL, 5.424 mmol, 60 eq) was added, and the resulting mixture was stirred at 60°C for 20h. The reaction mixture was cooled, and the solvent was evaporated. The residue

was diluted with EtOAc and the organic phase was washed with aq 1M NaOH (20 mL). The aqueous phase was extracted with EtOAc (4 x 15 mL). The combined organic layers were dried over anhydrous Na_2SO_4, filtered, and evaporated to give the product as yellowish oil (91% yield).

R_f: 0.15 (DCM/MeOH 9:1)

^{1}H NMR (600 MHz, CD_3OD) δ (ppm): 7.50 – 7.44 (m, 2H), 7.08 (d, *J* = 16.4 Hz, 1H), 6.94 (d, *J* = 16.4 Hz, 1H), 6.92 – 6.89 (m, 2H), 6.68 (d, *J* = 1.8 Hz, 2H), 6.37 (t, *J* = 1.8 Hz, 1H), 4.06 – 3.97 (m, 6H), 2.45 – 2.39 (m, 6H), 2.30 – 2.24 (m, 18 H), 1.84 – 1.76 (m, 6H), 1.74 – 1.65 (m, 6H).
^{13}C NMR (150 MHz, CD_3OD) δ (ppm): 161.8 (x2C), 160.2, 141.2, 131.4, 129.7, 128.8 (x2C), 127.6, 115.7 (x2C), 105.9 (x2C), 101.6, 68.7 (x3C), 60.4 (x3C), 45.4 (x6C), 28.3 (x3C), 24.9 (x3C).

(*E*)-4,4'-((5-(4-(4-(trimethylammonio)butoxy)styryl)-1,3-phenylene)bis(oxy))bis(*N*,*N*,*N*-trimethylbutan-1-aminium) iodide (134)

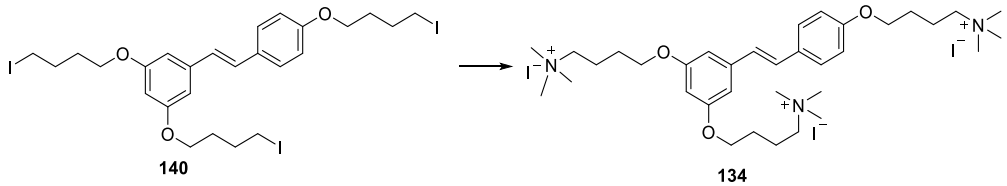

140 **134**

To a solution of compound **140** (60mg, 0.0775 mmol, 1 eq) in dry THF (3.4 mL) at room temperature, under N_2 atmosphere, trimethylamine 30-35% wt in EtOH (1.9 mL, 81.3 mmol, 105 eq) was added, and the resulting mixture was stirred for 24 h at 55°C. The solvent was evaporated and the product was obtained as a white solid, in quantitative yield.

M.p.: 151 – 152°C

^{1}H NMR (600 MHz, DMSO-d_6) δ (ppm): 7.56 – 7.50 (m, 2H), 7.02 (d, *J* = 16.4 Hz, 1H), 7.01 (d, *J* = 16.4 Hz, 1H), 6.98 – 6.93 (m, 2H), 6.75 (d, *J* = 1.6 Hz,

2H), 6.41 (t, *J* = 1.6 Hz, 1H), 4.09 – 3.99 (m, 6H), 3.43 – 3.33 (m, 6H), 3.12 – 3.01 (m, 27H), 1.91 – 1.80 (m, 6H), 1.78 – 1.69 (m, 6H).

^{13}C NMR (150 MHz, DMSO-d_6) δ (ppm): 161.7 (x2C), 160.1, 141.3, 131.5, 130.4, 129.7 (x2C), 127.9, 116.4 (x2C), 106.8 (x2C), 102.4, 68.7 (x3C), 66.9 (x3C), 54.1 (x9C), 27.5 (x3C), 21.1 (x3C).

3.3.6. Bibliography

WHO (2017) Global priority list of antibiotic-resistant bacteria to guide research, discovery, and development of new antibiotics. https://www.who.int/medicines/publications/global-priority-list-antibiotic-resistant-bacteria/en/

Bavo F, Pucci S, Fasoli F, Lammi C, Moretti M, Mucchietto V, Lattuada D, Viani P, De Palma C, Budriesi R, Corradini I, Dowell C, McIntosh JM, Clementi F, Bolchi C, Gotti C, Pallavicini M (2018) Potent Antiglioblastoma Agents by Hybridizing the Onium-Alkyloxy-Stilbene Based Structures of an α7-nAChR, α9-nAChR Antagonist and of a Pro-Oxidant Mitocan. J Med Chem 61:10531–10544. https://doi.org/10.1021/acs.jmedchem.8b01052

Biasutto L, Mattarei A, Marotta E, Bradaschia A, Sassi N, Garbisa S, Zoratti M, Paradisi C (2008) Development of mitochondria-targeted derivatives of resveratrol. Bioorganic Med Chem Lett 18:5594–5597. https://doi.org/10.1016/j.bmcl.2008.08.100

Bonandi E, Christodoulou MS, Fumagalli G, Perdicchia D, Rastelli G, Passarella D (2017) The 1,2,3-triazole ring as a bioisostere in medicinal chemistry. Drug Discov Today 22:1572–1581. https://doi.org/10.1016/j.drudis.2017.05.014

Chanawanno K, Chantrapromma S, Anantapong T, Kanjana-Opas A, Fun HF (2010) Synthesis, structure and in vitro antibacterial activities of new hybrid disinfectants quaternary ammonium compounds: Pyridinium and quinolinium stilbene benzenesulfonates. Eur J Med Chem 45:4199–4208. https://doi.org/10.1016/j.ejmech.2010.06.014

Coutts IGC, Southcott MR (1990) The conversion of phenols to primary and secondary aromatic amines via a Smiles rearrangement. J Chem Soc Perkin Trans 1 767–771. https://doi.org/10.1039/p19900000767

Csékei M, Novák Z, Kotschy A (2008) Development of a one-pot sequential Sonogashira coupling for the synthesis of benzofurans. Tetrahedron 64:8992–8996. https://doi.org/10.1016/j.tet.2008.05.100

Domalaon R, Idowu T, Zhanel GG, Schweizer F (2018) Antibiotic hybrids: The next generation of agents and adjuvants against gram-negative pathogens? Clin Microbiol Rev 31:1–45. https://doi.org/10.1128/CMR.00077-17

Đud M, Glasovac Z, Margetić D (2019) The utilization of ball milling in synthesis of aryl guanidines through guanidinylation and N-Boc-deprotection sequence. Tetrahedron 75:109–115. https://doi.org/10.1016/j.tet.2018.11.038

Garner LE, Park J, Dyar SM, Chworos A, Sumner JJ, Bazan GC (2010) Modification of the optoelectronic properties of membranes via insertion of amphiphilic phenylenevinylene oligoelectrolytes. J Am Chem Soc 132:10042–10052. https://doi.org/10.1021/ja1016156

Ghamrawi S, Bouchara J, Tarasyuk O, Rogalsky S, Lyoshina L, Bulko O, Bardeau JF (2017) Promising silicones modified with cationic biocides for the development of antimicrobial medical devices. Mater Sci Eng C 75:969–979. https://doi.org/10.1016/j.msec.2017.03.013

Gibtner T, Hampel F, Gisselbrecht JP, Hirsch A (2002) End-cap stabilized oligoynes: Model compounds for the linear sp carbon allotrope carbyne. Chem - A Eur J 8:408–432. https://doi.org/10.1002/1521-3765(20020118)8:2<408::AID-CHEM408>3.0.CO;2-L

Hagras M, Mohammad H, Mandour MS, Hegazy YA, Ghiaty A, Seleem MN, Mayhoub AS (2017) Investigating the Antibacterial Activity of Biphenylthiazoles against Methicillin- and Vancomycin-Resistant Staphylococcus aureus (MRSA and VRSA). J Med Chem 60:4074–4085. https://doi.org/10.1021/acs.jmedchem.7b00392

Heydarifard S, Pan Y, Xiao H, Nazhad MM (2017) Water-resistant cellulosic filter containing non-leaching antimicrobial starch for water purification and disinfection. Carbohydr Polym 163:146–152. https://doi.org/10.1016/j.carbpol.2017.01.063

Hider RC, Kong X (2010) Chemistry and biology of siderophores. Nat Prod Rep 27:637–657. https://doi.org/10.1039/b906679a

Hoshino J, Park EJ, Kondratyuk TP, Marler L, Pezzuto JM, van Breemen RB, Mo S, Li Y, Cushman M (2010) Selective synthesis and biological evaluation of sulfate-conjugated resveratrol metabolites. J Med Chem 53:5033–5043. https://doi.org/10.1021/jm100274c

Hu Y, Nawoschik KJ, Liao Y, Ma J, Fathi R, Yang Z (2004) Synthesis of Conformationally Restricted 2,3-Diarylbenzo[b]furan by the Pd-Catalyzed Annulation of o-Alkynylphenols: Exploring a Combinatorial Approach. J Org Chem 69:2235–2239. https://doi.org/10.1021/jo0303160

Katritzky AR, Rogovoy B V. (2005) Recent developments in guanylating agents. Arkivoc 2005:49–87. https://doi.org/10.3998/ark.5550190.0006.406

Kolb HC, Finn MG, Sharpless KB (2001) Click Chemistry: Diverse Chemical Function from a Few Good Reactions. Angew Chemie - Int Ed 40:2004–2021. https://doi.org/10.1002/1521-3773(20010601)40:11<2004::AID-ANIE2004>3.0.CO;2-5

Kong H, Cheng W, Wei H, Yuan Y, Yang Z, Zhang X (2019) An overview of

recent progress in siderophore-antibiotic conjugates. Eur J Med Chem 182:111615. https://doi.org/10.1016/j.ejmech.2019.111615

Krzyzanowski A, Saleeb M, Elofsson M (2018) Synthesis of Indole-, Benzo[b]thiophene-, and Benzo[b]selenophene-Based Analogues of the Resveratrol Dimers Viniferifuran and (±)-Dehydroampelopsin B. Org Lett 20:6650–6654. https://doi.org/10.1021/acs.orglett.8b02638

Kuppusamy R, Yasir M, Yee E, Willcox M, Black DS, Kumar N (2018) Guanidine functionalized anthranilamides as effective antibacterials with biofilm disruption activity. Org Biomol Chem 16:5871–5888. https://doi.org/10.1039/c8ob01699b

Li L, Yuan C, Dai L, Thayumanavan S (2014) Thermoresponsive polymeric nanoparticles: Nucleation from cooperative polymerization driven by dative bonds. Macromolecules 47:5869–5876. https://doi.org/10.1021/ma5015808

Markina NA, Chen Y, Larock RC (2013) Efficient microwave-assisted one-pot three-component synthesis of 2,3-disubstituted benzofurans under Sonogashira conditions. Tetrahedron 69:2701–2713. https://doi.org/10.1016/j.tet.2013.02.003

Mizuno M, Yamano M (2005) A new practical one-pot conversion of phenols to anilines. Org Lett 7:3629–3631. https://doi.org/10.1021/ol051080k

Pagliai F, Pirali T, Del Grosso E, Di Brisco R, Tron GC, Sorba G, Genazzani AA (2006) Rapid synthesis of triazole-modified resveratrol analogues via click chemistry. J Med Chem 49:467–470. https://doi.org/10.1021/jm051118z

Rasko DA, Sperandio V (2010) Anti-virulence strategies to combat bacteria-mediated disease. Nat Rev Drug Discov 9:117–128. https://doi.org/10.1038/nrd3013

Richter MF, Hergenrother PJ (2019) The challenge of converting Gram-positive-only compounds into broad-spectrum antibiotics. Ann N Y Acad Sci 1435:18–38. https://doi.org/10.1111/nyas.13598

Romero KJ, Keylor MH, Griesser M, Zhu X, Strobel EJ, Pratt D, Stephenson CR (2020) Synthesis of Vitisins A and D Enabled by a Persistent Radical Equilibrium. J Am Chem Soc 142:6499–6504. https://doi.org/10.1021/jacs.0c01714

Rostovtsev V V., Green LG, Fokin V V., Sharpless KB (2002) A stepwise huisgen cycloaddition process: Copper(I)-catalyzed regioselective “ligation” of azides and terminal alkynes. Angew Chemie - Int Ed 41:2596–2599. https://doi.org/10.1002/1521-3773(20020715)41:14<2596::AID-ANIE2596>3.0.CO;2-4

Salvio R, Volpi S, Cacciapaglia R, Sansone F, Mandolini L, Casnati A (2016) Phosphoryl Transfer Processes Promoted by a Trifunctional Calix[4]arene Inspired by DNA Topoisomerase I. J Org Chem 81:9016. https://doi.org/10.1021/acs.joc.6b01643

Schmidt B, Riemer M, Karras M (2013) 2,2′-Biphenols Via Protecting Group-Free Thermal or Microwave-Accelerated Suzuki-Miyaura Coupling in Water. J Org Chem 78:8680–8688. https://doi.org/10.1021/jo401398n

Song X, Yuan G, Li P, Cao S (2019) Guanidine-Containing Polyhydroxyl Macrolides: Chemistry, Biology, and Structure-Activity Relationship. Molecules 24:3913

Song YM, Ha YM, Kim JA, Chung KW, Uehara Y, Lee KJ, Chun P, Byun Y, Chung HY, Moon HR (2012) Synthesis of novel azo-resveratrol, azo-oxyresveratrol and their derivatives as potent tyrosinase inhibitors. Bioorganic Med Chem Lett 22:7451–7455. https://doi.org/10.1016/j.bmcl.2012.10.050

St. John SE, Jensen KC, Kang S, Chen Y, Calamini B, Mesecar AD, Lipton MA (2013) Design, synthesis, biological and structural evaluation of functionalized resveratrol analogues as inhibitors of quinone reductase 2. Bioorganic Med Chem 21:6022–6037. https://doi.org/10.1016/j.bmc.2013.07.037

Stockdale DP, Beutler JA, Wiemer DF (2017a) Synthesis of amide isosteres of schweinfurthin-based stilbenes. Bioorganic Med Chem 25:5483–5489. https://doi.org/10.1016/j.bmc.2017.08.016

Stockdale DP, Titunick MB, Biegler JM, Reed JL, Hartung AM, Wiemer DF; McLaughlin PJ, Neighbors JD (2017b) Selective opioid growth factor receptor antagonists based on a stilbene isostere. Bioorganic Med Chem 25:4464–4474. https://doi.org/10.1016/j.bmc.2017.06.035

Sundin C, Zetterström CE, Vo DD, Brkljaca R, Urban S, Eloffson M (2020) Exploring resveratrol dimers as virulence blocking agents – Attenuation of type III secretion in *Yersinia pseudotuberculosis* and *Pseudomonas aeruginosa*. Sci Rep 10:1–11. https://doi.org/10.1038/s41598-020-58872-0

Teng BH, Zhu Q Bin, Fan YY, Yao CS (2020) Total synthesis of the active resveratrol dimer dehydro-δ-viniferin. J Asian Nat Prod Res 22:947–955. https://doi.org/10.1080/10286020.2020.1776267

Tian WQ, Wang YA (2004) Mechanisms of Staudinger reactions within density functional theory. J Org Chem 69:4299–4308. https://doi.org/10.1021/jo049702n

Wan M, Hua L, Zeng Y, Jiao P, Xie D, TOng Z, Wu G, Zhoud Y, Tang Q, Mo F (2017) Synthesis and properties of novel stilbene-twelve alkyl

quaternary ammonium salts as antibacterial optical whitening agents. Cellulose 24:3209–3218. https://doi.org/10.1007/s10570-017-1323-9

Yamamoto K, Bruun T, Kim JY, Zhang L, Lautens M (2016) A New Multicomponent Multicatalyst Reaction $(MC)^2R$: Chemoselective Cycloaddition and Latent Catalyst Activation for the Synthesis of Fully Substituted 1,2,3-Triazoles. Org Lett 18:2644–2647. https://doi.org/10.1021/acs.orglett.6b00975

Yu J, Wang Y, Zhang P, Wu J (2013) Direct amination of phenols under metal-free conditions. Synlett 24:1448–1454. https://doi.org/10.1055/s-0033-1338703

Yue F, Lu F, Regner M, Sun Runcang, Ralph J (2017) Lignin-Derived Thioacidolysis Dimers : Reevaluation, New Products, Authentication, and Quantification. ChemSusChem 10:830–835. https://doi.org/10.1002/cssc.201700101

Zhou C, Chia GWN, Ho JCS, Seviour T, Sailov T, Liedberg B, Kjelleberg S, Hinks J, Bazan GC (2018) Informed Molecular Design of Conjugated Oligoelectrolytes To Increase Cell Affinity and Antimicrobial Activity. Angew Chemie - Int Ed 57:8069–8072. https://doi.org/10.1002/anie.201803103

3.4. STUDY OF XANTHOHUMOL METABOLITES IN HUMANS

ABSTRACT: Xanthohumol, a prenylated flavonoid present in hops and beer, has been studied for its several biological activities. However, its therapeutic use in humans could be affected by its conversion into the phytoestrogen 8-prenylnaringein (8-PN), mediated by gut microbiota. *In vitro* studies have showed that XN can be metabolized by Eubacterium species into 8-PN, *α,β*-dihydroxanthohumol (DXN) and *O*-desmethyl-*α*,*β*-dihydro-xanthohumol (DDXN). Therefore, the urine samples from a randomized, double-blinded, placebo-controlled cross-over study on 20 volunteers, who ingested 24 mg XN/day for 3 weeks, were analysed by LC-MS/MS. In all urine samples, 8-PN, DXN and DDXN were detected and three different metabotypes were revealed: 1) poor metabolizers, 2) prominent O-demethylation metabolizers, and 3) prominent hydrogenation metabolizers. Since gut microbiota was found to be responsible for both *O*-demethylation and hydrogenation of XN, the three metabotypes could be attributed to inter-individual differences in microbiota composition.

3.4.1. Introduction

As we explained in the introduction chapter, the activity of xanthohumol (XN) may be highly affected by its metabolism. Indeed, several *in vitro* and animal studies showed that XN can be spontaneously converted into its isomer isoxanthohumol (IX), which is demethylated by the human cytochrome CYP1A2 or by the microbiota into 8-prenylnaringenin (8-PN), a potent phytoestrogen with potential side effects (Possemiers et al. 2005). Moreover, in a previous work carried out by Prof. Fred Stevens group, in *in vitro* studies XN, 8-PN and DMX were demonstrated to undergo the metabolism of the gut microbe *E. ramulus* to give the corresponding hydrogenated products *α*,*β*-dihydroxanthohumol (DXN) and *O*-desmethyl-*α*,*β*-dihydroxanthohumol (DDXN) (Scheme 3.36) (Paraiso et al. 2019). However, the destiny of XN in humans has never been explored before. Therefore, we investigated the

conversion of XN and 8-PN into DXN and DDXN in humans by LC-MS/MS analysis.

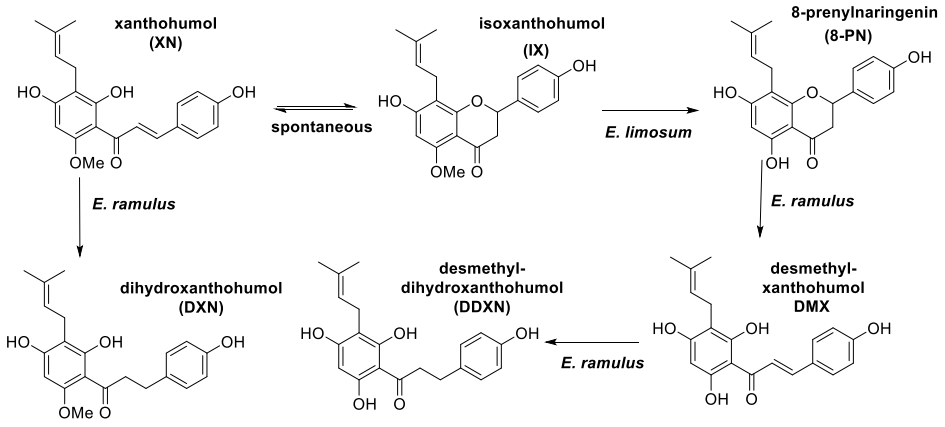

Scheme 3.36. Metabolism of XN and its related prenylated flavonoids by gut microbiota

3.4.2. Material and methods

Chemicals

XN (99+% purity) was a gift from Hopsteiner, Inc. (New York, NY, USA). IX, 8PN, and DMX were isolated and purified from hops as previously described (Stevens et al. 1997, 2000). DXN and ^{13}C-labeled O-desmethyl-*α*,*β*-dihydroxanthohumol (^{13}C-DDXN) were synthesized as previously reported (Ellinwood et al. 2017; Miranda et al. 2018; Paraiso et al. 2019). HPLC grade acetonitrile, ethyl acetate, methanol, and water were purchased from EMD Millipore (Gibbstown, NJ, USA). Dimethyl sulfoxide (DMSO) ACS reagent grade was obtained from Sigma-Aldrich Chemical Company (St Louis, MO, USA).

Clinical study design

Twenty people from the Corvallis area (Oregon, US) participated voluntarily in a randomized, double-blinded cross over trial. The twenty subjects (healthy men and women) for the clinical study were enrolled based on the following entry criteria: 18-50 years age, Body Mass Index (BMI) between 18.5 and 30 kg/m^2, normal metabolic blood panel, non-smokers or no other tobacco in the 3 months before the study, no current prescription drugs, no acute medical

conditions. The volunteers were asked to stop taking regular supplements, including anti-oxidants, and to avoid the consumption of high levels of flavonoids and xanthohumol in the normal diet (microbrew beers, teas, onions) for 2 weeks prior to study entry through conclusion of the study. The study was conducted at the Clinical Research Center (CRC) in the Linus Pauling Science Center (Corvallis, Oregon, US). The subject gave their written informed consent. The study was registered with the ClinicalTrials.gov identifier NCT02432651.

Subjects were randomized to 3 weeks of treatment of placebo, followed by 3 weeks of washout, and then three weeks of the alternative. Urine samples were collected at the beginning and at the end of each phase (4 samples per person).

Sample preparation

XN, IXN, 6-PN, and 8-PN: 100 µL of urine were added with 10 µL 500 ng/mL [$^{13}C_3$]-XN as internal standard and incubated with *Helix Pomatia* sulfatase/glucuronidase for 3h at 37°C. The samples were extracted twice with MTBE. The collected organic phases were dried under a nitrogen flow. The samples were then dissolved in 200 µL 50% methanol and used for the quantitation of XN, IXN, 6-PN, and 8-PN.

DXN and DDXN: 800 µL of urine were added with 10 µL 500 ng/mL [$^{13}C_3$]-XN as internal standard and incubated with *Helix Pomatia* sulfatase/glucuronidase for 3h at 37°C. The samples were extracted twice with MTBE. The collected organic layers were dried under a nitrogen flow. The samples were then dissolved in 100 µL 50% methanol and used for the quantitation of XN, IXN, 6-PN, and 8-PN.

LC-MS/MS analysis

Analysis was performed by HPLC performed on a Shimadzu LC system (Shimadzu; Columbia, MD, USA) coupled to a hybrid triple quadrupole-linear ion trap mass spectrometer (4000 QTRAP; AB Sciex; Concord, ,Ontario,

Canada) equipped with an electrospray ionization source. The samples were analysed using a ZORBAX 300SB-C8 column (2.1 x 50 mm, 3.5 µm), an injection volume of 1 µL and a mobile phase flow of 0.4 mL/min. The HPLC method used a gradient composed of solvent A (water + 0.1% formic acid) and B (acetonitrile + 0.1% formic acid). The solvent gradient started at 30% B and increased to 60% B until 1.5 min, was held at 60% from 1.5 to 2.5 min, increased to 100% from 2.5-3 min, was held at 100% from 3-3.8 min, decreased to 30% at 3.9 min, followed by re-equilibration of the column until 6.0 min. Negative ion electrospray was used with MRM for quantitative analysis of each compound. Data analysis was performed using MultiQuant software.

Method validation

The calibration curves were linear over the range of 0.2–204.8 ng/mL for XN, 2.0-512.0 ng/mL for IXN, 0.2-51.2 ng/mL for 8-PN and 6PN, and 0.05-6.4 ng/mL for DXN with $r^2 > 0.997$. The recovery of each probe samples at low, medium, high concentrations ranged from 83.7% to 115.0%. The accuracy of each QC sample at LLOQ, low, medium, and high concentrations ranged from 87.2% to 119.2%.

Statistical analysis

Heatmaps were made using MetaboAnalyst v.4.0. For a given metabolite, each cell represents the average of individual values from the same sample. To find differences in the metabolic profiles, after quantification of the different metabolites in the samples analysed, correlation analysis was performed using Pearson coefficient based on their interquantile range (IQR). Distance Measure: Euclidean; Clustering Algorithm: Ward; Data Source: Normalized by sum).

3.4.3. Results and discussion

Twenty healthy male and female volunteers (18-50 years old) from the Corvallis (Oregon) area were enrolled in a randomized, double-blinded, placebo-controlled cross-over trial. The twenty subjects were randomized to 3 weeks of treatment or placebo, followed by 3 weeks of washout, and then 3 weeks of the alternative.

During the treatment phase, the participating volunteers were asked to drink a non-alcoholic beverage (0.33 L) containing 8 mg of xanthohumol three times per day. There are no described toxicities for humans consuming oral xanthohumol-based supplements (Liu et al. 2015). A micrebrew ale beer may contain up to 4 mg/L of total prenylflavnoids (mainly xanthohumol and isoxanthohumol) (Stevens et al. 1999). In addition, capsules containing 5 mg xanthohumol are commercially available as dietary supplements. In human pharmacokinetic studies, 48 partecipants took a single dose of 20, 60, or 180 mg and no adverse effects were reported (Legette et al. 2014). Therefore, based on the available data on humans and on animal studies (Hussong et al. 2005; Vanhoecke et al. 2005; Legette et al. 2013), the dosage regimens of xanthohumol were assumed to be safe during the three-week exposure period.

Urine samples were collected at the beginning and at the end of each phase (4 samples per person) and levels of XN and its metabolites were determined by HPLC coupled to a hybrid triple quadrupole-linear ion trap mass spectrometer equipped with an electrospray ionization source. Data analysis was performed using MultiQuant software. Samples HPLC-MS/MS chromatograms are shown in Figure 3.28.

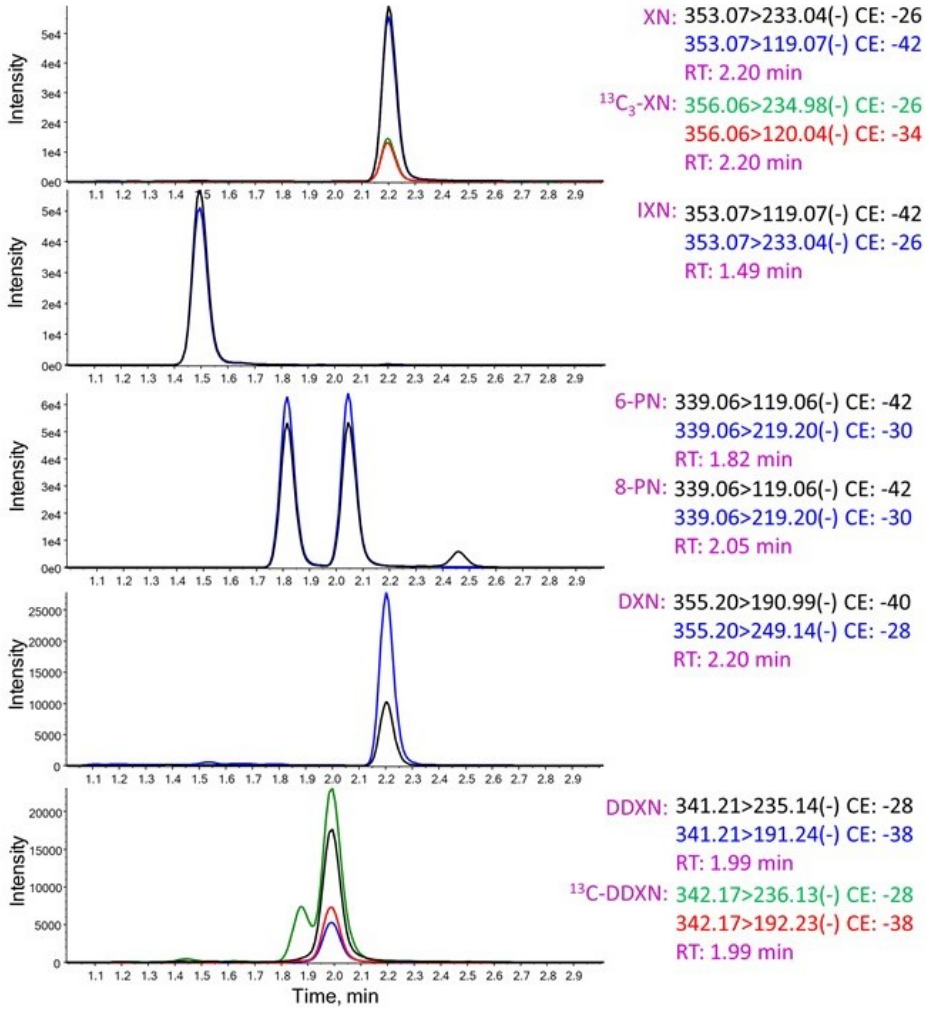

Figure 3.28 - *HPLC-MS/MS chromatograms of XN and its derivatives with their internal standards (IS). CE (Collision Energy), RT (Retention time).*

From the analysis of LC-MS/MS chromatograms of the urine samples deriving from the treatment phase, DXN and DDXN were detected and quantified in human samples for the first time. To confirm the identity of the new metabolite DDXN, ^{13}C-DDXN was spiked with the urine samples. Both retention time and MS/MS fragmentation pattern of the labeled compound matched those of the detected urine metabolite. Using hierarchical clustering analysis, the twenty samples could be subdivided into three groups by comparing the amount of

the different metabolites of xanthohumol in the urine samples (distance measure Pearson r) based on their interquantile range, IQR) (Figure 3.29).

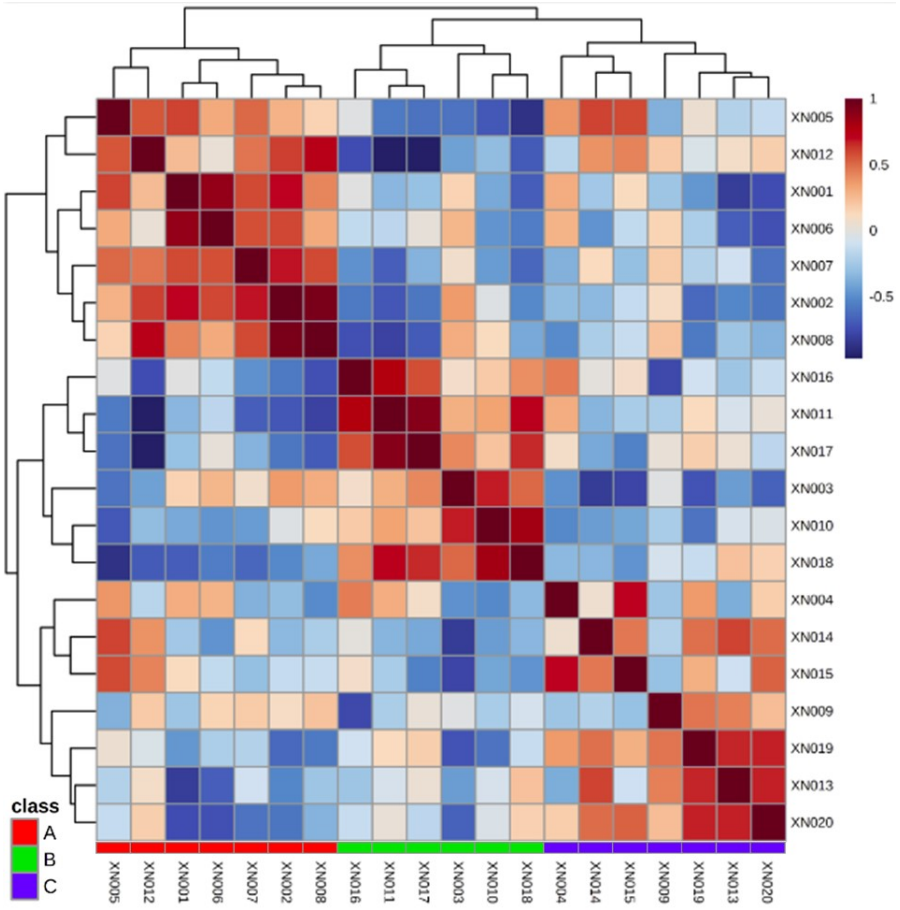

Figure 3.29. *Dendrogram representing the 20 samples which were divided into 3 groups using correlation analysis (distance measure: Pearson r) based on their interquantile range (IQR).*

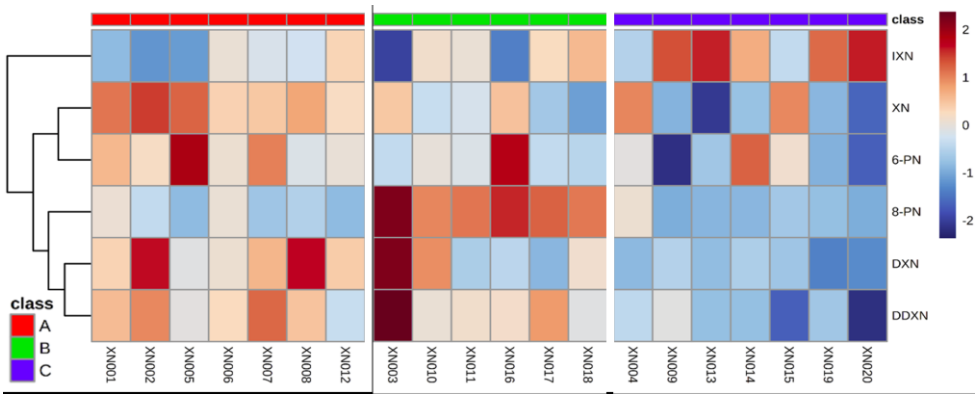

Figure 3.30. *The levels of XN and its metabolites in the 20 samples (urine samples with XN treatment from 20 participants) represented as heat map according to hierarchical clustering analysis (Distance Measure: Euclidean; Clustering Algorithm: Ward; Data Source: Normalized by sum). Group A (7 subjects) shows higher levels of DXN, DDXN, 6-PN; 8-PN is the most abundant metabolite in group B (6 subjects); in group C (7 subjects) the percentage of metabolites is lower compared to the other groups except for IX.*

In Figure 3.30, the levels of XN and its metabolites are represented as heat map ((Distance Measure: Euclidean; Clustering Algorithm: Ward; Data Source: Normalized by sum) (Chong et al. 2019). In particular, group A (7 subjects) showed higher levels of DXN and DDXN, which were demonstrated in *in vitro* studies to derive from the metabolism of the intestinal gut microbe *E. ramulus* (Paraiso et al. 2019). In group B, 8-PN was the most abundant metabolite, produced by hepatic metabolism and the intestinal gut microbe *E. limosum* (Possemiers et al. 2005). Group C appeared to be constituted by poor metabolizer, since the samples revealed high amount of , deriving from the spontaneous cyclization of XN in solution, with respect to the other groups. Therefore, these differences between the twenty subjects may reflect inter-individual differences in microbiota composition.

In particular, the similar trends of DXN and DDXN distributions in the twenty subjects suggested that they could derive from the same metabolic pathway, confirming previous studies in microbial cultures (Paraiso et al. 2019). Moreover, the quantititave analysis of xanthohumol metabolites in the urine samples showed three different metabotypes, which were correlated with a different microbiota composition, resulting in different metabolic profiles.

These findings highlight the importance of investigating intestinal microbial metabolism, which likely affects both beneficial and toxic effects of ingested molecules, like polyphenols, well known to be poorly absorbed in the upper gastrointestinal tract and to reach the colon where microbiota plays an important role for their destiny.

3.4.4. Bibliography

Chong J, Yamamoto M, Xia J (2019) MetaboAnalystR 2.0 : From Raw Spectra to Biological Insights. Metabolites 9:57. https://doi.org/10.3390/metabo9030057

Ellinwood DC, El-Mansy MF, Plagmann LS, Stevens JF, Maier CS, Gombart AF, Blakemore PR (2017) Total Synthesis of $[^{13}C]_2$-,$[^{13}C]_3$-, and $[^{13}C]_5$-isotopomers of xanthohumol, the principal prenylflavoid from hops. J Label Compd Radiopharm 60:639–648. https://doi.org/10.1002/jlcr.3571

Hussong R, Frank N, Knauft J, Ittrich C, Owen R, Becker H, Gerhauser C (2005) A safety study of oral xanthohumol administration and its influence on fertility in Sprague Dawley rats. Mol Nutr Food Res 49:861–867. https://doi.org/10.1002/mnfr.200500089

Legette LL, Karnpracha C, Reed RL, Choi J, Bobe G, Christensen JM, Rodriguez-Proteau R, Purnell JQ, Stevens JF (2014) Human pharmacokinetics of xanthohumol, an antihyperglycemic flavonoid from hops. Mol Nutr Food Res 58:248–255. https://doi.org/10.1002/mnfr.201300333

Legette LL, Moreno Luna AY, Reed RL, Miranda CL, Bobe G, Proteau RR, Stevens JF (2013) Xanthohumol lowers body weight and fasting plasma glucose in obese male Zucker fa/fa rats. Phytochemistry 91:236–241. https://doi.org/10.1016/j.phytochem.2012.04.018

Liu M, Hansen PE, Wang G, Qiu L, Dong J, Yin H, Qian Z, Yang M, Miao J (2015) Pharmacological profile of xanthohumol, a prenylated flavonoid from hops (*Humulus lupulus*). Molecules 20:754–779. https://doi.org/10.3390/molecules20010754

Miranda CL, Johnson LA, De Montgolfier O, Elias VD, Ullrich LS, Hay JJ, Paraiso IL, Choi J, Reed RL, Revel JS, Kioussi C, Bobe G, Iwaniec UT, Turner RT, Katzenellenbogen BS, Katnellenbogen JA, Blakemore PR, Gombart AF, Maier CS, Raber J, Stevens JF (2018) Non-estrogenic Xanthohumol Derivatives Mitigate Insulin Resistance and Cognitive Impairment in High-Fat Diet-induced Obese Mice. Sci Rep 8:1–17. https://doi.org/10.1038/s41598-017-18992-6

Paraiso IL, Plagmann LS, Yang L, Zielke R, Gombart AF, Maier CS, Sikora AE, Blakemore PR, Stevens JF (2019) Reductive Metabolism of Xanthohumol and 8-Prenylnaringenin by the Intestinal Bacterium *Eubacterium ramulus.* Mol Nutr Food Res 63:1–8. https://doi.org/10.1002/mnfr.201800923

Possemiers S, Heyerick A, Robbens V, De Keukeleire D, Verstraete W (2005) Activation of proestrogens from hops (*Humulus lupulus* L.) by intestinal microbiota; conversion of isoxanthohumol into 8-prenylnaringenin. J

Agric Food Chem 53:6281–6288. https://doi.org/10.1021/jf0509714

Stevens JF, Ivancic M, Hsu VL, Deinzer ML (1997) Prenylflavonoids from Humulus lupulus. Phytochemistry 44:1575–1585

Stevens JF, Taylor AW, Deinzer ML (1999) Quantitative analysis of xanthohumol and related prenylflavonoids in hops and beer by liquid chromatography-tandem mass spectrometry. J Chromatogr A 832:97–107. https://doi.org/10.1016/S0021-9673(98)01001-2

Stevens JF, Taylor AW, Nickerson GB, Ivancic M, Henning J, Haunold A, Deinzer ML (2000) Prenylfavonoid variation in *Humulus lupulus*: distribution and taxonomic significance of xanthogalenol and 4'-O-methylxanthohumol. Phytochemistry 53:759–775

Vanhoecke BW, Delporte F, Van Braeckel E, Heyerick A, Depypere HT, Nuytinck M, De Keukeleire D, Bracke ME (2005) A Safety Study of Oral Tangeretin and Xanthohumol Administration to Laboratory Mice. In Vivo (Brooklyn) 19:103–108

3.5. SYNTHETIC APPROACHES TOWARD THE SYNTHESIS OF A CHEMICAL PROBE OF XANTHOHUMOL

ABSTRACT: Despite of several studies on the biological effects on xanthohumol (XN), the specific targets involved in its bioactivity are still largely unknown. Therefore, a chemical probe of XN was conceived and designed. In particular, we developed a synthetic route to selectively functionalize the prenyl chain of XN without affecting the other parts of the molecule (hydroxy functions and *α*,*β*-unsaturated ketone) that were considered fundamental for the pharmacodinamycs of the natural precursor. The obtainment of a terminal aldehyde in place of the double bond of the prenyl chain would allow different xanthohumol derivatization for different biological applications.

3.5.1. Introduction

In order to find a way to determine the target of XN, we decided to build a chemical probe of the prenylflavonoid to perform biochemical assays. In the design of a chemical probe it is fundamental to maintain the structural features of the molecule involved in the mechanism(s) of action of the compound (Gunesch et al. 2020).

In 2016, a previous probe of XN was realized by Brodziak-Jarosz *et al* (Brodziak-Jarosz et al. 2016) (Figure 3.31). However, the probe designed and synthesized by Brodzia-Jarosz *et al* was demonstrated to be much less soluble than XN. Indeed, the authors decided to exploit one free hydroxy function of XN to place an alkyne chain that could react with biotin azide, by a click chemistry reaction, to identify biotinylated XN-protein adducts. The alkylation of the free phenolic function could explain the drastic solubility change of the alkynylated-XN analogue with respect to the natural precursor. In addition, this chemical modification could highly affect the bioactivity and thus the target(s) of the final probe, lacking an important functional group that could mediate XN molecular interactions.

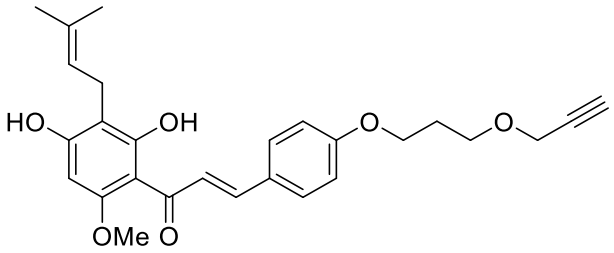

Figure 3.31. *Xanthohumol probe by Brodzia-Jarosz et al* (Brodziak-Jarosz et al. 2016)

Therefore, reasoning on the chemical features of XN and on the activity of its metabolites, we planned to modify XN on its prenyl chain. We decided to preserve its phenolic functions since they are likely involved in the interactions and/or in the effect of the molecule, as demonstrated by the loss of activity of methoxylated or acetylated resveratrol derivatives, for example. The *α*,*β*-unsaturated bond can be a site for Michael addition of cysteinyl thiolates conserved in several proteins. As a matter of fact, Brodziak-Jarosz *et al* (Brodziak-Jarosz et al. 2016) demonstrated that XN is able to form adducts with several thiol proteins, involved in different biological pathways, such as Keap1 (transcriptional factor in response to stressful conditions), Heat Shock Proteins (HSP), and glucose-6-phosphate dehydrogenase (G6PDH), involved in the tumor growth.

Looking at the structure of tetrahydroxanthohumol (TXN) (Figure 1.5, p 18), bearing a saturated prenyl chain and known to maintain the activity of XN (Miranda et al. 2018, Paraiso et al. 2020), we thought that modifying the prenyl chain of the natural precursor would have not highly affected the bioactivity of the final probe. The prenyl chain is assumed to give a lipophilic contribute to the otherwise hydrophilic XN, fundamental for its activity in a biological environment. Thus, trying to maintain the hydrophobic contribute of the prenyl moiety, we aimed at synthesizing a chemical probe of XN modifying its prenyl chain, while leaving the other parts of the molecule unaltered.

We planned to investigate how to selectively cleave the double bond of the prenyl chain in order to obtain a terminal aldehyde, which can be

functionalized in different ways to link directly, or through a spacer, a fluorescent dye or other markers for target visualization and identification. In particular, we envisioned to exploit the aldehyde to link an alkyl chain bearing a terminal alkyne or an azide, which could undergo Cu(I)-catalyzed [3 + 2] azido-alkyne cycloaddition (CuAAC) with different tags, like the widely used biotin (Figure 3.32).

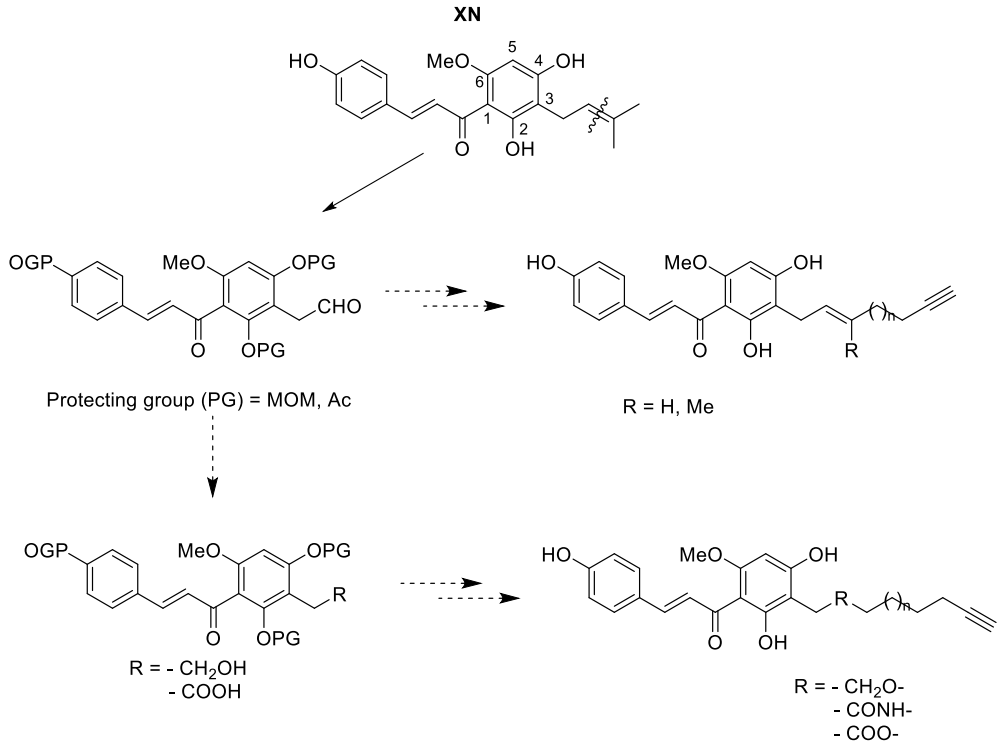

Figure 3.32. *Synthetic approach for the synthesis of XN chemical probe*

3.5.2. Materials and methods

Procedures for the synthesis, isolation, and characterization data for the various stilbenoids obtained are described in the experimental part 3.5.4.

3.5.3. Results and discussion

Firstly, we needed to protect the hydroxy groups, not only because of their reactivity in different reaction conditions, but also to avoid the spontaneous cyclization of XN into IX in solution. Obtaining a fully protected XN was not

trivial. The phenolic group at the position 2 of XN (Scheme 3.37) makes a strong hydrogen bond with the ketone group, resulting in high acidity of the proton and low reactivity in the protection reaction. Experimenting different conditions, we succeeded in the total protection of XN hydroxy group with MOMCl after treatment with NaH 60% at 0°C. The resulting compound **142** was treated with *m*-chloroperbenzoic acid (*m*-CPBA) to give epoxide **143.** Eventually, we tried to cleave the epoxide to give the corresponding diol and subsequently the aldehyde with $NaIO_4$ or HIO_4, but we could not isolate the pure product.

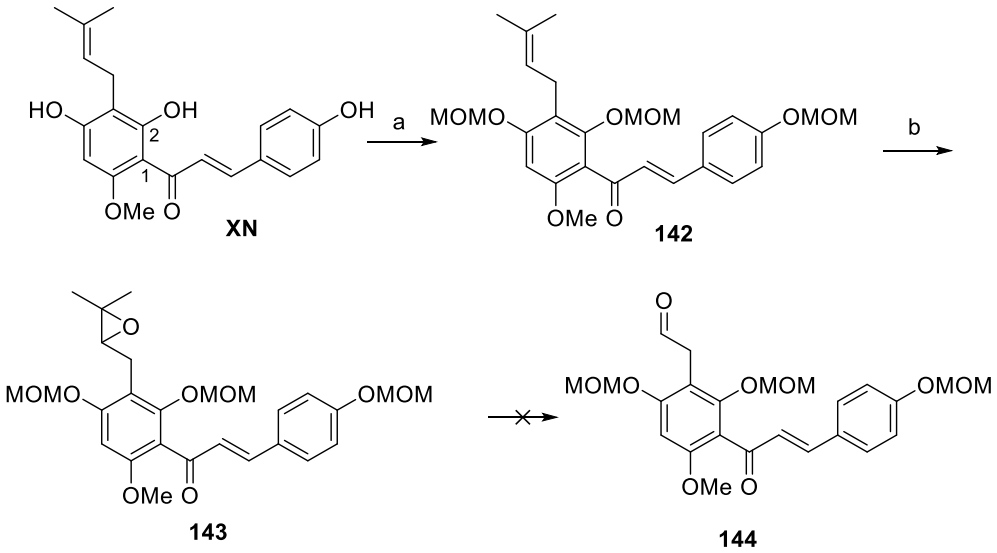

Scheme 3.37. *Reagents and conditions: a) MOMCl, NaH, DMF, 0°C, 2h, 90%; b) m-CPBA, DCM, 0°C to rt, 90 min, 64%.*

Therefore, we tried the same synthetic route starting from a completely acetylated XN. In this case, standard conditions (acetic anhydride and triethylamine in DCM) worked well to obtain smoothly the fully-protected xanthohumol **145** in 95% yield. The reaction with *m*-CPBA gave the corresponding epoxide **146** in 90% yield. We tried different conditions to obtain the final aldehyde **147**. In this case, direct cleavage and oxidation of epoxide with $NaIO_4$ gave the desired product, however with 10-15% of impurities, which were difficult to separate by standard column chromatography. Therefore, we previously performed the cleavage of the

epoxide to give the corresponding diol **148** (62% yield), which was then subjected to oxidation with $NaIO_4$ to give the desired aldehyde. However, when we scaled up the reaction (scale > 200 mg), this approach did not work. Eventually, we treated **146** with HIO_4 in a mixture of THF/Et_2O (1:2) and we obtained the pure aldehyde **147** in 80% yield, even on a hundreds milligrams scale (Scheme 3.38).

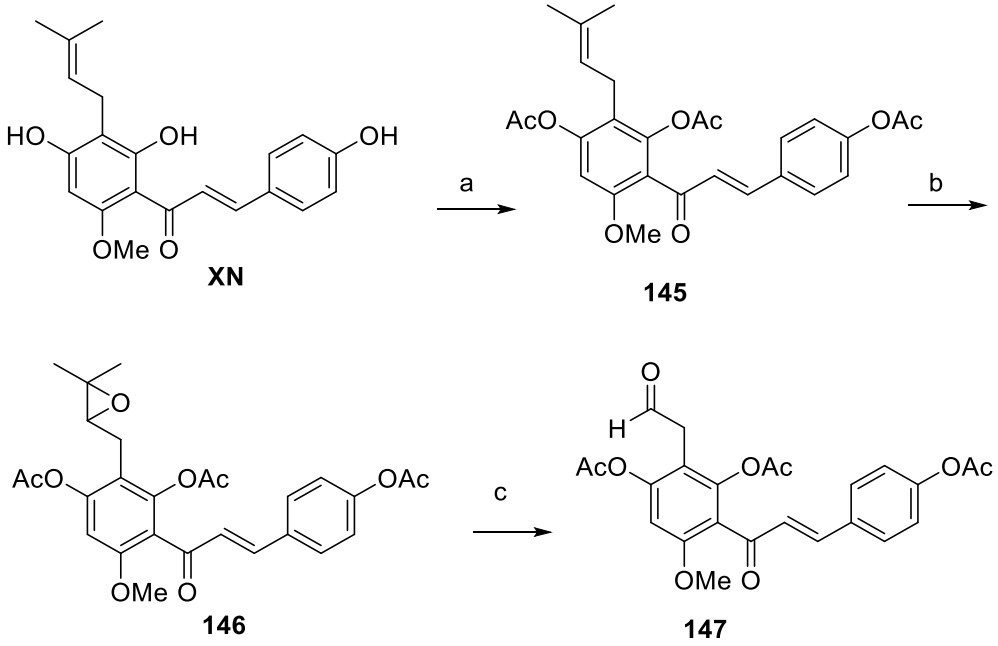

Scheme 3.38. Reagents and conditions: a) Ac_2O, TEA, DCM, rt, overnight, 95%; b) *m*-CPBA, DCM, 0°C to rt, 90 min, 90%; c) HIO_4, THF/Et_2O (1:2), 2h, 80%.

The aldehyde is a scaffold that can be functionalized in different ways. Unfortunately, the reactions we could perform in this case were limited by the labile acetyl groups, used to easily protect the phenolic portions of XN.

We tried to perform a Wittig reaction but we obtained a complex mixture. Also a reductive amination with propargylamine and sodium triacetoxyborohydride resulted in a mixture of products. Therefore, we oxidized the aldehyde in the mild Pinnick conditions to yield the corresponding acid **149** in good yield (62%). The acid **149** can be used to build an amide bearing an alkyl chain,

which should be stable to the deprotection conditions of the acetyl groups. As representative example for this approach, we perfomed a coupling reaction between the obtained acid and propargylamine in presence of HOBt and EDC·HCl, followed by deprotection of the acetyl group with aq 2M $LiOH·H_2O$ in THF at 0°C to give the amide **150** in 42% yield, over two steps (Scheme 3.39).

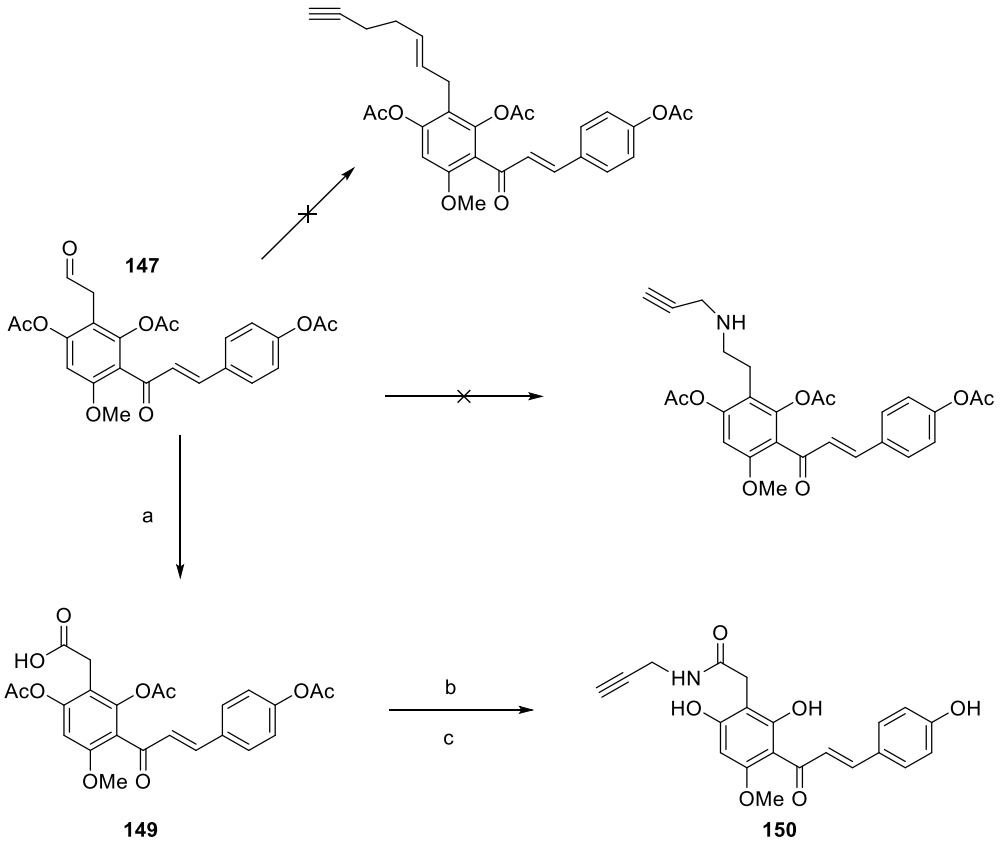

Scheme 3.39. Reagents and conditions: a) $NaClO_2$, NaH_2PO_4, *t*-BuOH/H_2O, rt, 20 min, 62%; b) DIPEA, HoBt, EDC·HCl, DMF, rt, overnight, c) aq 2M $LiOH·H_2O$, THF/water, 0°C, 30 min, 42% over two steps.

The amide obtained was actually more hydrophilic than xanthohumol. Further investigations on the amide coupling with different amines are underway, besides studies on different ways to exploit the obtained aldehyde for other derivatization reactions.

In conclusion, we explored the reactivity of XN, which in spite of its apparent structural simplicity demonstrated to be sensitive to both acidic and basic conditions. The hydroxy functions were found to have very different reactivities, making troublesome even their protection. Moreover, the presence of an *α*,*β*-unsaturated ketone implies its reactivity in nucleophilic reaction, such as the Michael-addition that spontaneously occurs in solution leading to XN isomerization into its flavanone derivative IX.

With respect to this, we achieved XN full protection which was not trivial because of the very acidic hydroxy group forming a strong hydrogen bond with the ketone group of the *α*,*β*-unsaturated portion of the molecule. We applied a new way to approach this molecule, since attempts to modify XN have always been focused on the alkylation or on other functionalization of the phenolic moieties, resulting in lack of regioselectivity or requiring a total synthesis approach. The obtainment of the terminal aldehyde on the prenyl chain and the initial investigation to exploit this scaffold for the construction of a chemical probe could be considered a promising starting point for the derivatization of XN with different biological applications.

3.5.4. Experimental section

3.5.4.1. General information

See chapter 3.1.4.1 for General information. In this case, NMR data were acquired using 700MHz NMR and 400 MHz NMR spectrometers (Bruker, MA; USA). Chemical shifts (δ values) and coupling constants (J values) are given in ppm and Hz, respectively. Number in parentheses following carbon atom chemical shifts refer to the number of attached hydrogen atoms determined by DEPT experiments.

3.5.4.2. Experimental procedures

(E)-1-(6-methoxy-2,4-bis(methoxymethoxy)-3-(3-methylbut-2-en-1-yl)phenyl)-3-(4-(methoxymethoxy)phenyl)prop-2-en-1-one (142)

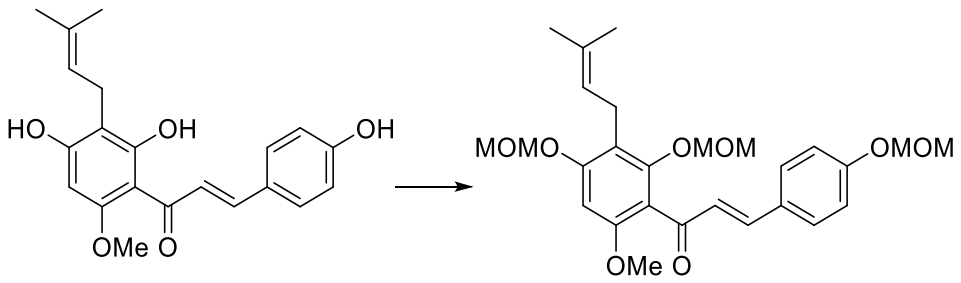

XN **142**

To a solution of XN (200 mg, 0.565 mmol, 1 eq) in dry DMF (5.6 mL) at 0°C under argon atmosphere, NaH 60% (122 mg, 5.08 mmol, 9 eq) was cautiously added. The mixture turned red and was allowed to stir at room temperature for 20 min. Then, the mixture was cooled again to 0°C and chloromethyl methyl ether (MOMCl) (204 mg, 193 µL, 2.54 mmol, 4.5 eq) was slowly added and the mixture was allowed to warm to room temperature and stirred for 2 hours. The mixture was quenched with conc NH_3 (2 mL) and stirred for 10 min. Then, the mixture was partitioned between water (20 mL) and AcOEt (20 mL), and the aqueous phase was further extracted with EtOAc (2 x 20 mL). Combined organic phases were washed with water (40 mL), brine (40 mL), dried over anhydrous Na_2SO_4, filtered and evaporated. The residue was

purified on silica gel by column chromatography using as eluent hexane/AcOEt 7:3 to give the corresponding product as a pale yellow oil in 90% yield.

R_f: 0.3 Hex/AcOEt 7:3

^{1}H NMR (400 MHz, C*D*Cl$_3$) δ (ppm): 7.50 – 7.44 (m, 2H), 7.36 (d, *J* = 16.0 Hz, 1H), 7.05 – 6.99 (m, 2H), 6.89 (d, *J* = 16.0 Hz, 1H), 6.58 (s, 1H), 5.23 (s, 2H), 5.21 – 5.15 (m, 3H), 4.90 (s, 2H), 3.75 (s, 3H), 3.50 (s, 3H), 3.47 (s, 3H), 3.42 (s, 3H), 3.35 (d, *J* = 6.8 Hz, 2H), 1.76 (s, 3H), 1.67 (s, 3H).

(*E*)-1-(3-((3,3-dimethyloxiran-2-yl)methyl)-6-methoxy-2,4-bis(methoxymethoxy)phenyl)-3-(4-(methoxymethoxy)phenyl)prop-2-en-1-one (143)

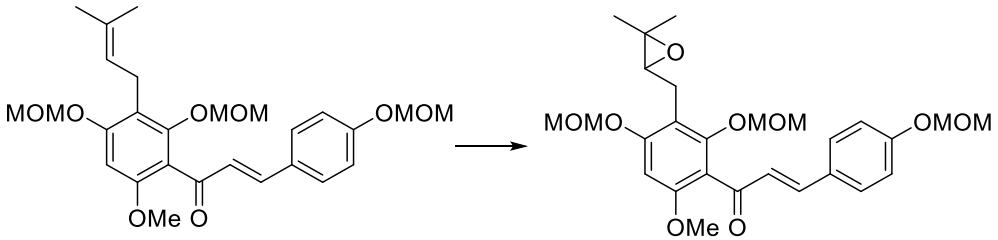

142 **143**

To the solution of **142** (30 mg, 0.062 mmol, 1 eq) in DCM (2 mL) at 0°C *m*-CPBA 50% wt (24 mg, 0.068 mmol, 1.1 eq) was added and the mixture was stirred for 90 min at room temperature. The mixture was quenched with ice and aq saturated $Na_2S_2O_3$. The aqueous phase was extracted with EtOAc (3 x 10 mL). The combined organic layers were washed with aq 5% $NaHCO_3$ (3 x 10 mL), dried over anhydrous Na_2SO_4, filtered, and evaporated. The crude was purified on silica gel by column chromatography, using as eluent hexane/EtOAc 6:4 to give the product as foamy white solid (467 mg, 96%).

R_f: 0.2 Hex/AcOEt 7:3

^{1}H NMR (700 MHz, C*D*Cl$_3$) δ (ppm): 7.53 – 7.47 (m, 2H), 7.38 (d, *J* = 16.0 Hz, 1H), 7.07 – 7.02 (m, 2H), 6.91 (d, *J* = 16.1 Hz, 1H), 6.65 (s, 1H), 5.28 (s, 2H), 5.22 (s, 2H), 4.97 (dd, J_1 = 6.0 Hz, J_2 = 17.9 Hz, 2H), 3.79 (s, 3H), 3.54 (s, 3H), 3.49 (s, 3H), 3.46 (s, 3H), 3.05 – 2.97 (m, 2H), 2.79 (1H, t, *J* = 5.4 Hz), 2.92 – 2.86 (m, 1H), 1.44 (s, 3H), 1.32 (2, 3H, s).

^{13}C NMR (175 MHz, CDCl$_3$) δ (ppm): 193.8 (0), 159.1 (0), 158.0 (0), 156.9 (0), 154.8 (0), 144.2 (1), 130.1 (x2C, 1), 128.5 (0), 126.9 (1), 118.5 (0), 116.4 (x2C), 115.4 (0), 113.7 (0), 101.1 (2), 94.8 (1), 94.5 (2), 94.2 (2), 63.9 (1), 57.6 (3), 56.3 (3), 56.2 (3), 56.0 (3), 24.9 (3), 23.7 (2), 19.0 (3).

(*E*)-4-(3-(4-acetoxyphenyl)acryloyl)-5-methoxy-2-(3-methylbut-2-en-1-yl)-1,3-phenylene diacetate (145)

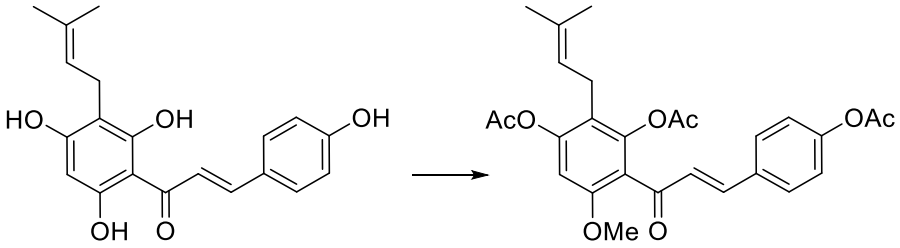

XN **145**

To the suspension of XN (400 mg, 1.13 mmol, 1 eq) in DCM (6 mL), Ac_2O (0.48 mL, 5.084 mmol, 4.5 eq) and TEA (1.41 mL, 10.17 mmol, 9 eq) were added and the resulting mixture was stirred overnight at room temperature. The reaction mixture was diluted with DCM and washed with water (2 x 15 mL). The combined aqueous layers were further extracted with DCM (2 x 20 mL). The collected organic layers were dried over anhydrous Na_2SO_4, filtered, and evaporated. The crude was purified on silica gel by column chromatography, using as eluent hexane/EtOAc 6:4 to give the product as foamy white solid (528 mg, 97%).

R_f: 0.5 Hex/AcOEt 6:4

^{1}H NMR (700 MHz, C*D*Cl$_3$) δ (ppm): 7.67 (2H, AB system, *J* = 8.7 Hz), 7.45 (1H, d, *J* = 16.1 Hz), 7.11 (2H, AB system, *J* = 8.7 Hz), 6.92 (1H, d, *J* = 16.1 Hz), 6.64 (1H, s), 5.03 – 4.99 (1H, m), 3.77 (3H, s), 3.11 (2H, d, *J* = 6.7 Hz), 2.31 (6H, s), 2.16 (3H, s), 1.69 (3H, s), 1.67 (3H, s).

^{13}C NMR (175 MHz, C*D*Cl$_3$) δ (ppm): 192.0 (0), 169.3 (0), 168.9 (0), 168.8 (0), 156.0 (0), 152.4 (0), 151.2 (0), 147.8 (0), 144.1 (1), 132.5 (0), 132.2 (0), 129.9 (2C, 1), 127.6 (1), 122.3 (2C, 1), 121.4 (1), 121.3 (0), 120.1 (0), 104.5 (1), 56.3 (3), 25.7 (3), 23.9 (2), 21.3 (3), 21.1 (3), 20.7 (3), 18.0 (3).

(E)-4-(3-(4-acetoxyphenyl)acryloyl)-2-((3,3-dimethyloxiran-2-yl) methyl)-5-methoxy-1,3-phenylene diacetate (146)

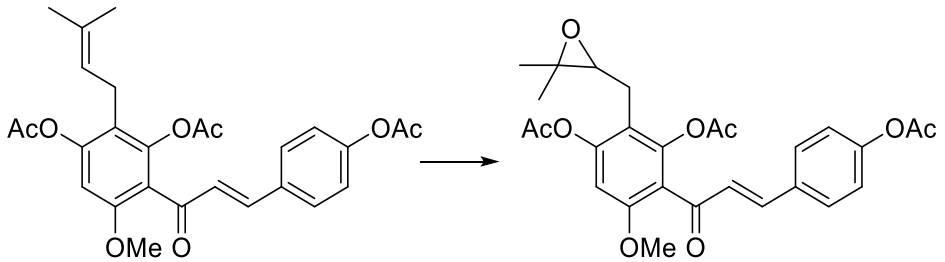

To the solution of **145** (465 mg, 0.9677 mmol, 1 eq) in DCM (3.6 mL) at 0°C *m*-CPBA 50% wt (367 mg, 1.064 mmol, 1.1 eq) was added and the mixture was stirred for 3 h at room temperature. The mixture was quenched with ice and aq saturated $Na_2S_2O_3$. The aqueous phase was extracted with EtOAc (3 x 15 mL). The combined organic layers were washed with aq 5% $NaHCO_3$ (3 x 15 mL), dried over anhydrous Na_2SO_4, filtered, and evaporated. The crude was purified on silica gel by column chromatography, using as eluent hexane/EtOAc 1:1 to give the product as foamy white solid (467 mg, 96%).

R_f: 0.3 Hex/AcOEt 6:4

^{1}H-NMR (700 MHz, C*D*Cl$_3$) δ (ppm): 7.56 (2H, AB system, *J* = 8.4 Hz), 7.45 (1H, d, *J* = 16.1 Hz), 7.12 (2H, AB system, *J* = 8.4 Hz), 6.92 (1H, d, *J* = 16.1

Hz), 6.69 (1H, s), 3.79 (3H, s), 2.79 (1H, t, J = 5.4 Hz), 2.68 (1H, dd, J_1 = 4.9 Hz, J_2 = 14.9 Hz,) 2.61 (1H, dd, J_1 = 6.0 Hz, J_2 = 14.9 Hz), 2.37 (3H, s), 2.31 (3H, s), 2.20 (3H, s), 1.34 (3H, s), 1.27 (3H, s).

^{13}C NMR (175 MHz, C*D*Cl$_3$) δ (ppm): 191.8 (0), 162.3 (0), 169.0 (0), 168.9 (0), 156.7 (0), 152.5 (0), 151.6 (0), 148.2 (0), 144.3 (1), 132.5 (0), 129.9 (2C, 1), 127.5 (1), 122.3 (2C, 1), 121.4 (0), 117.4 (0), 104.6 (1), 62.9 (1), 58.6 (0), 56.3 (3), 24.7 (2), 24.6 (3), 21.3 (2C, 3), 20.9 (3), 19.1 (3).

(*E*)-4-(3-(4-acetoxyphenyl)acryloyl)-2-(2,3-dihydroxy-3-methylbutyl)-5-methoxy-1,3-phenylene diacetate (148)

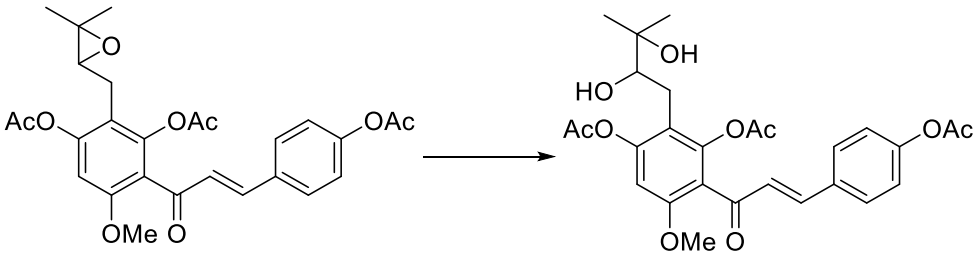

146 **148**

To a solution of compound **146** (140 mg, 0.282 mmol, 1) in a mixture THF/water 1:1 (v/v) (3 mL), some drops of H_2SO_4 were added and stirred for 2 h at room temperature. The mixture was partitioned between water (10 mL) and AcOEt (10 mL) and the aqueous phase was further extracted with EtOAc (2 x 20 mL). The combined organic layers were washed with brine (20 mL), dried over anhydrous Na_2SO_4, filtered and evaporated. The crude was purified on silica gel by column chromatography, using as eluent hexane/AcOEt 1:1 to give the desired compound as a pale yellow oil.

R_f: 0.2 Hex/AcOEt 6:4

^{1}H NMR (700 MHz, C*D*Cl$_3$) δ (ppm): 7.62 – 7.57 (m, 2H), 7.48 (d, J = 16.1 Hz, 1H), 7.15 – 7.11 (m, 2H), 6.95 (d, J = 16.1 Hz), 6.70 (1H, s), 3.81 (s, 3H), 3.59

– 3.53 (m, 1H), 2.65 – 2.60 (2H, m), 2.36 (s, 3H), 2.33 (3H, s), 2.20 (3H, s), 1.27 (3H, s), 1.23 (3H, s).

(*E*)-4-(3-(4-acetoxyphenyl)acryloyl)-5-methoxy-2-(2-oxoethyl)-1,3-phenylene diacetate (147)

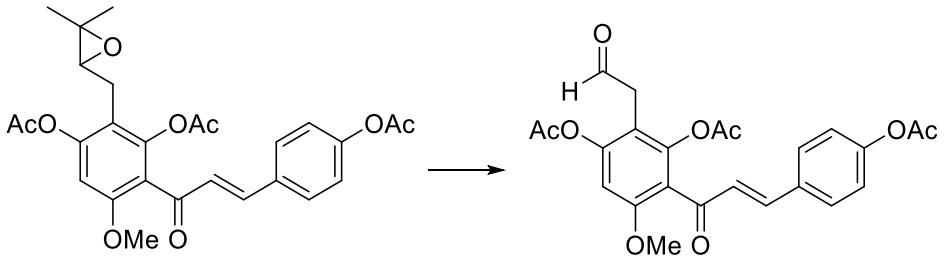

146 **147**

To the solution of **146** (500 mg, 1.007 mmol, 1 eq) in Et_2O (5 mL) at 0°C a solution of $HIO_4 \cdot H_2O$ (253 mg, 1.1077 mmol, 1.1 eq) in THF (2.5 mL) previously stirred for 15 min was slowly added and the mixture was stirred for 2 h at 0°C and then 15 min at room temperature. The mixture was diluted with EtOAc (15 mL) and washed with water (15 mL). The aqueous layer was further extracted with EtOAc (2 x 10 mL). The combined organic layers were washed with aq 5% $NaHCO_3$ (25 mL), dried over anhydrous Na_2SO_4, filtered, and evaporated. The crude was purified on silica gel by column chromatography, using as eluent hexane/acetone 3:2 to give the product as foamy yellow solid (400 mg, 87%).

R_f: 0.4 hexane/acetone 6:4

^{1}H NMR (700 MHz, C*D*Cl$_3$) δ (ppm): 9.50 (1H, t, *J* = 2.2 Hz), 7.57 (2H, AB system, *J* = 8.6 Hz), 7.43 (1H, d, *J* = 16.1 Hz), 7.14 (2H, AB system, *J* = 8.6 Hz), 6.93 (1H, d, *J* = 16.1 Hz), 6.76 (1H, s), 3.81 (3H, s), 2.38 (2H, d, *J* = 2.2 Hz), 2.33 (3H, s), 2.31 (3H, s), 2.17 (3H, s).

^{13}C NMR (175 MHz, C*D*Cl$_3$) δ (ppm): 198.2 (0), 191.5 (0), 169.3 (0), 168.8 (0), 168.7 (0), 157.5 (0), 152.6 (0), 151.8 (0), 148.3 (0), 144.7 (1), 132.3 (0), 129.9 (2C, 1), 127.4 (1), 121.4 (2C, 1), 121.3 (0), 112.1 (0), 104.5 (1), 56.4 (3), 39.6 (2), 21.3 (3), 21.0 (3), 20.6 (3).

(*E*)-2-(2,6-diacetoxy-3-(3-(4-acetoxyphenyl)acryloyl)-4-methoxyphenyl)acetic acid (149)

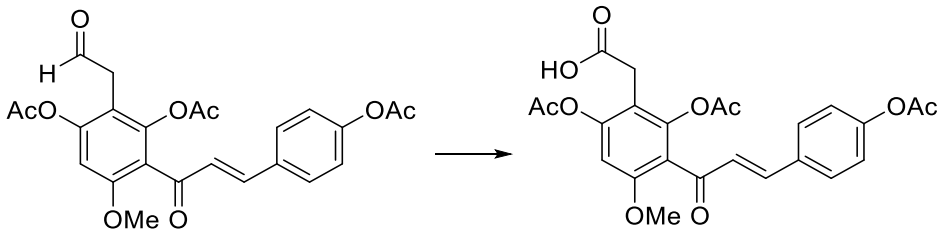

To the solution of aldehyde **147** (140 mg, 0.308 mmol, 1 eq) in a mixture of *t*-BuOH (3mL) and H_2O (1.5 mL) 2-methyl-2-butene (0.36 mL, 3.388 mmol, 11 eq), was added, followed by aq 2M NaH_2PO_4 (0.77 mL, 1.54 mmol, 5 eq) and aq 1.2 M $NaClO_2$ (0.77 mL, 0.924 mmol, 3 eq), and the resulting mixture was stirred at room temperature for 20 min. The solution was quenched with brine (5 mL) and extracted with EtOAc (3 x 10 mL). The combined organic layers were dried over anhydrous Na_2SO_4, filtered, and evaporated. The crude was purified on silica gel by column chromatography, using as eluent DCM/MeOH (from 95:5 to 9:1) to give the product as foamy yellow solid (400 mg, 87%).

R_f: 0.3 DCM/MeOH 95:5

^{1}H NMR (700 MHz, C*D*Cl$_3$) δ (ppm): 7.57 (2H, AB system, *J* = 8.6 Hz), 7.45 (1H, d, *J* = 16.1 Hz), 7.12 (2H, AB system, *J* = 8.6 Hz), 6.93 (1H, d, *J* = 16.1 Hz), 6.77 (1H, s), 3.80 (3H, s), 3.47 (2H, s), 2.34 (3H, s), 2.31 (3H, s), 2.20 (3H, s).

^{13}C NMR (175 MHz, C*D*Cl$_3$) δ (ppm): 191.4 (0), 169.3 (0), 168.9 (0), 168.6 (0), 157.3 (0), 152.5 (0), 151.5 (0), 148.0 (0), 144.2 (1), 132.4 (0), 131.2 (0), 129.9 (2C, 1), 127.4 (0), 122.3 (2C, 1), 121.2 (0), 113.3 (0), 104.5 (1), 56.4 (3), 29.8 (2), 21.8 (3), 21.1 (3), 20.6 (3).

(*E*)-2-(2,6-dihydroxy-3-(3-(4-hydroxyphenyl)acryloyl)-4-methoxyphenyl)-*N*-(prop-2-yn-1-yl)acetamide (150)

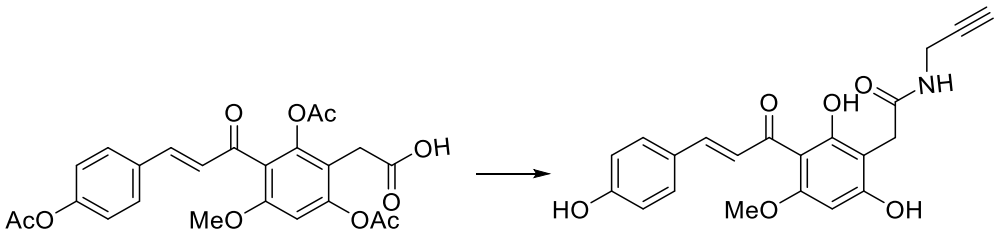

149 **150**

To the solution of **149** (30 mg, 0.0638 mmol, 1 eq) in DMF (0.5 mL) and DIPEA (13.3 µL, 0.0756 mmol, 1.2 eq), EDC·HCl (14.7 mg, 0.0756 mmol, 1.2 eq) was added, followed by HOBt (9.8 mg, 0.0702 mmol, 1.1 eq) and propargylamine (4.5 µL, 0.0702 mmol, 1.1 eq) and the mixture was stirred overnight at room temperature. The mixture was acidified with aq 1M HCl and extracted with EtOAc (3 x 10 mL). The combined organic layers were dried over anhydrous Na_2SO_4, filtered, and evaporated. The crude was purified on silica gel by column chromatography, using as eluent hexane/acetone 6:4 (R_f: 0.3). The product was dissolved in THF (0.4 mL) at 0°C and aq 2M LiOH (0.2 mL) was slowly added and the mixture was stirred for 15 min at 0°C. The mixture was then quenched with saturated NH_4Cl solution until pH 7. The aqueous layer was extracted with EtOAc (3 x 10 mL). The combined organic layers were dried over anhydrous Na_2SO_4, filtered, and evaporated. The crude was purified on silica gel by column chromatography, using as eluent DCM/MeOH (from 98:2 to 96:4). A yellow solid was obtained (10 mg, 42% after 2 steps).

R_f: 0.3 DCM/MeOH 95:5

^{1}HNMR (700 MHz, d_6-DMSO) δ (ppm): 10.79 (1H, brs), 10.09 (1H, s), 8.11 (1H, t, *J* = 5.2 Hz), 7.78 (1H, d, *J* = 15.5 Hz), 7.69 (1H, d, *J* = 15.5 Hz), 7.58 (2H, AB system, *J* = 8.7 Hz), 6.84 (2H, AB system, *J* = 8.7 Hz), 6.09 (1H, s), 3.89 (3H, s), 3.82 (2H, dd, J_1 = 2.5 Hz, J_2 = 5.6 Hz), 3.09 (1H, t, *J* = 2.5 Hz).
^{13}C NMR (175 MHz, d_6-DMSO) δ (ppm): 191.5 (0), 170.2 (0), 165.3 (2C, 0), 161.2 (0), 160.0 (0), 142.8 (1), 130.6 (2C, 1), 126.0 (0), 123.6 (1), 116.0 (2C, 1), 104.4 (0), 102.3 (0), 91.0 (1), 81.7 (0), 72.7 (1), 55.8 (3), 29.0 (2), 28.0 (2).

3.5.4. Bibliography

Brodziak-Jarosz L, Fujikawa Y, Pastor-Flores D, Kasikci S, Jiràsek P, Pitzl S, Owen RW, Klika KD; Gerhauser C, Amslinger S, Dick TP (2016) A click chemistry approach identifies target proteins of xanthohumol. Mol Nutr Food Res 60:737–748. https://doi.org/10.1002/mnfr.201500613

Miranda CL, Johnson LA, De Montgolfier O, Elias VD, Ullrich LS, Hay JJ, Paraiso IL, Choi J, Reed RL, Revel JS, Kioussi C, Bobe G, Iwaniec UT, Turner RT, Katzenellenbogen BS, Katzenellenbogen JA, Blakemore PR, Gombart AF, Maier CS, Raber J, Stevens JF (2018) Non-estrogenic Xanthohumol Derivatives Mitigate Insulin Resistance and Cognitive Impairment in High-Fat Diet-induced Obese Mice. Sci Rep 8:1–17. https://doi.org/10.1038/s41598-017-18992-6

Paraiso IL, Revel JS, Choi J, Miranda CL, Lak P, Kioussi C, Bobe G, Gombart AF, Raber J, Maier CS, Stevens JF (2020) Targeting the Liver-Brain Axis with Hop-Derived Flavonoids Improves Lipid Metabolism and Cognitive Performance in Mice. Mol Nutr Food Res 64:1–10. https://doi.org/10.1002/mnfr.202000341

Gunesch S, Soriano-Castell D, Lamer S, Schlosser A, Maher P, Decker M (2020) Development and Application of a Chemical Probe Based on a Neuroprotective Flavonoid Hybrid for Target Identification Using Activity-Based Protein Profiling. ACS Chem Neurosci 11:3823–3827. https://doi.org/10.1021/acschemneuro.0c00589

4. CONCLUSIONS AND FUTURE PERSPECTIVES

Efficient synthetic and biocatalytic strategies were developed to obtain natural resveratrol-derivatives and their analogues in substantial amounts for their biological evaluation. This allowed systematic studies of single pure compounds, in particular as inhibitors of α-amylase, involved in the glucose metabolism, and as antimicrobials.

The biological studies showed the potential of resveratrol-derived stilbenoids, which were demonstrated to have higher activity than the most-studied resveratrol in the biological models investigated. In particular, *trans*-viniferins resulted to inhibit pancreatic α-amylase more efficaciously than the reference drug acarbose, highlighting the importance of their three-dimensional shape and their geometric molecular features in the interaction with the enzymatic target. These findings are of particular interest, if we take into consideration that the intestinal concentrations of the stilbenoids dimers may be higher than expected for a given food on a composition-only basis. Indeed, it is important to remind that oligomeric stilbenoids may derive from simple metabolic transformations of their monomeric precursors, usually much more abundant than oligomers in common food and beverages.

Evaluation of the antimicrobial activity on foodborne pathogens revealed that dimeric stilbenoids exerted significant antibacterial activity on Gram-positive bacteria strains, with dehydro-δ-viniferin resulting the most active compound of the series. Investigation of the mechanism of action showed that dehydro-δ-viniferin was able to damage the cytoplasmic membrane of *L. monocytogenes*, causing membrane depolarization and loss of membrane integrity.

SAR studies were conducted to elucidate the molecular features relevant to the bioactivity of the benzofuran-containing viniferins. A series of novel simplified analogues of dehydro-δ-viniferin and dehydro-ε-viniferin was designed and synthesized. The selective removal of the phenolic moieties

from dehydro-δ-viniferin resulted in a severe drop of the antibacterial activity, whereas a simplified analogue of dehydro-ε-viniferin was found to exert two-fold higher potency than the natural precursor. These results evidenced the potential use of the stilbenoids obtained as both antimicrobial agents and food preservatives against foodborne pathogens as well as antibiotic adjuvants. Studies of combinations of stilbene derivatives and antibiotics hold promise for future investigation of effective combination therapies.

Following the current strategies to address Gram-negative bacteria, we developed synthetic approaches to build a series of new analogues of resveratrol-based derivatives to broaden the spectrum of the antimicrobial activity of their precursors also on Gram-negative pathogens. In particular, we obtained a small collection of stilbenoids bearing a basic nitrogen function, which was supposed to help the interaction with the negatively charged portion of the outer membrane of Gram negative bacteria. In addition, we investigated how to differently functionalize the benzofuran scaffold of dehydro-δ-viniferin in order to build a series of bioisosteres and analogues for further SAR studies. At the same time, the synthetic procedures developed could be exploited to build hybrid antibiotics, containing siderophores or antibiotics, to address Gram-negative bacterial infections.

The second part of the thesis dealt with studies on the prenylflavonoid xanthohumol. From the LC-MS/MS analysis of urine samples from a randomized, double-blinded, placebo-controlled cross over study on twenty subjects, three metabotypes emerged, which may reflect inter-individual differences in microbiota composition and/or functional capacity. This finding highlights the importance of investigating intestinal microbial metabolism, which likely affects both beneficial and toxic effects of dietary polyphenols.

Eventually, the chemical reactivity of xanthohumol was investigated, and a synthetic approach to selectively functionalize the prenyl chain of xanthohumol was developed. This would allow the derivatization of

xanthohumol for the construction of a chemical probe to investigate the target(s) of this compound by biochemical assays.

5. SCIENTIFIC PRODUCTION

PAPERS

L. Mattio, G. Catinellla, S. Dallavalle, A. Pinto (2020) "*Stilbenoids: A Natural Arsenal against Bacterial Pathogens*" Antibiotics, 9, 336, doi:10.3390/antibiotics9060336.

L. Mattio, G. Catinellla, A. Pinto, S. Dallavalle (2020) "*Natural and nature-inspired stilbenoids as antiviral agents*" Eur. J. Med. Chem., 202, 112541, doi: 10.1016/j.ejmech.2020.112541.

G. Catinella, L. M. Mattio, L. Musso, S. Arioli, D. Mora, G. L. Beretta, N. Zaffaroni, A. Pinto, S. Dallavalle (2020) "*Structural Requirements of Benzofuran Derivatives Dehydro- δ - and Dehydro- ε -Viniferin for Antimicrobial Activity Against the Foodborne Pathogen Listeria monocytogenes*" Int. J. Mol. Sci., 21, 2168, doi: 10.3390/ijms21062168

L. Mattio, S. Dallavalle, L. Musso, R. Filardi, L. Franzetti, L. Pellegrino, P. D'Incecco, D. Mora, A. Pinto, S. Arioli (2019) "*Antimicrobial activity of resveratrol-derived monomers and dimers against foodborne pathogens*" Scientific Reports, 9, 19525, DOI: 10.1038/s41598-019-55975-1

L. Mattio, M. Marengo, C. Parravicini, I. Eberini, S. Dallavalle, F. Bonomi, S. Iametti, A. Pinto (2019) "*Inhibition of Pancreatic α-amylase by Resveratrol Derivatives: Biological Activity and Molecular Modelling Evidence for Cooperativity between Viniferin Enantiomers*." Molecules, 24, 3225, doi: 10.3390/molecules24183225

POSTER COMMUNICATIONS

14-16 August, 2019 – Corvallis (OR – USA) - Linus Pauling Institute International Conference: "*Global natural products social molecular networking (GNPS) analysis integrated with model-predicted bioactives in*

hops extract"- L. Mattio, W. Wu, K. Brown, C. Miranda, A. Vaswani, A. Alcazar Magana, J. Morré, C. S. Maier, J.F. Stevens

2-6 June 2019 – Atlanta – 67th ASMS Conference on Mass Spectrometry and Allied: "*Gut microbial and hepatic metabolism of the hop flavonoid xanthohumol in humans*" - Wu, I. L. Paraiso, L. Mattio, R. Reed, J. Morré, A. F. Gombart. C. S. Maier, J.F. Stevens

24-27 September 2018 – Camerino – CHIMALI – XII Italian Food Chemistry Congress: "*Structure-dependent biological activities of natural resveratrol derivatives*" – L. Mattio, F. Braggio, M. Marengo, A. Scarafoni, S. Iametti, S. Dallavalle, A. Pinto.

19-21 September 2018 – Oristano – XXIII Workshop on the developments in the Italian PhD Research on food science, technology and biotechnology: "*Synthesis and biological evaluation of resveratrol derivatives*" L. Mattio, S. Dallavalle

ORAL COMMUNICATIONS

18th September – Milan (MI) Italy – Workshop in Food Systems 2020 – "*Synthesis, SAR and biological studies of natural polyphenols and their metabolites*" – L. Mattio

30th September – 1st October, 2019 – La Valletta, Malta – 13th World Congress on Polyphenols Applications: "*Quantitative profiling of urinary xanthohumol metabolites in humans reveals metabotypes that reflect differences in gut microbiomes*" - L. Mattio, W. Wu, I. L. Paraiso, R. Reed, J. Morré, A. F. Gombart, C. S. Maier, J.F. Stevens

2-4 May 2018 – Bergamo – School of Food Proteins: "*Polyphenols: Chemistry, metabolites, structure activity relationships*", L. Mattio.